The dry beneficiation of South African small coal in a dense medium fluidized bed

N Hughes

Orcid.org 0000-0000-0000-0000

Dissertation submitted in fulfilment of the requirements for the degree *Master of Engineering in Chemical Engineering* at the North-West University

Supervisors: Prof M Le Roux

Prof Q.P. Campbell

Graduation May 2018

Student number: 22775900

Student identification and Information:

Surname: Hughes

Names: Nikki

Identification number: 910314 0265 086

Student number: 22775900

Highest qualification: B.Eng. Mineral (2015)

Contact details: 060 525 8136

nikki11hug@gmail.com

Thesis details:

Project title: The dry beneficiation of South African small coal in a dense medium fluidized bed

Study level: M. Eng. (Chemical)

Completion year: 2017

Institute: North-West University Potchefstroom campus

Faculty: Faculty of Chemical and Minerals Engineering

Group: Coal Research Group

Supervisors: Prof M. Le Roux

Prof Q.P. Campbell

Deliverables of the study:

- National conference (Presentation and published conference paper)
  South African Coal Processing Society (SACPS - 2017) – Secunda, South Africa 20-24 August 2017

  M. Le Roux, Q.P. Campbell & N. Hughes. 2017. The dry beneficiation of South African small coal in a dense medium fluidized bed.

Declaration:

Herewith I, **Nikki Hughes**, declare that the dissertation entitled:

“The *dry beneficiation of South African small coal in a dense medium fluidized bed”*

Which is herewith submitted in the fulfilment of the requirements as stipulated for the degree Master of Engineering in Chemical Engineering to the North-West University Potchefstroom campus, is a representation of my own unique and individual work and has not been previously submitted to this or any other institute.

Signed:

Nikki Hughes Date: 20/11/2017

Dedication

I would like to dedicate my work in two parts, each to a very special person firstly, of whom has had an immense impact in my life and secondly whose of life I wish to touch.

Part 1

To my father, Jack Hughes, whom without I would have had none of the opportunities that has led me this far. I admire your persistence, perseverance and passion with regard to your work and family. I thank you for every day that you took head on, regardless of the pain, torment and suffering that you endured. I respect you so much for it and can only hope to be able to show the same dedication to my work, family and life. May this work be but a reminder (in a very small way) of how I am working towards being as strong, focussed and dedicated as you.

Part 2

To my god-daughter, Willow Jordaan, this study is but the small bit that I can do to ensure that you and generations to come can enjoy the wonders energy has to offer. It forms a part of forward thinking and pushing the boundaries of life as we know it so as to explore and improve. I can only wish that you remain as adventurous and curious as you are and when you are able, that you will push the boundaries and be daring. Change might be inevitable but it will force you to live and grow in ways unimaginable.

Acknowledgements:

Most importantly, I would like to give gratitude to the North-West University for bestowing upon me the opportunity to obtain a degree in Masters of Engineering. More specifically, I would like to provide a special thanks towards the following people for their influence, contributions and guidance towards the completion of this study.

- Firstly, in gratitude to my study supervisor, Professor M. Le Roux, for the guidance, support, encouragement and understanding throughout the course of this study. His vision, knowledge and mentorship is what helped make this project a success.
- I would also like to express appreciation to my co-supervisor, Professor Q.P. Campbell, for the unique insight and assistance that he provided throughout the duration of this course.
- To my mentor, E.S. Peters, for her advice and devotion towards making this study a success and most importantly for her compassion during the toughest times.
- The laboratory and workshop personnel at the North West University, for their hard work and contributions towards the experimental portion of my study. A special thanks to Mr. Adrian Brock for his vision and dedication in the design and building of the equipment required for the study.
- The most special thanks to my best friend, Justine Jordaan, whom without I could not make anything a success. Her constant support, motivation and sincere understanding has helped me in every aspect of life including my studies.
- To my god child, most beautiful little Willow Jordaan, for having the power to lift my spirits with the simplest of acts (a smile, hug or kiss). True happiness and positivity emanates from you and touches all in your presence.
- My family (especially my father, mother and sister) for their guidance, prayers and love. Moreover for their constant inspiration and devotion to help make me a successful woman and for their overwhelming pride in me.
- Finally, with the highest sense of gratitude, I offer my sincere thanks to our Almighty God for the wonderful blessings that He has bestowed upon me.

ABSTRACT

Conventionally, wet processing was preferred to beneficiate coal based on its sharp separation efficiency; however, the excessive process water constraint is an extreme drawback and proves that wet beneficiation is currently an unsustainable coal washing technique in some parts of the world. Therefore, research into the development of dry beneficiation technologies, especially in coal-rich, semi-arid countries like South Africa is strongly motivated.

In principle, dry technologies are similar to most wet beneficiation techniques that are currently industrialized. These operate based on the relative movement of a particle within a medium in accordance to the difference in said particle and medium density. In the simplest terms, particles denser than the medium sink and those less dense, float. The preferred method of dry dense medium separation is proving to be the air dense medium fluidized bed (ADMFB) technology. In the ADMFB, air at specific velocity is blown through a particulate bed of suitable dense medium. This forms a fluidized bed of particles with pseudo-fluid properties such as, and most applicable to this study, density. Upon the addition of coal to the suspended medium, stratification occurs and the heavier coal particles (associated with high mineral content and low calorific value) sink to the bottom of the bed, and in turn the lighter, better quality particles float. Experimentally, a mixture of coal and medium is loaded into a column and fluidized with air for a period of time. After completion the particulate suspension is allowed to settle into to a packed bed state which is cut in layers of specific height and sampled for analyses. The extent of separation is observed from the quality of the coal in terms of the ash yield, calorific value and density, reporting to each layer.

The purpose of this study was to determine whether ADMFB is suited for the effective beneficiation of South African small (+5.6-13.2mm) coal particles. The separation efficiency of the fluidized bed, (how effectively high-density gauge and low-density coal are separated in the ADMFB), was evaluated by considering the following objectified variables: the effects of differing particle size distributions, variance in medium-to-coal ratios and the influence of activated vibration. Auxiliary investigations toward the quality of the feed coal were also conducted to further comprehend the significance of this variable on the separation efficiency of the fluidized bed.

Another major outcome of this study was to design an enlarged ADMFB for processing of large particle sizes and increased bed loads. This was approached by an initial fundamental process design in which the modified Ergun and associated fluidization equations were used to obtain the minimum fluidization velocities and corresponding bed pressure drop and height for each variable considered. From these results, the bed geometry and dimensions of the new assembly were decided upon. A 0.3m by 0.3m square bed structure was selected, made up of eight 0.05m transparent PVC layers that fit perfectly into another to prevent air and material leakages. This makes up the fluidizing layer of the bed, which is mounted on an air distributer mechanism that is affixed to a centrifugal fan delivering an even distribution of air at the required velocity. The effect of vibration is of interest to this study and bed vibration, when required, is induced by means of an oscillating vibratory motor with adjustable frequency and amplitude. Accurate flow and pressure readings, required for establishing a stable fluidized bed, were attained from an air velocity sensor and water based manometer, respectively.

Dry beneficiation of the coal was attained within the ADMFB, in varying degree, for each of the variables listed above. For a theoretical product of 75% bed volume (or the top 3 bed layers), ash yields obtainable are recorded to vary between 13 and 17.6% with a corresponding mass yield percentage range of 27.6-34.2. For the experiments conducted in this study, these values worsen slightly when considering the addition of dense medium and vibration.

When focussing on the ash values in the feed, top and bottom layers of the bed, a decrease in coal particle size distribution (PSD) proves to have an effect on the extent of separation in the bed. All considered PSD ranges yielded comparable ash values in the top, intermediate and bottom bed layers but the larger PSD (+11.2-13.2mm) yielded the best performance curves when considering ash value and mass yield. Ash content values ranging from 18-30%$_{wt}$ were obtained in the top bed layers over all variables considered, depending on the ash content of the feed and whether dense medium or vibration are present during operation. It was further established that the addition of dense medium (magnetite) did not have a remarkable effect on the separation efficiency of the ADMFB. The experimental runs conducted with dense medium yielded less desired results in the top, intermediate and bottom layers of the bed when compared to those of only coal. The activation of vibration too, showed no improvement to the extent to which the ADMFB separates the coal, middling and gangue products. However, noticeable was that a decrease in PSD, addition of dense medium and activation of vibration had a significant impact on the operability of the ADMFB in terms of minimum fluidization requirements and bed stability.

Coal with considerable amounts of intrinsic ash forming minerals, which cannot be liberated by means of crushing, prove extremely difficult to beneficiate. Conclusively, it was established that the quality of the coal in terms of amount of inorganic matter (minerals) present and the measure to which these are intimately mixed with the organic matter (microlythotypes), significantly influenced bed segregation. From this it can be noted that a blended feed coal, containing a variety of qualities, is best suited for the dry beneficiation of coal in an ADMFB and that extensive optimization of the operation in all aspects is crucial. Furthermore continuous operation of the bed is required to ensure that the drawbacks of a batch-type experimental run, most especially with regard to vibrated dense medium beds, are negated.

- ***Keywords:*** South Africa, water scarcity, dry coal beneficiation, dense medium separation, minimum fluidization velocity, air dense medium fluidized bed, magnetite and liberation.

TABLE OF CONTENTS

LIST OF FIGURES

LIST OF TABLES

LIST OF EQUATIONS

TABLE OF ABBREVIATIONS

Abbreviation	Description	Abbreviation	Description
ADMF	Air dense medium fluidization	**ADMFB**	Air dense medium fluidized bed
Al	Aluminium	**AR**	As received
ARD	Apparent relative density	**BD**	Bulk density
C	Carbon	**Ca**	Calcium
CI	Confidence interval	**CUMT**	Chinese University of Mining and technology
CV	Calorific value	**DDM**	Dry dense medium
DDMS	Dry dense medium separation	**DMR**	Department of mineral resources
DM	Dense medium	**DMS**	Dense medium separation
DOE	Department of energy	**DVD**	Digital video disc
EDS	Electron dispersive X-ray spectroscopy	**Fe**	Iron
HAZOP	Hazard and operability study	**HIRA**	Hazard identification risk assessment
HV	Heating value	**H_2O**	Water
IEA	International energy agency	**IEC**	International energy council
K	Potassium	**MFV**	Minimum fluidization velocity
Mg	Magnesium	**Na**	Sodium
NWU	North-West University	**O**	Oxygen
PSD	Particle size distribution	**PVC**	Poly vinyl chloride
QUEMSCAN	Quantative evaluation of minerals by scanning electron microscopy	**RH**	Relative humidity

ROM	Run-of-mine	**RPM**	Revolutions per minute
S	Sulphur	**SA**	South Africa
SACPS	South African coal processing society	**SANEDI**	South African
SANS	South African national standard	**SAWS**	South African weather service
SEM	Scanning electron microscopy	**SG**	Specific gravity
Si	Silica	**SPI**	Standard precipitation index
STDev.	Standard deviation	**TGA**	Thermogravimetric analysis
Ti	Titanium	**TRD**	True relative density
VA	Vibration activated	**VD**	Vibration deactivated
USA	United States of America	**WCA**	World coal association
WCI	World coal institute	**WEC**	World energy council
wt	Weight		

TABLE OF SYMBOLS

Symbol	Description	Unit
A_t	Cross sectional area	m^2
d_p	Particle diameter	m
F_b	Force of buoyancy	N
F_{gd}	Drag force of fluid on particle	N
F_{sg}	Drag force of particle on fluid	N
G	Force of gravity	N
g	Gravitational acceleration	m/s^2
W	Weight	N
ΔP_b	Bed pressure drop	Pa
ΔP_{mf}	Bed pressure drop at minimum fluidization	Pa
H_{mf}	Bed height	m
ε	Bed voidage	-
ε_{mf}	Bed voidage at minimum fluidization	-
u	Superficial velocity	m/s
u_{mf}	Minimum fluidization velocity	m/s
u*	Scaling factor	-
M	Mass	kg
S_{bed}	Cross sectional be area	m^2
Φ_s	Sphericity	-
μ	Viscosity	Pa.s
ρ_f	Fluid density	Kg/m^3
ρ_s	Particle density	Kg/m^3

Chapter 1: INTRODUCTION AND OVERVIEW

This chapter provides the reader with an introduction to the project entitled *"The dry beneficiation of South African small coal in a dense medium fluidized bed"*. It includes the necessary background knowledge to ensure a general understanding of the problem at hand and lists the motivation, aim and various objectives of the investigation. The following sections compose *Chapter 1*:

- **Section 1.1:** Summarizes the necessary background knowledge required to understand the problem and produces motivations for the possible solution as investigated during this study.
- **Section 1.2:** Provides a brief problem statement and general hypothesis for the investigation given the background regarding coal processing and the future thereof.
- **Section 1.3:** Presents the scope and limitations of the project by detailing, with reasons, all which is deemed within consideration for the investigation.
- **Section 1.4:** Provides the reader with the main aim and listed objectives pertaining to the investigation within the scope as presented in Section 1.3.
- **Section 1.5:** Offers the reader a detailed outline of the dissertation ordaining the flow of the document and providing a description of what is expected in each chapter.
- **Section 1.6:** Concludes the chapter and provides a brief introduction for the chapter that follows.

1.1 Background and motivation

Globally, coal is considered as one of the most important sources of energy mainly due to its affordability, abundance and wide distribution (WEC, 2017). With 892 billion tonnes of recoverable reserves worldwide, it is in no doubt that coal is responsible for meeting a great deal of the international energy demand (WCA, 2017). According to the WEC (2017), coal is used to fuel approximately 29% of the planet's energy requirements and will contribute significantly for roughly thirty more years.

South Africa (SA) houses the 9th largest coal reserve worldwide, with vast coalfields that are spread mostly across the north-eastern region of the country (IEA, 2014). Due to such a notable coal supply, the SA economy relies greatly on coal production and is accordingly listed as the seventh largest coal producer in the world succeeding China, America, India, Indonesia, Australia and Russia (WEC, 2017). SA primarily utilizes coal as the main national source of energy, with an astounding 77% of the overall power requirements being provided by coal fired power stations (DOE, 2017). Coal also plays a key role in the SA export market as stipulated by the Department of Mineral Resources (2014). An average of 28% of the total coal produced is exported to the Middle East, Africa and Europe. Various metallurgical applications such as steel, iron and cement production also rely heavily on coal as fuel and chemical reductant (IEA, 2011). Coal mining operations further makes up 17% of the total employment of SA citizens and is therefore the third largest employer in the mining sector (Stats SA, 2013). Coal, for these reasons, is a key source of energy and of paramount economic importance to South Africa and the rest of the globe. As such, the continuing decline in economically recoverable coal reserves proves to be a major issue facing all prominent coal processing countries (Jeffrey *et al*., 2014). Great importance has consequently been placed on the efficiency of coal processing practices so as to guarantee the sustainable use of this valuable resource.

Coal, in essence, is a combustible rock predominantly consisting of carbonized plant material together with various inorganic sediments. Owing to its heterogeneous nature, it is often necessary to remove certain impurities from the coal prior to utilization. This produces a coal with higher overall quality and results in fewer environmental penalties and decreased energy losses (Chen and Yang, 2003). Coal beneficiation is the process by which these impurities are removed through employing extensive mechanisation and assorted water treatments. Beneficiation processes induce a separation of the desired materials and unwanted gangue present in the coal (World Coal Institute, 2009). Although the currently industrialized, wet beneficiation processes yield high separation efficiencies, it requires substantial amounts of water. These large amounts of water lead to difficulty in handling, transport and storage of the coal and, furthermore, increased capital, operating and transportation costs (Choung *et al*., 2006). Additionally, in semi-arid coal processing countries such as Australia, China, India, Mongolia and South Africa, limited amounts of clean process water have manifested wet coal beneficiation techniques as non-ideal (Chen & Yang, 2003; Zhao *et al*., 2015).

Upon detailed studies of the water resources in SA it was discovered that the average annual rainfall is 492mm, which is well below the global average of 985mm, therefore classifying SA as a water stressed country (Rand Water, 2017). Data obtained from The South African Weather Service (SAWS, 2017) shows that the country experiences uneven distribution of rainfall accompanied by periods of severe drought. *Figure 1.1* provides a map showing the standardized precipitation index (SPI) for SA from April 2015 to January 2017.

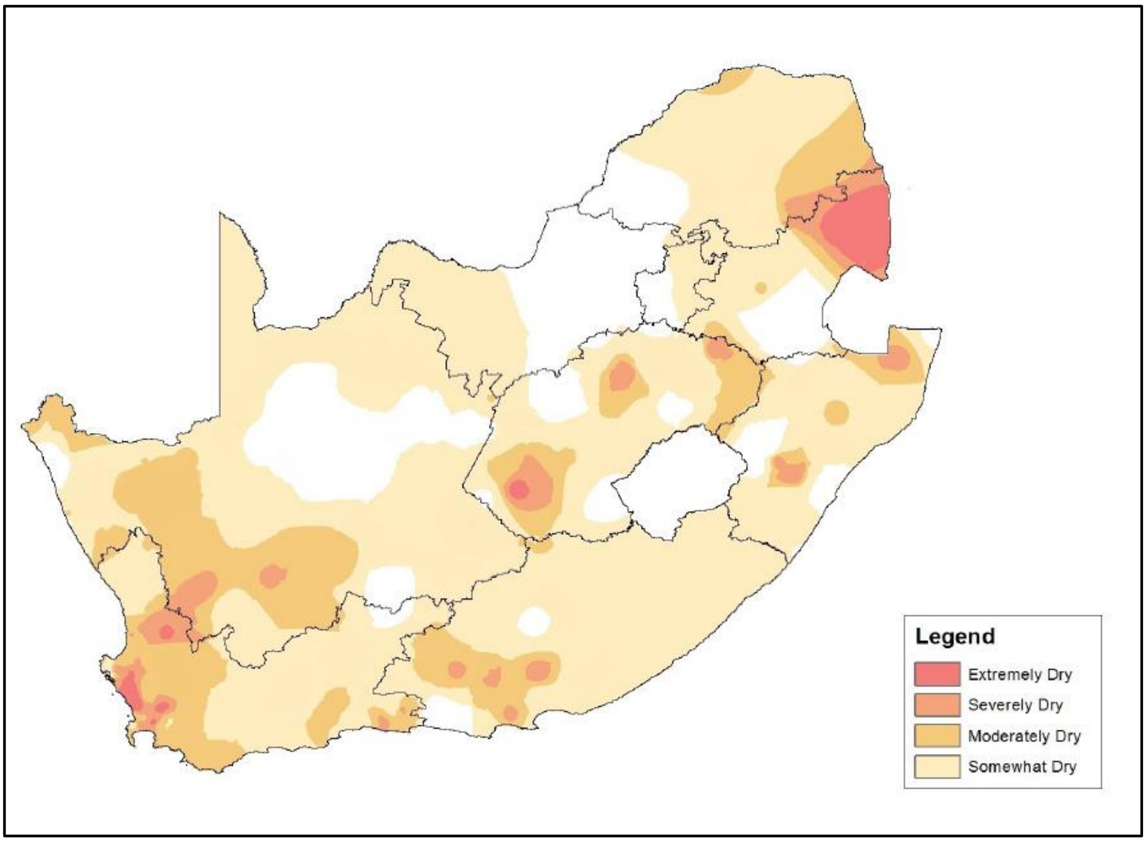

Figure 1.1: Standard precipitation index for SA from Apr 2015 - Jan 2017 (SAWS, 2017)

The above map indicates the areas that were subject to drought throughout the given period and unveils that a vast portion of SA suffered from a parched climate. Notably dry conditions are visible in the north-eastern region which is known to consist of the coal rich areas. From this, it is evident that SA has endured a prolonged period of drought which bears concern especially to the citizens and all industries relying on water. Henceforth, rainfall and temperature forecasts provided by SAWS do not show desirable improvements with the likelihood of decreased rainfall anticipated in future.

The predictions of continued decreasing rainfall especially in the coal rich areas in SA and various other countries, gives further rise to the importance of sustainable use of process water. As a result, research into the alternative dry coal beneficiation methods has been undertaken in South Africa and globally in the hopes of yielding comparably high separation efficiencies, as obtained with wet techniques, without the requirement of water. Various techniques have been investigated of which pneumatic oscillating tables, specialized air jigging and air dense medium fluidized bed (ADMFB) technology yielded closely comparable efficiencies when considering those of wet beneficiation methods (Chen & Wei, 2003; Dwari & Rao, 2007, Zhao *et al.,* 2015). Of these, the air dense medium fluidization (ADMF) process has recently received much attention as the preferred alternative dry beneficiation technique and has been proven effective in China for coal particles above 6 mm (Mohanta *et al.,* 2011). This process may yield separation efficiencies that are closely comparable to those of wet beneficiation techniques and reduces capital and operational costs as well as lowers air and water pollution (Chen & Yang, 2003).

The principle of operation of an ADMFB is similar to that of the wet beneficiation processes that are based on density separation. It consists of a bed of uniquely shaped and sized dense medium particles through which air is percolated at a velocity slightly above the incipient fluidization point. This induces a suspension of the particles which in turn exhibits pseudo-fluid characteristics and possesses a uniform and stable specific density. Upon addition of coal particles to the suspended dense medium, stratification occurs in which the high density coal fractions (mineral rich) sink to the bottom while the low density coal fractions (organic rich) float to the bed surface. This means of separation is in accordance with the Archimedes principle of buoyancy and is generally affected by the difference in density, size and shape of the individual coal particles (Zhao *et al.,* 2015; Sahu *et al.,* 2013). In some cases varying the amount of dense medium, and/or applying vibration to the bed, enhances the ease of fluidization and may yield more desired results. It is thus possible to obtain a high quality coal product and low quality, high ash waste at a specific cut point along the height of the fluidized bed.

From the above discussion *(Section 1.1*), the importance of considering dry beneficiation technologies for coal processing in South Africa is clear. Moreover, it appears that the ADMFB method is most suitable due to its high separation efficiency and low cost when compared to other dry techniques (Chikerema & Moys, 2012; Kumar *et al*., 2010). From here a general problem statement is developed on the basis of both, the large demand for coal and current water crisis in South Africa.

1.2 Problem statement and hypothesis

As stated above, quite a bit of research has been conducted in the dry beneficiation of coal with the ADMFB technique. Chen & Wei, 2003; Dwari & Rao, 2007; Chikerema & Moys, 2012; Firdaus *et al.*, 2012; Prusti *et al.*, 2015 and Zhao *et al.,* 2015 are among the many that have published articles in regards to dry coal processing in countries such as China, India and Australia. There is, however, a lack of data pertaining to the separation of South African small and coarse coal (ranging more or less in +1-50mm) in an ADMFB. Studies regarding the beneficiation of fine and ultra-fine coal in a dense medium bed has been undertaken, on small scale, by the North-West University (NWU) but none on the small and coarse size fractions and additional larger scale tests.

It was therefore considered necessary to conduct research on South African coal in the above mentioned size fractions and also on a larger scale. This is so as to obtain a broad understanding of the separation mechanisms and efficiencies that can be obtained from the ADMFB method. From the knowledge gained a suitable means of implementing such a process industrially can be developed if deemed successful.

The coal found in South Africa originated in the Permian period on the Gondwanaland super-continent, which has now separated into many countries including Africa, India and Australia (Encyclopaedia Britannica, 2015). It is expected that the coal behave in a similar manner to the research conducted by these countries on ADMFB separation given that the procedure is optimized and operated correctly. The research conducted by Firdaus *et al.*, (2012) on Australian coal produced a product with an ash value of 8.2%$_{wt}$ at a yield of 78.3% for a PSD ranging from +5-31mm. It is expected that the beneficiation of the South African small and coarse coal would yield similar results when separated in an ADMFB that is operated at optimal condition.

1.3 Scope of the study

The overall scope of this investigation is primarily focussed on successfully employing an ADMFB to beneficiate coal and obtain a saleable product. Various considerations play a part in determining the effectivity of such a process and it is therefore necessary to imprint the boundaries of this investigation.

This study includes a fundamental process and mechanical design followed by the construction and commissioning of a suitable ADMFB for beneficiation of South African small coal particles ranging from +5.6-13.2mm with +0.3mm coarse grade magnetite as dense medium. The effects of coal feed particle size distribution (PSD), amount of magnetite and vibration of the bed on the ability and extent of separation are considered. This is quantified through proximate, helium pycnometry and bomb calorimetry analyses to determine the variations in the ash contents, densities and calorific values (CV's), respectively, along the bed height. The experimental work is conducted in ambient air temperature, pressure and relative humidity conditions with sample that is dried to below 5% moisture by weight. The results obtained are examined to determine the suitability of the ADMFB technology for South African small coal particles at the conditions specified. *Section 1.4* details the aim and objectives of the study as outlined in the scope.

1.4 Aim and objectives

The aim of this research project is to investigate whether an ADMFB is suitable for the effective dry beneficiation of South African small coal particles (+5.6 -13.2 mm). The study is divided into the following objectives.

1. Conduct an extensive review of existing literature on the topic and gather all relevant information in an ordered summary.
2. Perform a fundamental process design in order to determine the necessary fluidization conditions in terms of material, pressure and air flow requirements.
3. Undertake a general mechanical design of the ADMFB in order to ensure the correct bed dimensions, sufficient blower and vibration power, and finally, accurate flow and pressure readings.

4. Construction and commissioning of the ADMFB along with a set of initial experiments to ensure safe and correct operation.
5. Conduct a set of investigations to determine the maximum, minimum and optimal operation points for the equipment.
6. Determine the separability and quality of the feed coal by means of performing an initial washability analysis.
7. Investigate the final ash, density and calorific values obtainable from the ADMFB and determine whether a significant improvement was made to the separation efficiency while considering the following research questions:
    i. What is the effect of coal quality on the separation efficiency of the ADMFB?
    ii. Does coal feed PSD influence the separation efficiency of the ADMFB?
    iii. Will the separation efficiency of the ADMFB be influenced by the mass ratio of coal to dense medium in the feed?
    iv. Does the state of vibration of the ADMFB have a significant improvement on the separation efficiency within the bed?
8. Perform repeatability and verification investigations on selected variables and the accompanying analyses in order to prove the repeatability of the experiments.
9. Determine the strength of the effect that the different variables have on one another by means of a statistical analysis.

1.5 Dissertation outline

The general flow of the dissertation is broadly divided into 7 chapters that detail the theory pertaining to the study as well as the procedure of experimentation and discussion of the results. The introduction *(Chapter 1)* provides an overview of the study and includes the required theoretical background, aim, objectives and scope of the investigation. This is followed by an extensive literature review in which the knowledge obtained regarding coal; the beneficiation of coal; fluidising principles and dry beneficiation techniques are compiled into a neat summary in *Chapter 2*. *Chapter 3* contains the detailed equipment design procedure of the fluidized bed and encompasses process and mechanical fundamentals. The materials required for the study and sample preparation thereof are discussed in *Chapter 4* coupled with the coal and magnetite characterization. It also stipulates the experimental procedure and sampling techniques observed during the investigation. The results procured throughout the study are portrayed and discussed in *Chapters 5* and *6*. The last chapter embodies a comprehensive conclusion of the findings during the study and how they relate to the objectives as stipulated in *Section 1.4*. The figure that follows, *Figure 1.2,* depicts the general flow and outline of the dissertation.

Chapter 1: Introduction and overview

1.1. Background and motivation
1.2. Problem statement and hypothesis
1.3. Scope of the study
1.4. Aim and objectives

Chapter 2: Literature review

2.1. Chapter overview
2.2. Coal resource
2.3. Coal preparation and beneficiation
2.4. Fluidization
2.5. Dry beneficiation of coal using ADMFB technology
2.6. Chapter summary

Chapter 3: Bed design and commisioning

3.1. Chapter overview
3.2. Experimental set-up
3.3. Fundamental bed design
3.4. Mechanical considerations
3.5. Air distribution
3.6. Control and measurement
3.7. Bed structure
3.8. HAZOP
3.9. Commisioning

Chapter 4: Materials, Equipment and Experimental

4.1. Chapter overview
4.2. Coal
4.3. Magnetite
4.4. Experimental procedure
4.5. Safety
4.6. Observations
4.7. Chapter summary

Chapter 5: Initial results and discussion

5.1. Chapter overview
5.2. Optimization
5.3. Results
5.4. Auxiliary investigations
5.5. Chapter summary

Chapter 6: Results and discussion

6.1. Chapter overview
6.2. Results
6.3. Statistical analysis

Chapter 7:Conclusions, recommendations and contributions

Figure 1.2: Dissertation outline

1.6 Chapter summary

Dry coal beneficiation methods prove an important research topic due to the increasing water related issues associated with wet beneficiation processes. This is most especially experienced in countries such as Australia, China, India and South Africa suffering from drought and/or sub-zero conditions. The exceedingly stringent water usage and pollution restrictions in these countries have placed large emphasis on the need for moving either slightly or entirely away from the use of water in coal processing. From this chapter the motivation for the investigation at hand is fully understood and a clear aim and scope have been detailed for the desired outcome along with a well-defined list of objectives. Here after, *Chapter 2* follows detailing the necessary literature pertaining to ADMFB technology for coal beneficiation.

Chapter 2: LITERATURE REVIEW

Chapter 2 is a compilation of literature that pertains to the investigation entitled "The *dry beneficiation of South African small coal in a dense medium fluidized bed".* It consists of theory regarding the materials, coal preparation, fluidization principles and beneficiation of coal on a dry basis. This chapter is divided into the following sections:

- **Section 2.1:** Provides a brief overview of the investigation and its purpose, followed by a declaration of the topics that are of importance for the study.
- **Section 2.2:** Describes the coal resource in terms of origin, composition, uses and processing.
- **Section 2.3:** Details the importance of coal preparation and provides brief summaries of both the current and advancing beneficiation techniques.
- **Section 2.4:** Gives an in depth discussion of the fluidization principle on which the ADMFB operates.
- **Section 2.5:** Discusses the dry beneficiation of coal using ADMFB at length and identifies and further elaborates upon the related topics that prove important.
- **Section 2.6:** Concludes the chapter and provides a brief introduction to the chapter that follows.

2.1 Overview

Due to the abundance and affordability of coal, it is a vital source of energy around the globe. Coal, however, remains a non-renewable resource and therefore great importance is placed on optimal preparation and beneficiation techniques to ensure its sustainability. Furthermore, the recent shortages of water in areas where coal is most abundant has forced the coal industry to steer focus to the sustainable use of water as well. As mentioned in *Chapter 1*, much research is therefore being done, globally, into dry beneficiation technology for coal.

The aim of this research project has been established, in *Chapter 1*, as determining if the ADMFB process can effectively beneficiate South African small coal particles and to further ascertain which variables play a vital role. It is thus of importance to fully comprehend the major 'coal related' topics such as the origin, geology, properties and preparation as well as the effects these may have upon each other.

2.2 Coal resource

Coal, as will be elaborated in the sections that follow, is a complex compound containing valuable carbon and undesired mineral matter and moisture. These unwanted elements ultimately lead to a reduced coal quality and a number of associated handling and environmental issues. Coal preparation or beneficiation processes are therefore conducted upon run-of-mine (ROM) coal in order to reduce the unwanted components present and produce a coal of higher quality. These operations typically make use of density separation techniques that are based on the differences in density between the mineral matter and valuable carbon of a coal (SA Roadmap, 2011).

2.2.1 Definition and Origin

Coal is a carbonaceous and readily combustible sedimentary rock that originated from the compaction and induration of variously metamorphosed plant remains (SACPS, 2015). Consequently, it contains both organic and inorganic materials and does not have a crystalline structure or chemically homogeneous composition. It generally materializes as banded strata of alternate coal, shale and sandstone sediments along with infrequent conglomerates (SACPS, 2011).

The formation of coal occurred over millions of years ago as prehistoric vegetation decayed and biochemically altered to produce peat. Coalification transpires when peat is transformed into coal through a number of phases that involve numerous biological, physical and chemical processes. As the stages during coalification progress, the maturity or rank of the coal increases, with peat consisting of the lowest rank and being associated with high moisture and low a heating value (SACPS, 2015). The coalification process and its related progressive attributes can be arranged as depicted in *Figure 2.1*.

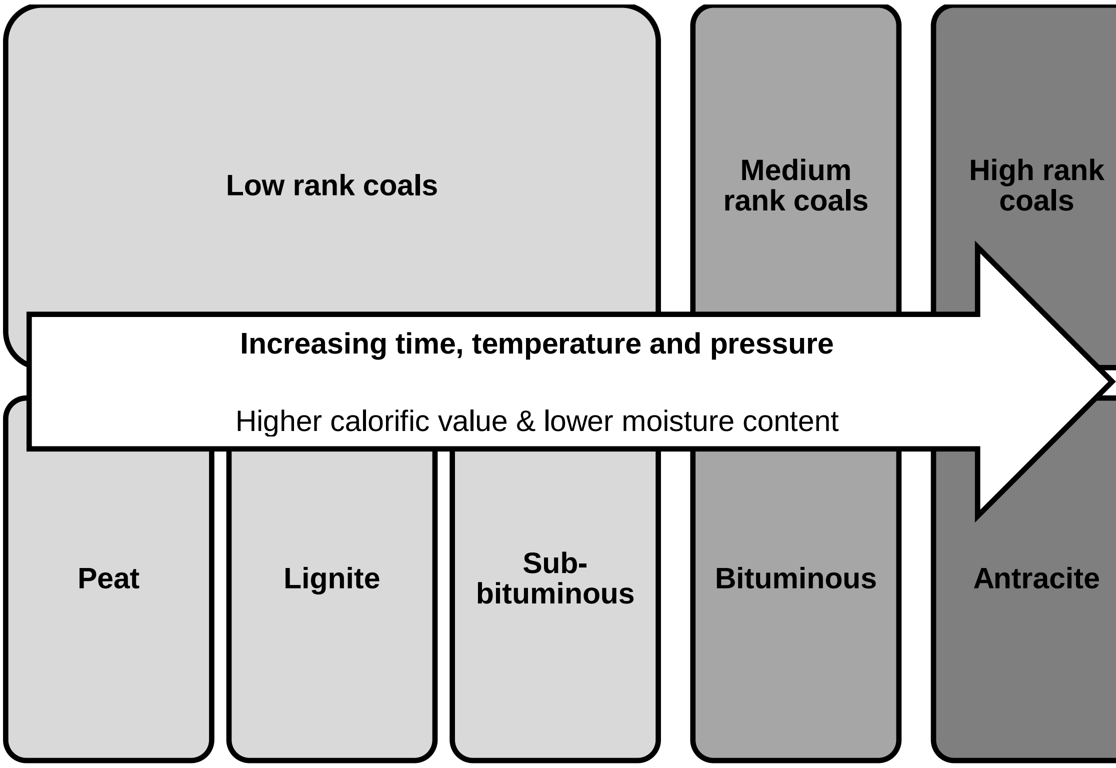

Figure 2.1: Coalification stages adapted from (WCI, 2009)

During the first phase of maturation, peat forms lignite by partial decomposition and compaction of the raw plant material. In the metamorphic or second stage of coalification, lignite is buried by sediments and thereby compacted and heated for extended periods of time. Progressively, with the continued effects of temperature and pressure, lignite matures and mesomorphs into bituminous coal. Ultimately, through continuation of heating and compression, anthracite or high rank coal is formed provided that the environment remains ideal (SACPS, 2015). The differences in the variety of plant remains (type), range of impurities (grade) and degree of metamorphism (rank) help characterize a coal and are greatly reliant on the unique climate experienced during particular times in the earth's history when the coal was formed (SACPS, 2015).

2.2.2 Coal characterization

Due to the variety of conditions upon its formation, coal is an inherently complex mixture of organic and inorganic matter. As such, accurate and complete classification of a coal is reliant on a number of chemical, physical and thermal properties. More specifically, it concerns the amount of organic matter (macerals) present; moisture and mineral contents and the associated density and heating values.

These characteristics all have a major impact on the quality of a coal and bear great effect on its behaviour during processing. Good quality coals are generally expressed by high heating values, intermediate densities; low moisture content and decreased mineral matter. In the sub-sections below, coal characterization is wholly detailed while placing focus on moisture and density as these are expected to have the greatest impact during the current investigation.

2.2.2.1 Rank

The rank or type of coal is described as the progression from peat to anthracite due to increased compaction and calefaction. As the coalification process advances, differences in the moisture content, calorific value, density and appearance of the coal are perceived (SACPS, 2015). As portrayed in *Section 2.2.1,* peat, lignite and sub-bituminous coals (forming the lower ranks) are associated with high moisture contents and decreased calorific values. These are further known for their dull and earthy appearance along with friable texture. High rank coals (bituminous and anthracite) have a harder texture and near black lustre with higher carbon contents and scanty moisture levels (WCI, 2009). Density changes with increasing rank by the following guideline provided by Xie (2015). The coal density ranges for peat, lignite, bituminous and anthracite are roughly 0.72, 0.8-1.35, 1.25-1.5 and 1.36-1.8g/cm^3, respectively. Clearly, a detailed knowledge of a coals appearance, components (organic and inorganic) and related physical and thermal properties is vital in specifying the rank and thereby the quality.

2.2.2.2 Lithotypes

Macroscopically, bands of different brightness and texture are visible at the coal face. These bright and dull bands are called lithotypes and are categorized either as vitrain, durain, clarain or fusian. This classification is mostly used as a general visual description of the coal sample and is therefore only briefly considered as follows (SACPS, 2015).

I. *Vitrain lithotypes* occur in hard bituminous and anthracitic coals as thin layers of jet-black lustre and soft brittle grain.

II. *Durian lithotypes* are distinguished into black and grey durain. The former is composed mostly of the residues of leaves and seeds. Grey durain is similar in appearance to black durain but consists of a complex mixture of vitrain and fusain lithotypes.

III. *Clarain lithotypes* are comprised of alternate bands of vitrain and black durain which are identified as thin bands with a satin appearance.

IV. *Fusain lithotypes* are not generally constituted as hard continuous bands, but come forth as discrete flattened pieces occurring at certain depths of a coal seam. Fusain represents plant matter that was subjected to oxidation during the initial stages of coalification.

2.2.2.3 Coal macerals

Of the macerals in occurrence of bituminous and anthracitic coals, three are deemed relevant and these are briefly discussed. Macerals are defined as the coalified remnants of the prehistoric plants and animals that have been preserved in the coal and rock formations. The macerals make up the organic component of a coal and are established as either vitrinite, inertinite or liptinite (Falcon and Ham, 1988).

I. *Vitrinite* forms the main organic component of the vitrain, clarain and grey durain lithotypes and is identified with a glass-like shimmer. It is mostly composed of cellular plant matter such as roots, stems, trunks and barks and is responsible for the coking properties of coal.

II. *Liptinite* is formed from spore coats, leaf cuticles, waxes and resins that are the most resistant to biochemical actions and are therefore only slightly changed from the original plant material. This maceral is the major constituent in black durain and clarain.

III. *Intertnite is* mostly seen in fusian and represents the most highly-altered plant remains in coal. It is the most common maceral in almost all types of coal.

The macerals can additionally be classified based on their reactivity with vitrinite and liptinite included in the reactive category and intertinte branded as non-reactive (Falcon and Ham, 1988). Maceral class, further, has an effect on the density of a specified coal rank with density increasing in the order of liptinite, vitrinite and finally inertinite. For coals with very high carbon contents the three become similar and also undergo a sharp increase in density (Xie, 2015).

2.2.2.4 Minerology

The inorganic constituents of coal are comprised of mineral matter such as carbonates, sulphides, pyrites, quartz and clays. These minerals can further be defined as inert solid materials that ultimately lead to a reduced coal quality by means of dilution and do not ignite but remain as an ash residue post complete combustion (SACPS, 2015). Two types of mineral matter can be categorized, inherent and extraneous with the former consisting of solid minerals that are intimately mixed within the coal and were present in the original vegetation from which the coal was formed. Extraneous mineral matter is made up of the dirt bands and lenses within the coal seam and also the shales, sandstones and intermediate rocks that are introduced into the mined product (SACPS, 2011).

The grade of a coal is determined by the type and amount of mineral matter present and will vary according to the area of formation and rank. Moreover, the ash yield of a coal (grade), is associated with various environmental and technological issues during preparation and use (Schweinfurth, 2009). A reduced efficiency of a coal processing plant is expected due to the presence of mineral matter in the coal and processing and combustion equipment may also be negatively affected.

Of notable importance, especially for beneficiation, is the effect that the mineral matter, or ash yield, has on coal density. Mineral densities are as a whole significantly higher than that of organic matter and as a result the content and composition of said minerals drastically influence the density of a coal. Xie (2015) states that an increase in coal density of 0.01% is roughly anticipated for every 1% increase in coal ash yield. This greatly affects the behaviour of coal particles during processes that are especially based on density, such as dense medium separation.

2.2.2.5 Other properties of relevance

Aside from the ash yield of a coal, three other constituents bare great importance. These are defined as moisture content, volatile matter and fixed carbon content. Most coal mining and operations utilize water which results in coal with high free and surface moisture contents. The moisture content of a coal has an adverse effect on the quality of a coal much in the same manner as ash content. Energy is required to evaporate the water and the efficiency of the combustion is thereby reduced. As such, moisture forms an important property and plays a major role in the performance of coal during processing.

The second component consists of a mixture of short and long chain hydrocarbons and also sulphur. This is termed the volatile matter in a coal and is liberated at high temperatures in the absence of oxygen. These volatiles are the root of the harmful carbon-, sulphur- and nitrogen-oxide emissions associated with the combustion of coal (Schweinfurth, 2009). As such, the volatile matter in coal is considered key and dealing therewith is cardinal. Lastly, the fixed carbon is determined by the difference in mass of a sample after moisture, volatiles and mineral matter have been removed. This is ultimately used to estimate the amount of pure carbon that can be yielded from the sample.

The chemical components of a coal sample, as listed and described above, are quantified by means of ultimate and proximate analyses. These techniques essentially drive off each component individually using high temperatures and calculates the moisture, volatile, ash and fixed carbon amounts by mass difference.

2.2.2.6 Density

Among the many physical properties of coal, the density proves of utmost importance for the current study. It provides an indication of the nature and structure of the coal substance and further aids in determining the coal grade. As noted earlier, the inorganic mineral matter constituents in a coal specimen are closely related to its density. Due to the inhomogeneous nature of coal, a large density profile is experienced throughout coal fields and seams. It is thus important to fully understand density and how it is related to coal classification.

Density can be distinguished into three types, true relative density (TRD), apparent relative density (ARD) and bulk density (BD). An understanding of the difference in these classes is essential. TRD refers to a density value determined while excluding the pores of the coal. This is mostly used in quality research and is determined by using a pycnometer analysis. The second measure of the density of coal termed ARD, is calculated as the ore mass per unit volume whilst including the pores structures. Finally, BD refers to the ratio of coal mass filling a container and to the vessel volume. Placed into perspective, TRD usually presents the highest density value followed by ARD and then BD (Xie, 2015).

In conclusion, it is transparent that coal is extremely heterogeneous and, additionally, can be classified by various means. Each parameter and determination method thereof, provides useful information regarding a coal's abilities and its behaviour during processing. It is therefore imperative to understand and critically define the various characteristics of coal as detailed above. Moreover, a comprehensive understanding of the expected effects of said properties on the ongoing investigation is necessary. As such, the formation and quality, in terms of rank, type, grade, composition and density, of coals originating in South Africa will be explained in the section that follows along with their expected effect on the current study.

2.2.3 Coal in South Africa

The coal deposits in South Africa were formed in the Permian period approximately 300 million years ago and are hosted in the sedimentary rocks of the main Karoo Basin (SACPS, 2011). This retro-foreland basin was created when tectonic movements resulted in a portion of the Gondwanaland super-continent, to perpetually subside. Peat swamps developed within the basin and the forming coal deposits were thereafter affected by igneous intrusions associated with the rising of the Drakensberg. This provided the ideal conditions that ultimately led to the improved coal rank and the tendency for rank to increase from southwest to northeast regions (SA Roadmap, 2011).

Low rank coals are considered negligible and superficial to the South African coal market and most mined coals fall into the range that extends from bituminous to anthracite. These hard coals consist mostly of vitrain and grey durain lithotypes and are associated with vitrinite and inertinite macerals (SACPS, 2015). Extraction of high ash, or low grade, coal is however becoming increasingly frequent in South Africa with ash yield values as high as $40\%_{wt}$ being reported (Jeffrey, 2005).

The South African coal seams that are of economic significance are generally mined in the Ecca and Beaufort groups of the Karoo basin. There are a number of prominent coalfields occurring across the north eastern region of the country and are generally located in the Mpumalanga, Free State and Limpopo regions which are associated mainly with mud- and sandstone sediments (SA Roadmap, 2011; Jeffrey, 2005). Approximately 70% of the remaining South African coal reserves are found within the Highveld, Witbank and Waterberg coalfields in Mpumalanga and Limpopo respectively. *Figure 2.2* provides a depiction of the major coal occurrences and activity in South Africa, with special regard to the location of the coalfield from which the coal utilized during the study was obtained.

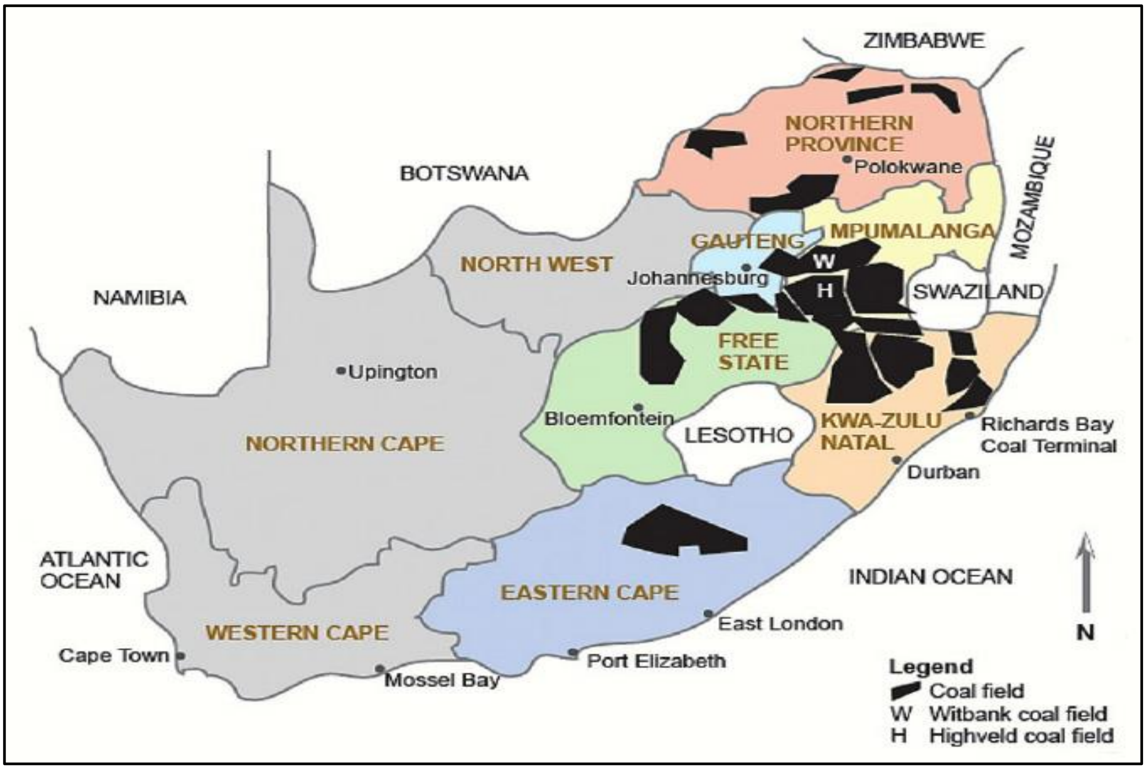

Figure 2.2: The main economically viable coalfields in South Africa (SACPS, 2015)

The coalfields are portrayed in black across the map of South Africa, in *Figure 2.2*, with those of the Highveld and Witbank indicated by H and W, respectively. Coal from the Witbank coalfield in Mpumalanga, indicated by the W, is considered for the ongoing investigation and is therefore characterized with a semi-bituminous to bituminous rank, reasonable calorific values and ash yields within the range of 35%$_{wt}$ (Jeffrey, 2005).

2.2.3.1 Coal products and utilization

Coal is used for numerous applications in South Africa namely, coking in metallurgical processes, preparation of synthetic fuels, local electricity generation and lastly for export. Each application requires a coal of specific quality in terms of its unique properties such as calorific value, ash yield, volatile matter, sulphur present and moisture content. South Africa typically produces four main coal grades, A, B, C and D. *Table 2.1* presents some characteristics of South African ROM coal and those of the four main coal grades (IPC Coal, 2016; SA Roadmap, 2011).

Table 2.1: Typical characteristics of SA ROM and coal products (IPC, 2016; SA Roadmap, 2011)

Characteristic	ROM	A Grade	B Grade	C Grade	D Grade
Sulphur (%)	< 2	< 0.6	< 0.6	< 1.0	< 1.5
Calorific value (MJ/kg)	16 – 21	27 – 28.5	26 – 27.5	24 – 26	21 - 23
Ash ($\%_{wt}$)	20 – 40	12 – 14	14 – 16	16 - 18	20 - 25

From *Table 2.1*, it is clear that the quality increases from grade D to A with the ROM coal being of moderately low quality. Metallurgical coal is used in the coking applications of steel production and requires relatively low ash and sulphur yields with the associated calorific value being higher than 23MJ/kg. The coal used as an export product necessitates a similar quality (Eberhard, 2011). When considering the ROM coal characteristics, it is clear that coal preparation and improvement is essential to obtain the desired quality for these products. The quality of thermal coal used in local electricity generation and synthetic fuel production is generally much lower. Being associated with Grade D coal having calorific values smaller than 23MJ/kg and ash yields ranging from 20-35$\%_{wt}$, these coals can in many cases be utilized without beneficiation (Eberhard, 2011). The ROM coal grade and product specifications do not solely dictate the need for and extent of beneficiation. The economic feasibility regarding operation and transportation are considered and as a result many coal mining operations produce a dual product consisting of beneficiated coal for metallurgical and export purposes, and a middling product suitable for local consumption (SA Roadmap, 2011).

Coal utilized during this investigation, as previously mentioned, was obtained from the Witbank coalfield in the Mpumalanga region of South Africa. Coal mining operations in this coalfield are in the number 1, 2, 4 and 5 seams and produce high quality metallurgical and export coal, local steam coal and blended coking coal respectively (SA Roadmap, 2011). Furthermore, the coal sample was extracted from seam 4 and as a result the investigation is aimed at yielding a high quality thermal coal (grade D).

2.3 Coal preparation and beneficiation

The desire to yield a coal product of the necessary quality for its intended purpose is proved imperative in the South African coal market. Beneficiation processes are thereby deemed vital in eliminating the various issues related to the sheer amount of extraneous and non-combustible matter in coal. These problems include a reduction in calorific value; increase in the volume of materials to be handled and transported; increased wear and tear on processing equipment and the release of hazardous gases and particulate emissions. The preparation of ROM coal results in the removal of the unwanted impurities and thereby generates a uniform and more suitable product (SA Roadmap, 2011).

2.3.1 Preparation

In South Africa, two coal preparation stages are currently used namely, screening and washing. A primary screening stage is initially used to remove large foreign objects from the coal, which is then crushed to reduce the overall top size. Another screening stage follows this in order to separate the coal into desired ranges for either direct sale or further processing by beneficiation (SA Roadmap, 2011). Typical values, mass distributions and moisture contents of the various size fractions as classified in South Africa are presented in *Table 2.2*.

Table 2.2: Typical classification and characteristics of coal size fractions (SA Roadmap, 2011)

Classification	Particle size (mm)	Mass distribution (% of total product)	Moisture content (AR $\%_{wt}$)
Coarse	12-250	61	5
Small	1-12	28	9
Fine	0.1-1	7	13
Ultra-fine	0.1-0.15	4	27

Coal particles ranging in size from 5.6mm to 13.2mm are deemed as part of the scope for the study. These fall within the span classified as small coal particles, as listed in *Table 2.2*, and are associated with 28% of the total coal product and relatively low moisture contents (9%$_{wt}$).

2.3.2 Beneficiation

Beneficiation processes are conducted in order to reduce the amount of minerals present in coal and essentially generate a coal that meets the product specifications. Density separation techniques are typically used due to the large differential in density between the inorganic or ash forming materials present, and the valuable coal organic (SA Roadmap, 2011).

Density separation methods are used to separate minerals of differing specific gravity (SG) by making use of their relative movement in response to gravity and one or more other forces. This is usually related to the resistance of motion by means of a vicious fluid (medium) such as water or alternatively, air (Wills & Napier-Munn, 2008). Depending on the chosen medium, beneficiation can be categorized as either wet (operating with water) or dry (operating with air), both based on the same principle. In dense medium separation, ore particulates are added to a medium (wet or dry) of suitable density and depending on the density of each individual particle, a float or sink action is experienced. Those particles with a relative density higher than that of the medium, will sink and those lighter will float (Wills & Napier-Munn, 2008). As the ash value of coal is related to its relative density, in that coal with high mineral content is denser, beneficiation to remove the undesired ash forming minerals is possible with dense medium separation (SA Roadmap, 2011). *Figure 2.3* provides a basic portrayal of the principle of dense medium separation.

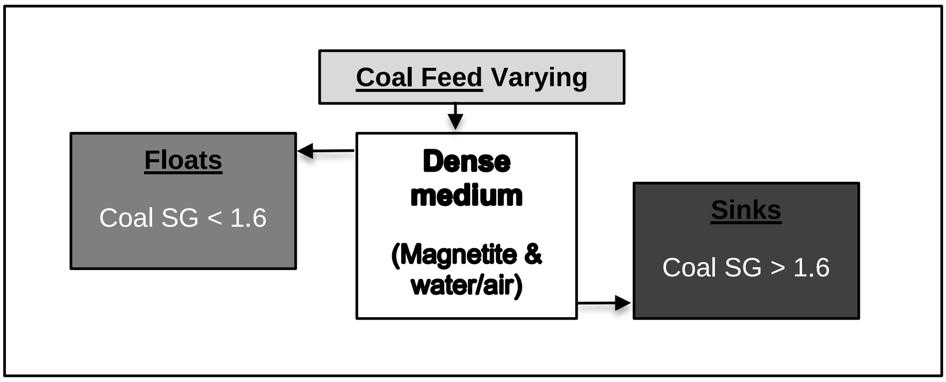

Figure 2.3: The principle of dense medium separation

Portrayed in *Figure 2.3*, a coal feed of varying relative density is placed into a suitable dense medium of 1.6g/cm^3. The coal heavier than this density and associated with high ash content, sinks and those less dense, low ash yield coal particles float. Effective separation is only possible if a marked density difference exists between the valuable ore and gangue. Additionally, the effect of particle size must be considered as the effectiveness of gravity separation will reduce when the movement of particles are not governed by density but rather surface friction and usually occurs with finer particles (Wills & Napier-Munn, 2008). Size further affects the volume of a system with an increased mass of particles reporting to the same density and causing a behaviour similar to that of smaller denser particles.

Most dense medium separation techniques that are exploited globally for the beneficiation of coal are based on wet beneficiation (Yang *et al.*, 2013). The coal is washed by means of dense medium drums, cyclones, spirals and froth floatation, all of which make use of copious amounts of water yielding a moist product with reduced calorific value. As a result, wet beneficiation processes require additional infrastructure for tailings disposal and water recovery (Yang *et al.*, 2013). *Figure 2.4* provides a generic flowsheet for a complex coal beneficiation plant in South Africa.

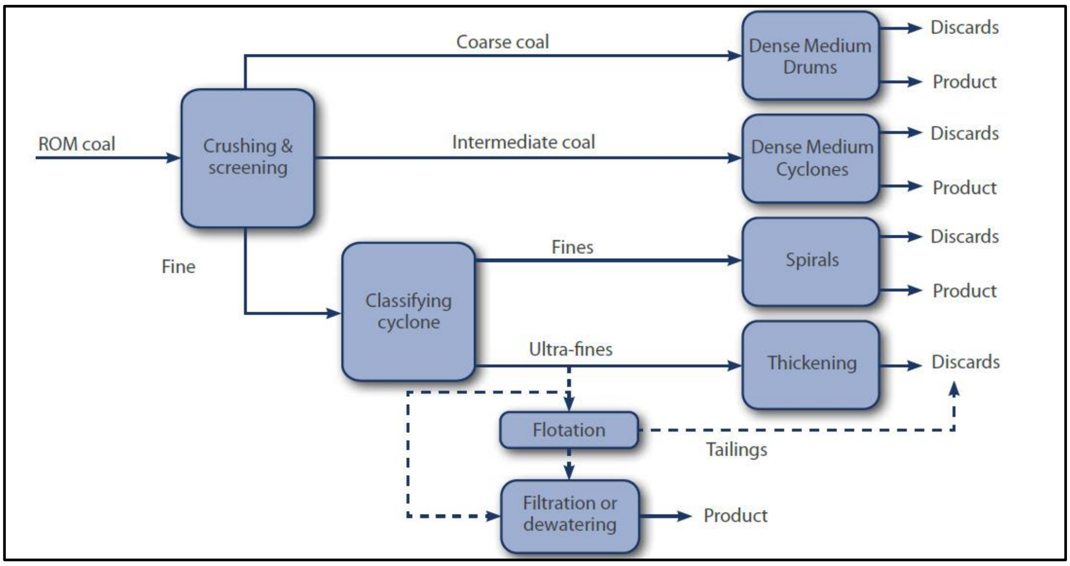

Figure 2.4: Generic block flow diagram of the coal washing process adapted from (SA Roadmap, 2011)

As visible from the flow diagram in *Figure 2.4*, after initial crushing and screening, the oversize coal is divided into coarse and intermediate classes and beneficiated using dense medium drums and dense medium cyclones respectively. The undersize or fine coal fraction proceeds to a classifying cyclone yielding fine and ultra-fine coal products. The fine portion is then washed in a spiral concentrator and the ultra-fine fraction continues to the thickeners or froth flotation tanks. Of importance for this dissertation, as noted previously, is the intermediate coal fraction currently beneficiated, mostly, by means of dense medium cyclones. This unit utilizes fine particulates (such as magnetite) suspended in water as dense medium and make use of the gravity difference and a centrifugal force to separate the heavy mineral rich coal from the light and desired product (Wills & Napier-Munn, 2008).

The methods that are currently used to prepare coal in South Africa will need to adapt to the current resource, market and environmental trends. It is vital to ensure maximum throughput at reduced operation costs and in the face of declining ore grades and environmental concerns. The above mentioned drawbacks have led to various branches of research investigations in order to maintain and improve upon the current standard. The development of dry coal beneficiation technology is considered extremely important most specifically to countries with abundant coal resources facing extended periods of drought. As stipulated in Chapter 1, establishing a means of coal processing without the requirement of water would prove most useful and may further lead to reduced capital and operating costs, decreased difficulty in coal handling and storage and the elimination of water pollution related to coal processing (Sahu *et al.*, 2009).

2.3.3 Dry preparation technologies

A number of dry coal preparation technologies have been introduced into the coal washing market since the early 1900's and these include; hand picking, frictional separation, gravity separators, electrostatic separators, microwave separation, air jigging, specialized air jigging (FGX) and gas-solid fluidized beds (Chen & Wei, 2003; Dwari & Rao, 2007, Zhao *et al*., 2015). These processes each manipulate specific differences between coal and gangue properties to induce a separation of desired material from undesired material. Some of the afore-mentioned properties can be listed as, density, size, shape, lustrousness, magnetic conductivity, electric conductivity, radioactivity and frictional coefficient, to name a few (Chen & Wei, 2003).

Dry coal processing rose quickly in popularity among various countries most especially USA and China (Honaker *et al*., 2008; Chen & Wei, 2003). This was mostly as result of the favoured reduction in capital and operational cost, no additional water treatment requirements and the deliverance of an upgraded coal product with low moisture contents. A decline in this prevalence was however experienced from 1990 due to the increased ROM moisture levels and more stringent dust suppression requirements. Moreover, the climbing demand for superior coal qualities at the best separation efficiencies became of utmost importance (Honaker *et al*., 2008).

Extensive research into dry coal processing did however, not seize entirely as the benefits of such technologies were still seen attractive in both arid and freezing regions of the globe. As a result, investigations into pneumatic beneficiation methods such as air jigging and ADMFB were undertaken (Chen & Wei, 2003). Some difficulties are in acquaintance with pneumatic processes and these include strict restrictions on feed particle size; lower separation efficiencies; high airflow specifications and dust pollution (Chen & Yang, 2003). Of the pneumatic methods the ADMFB proves to be the most promising in delivering a more favourable product with the least amount of pitfalls (as listed above).

Table 2.3 provides the Ecart Probable Moyen (E_p) values for selected coal beneficiation processes. This parameter is generally used to provide an idea of the degree of efficiency of separation. A predominantly lower E_p value is indicative of a better separation with a value of zero portraying ideal separation.

Table 2.3: Comparison between beneficiation processes (taken from Chikerema & Moys (2012))

Method	Ecart Probable Moyen (E_p) range
Air jigging	0.200 - 0.300
FGX	0.150 - 0.300
ADMFB	0.040 - 0.150
Wet DMS	0.015 - 0.120

Table 2.3 shows that the ADMFB technology compares well with that of wet dense medium separation methods (Chikerema & Moys, 2012). Henceforth, the current investigation focusses primarily on the desired beneficiation of coal using the ADMFB process.

In summary and as mentioned previously, an ADMFB operates similarly to most DMS processes where particles are separated based on the float and sink principle as a result of the difference in size, shape and density. In the sections that follow, the topics of fluidization and everything relating thereto are discussed.

2.4 Fluidization

Fluidization is described as the process by which particulates packed in a bed are transformed into a fluid like state by suspending them in an upward flowing fluid, either liquid or gas. A method of contacting, such as fluidization, generates a few unusual characteristics which can be utilized to the desired advantage (Kunii & Lievenspiel, 2001). DMS processes specifically relating to fluidized dense medium beds are an example of the fluidization principle and this phenomenon is therefore detailed in the sections that follow.

2.4.1 Fluidization principle

The fluidization phenomenon is based on the principle of buoyancy as stipulated by Archimedes.

> *An object, whether fully or partially submerged in a fluid, is subjected to an upward buoyancy force equivalent to the weight of the fluid displaced by the object.*

More specifically, the object would be caused to rise and continue rising, float or sink depending on the magnitude of the upward force provided by the fluid and the weight of the object (Luo & Chen, 2011).

Fluidization is characterized into three distinct states depending on the particulate behaviour within the system. In the first state, named fixed state, the particles remain packed together with nearly no movement. The upward fluid simply percolates through the void spaces between the stationary particles. A slight increase in the velocity of the fluid causes the bed to expand and allows the particles to move apart with some vibrating into restricted regions. At a specific flow of the fluid, each particle becomes suspended. This state is termed incipient or minimum fluidization and the particles in the system are free to move and rearrange. A further bed expansion is experienced due to the formation of bubbles. The last state is where particles are subjected to a very high medium flow and the system enters a turbulent region with vigorous particulate and fluid movement (Kunii & Lievenspiel, 2001).

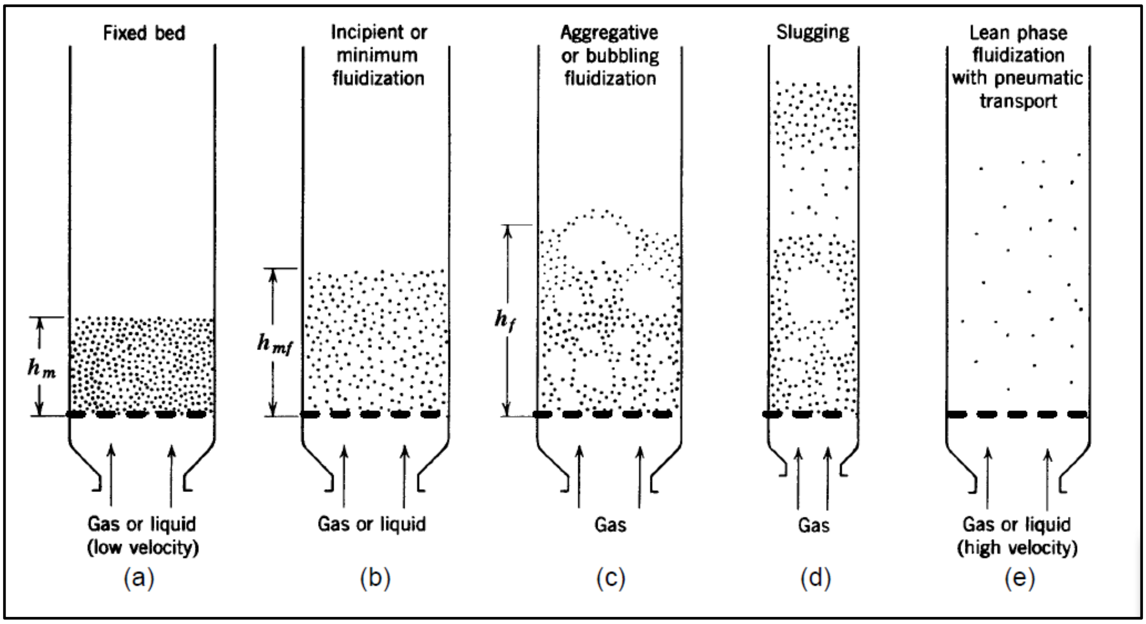

Figure 2.5: Stages of contacting during fluidization (adapted from Kunii & Lievenspiel, 2001)

At fluid velocities higher than the incipient fluidizing point a difference in particulate behaviour is observed for liquid-solid and gas-solid systems. In the former, a smooth and progressive expansion of the bed is obtained and gross flow instabilities are damped and remain relatively small. In the gas-solid system, for example an ADMFB, such a bed is only observed under special conditions usually attributed to fine and light particles fluidized by a dense gas (Kunii & Lievenspiel, 2001). These systems usually experience large instabilities with bubbling and channelling of the gas once operating above minimum fluidization. As the flow rate of the gas continues to increase the particles become more violently agitated and particulate movement tends to be much more vigorous. In this state, the bed expands no further than that observed at incipient fluidization. *Figure 2.5* provides a depiction of the various states of fluidization as discussed. When fluidized at a sufficiently high fluid flow rate, the terminal velocity of the particles is exceeded and the upper surface of the bed disappears. One then observes entrainment, and bubble formation is not appreciated as extreme turbulent motion of solid clusters and voids of gas occurs in various shapes and sizes. Further increasing the gas flow would yield a bed where the solids are removed from the bed with the fluid (Kunii & Lievenspiel, 2001).

Gas-solid fluidization systems may encounter some further issues relating to bubble formation and entrainment of particles. Coalescence of gas bubbles may occur, causing the bubbles to grow while rising along the bed. In a bed of enough depth and small diameter these coalesced bubbles may grow large enough to spread across the vessel. This causes the particles to behave differently than expected. Fine particles would flow smoothly down along the wall around the rising void of gas causing axial slugging. In a coarser particulate bed, the portion above the gas void is forced upward and particles fall from the void which eventually ruptures and disintegrates. This continues and forms an unstable oscillatory motion which is undesired for effective fluidization (Kunii & Lievenspiel, 2001).

One of the unusual properties of a gas-solid fluidized bed is its pseudo-fluid state which is made useful in the ADMFB process. Visually, this system compares to that of boiling water and exhibits a fluid-like behaviour (Kunii & Lievenspiel, 2001). This is best explained pictorially by *Figure 2.6*.

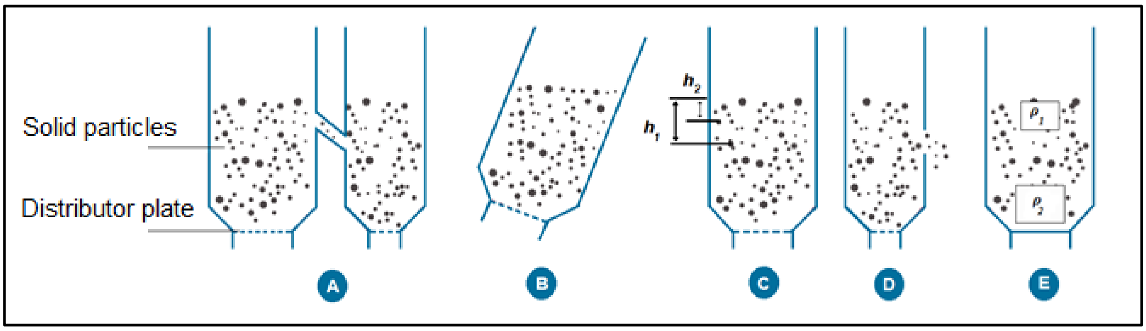

Figure 2.6: Pseudo fluid bed properties (adapted from Luo & Chen (2001); Mohanta *et al*. (2011))

Not displayed in the image (*Figure 2.6*), but still a property of the fluidized bed is that upon the addition of a large and light object to a stable fluidized bed, it will float on the surface of the bed. The first (A) and second (B) images indicate that the levels of two connected fluidized beds would equalize and if tipped the upper level of the bed remains horizontal. Sketch C shows that the difference in pressure between two points in the bed is relatively equal to the static head between these points and the fact that solids would jet from a hole in the side of the container is depicted in D. Furthermore, a density segregation is experienced in which the more dense material sinks to the floor of the bed and the less dense material floats to the surface (Mohanta *et al.*, 2011). These are all common properties of liquids that exhibit themselves in a gas-solid fluidized bed.

A well-developed fluidized bed, void of turbulence and large bubble formation, is observed at a certain fluid velocity usually related to the minimum fluidizing velocity or a point slightly above. At the incipient fluidization point, particles begin to move due to the various forces acting upon them of which gravitation and buoyancy are the most observed (Rhodes, 2008). Some particles, most likely those which are dense, would sink due to gravity and others that are lighter would float due to buoyancy (Choung, *et al.*, 2006; Luo & Chen, 2001). The fluid-like properties of the suspension within the system are the reason a separation in density is experienced (Sahu *et al.*, 2009). A particulate bed in this state is known to behave similarly to that of a Bingham fluid with rheological characteristics generally explained by the falling sphere principle (Wei & Chen, 2001). The forces, as portrayed in *Figure 2.7*, that influence particles in a fluidized bed are namely, force of gravitation (G in Newton), buoyant force (F_b in Newton), drag force as a result of friction (F_{gd} in Newton), drag force of the fluid put forth on the particle (F_{sd} in Newton) (Sahu *et al.*, 2009).

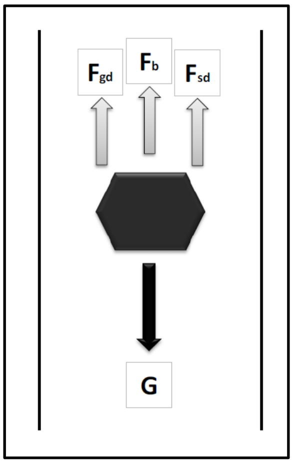

Figure 2.7: The forces that act on a particle during fluidization (adapted from Sahu *et al.*, 2009)

The frictional drag force of the fluid onto the particle can be considered negligible since the diameter of such a particle is much larger than that of the dense medium. As a result, only three main forces act upon a particle suspended in a fluid.

It is assumed that in practice a perfect separation can be achieved through ideal particle distribution, however, in reality, both light and dense particles can be misplaced. In more general terms, a heavy particle that should sink, rather floats and alternatively a light particle that should float would sink. This occurrence is referred to as the displaced distribution effect (Chen & Wei, 2005; Sahu *et al*., 2009). Many factors can attribute to this phenomenon with movement and viscosity effects being predominant. The displaced movement effect is significant when the gas flow is either too high or too low (Chen & Wei, 2005). As a result the feed air velocity significantly affects the separation efficiency of the system. Particle size, moreover, bears great effect on the displacement theory. It is found that larger less dense particles can sink whilst smaller, denser particles could float.

Naturally, the gas velocity is a crucial parameter in ensuring stable fluidization and also effective separation within the bed. The velocity of the fluid must be controlled and remain between minimum fluidization point and bubbling velocity. The minimum fluidization velocity is discussed in detail in *Section 2.4.2* to ensure a full comprehension of fluidization.

2.4.2 Minimum fluidizing velocity

The minimum fluidization point is deemed the velocity at which the particles transform from the packed bed state to a state of fluidization. The particles tend to behave as a fluid and are free to rearrange and move in the bed according to its density relative to that of the entire fluidized system (He *et al*., 2016a; Zhao *et al.*, 2015). The incipient fluidization point is therefore vital in the stability of the fluidized bed and consequently the separation efficiency of the process.

The velocity required for fluidization is proportional to the drag force able to cause the suspension of the solid particles within the bed (Escudero & Heindel, 2011). An equation derived by Kunii & Levenspiel (1991) is commonly used to predict the incipient fluidization point in a system. Some parameters affecting the minimum fluidization velocity are considered important when designing a proper fluidized bed and listed as follows (Escudero & Heindel, 2011):

- Particle properties
- Fluid properties
- Bed geometry

According to Kunii and Levenspiel (1991), minimum fluidization occurs at the point when the drag force created by the upward flowing fluid is equal to the weight of the particles.

$$(drag\ force\ created\ by\ uwards\ flowing\ fluid) = (weight\ of\ the\ particles) \quad \ldots [2.1]$$

$$\Delta p_b A_t = W = A_t L_{mf}(1-\varepsilon_{mf})\left[(\rho_s-\rho_g)_{ggc}\right] \quad \ldots [2.2]$$

Where the symbols used are described as follows:

Symbol	Description	Unit
Δp_b	Pressure difference	Pa
A_t	Cross-sectional bed area	m^2
W	Bed weight	N
H_{mf}	Bed height	m
ε_{mf}	Bed voidage	-
$\rho_{s/}\ \rho_g$	Particle/fluid density	kg/m^3
ρ_g	Gravitational acceleration constant	m/s^2

By rearranging *Equation 2.2*, the condition for minimum fluidisation can be described by:

$$\frac{\Delta p_b}{L_{mf}} = (1-\varepsilon_{mf})(\rho_s-\rho_g)\frac{g}{g_c} \quad \ldots [2.3]$$

The superficial velocity at minimum fluidising conditions, u_{mf}, is given by

$$\frac{1.75}{\varepsilon_{mf}^3\varphi_s}\left(\frac{d_p u_{mf} p_g}{\mu}\right)^2 + \frac{150(1-\varepsilon_{mf})}{\varepsilon_{mf}^3\varphi_s^2}\left(\frac{d_p u_{mf} p_g}{\mu}\right) = \frac{d_p^3\rho_g(\rho_s-\rho_g)g}{\mu^2} \quad \ldots [2.4]$$

Where the symbols used are described as follows:

Symbol	Description	Unit
u_{mf}	Minimum fluidization velocity	m/s
d_p	Particle diameter	m
φ_s	Particle sphericity	-
μ	Fluid viscosity	Pa.s

By rearranging *Equation 2.4*, *Equation 2.5* is attained as

$$\frac{1.75}{\varepsilon_{mf}^3 \varphi_s} Re_{p\,mf}^2 + \frac{150(1-\varepsilon_{mf})}{\varepsilon_{mf}^3 \varphi_s^2} Re_p = Ar \qquad \ldots [2.5]$$

With *Re* being the Reynolds number (*Equation 2.6*) and *Ar* being the Archimedes number (*Equation 2.7*):

$$Re = \left(\frac{d_p u_{mf} p_g}{\mu}\right) \qquad \ldots [2.6]$$

$$Ar = \frac{d_p^3 \rho_g (\rho_s - \rho_g) g}{\mu^2} \qquad \ldots [2.7]$$

Equation 2.5 can therefore be simplified to give the minimum fluidisation velocity of small particles as (Kunii & Levenspiel, 1991):

$$u_{mf} = \frac{d_p^2(\rho_s - \rho_g) g}{150\mu} \frac{\varepsilon_{mf}^3 \varphi_s^2}{1-\varepsilon_{mf}} \qquad Re_{p_{mf}} < 20 \qquad \ldots [2.8]$$

The last equation (*Equation 2.8*) is defined as the Ergun equation and it specifies that an increased particle size (d_p) will result in the requirement of a quadratic increase in minimum fluidization velocity. Also observed from the equation is that the bed voidage (ε_{mf}) is proportional to the incipient velocity and similarly the minimum fluidization point will increase with increase particle density.

The position of a particle in the bed is dictated by the relative velocity between the particle and medium. This contributes to the separation efficiency as it is dependent on the bed viscosity and velocity of the medium as discussed with the misplacement effects. The importance of accurate determination of the minimum fluidization velocity is therefore emphasized. Incorrect fluidization conditions will contribute to the displacing effect and also lead to ineffective separation. The following section therefore deals with the correct determining of the minimum and operating fluidization velocity.

2.4.3 Pressure and velocity relations

The extent of fluidization can, in most cases, be easily observed, but there are times when this is not possible. Experimentally, an estimation of the minimum fluidization point can be made by constructing a pressure drop versus superficial gas velocity curve as demonstrated in *Figure 2.8* and obtained from the *Equation 2.9* with the use of uniformly sized particles.

$$\frac{\Delta p_{fr}}{L_m} g_c = 150 \frac{(1-\varepsilon_m)^2}{\varepsilon_m^3} \frac{\mu u_o}{(\varphi_s d_p)^2} + 1.75 \frac{1-\varepsilon_m}{\varepsilon_m^3} \frac{\rho_g u_o^2}{\varphi_s d_p} \quad \ldots [2.9]$$

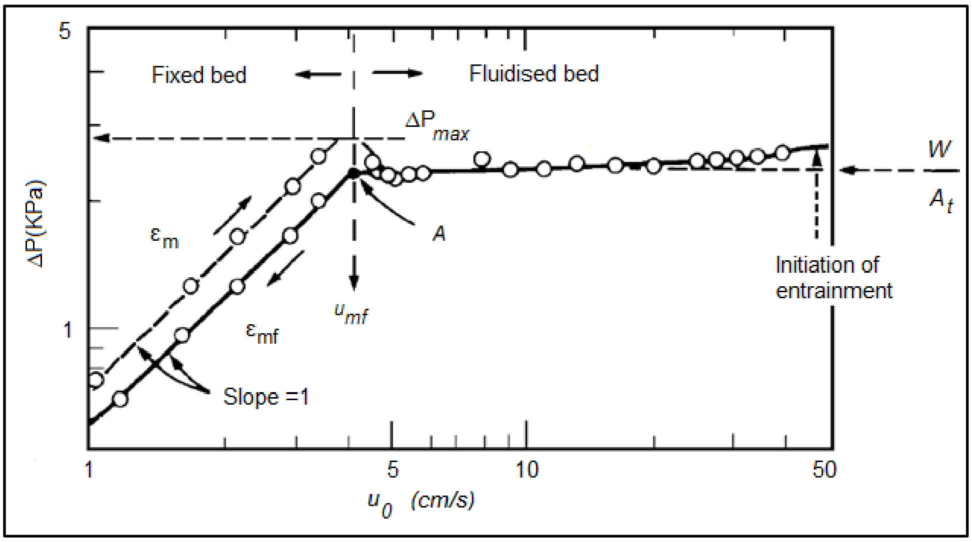

Figure 2.8: Pressure vs. velocity diagram of uniform sand particles (taken from Kunii & Levenspiel, 1991)

When considering *Figure 2.8*, the pressure drop across the bed is measured at increasing gas superficial velocities and recorded. A point of maximum pressure (*ΔP_{max}*) is observed in which the pressure in the bed is slightly above the static pressure of the bed. The bed remains in a fixed or packed state until this point is reached and is depicted by the straight line with a slope of 1. A slight decrease in pressure is observed after the maximum pressure point which is an indication that initial fluidization has occurred in the bed. Upon slightly increasing the velocity, formation of small bubbles occurs and the bed expands slightly transforming into the fluidized state (Kunii & Levenspiel, 1991). From this the minimum fluidizing point can be established during operation of the bed.

The fluidization velocity is generally chosen to be slightly higher than the incipient fluidization point to ensure complete fluidization. It is however essential to closely observe the bubble formation in the bed as it bears great influence on the gas velocity within the bed (Luo *et al.*, 2012). The extent to which the velocity should be increased higher than minimum fluidization point for a specific size range of coal is elaborated on by He *et al*. (2016a). Laboratory scale experiments were performed by He *et al*. (2016a) on a dense medium fluidised bed with Chinese coal sized at +3-25mm and magnetite sized +0.074-0.3mm as dense medium. The coal and magnetite were fluidized at different superficial velocities ranging from a factor of 1.2 to 2.0 times the minimum fluidization point. From this it was found that slight segregation occurred at a factor of $1.3U_{mf}$ due to the formation of more small bubbles and the further expansion of the bed. Further increases in gas velocities (from $1.3U_{mf}$ to $1.8U_{mf}$) provides efficient separation as enough small bubbles were produced. The best separation was found at a velocity that is 1.6 times the minimum fluidization velocity. Increase in air flow above $1.8U_{mf}$ caused severe back mixing and resulted in many displaced particles and consequently worsened the separation efficiency as the stability of the bed was decreased due to the formation of large bubbles (He *et al.*, 2016a).

Zhao *et al.* (2016) conducted similar experiments on coal sized +1-3mm with magnetite sized 232µm in a 4:1 coal to magnetite volume ratio. The results obtained were however different from those obtained by He *et al.*, (2016a). He *et al.* (2016a) stated that $U = 1.6U_{mf}$ is the optimum while a bed operating above 1.8Umf would experience severe back mixing. From the work conducted by Zhao *et al*. (2016) the back mixing was only observed at $U > 2.4U_{mf}$. This might be attributed to the different coal and magnetite particle size ranges used by the two studies. There is thus no exact recommendation for the extent to which the velocity should exceed minimum fluidization velocity as it is relative to size range and would therefore differ from case to case.

2.4.4 Bubble formation and behaviour

It is crucial to incorporate both the gas velocity and minimum fluidization velocity, as seen for the studies conducted by He *et al*. (2016a) and Zhao *et al*. (2016). These are the factors that mostly dictate the formation of bubbles in the bed which is essential for the effective separation in a gas-solid dense medium fluidized bed.

Bubbles may have advantages and disadvantages on the effective and stable fluidization of a particulate bed. These are as follows (Luo *et al.*, 2012; Sobrino, 2009):

- One important result of bubble formation is remixing. Initially, mixing of the material in the bed is required as it enhances the uniformity of the density throughout the bed. This is generally caused by small bubbles. However remixing of particles caused by large bubbles can hinder the effective stratification of particles due to the entrainment and displacement of particles
- Small bubbles moving along the bed initiate a loosening effect on the particles and thereby allows for better separation. Once again larger bubbles can negatively affect the bed by causing variations in the bed height.

Smaller bubbles provide favourable effects on the fluidization process and promote a well-developed fluidized bed, whilst larger bubbles reduce the stability of the bed and thereby supress segregation (Luo *et al.*, 2012).

2.4.5 Classification of particles

Another vital consideration in fluidization is, as discussed above, the minimum fluidizing velocity which is a function of particle properties, particle and bed geometry and also fluid properties (Escudero & Heindel, 2011). The behaviour of the particles in a fluidized bed differ for varying particles, however, four main classes have been labelled by Geldart (Kunii & Lievenspiel, 2001).

- **Group A**
  These particles fluidize easily with relatively controllable bubble formation at low gas velocities. The particles within this class are generally characterized by low particle densities (<1.4 SG) and small mean particle sizes.
- **Group B**

Vigorous bubbling is experienced in a fluidized bed containing this class of particle due to the small size range (40-500 micron) and large density range (1.4 - 4.0 SG).

- **Group C**
  The particles forming this group, are very fine and fluidization is therefore nearly impossible. This is due to the interaction forces between the particles being much larger than the particle-gas forces.
- **Group D**
  The particles in this class are very large and/or dense particles which negatively affects fluidization due to the formation and eruption of large bubbles. Serious gas channelling and back-mixing is also more common with these particles (Yang *et al.*, 2015).

The coal particles considered for this investigation can be classed into the Geldart A or Geldart D types and is consequently expected to fluidize quite easily without dense medium. The dense medium powders are classified as Geldard group B and their ultra-fine nature can cause vigorous bubbling which should be carefully observed.

2.5 Dry beneficiation of coal using ADMFB technology

The first traceable account of the beneficiation of coal in an ADMFB occurred in 1926 when Yancey and Frazer published a paper and issued a patent for the process. Their research was developed on beneficiating coal with a particle size ranging from 10 to 50 mm using sand with a bulk density of 1.45 SG as a dense medium (Houwelingen & de Jonge, 2004; Mohanta *et al*., 2013). The verification of the process was however never determined on pilot or industrial scale and consequently the separability remain unclear.

Dry dense medium separation using fluidized beds have since then been globally explored for many related applications in coal and other industries such as iron ore, for example (Zhao *et al.*, 2011; Oshatani *et al.,* 2011). Separation of large coal particles +6-50mm by ADMFB technology has been tested by a number of research institutions with successful results and E_p values at 0.05 (Firdaus *et al.*, 2012; Luo *et al*., 2003; Wei *et al*., 2003; Luo & Chen, 2001).

The first pilot scale ADMFB plant was constructed by the Chinese University of Mining and Technology (CUMT) and reported to annually process approximately 320 000 tonnes of +6-

50 mm coal yielding an E_p of 0.05. Since then, larger commercial plants have been constructed with outputs of 700 000 tonnes per annum (Chen & Wei, 2005). An image of the dry dense medium (DDM) plant in operation located in Shenhua, China is provided in *Figure 2.9*.

Figure 2.9: Dry dense medium plant in Shenhua, China (taken from de Korte (2016))

Some additional studies conducted by CUMT with regards to dry coal beneficiation yielded the following conclusions:

- **Air dense medium fluidized beds with added vibration**
  Chen & Wei (2005) reduced the ash yield from 16.57%$_{wt}$ to 8.35%$_{wt}$ (by 8.22 percentage points) and obtained a yield of 80.2% for the beneficiation of fine coal (-0.5+6.0mm) in an ADMFB accompanied by vibration. Furthermore, the E_p value associated to the experimental work was found to be 0.065.
- **Air dense medium fluidized beds that are deep**
  By investigating deeper beds, Chen and Wei (2005) determined that an E_p value of 0.02 is possible when beneficiating coal smaller than 50mm. This was especially useful to the large surface mines in China that require waste removal from feedstocks.
- **Triboelectric cleaning technology**

When considering ultra-fine coal having an averaged particle size of 43μm, the triboelectric cleaning technology yielded extremely low ash yields in the product, even well below 2$\%_{wt}$. This is however due to the coal being completely liberated beforehand (Chen & Wei, 2005).

- **Dual-density air dense medium fluidized beds**

  A three stream coal product is obtainable from this technology namely; clean, middling and discard. Chen and Wei (2005) determined the densities for the upper and lower layers as 1.52 and 1.87g/cm^3, and E_p values of 0.07 and 0.1, respectively.

Some further investigations regarding the effects of dense medium; vibration; bed geometry and particulate size and shape are detailed in the sections that follow. The aim is to provide an expectation of the behaviour of the fluidization and separation in the experiments for the investigation at hand.

2.5.1 Dense medium

The dense medium utilized in DMS processes is generally a suspension of a relatively dense mineral in a fluid such as water (for wet methods) or air (for dry technologies). A specific and uniform density over the depth of the bed is thereby obtained. Due to the large difference in density of the desired coal product and undesired gangue and also the specific gravity of the medium, gravity separation occurs as discussed previously. Furthermore, the addition of a medium can aid in preventing the back mixing of particles in the bed (Prusti *et al.*, 2015) and also inhibit vigorous bubbling inside the bed (Fan *et al.*, 2001)

Magnetic materials (such as magnetite) are the preferred medium used during DMS operations due to the fact that recovery and cleaning is made easier by magnetic separation processes (Maoming *et al.*, 2003). A number of successful studies have been conducted with other dense medium types such as silica, zircon and fine coal either purely or as mixtures (Lagner *et al.*, 2016; Firdaus *et al.*, 2012). Magnetite was selected as the medium for the purposes of this study and therefore only reference to it shall be made when discussing dense medium henceforth.

The particle size of the added medium should be considered important. Magnetite that is too small will fluidize poorly because the inter-particulate cohesive forces are extremely strong between the ultra-fine particles and therefore plug flow and dead zones can be caused in the bed (Luo *et al.,* 2002; Zhao *et al.,* 2010b). This further leads to aggressive bubbling and the blowing of the fine material directly out of the bed (De Korte, 2016; He *et al.*, 2016a). Conversely, a medium that is too coarse would not fluidize easily. This would lead to the necessity of larger gas velocities and increasing energy requirements. Moreover, the bed voidage would most likely be larger causing an increase in larger bubbles (He *et al.*, 2016b). An additional size consideration is that the coal and magnetite particle sizes should not be too closely related once again due to the inter-particulate surface forces providing a hindrance for fluidization.

Some work was conducted by He *et al*. (2016a) to elaborate on the issue of magnetite size. The study entailed the investigation into minimum fluidization requirements, pressure drop and stability of three different magnetite sizes categorized as Geldart B powders; +0.15-0.3mm, +0.074-0.15mm and -0.074mm. *Figure 2.10* depicts the static pressure drop across the bed versus superficial velocity for the three magnetite sizes used in the above study.

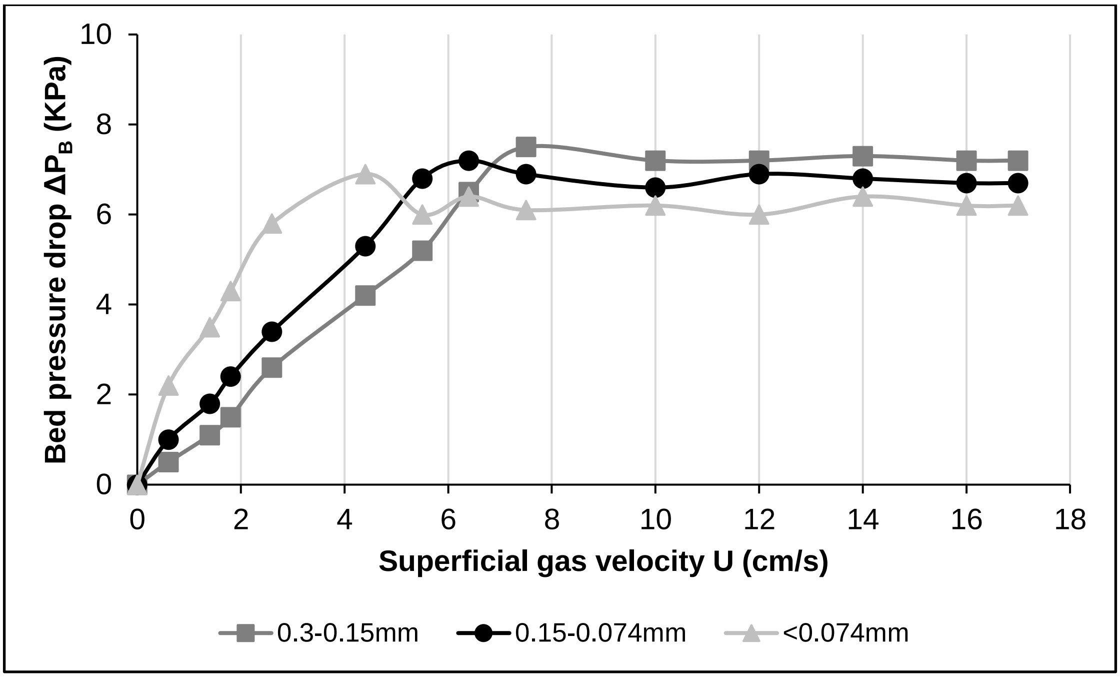

Figure 2.10: Pressure drop across a fluidised bed as a function of superficial velocity (adapted from He *et al.* (2016a))

Figure 2.10 clearly shows that the finest medium had the lowest minimum fluidizing point and so increasing in ascending order of the particle size. The overall pressure drop remained constant once minimum fluidization was reached but the stability of the bed pressure drop improved as the magnetite size was increased. A bed with lower bulk density, larger porosity and increased expansion was created with the finer magnetite resulting in an unstable bed (He *et al.*, 2016a). Additionally, the finer powder was more sensitive to step changes in the feed gas velocity. The -0.074mm magnetite yielded an unstable bed and is therefore inadequate for use as a fluidizing medium. Alternatively, the larger of the three sizes +0.074-0.3mm produced a fluidized bed with better stability. Furthermore, it was determined that a mixture of the two larger size ranges could still result in a bed that is reasonably stable.

Magnetite is available in South Africa as a by-product from the tailings of copper production, but is much too fine in comparison to that used in the pilot plants in operation in China (De Korte, 2016). *Figure 2.11* portrays a size analysis for magnetite from various sources in South Africa as compared to that of China.

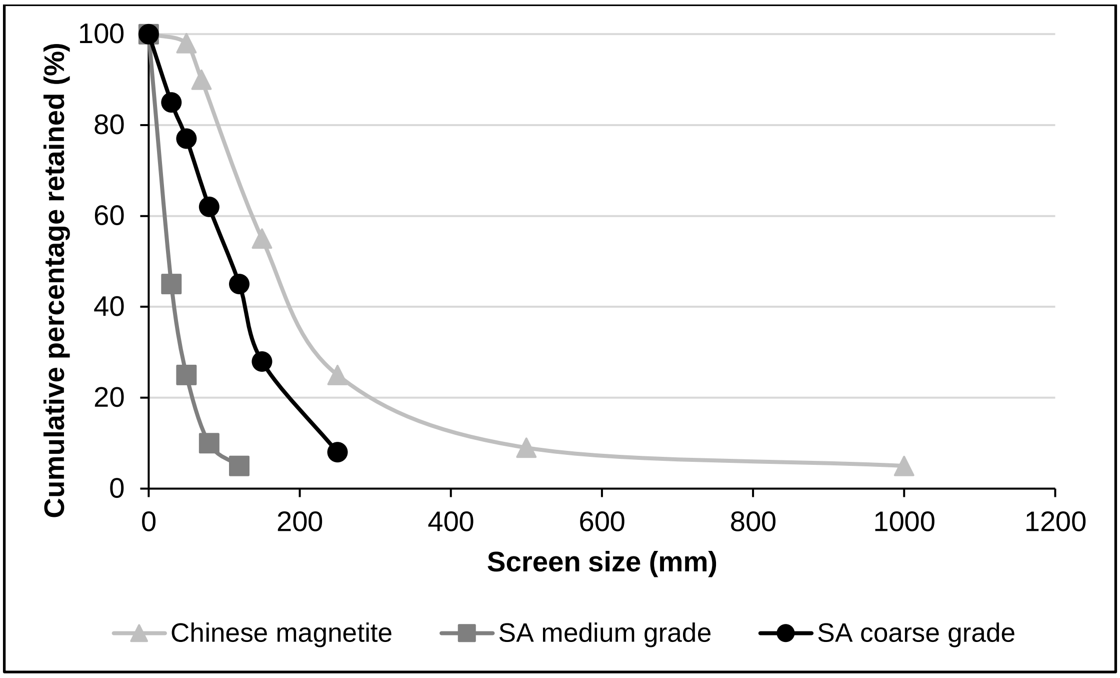

Figure 2.11: Comparison between magnetite sizes from three sources (adapted from de Korte (2016))

The plot portrays the cumulative mass percentage retained versus screen size for magnetite obtained from China and the South African medium and coarse grades. From *Figure 2.11*, it can be seen that the magnetite that is available in South Africa is very fine when compared to that used in China. The scarcity of a preferred coarser magnetite in South Africa is a major issue related to the implementation of ADMFB technology and requires immediate attention (De Korte, 2016). There are some difficulties associated with the removal of the medium from the coal after separation and as a result dense medium consumption can be relatively high (Sahu *et al.*, 2009). Furthermore, additional capital and operational costs are required as a result of recycling the magnetite and product deterioration is also experienced (Yang *et al.*, 2013). Some attrition of the particles may cause fine coal to accumulate in the medium which results in a medium of inconsistent density. This accumulated coal will need to be removed. Mixing the finer magnetite with a slightly coarser coal (autogenous medium) could provide a solution for the constraint on the availability of coarse magnetite and some promising results were obtained for this through He *et al.* (2016c); Luo and Chen (2001) and Yang *et al*. (2013b). The use of an autogenous medium further provides a solution to the recovery and cleaning problems related to the use of other media.

2.5.2 Vibrated air dense medium fluidized beds

The separation of coal particles occurs mainly due to the presence of bubbles in the bed. The rise of a bubble through the bed causes a region to be momentarily disturbed thereby inducing a lower solid volume than the surrounding area. A particle within this region will therefore be able to move freely, in that a denser particle will sink and less dense one would float. The addition of vibration produces a loosening effect and thereby enhances the formation of bubbles in the bed and improves the segregation (Yang *et al.*, 2013a). Additionally a well dispersed fluidized bed is obtained from a vibrating dense medium bed as the gas-solid interactions are increased (He *et al*., 2015). The channelling of the air feed is also reduced upon the addition of vibration most especially with the smaller size fractions (Moaming *et al.*, 2003). Macpherson and Galvin (2010) further discovered that vibration can aid in lowering the minimum fluidizing point; aid in the stability of the bed and reduce any additional forces acting on a particle. The pressure drop of a vibratory dense medium fluidized bed was also determined to be lower than that of a bed with no vibration (He *et al.*, 2015). The results of the above mentioned study are depicted in *Figure 2.12*.

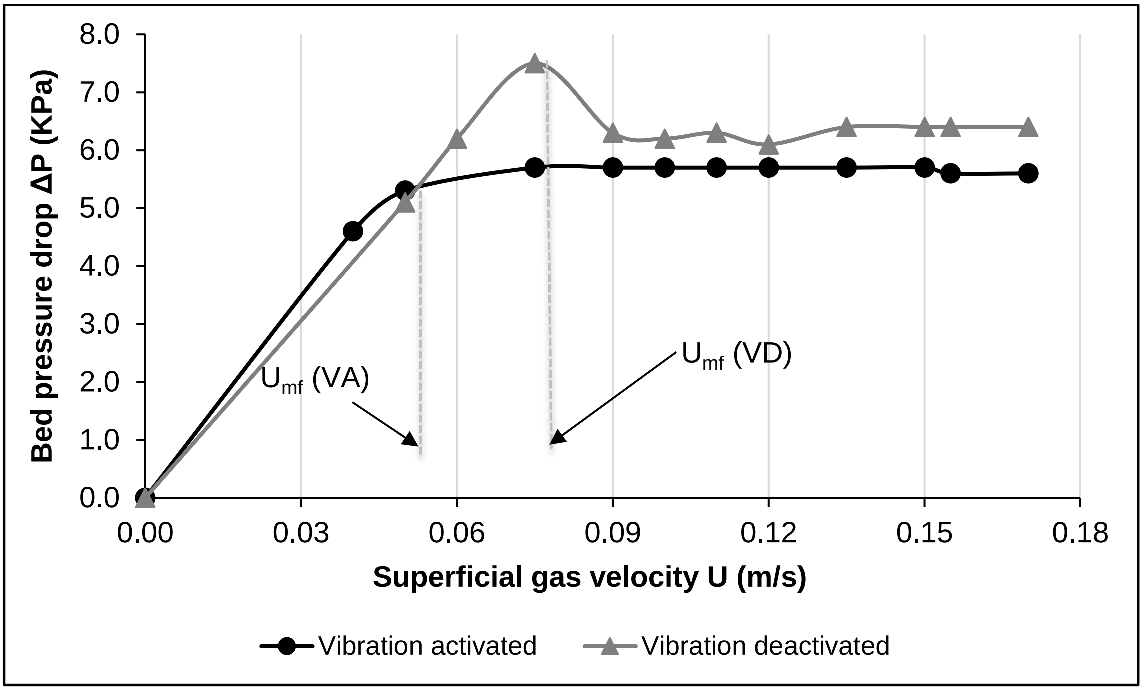

Figure 2.12: Pressure drop fluctuation of the bed with and without vibration (adapted from He *et al*., 2015)

In the figure, the bed pressure drop versus superficial gas velocity relations are depicted for a bed with and without vibration. The minimum fluidization points for each bed are indicated with U_{mf} (VA) and U_{mf} (VD) showing that of the bed with vibration activated and deactivated, respectively. Clearly the addition of vibration ensures a lower and more stable bed pressure drop also reaching incipient velocity at lower superficial gas flows. This provides evidence that the addition of vibration energy could form a well-developed fluidized bed at lower superficial velocity and in a shorter period of time.

Various studies have been conducted on the effects and conditions of adding vibration to an air dense medium fluidized bed. Yang *et al*. (2013a) conducted studies on coal of +1-3mm and +3-6mm in order to determine if a vibrating fluidized bed would be successful. A reduction of the ash content ranging in 15%$_{wt}$ was obtainable for both sizes from a feed averaging in 40%$_{wt}$ ash with a gangue containing an ash value as high as 70%$_{wt}$ (Yang *et al.*, 2013a). Studies conducted by He *et al.*, (2015) on fine coal yielded prominent results in reducing coal with approximately 28%$_{wt}$ ash content to a product with ash content of more or less 10%$_{wt}$ with very high yields and E_p values ranging from 0.065 and 0.055 depending on particle size. A dense medium vibratory fluidized bed was proven to be able to produce a coal product with ash value below 10%$_{wt}$ and E_p of 0.07 in a study conducted by Luo *et al.*, (2008). Dwari and Rao (2007) found similar results for ultra-fine coal (125µm) in a laboratory set-up able to produce a yield reaching 80.2% and ash reduction of 8.22 % points.

The frequency and amplitude of the vibration are variables to consider during operation of a vibrated ADMFB. If too small, the frequency and amplitude create a vibration that is too weak to prevent the formation of de-fluidized zones and big bubbles. Conversely, if too large, particle circulation and back-mixing tend to occur in the lower parts of the bed (Yang *et al.*, 2013b). A study conducted by He *et al.* (2015) on the required amplitude and frequency during vibration yielded that, between the two, the amplitude of vibration has the largest effect on the fluidization of- and segregation in the bed. These factors should therefore be adjusted in a suitable range so as to maintain a preferred bed stability and uniform bed density in a vibratory dense medium fluidized bed. A value of 1 mm amplitude and frequency of 15Hz was determined most effective by He *et al*. (2015) for +1-6mm coal particles and magnetite of +0.074-0.3mm as dense medium. Yang *et al.* (2013b) on the other hand found that frequencies between 18-33Hz and an amplitude ranging from 2.6-3.8mm is optimal. The differences in findings prove that the perfect vibratory conditions are bed and coal dependant.

2.5.3 Effects of moisture

Inefficient separation is expected when both coal dense medium particles contain moisture levels that are deemed high. This is as a result of the particles agglomerating and sticking to the walls of the bed, thereby preventing good fluidization due to poor interaction between the solid and gas phases. Investigation conducted by Terblanche (2011) proved that particles with initial moisture contents larger than 7%$_{wt}$ will not fluidize well. He *et al.* (2015) proposed that the feed coal surface moisture for particles ranging from 1-6mm should generally be less than 2.5%$_{wt}$. Drying of the feed coal processed in an ADMFB is therefore a necessity as most South African coals contain an average surface moisture ranging between 5 and 6 %$_{wt}$ (De Korte, 2016). The moisture content of the feed air to the ADMFB is also of utmost importance and should be extremely low. The moisture in the air could condense in the bed and cause a hindrance in fluidization and problems with medium recovery (De Korte, 2016).

2.5.4 Particle size, shape and density

Individual particle size, shape and density bears great influence on the positioning of the particles in the bed. A linear relationship is observed for the positioning of coal particles that are less dense than the bed. These particles will float at different heights depending on the difference in their relative density when compared to that of the bed. The position of coal particles with densities approaching that of the bed decreases rapidly (Prusti *et al.*, 2015).

It was further discovered that for a specific particle shape, coal with a small projected area and increasing density will move gradually down the length of the bed whereas larger coal particles would rapidly fall to the bottom of the bed when increasing in density. This behaviour can be attributed to dissimilar dead zones formed due to larger size and shape that may lead to a change in the effective density of the particle and therefore it's positioning in the bed (Prusti *et al.*, 2015). Yang *et al*. (2013) determined that the performance of an ADMFB decreases with decreasing particle size and is due to the reduction in settling velocity and increase in the remixing effect caused by bubbles. Increasing particle size in relation to the bed diameter also affects the effectivity of fluidization. As the ratio of the diameter of the particle to the diameter of the bed increases, the minimum fluidization point increases as well causing a more significant wall effect (Rao *et al.*, 2010).

Prusti *et al.* (2015) observed that particle shape influences the behaviour and movement of an individual coal particle. Particles in the shape of triangular prisms generally attain higher positions in the bed irrespective of size or density with the positioning of the cubic, rectangular prism and spherical shapes following in descending order. This is as a result of the lower dead zone area formed upon the triangular particles in comparison to the other shapes with spherical having the largest. A larger dead zone increases the effective density of a particle due to the deposition of medium and accumulated fines in the dead zone. This causes the particle to attain a heavier apparent weight and leads to a deeper position in the bed than expected (Prusti *et al*., 2015). *Figure 2.13* provides the expected positioning of a particle versus the coal density for different sizes and shapes of particles as determined by Prusti *et al.* (2015).

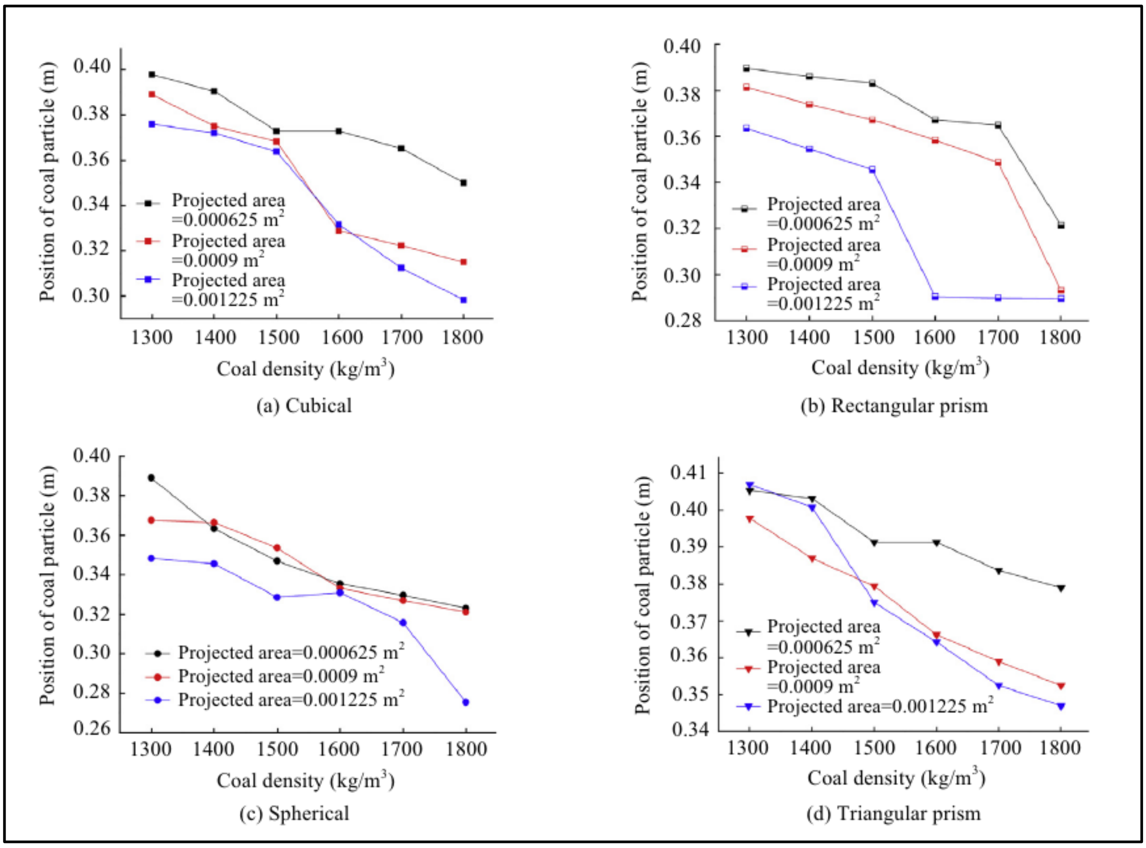

Figure 2.13: Effect of particle shape on the ADMFB separation (taken from Prusti *et al*., 2015)

2.5.5 Static bed height and column shape

The packed bed height and columnar shape have been proven to influence the minimum fluidization point of a particular bed. Rao *et al*. (2010) found that an increase in minimum fluidization velocity is expected as the ratio of column height to diameter increases for a fixed column diameter. The column consequently becomes much taller and the wall effects become more prominent causing difficulty in fluidization of the particles. Fluidization is therefore nearly impossible in a bed with a large static height to diameter ratio. Similar results were obtained by Fardaus *et al.*, 2012, indicating that the separation efficiency increased with decreasing static bed height as a result of the bubble size remaining small in comparison to the particle size. The larger bubbles (in comparison to particle size and bed diameter) contain a strong wake which causes the coal particles to be dragged upwards and increases the fluidization intensity which affects fluidized bed destiny and may result in the back-mixing of particles (Fardaus *et al.*, 2012). Conversely, if the initial bed height is too low, most of the fine particles are blown away from the interspace between the coarse particles and fluidization is hindered as well (Yang *et al.*, 2013b).

It was determined by Sahu *et al.* (2013) that the cross sectional shape of the bed also affects the minimum fluidization velocity. In this study rectangular, square and circular beds were investigated to determine which yields a more stable fluidization bed. The stability of fluidization is determined from the range between the minimum fluidization point and minimum bubbling point. These were determined for the three cross sectional bed shapes mentioned and from the results it was clear that stable fluidization increases from circular to square to rectangular. This is due to the high porosity of the bed and dead zones created at the corners of the bed increasing the static bed height (Sahu *et al.*, 2013).

2.6 Chapter summary

ADMFB beneficiation of coal is clearly an intricate technology with various factors playing a vital role in its effectivity. These are all considered when investigating the process for the objectives as stipulated in *Chapter 1*. At this point, the concepts relating to coal and dry beneficiation technologies should be fully understood and with this comprehensive knowledge the design, experimental and results chapters can follow.

Chapter 3: BED DESIGN AND COMMISSIONING

Chapter 3 focusses on the design of a new ADMFB assembly in order to achieve the objectives for the project. This chapter details the fundamental processes design and any associated mechanical considerations for implementing an enlarged ADMFB design. This chapter further brings focus to certain shortcomings on the equipment used in previous studies at the North-West University (NWU) and the improvements made thereupon. *Chapter 3* consists of the following sections:

- **Section 3.1:** Overviews the study problem and details the necessity of an improved ADMFB design for the objectives of the investigation.
- **Section 3.2:** Provides a brief description of the fluidized bed assembly and experimental procedure and stipulates the design objectives.
- **Section 3.3:** Details the theoretical fundamental process design of the fluidized bed in terms of both air velocity and pressure requirements.
- **Section 3.4:** Consists of the mechanical considerations regarding the accumulation of air in the bed, dust control mechanism and adding vibration to the fluidized bed structure.
- **Section 3.5:** Entails a detailed description of the bed structure and dimensions as relating to the design objectives, process design and mechanical considerations.
- **Section 3.6:** Discusses the air flow and distribution mechanisms implemented in the bed design.
- **Section 3.7:** Explains the control and measuring systems in place for adjusting the air flow and extent of vibration and measuring the air velocity and bed pressure drop, respectively.
- **Section 3.8:** Provides a basic hazard and operability (HAZOP) study that was conducted for the fluidized bed in terms of machinery and equipment and all interlinking process lines and sensors there between.
- **Section 3.9:** Discusses in detail the commissioning phase of the ADMFB in terms of bed operation, design shortcomings and the improvements thereon.
- **Section 3.10:** Provides a conclusion to the chapter and brief introduction to the chapter that follows.

3.1 Overview

For the applicability of the experimental set-up of this study, a batch type process is undertaken and the bed is loaded with a homogenous coal-dense medium mixture. The packed particulate bed is allowed to fluidize for a period of time to ensure effective stratification of the coal particles. On completion, the particles are allowed to slowly settle back into a packed bed state which is sampled by layering the coal at specific heights along the column and the extent of fluidization is determined from the results of conducting relevant analyses thereon.

A well-developed and stable fluidized bed is of utmost importance for effective density separation. However, this is reliant on the bed geometry; fluid, particle and air flow specifications and the stability of bed pressure drop. As such a comprehensive process design and some additional mechanical considerations are necessary which is discussed in the sections that follow.

3.2 Experimental set-up

Ensuring the correct experimental set-up and optimal operating conditions for the process equipment is of immense importance. When deciding upon a suitable apparatus for conducting the necessary experiments, it is essential to note the various interdependent factors that could affect the accuracy of the unit's operation. Even more emphasis is placed on these parameters when designing equipment from fundamentals. It has been established that the factors most affecting the minimum fluidization velocity (MFV), and thereby the effective operation of the ADMFB, are those relating to the particle and fluid properties as well as bed geometry and air distributor design (Fardaus et al., 2012; Escudero & Heindel, 2011).

3.2.1 Fluidized bed description

The North-West University (NWU) has conducted numerous studies ADMFB separation on for fine coal fractions, more specifically 0.5mm to 5.6mm. The fluidized bed used for the above-mentioned studies was made up of a stack of circular polyvinyl chloride (PVC) rings with a diameter of 0.15m and individual height of 0.04m. Once clamped together, the bed reaches an overall height of 0.4m and is placed atop a distribution plate layer of perforated steel sheeting and marbles. This set-up is affixed to a TrbD-450 Radial Bladed Centrifugal Fan that delivers air at 30m^3/min and also an industrial sieve shaker for the addition of vibration. The existing fluidized bed, as described above, was enlarged in order to accommodate the larger PSD (+5.6-13.2mm) and feed mass considered for this study. In addition, some shortcomings identified during the operation of the above mentioned bed were improved upon in the newly designed bed.

3.2.2 Design objectives

The objective of the new assembly is to implement an enlarged fluidized bed design that can accommodate an increased PSD as well as elevated feed mass. This structure is to be retrofitted to the existing centrifugal fan as named in *Section 3.2.1* and be operated as briefly described in *Section 3.1*. Some additional considerations were made during drafting to allow for future improvement and to contrive some issues noted during operation of the previous bed.

1. A square cross sectional area was considered for the new set-up. As mentioned cross sectional bed geometry influences the fluidization with its stability increasing from circular to square to rectangular (in a study by Sahu *et al.*, 2013). Furthermore, the square shape was selected in order to attempt layered sampling during fluidization without needing the particles to settle first. This is a consideration that proves most viable when pondering the physical and mechanical mechanisms of such a sampling system.
2. An improved air distribution layer was given thought to so as to ensure enough of an even supply of air throughout the cross sectional area of the bed. Hence, an air accumulation plenum and new distributor plate were drafted.
3. Some changes to the overall bed structure height were contemplated to combat an observed accumulation of air in the top section of the previous bed (mentioned in 3.2.1) due to the inability for the air to escape the bed quickly enough. As such, a fluidized bed with an increased height was considered in order to allow sufficient room for the particles to fluidize and eliminate any hindrance of air flow out of the bed which could result suppression of fluidization and poor separation.

4. An additional dust control layer was designed for the top of the bed. This is to ensure minimal dust pollution to the air by making certain that any ultra-fine particles accumulating during operation remain in the bed.
5. A new system of vibration of the bed was established with the aid of a vibrating oscillatory motor that is affixed to the frame of the bed with frequency and amplitude outputs that can be adjusted by a variable speed drive and the adjustment of weights, respectively.
6. A refined method of measuring air flow from the centrifugal fan was further taken into account with the implementation of a flow sensor that is better suited for the application and maximum air flow requirements for the study at hand.

With these design objectives in mind, the fundamental process design and basic mechanical considerations can follow. These entail the MFV, pressure drop and required bed design ratio calculations for various PSD's at a range of densities. The design further comprises a detailed look into the mechanical requirements from the blower, vibration motor, air accumulation prevention, dust control layer and sensor readings. Lastly, a bed structure is proposed and dimensions thereof stipulated.

3.3 Fundamental process design

The particle and fluid properties are firstly considered when establishing a fundamental process design as they mostly affect the MFV. For the initial design, particle size and density are considered to have the greatest effect and the other properties relating to the particles and fluid are assumed constant. The MFV requirements, for the dense medium and coal, are evaluated, for various sizes and densities, under certain ideal conditions by means of a rearranged Ergun equation (3.1) as follows:

$$(\rho_p - \rho_f)g = \frac{\rho_f u_{mf}^2}{\varphi_s D_p \varepsilon^3}\left[\frac{150(1-\varepsilon)}{\varphi_s d_p u_{mf} \rho_f} + 1.75\right] \qquad \dots [3.1]$$

Where the symbols used are as follows,

Symbol	Description	Unit
ε	Bed voidage	-
φ_s	Particle sphericity	-
d_p	Particle diameter	m
u_{mf}	Minimum fluidization velocity	m/s
ρ_f	Fluid density	kg/cm^3
μ	Fluid Viscosity	Pa.s
ρ_p	Particle density	kg/cm^3

Of the parameters listed above, a few are assumed constant with regards to the particle and fluid properties and are listed in *Table 3.1*.

Table 3.1: Constant parameters as stipulated for the Ergun equation

Variable	Amount	Unit
ρ_f (Rhodes, 2008)	1.225	kg/m^3
g (Rhodes, 2008)	9.8	m/s^2
μ (Rhodes, 2008)	1.983e-05	Pa.s
φ (Kunii & Levenspiel, 2001)	0.63	-
ε_{mf} (Wen and Yu, 1966)	0.48	-

The minimum fluidization velocities as calculated from *Equation 3.1* for the coal over an array of particle sizes and SG's while considering the constant parameters as stipulated in *Table 3.1* are summarised in *Table 3.2* below.

Table 3.2: Minimum fluidization velocities (m/s) for an array of coal particle sizes and densities

Particle size (m)	Minimum fluidization velocity (m/s)									
	SG 1.0	SG 1.1	SG 1.2	SG 1.3	SG 1.4	SG 1.5	SG 1.6	SG 1.7	SG 1.8	SG 1.9
0.0056	1.25	1.32	1.38	1.44	1.50	1.55	1.61	1.66	1.71	1.76
0.0067	1.40	1.47	1.54	1.60	1.67	1.73	1.79	1.84	1.90	1.95
0.0080	1.55	1.62	1.70	1.77	1.84	1.90	1.97	2.04	2.10	2.15
0.0095	1.70	1.79	1.87	1.95	2.02	2.10	2.17	2.24	2.30	2.37
0.0112	1.86	1.95	2.04	2.13	2.21	2.29	2.37	2.44	2.51	2.58
0.0132	2.03	2.13	2.23	2.37	2.41	2.50	2.58	2.66	2.74	2.82

From *Table 3.2*, indicated in red for all particle sizes at and SG of 1.0 and all SG's at a PSD of 0.0056m, the MFV clearly increases for increasing particle size as well as increasing particle density. This is because of the weight and equivalent cross sectional area of the particles requiring a larger buoyancy force in order to suspend. On assuming that the feed sample of each PSD varies in accordance to the density as stipulated in *Table 3.2*, a range of theoretical MFV's were established for fluidization operation. This is summarized as below.

- +5.6-6.7mm – 1.25 to 1.95m/s
- +6.7-8.0mm – 1.40 to 2.15m/s
- +8.0-9.5mm – 1.55 to 2.37m/s
- +9.5-11.2mm – 1.70 to 2.58m/s
- +11.2-13.2mm – 1.86 to 2.82m/s

Further assuming the same bed voidage, sphericity and fluid properties as in *Table 3.1*, the MFV obtained for magnetite particles of 0.3mm and TRD equal to 4800kg/m^3, is approximately 0.12m/s. The much lower MFV of the magnetite powder regardless of its large density is attributed to the very fine particle size range. From *Equation 3.1*, the particle size affects the MFV by means of a quadratic multiplication whereas density is in the zeroth order of multiplication.

Of noteworthy importance is the fact that the Ergun equation aids in calculating the MFV for singular particles suspended in a fluid. As such the values as discussed above, are only theoretical MFV's for individual particles and may be considerably higher in practice when considering an entire particulate bed. This is due to the total mass and static bed height of the sample and also the particulate interactions with one another and the bed walls. A more accurate MFV calculation for a bed of particles is done experimentally as described in *Section 2.4.2* and will be dealt with in *Chapter 5*. Following from here are the bed pressure drop and fluidized bed height calculations for assumed bed mass and properties as listed in *Table 3.1*. These parameters factor into account the cross sectional area of the bed and hence provided the data from which the bed diameter was designed.

The fluidized bed height and frictional pressure drop across the bed for a specific sample mass and particle density are given by *Equations 3.2 and 3.3,* respectively.

$$H_{mf} = \frac{M}{S_{bed}(1-\varepsilon_{mf})\rho_p} \qquad \text{… [3.2]}$$

$$\frac{\Delta P_{bf}}{\Delta H_{mf}} = 150\frac{u_{mf}\mu(1-\varepsilon_{mf})^2}{(\varphi_s d_p)^2\varepsilon_{mf}^3} + 1.75(\frac{\rho_f u_{mf}{}^2(1-\varepsilon)}{\varphi_s d_p \varepsilon^3}) \qquad \text{… [3.3]}$$

Where,

Symbol	Description	Unit
H_{mf}	Bed height at MFV	m
M	Bed mass	kg
S_{bed}	Cross-sectional bed area	m^2
ε_{mf}	Bed voidage	-
ρ_p	Particle density	kg/m^3
ΔP_{mf}	Bed pressure drop	Pa
u_{mf}	MFV	m/s
μ	Fluid viscosity	Pa.s
φ_s	Particle sphericity	-
d_p	Particle diameter	m
ρ_f	Fluid density	kg/m^3

Table 3.3 sums up the results obtained for the fluidized bed height and frictional pressure drop as calculated from *Equations 3.2* and *3.3,* respectively, with a bed mass of 15 kg and for bed widths of 0.15, 0.2, 0.3 and 0.4m.

Table 3.3: Fluidized bed height (m) and pressure drop (Pa) values for four different bed widths

Bed width (m)	H_{mf} (m)	ΔP_{fb} (Pa)
0.15	0.65-1.29	6525-6529
0.20	0.36-0.72	3670-3673
0.30	0.16-0.32	1631-1632
0.40	0.09-0.18	918

The maximum and minimum values portrayed in *Table 3.3*, for frictional pressure drop across the bed and fluidized bed height, link to the maximum and minimum coal SG's of 1.0 and 2.0, respectively. Clearly an increasing density does not have a major effect on the frictional pressure drop but does severely affect the bed height. This provides further proof to the fact that stratification does occur, according to density, in an ADMFB. When considering increasing bed width, ΔP_{fb} decreases and a similar trend is noticed in H_{mf}. This is due to the larger surface area allowing for a smaller initial static bed height when considering the same mass. The particles are spread out and therefore need to undergo less particle to particle and particle to wall interactions to properly fluidize, thus reducing the frictional pressure drop. From this it is clear that the larger square fluidized beds would be better suited as they yield the lowest frictional pressure drop and fluidized bed heights.

In a study conducted by Rao *et al.* (2010), it was determined that the column height to column diameter ratio (H/D) and particle diameter to column diameter ratio (d/D), play a major role in the wall effects experienced in a fluidized bed. As these ratios increase, the MFV increases which leads to more prominent wall effects and escalated difficulty in fluidizing. Therefore a fluidized bed should be designed to ensure that both these ratios remain as low as possible. *Table 3.4* portrays the H/D ratio range for each column width as well as the minimum (d_{min}/D) and maximum (d_{max}/D) ratios correlating with the smallest and largest particle sizes, respectively. From *Table 3.4*, an increase in H/D and d/D is expected for decreasing bed width and the lowest values, as recommended by Rao *et al.* (2010), are associated to the largest bed width of 0.4 m.

Table 3.4: Column height to diameter and particle to column diameter ratios

Column width (m)	H/D	d_{min}/D	d_{max}/D
0.15	3.9-7.9	0.037	0.088
0.2	1.7-3.3	0.028	0.066
0.3	0.5-1.0	0.019	0.044
0.4	0.2-0.4	0.014	0.033

From the above calculations relating to the particle and fluid properties, it was determined that the largest possible theoretical velocity required for fluidizing the coal is approximately 2.82m/s and that of magnetite is 0.12m/s. The current blower is capable of handling maximum airflow rates ranging around 18m/s, which is adequate for the new design. Once again, some emphasis is placed on the difference in theoretical values obtained from the Ergun and experimental MFV from the pressure drop versus superficial velocity relations. The experimental method is more accurate for the application at hand as it considers the entire bed mass and particle-particle and particle-bed wall interactions. These determinations are done in the respective *Chapters 5* and *6* where the optimization of the ADMFB is discussed.

From the fluidized bed height, pressure and design ratio calculations it is clear that when considering stable fluidization larger bed widths prove best suited. This is due to the low bed heights, pressure drops, H/D and d/D ratios which are generally associated with good fluidization behaviour. Due to the sizing of the frame and ducts connected to the blower, a bed width of 0.3m was selected for the new set-up. The parameters as calculated above for this bed width are considered within reason for the objectives of this study. Furthermore, beds of this diameter have been used in studies as reported by Zhao *et al*. (2015). In the sections that follow, some basic mechanical considerations in terms of vibration, particle transport disengagement and dust control are detailed.

3.4 Basic mechanical considerations

Similar to the small-scale fluidized bed previously used, the new ADMFB design consists of a stack of transparent PVC layers (but only in a cubic shape) of 0.3m width and 0.05m layer height. The bed consists of eight of layers stacked on top of one another, yielding a total bed height of 0.4m. The PVC layers are machined to fit into one another, effectively sealing the bed and eliminating air leakages from the sides. Sampling of the bed layers consists of dissembling the stacked column and analysing the coal within. For this purpose, each layer is fitted with a 2mm opening through which a steel sample cutter can be inserted to effectively cut the packed bed and remove the desired coal layer. The opening is sealed with a rubber stopper in order to prevent air and fine particle leakages during operation, and is removed when the bed is sampled. The methods for assembly, disassembly and sampling will be discussed in more detail in *Chapter 4*.

3.4.1 Particle transport disengagement and dust control

As stipulated by design objectives 3 and 4, with regard to the movement of particles out of the fluidized bed, evasion of air accumulation in the top of the bed structure and also dust pollution prevention, two extra bed layers were constructed. These are visible in *Figure 3.1*.

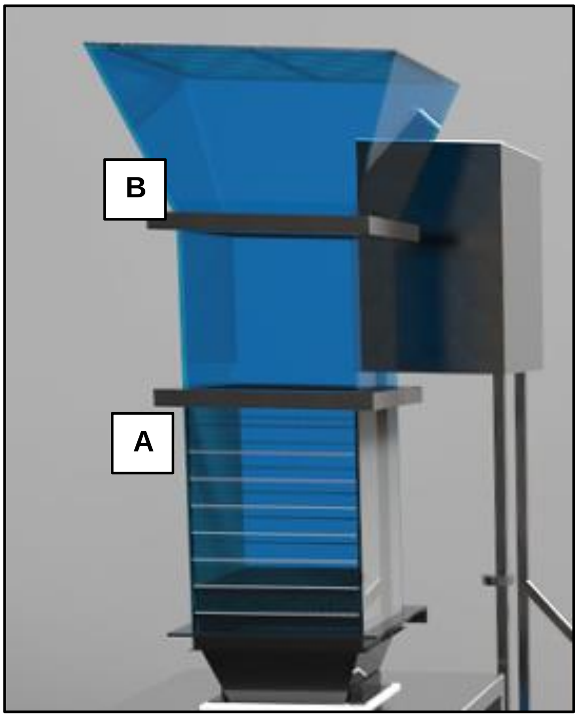

Figure 3.1: Bed structure and control measure additions

In *Figure 3.1*, the labels A and B depict the bed layers and transport disengagement layer and dust control layer, respectively. Once stacked, the bed stands approximately 1 m tall and is fastened with an array of nuts, bolts and clamps to ensure its rigidity and stability during operation. The entire structure, as detailed above, is retrofitted to the centrifugal fan by means of an air distribution layer which is discussed in *Section 3.5* below.

Since the bed is cubical in shape, with the bed width and bed height being relatively close to one another, a build-up of air in the top of the bed during operation was a probability. It was observed, in the previous bed, that when the coarser material was processed at a bed height larger than that of the bed width, the air did not flow quickly enough from the top of the bed. Consequently, the air accumulated in the top portion of the bed and began to supress the coal particles being fluidized. Resultantly, a 9^{th} 0.3m bed layer was added to the bed structure, making up a total bed height of 0.7m, and ensuring sufficient space for the particles to fluidize without an undesired build-up of air and also ensuring particle transport disengagement for the smaller and lighter coal particles flowing out of the coal-magnetite suspension.

Lastly, an inverted tapered trapezoidal layer, with 0.1mm wire mesh covering the top, was affixed to the bed. This layer is in place to ensure that no fine and ultra-fine particles escape the bed and thereby reduces dust pollution to the air during operation. The incline angle is at approximately 20° and results in an increase in layer width from 0.3m to 0.66m. The total surface area of the layer thereby increases from a $0.09m^2$ to $0.44m^2$.

The increase in surface area causes the particles fluidizing in the bed below the dust control layer to experience a lesser buoyant force as provided by the cross-sectional air flow. The ultra-fine magnetite and coal particles reporting to the higher parts of the bed therefore fall back into the particulate bed. The sieve at the top of the bed is to ensure any particles not affected by the increase in surface area remain in the bed. *Figure 3.2* shows the 9^{th} particle transport disengagement and tapered dust control (A and B) layers.

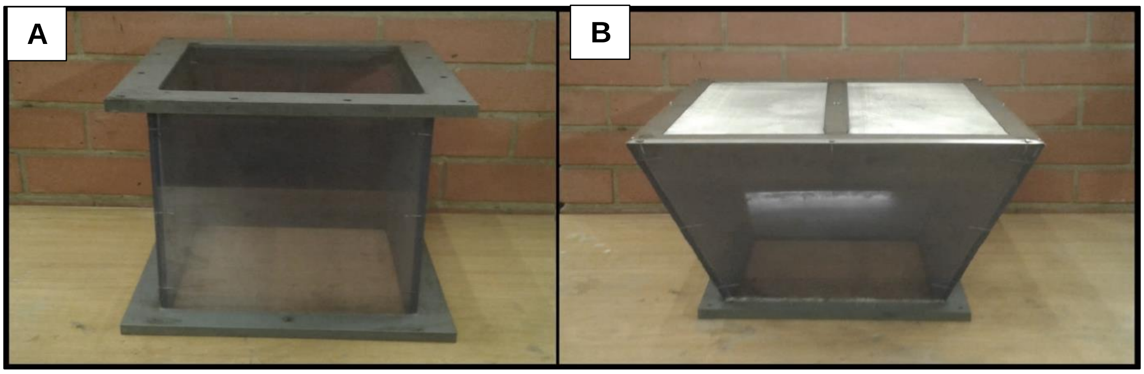

Figure 3.2: Bed layers for particle transport disengagement and dust pollution (A and B)

3.4.2 Bed vibration

The specification of a suitable means of vibration is considered as part of the basic mechanical design of the bed. As stipulated in *Chapter 2, Section 2.5.2*, vibration may lead to improved fluidization as a result of increased gas-solid interactions and reduced aperture blinding and air channelling (Yang *et al.*, 2012b; Maoming *et al*., 2003). Of further importance is the effect that both the frequency and amplitude have on vibration. Values that are too low create weak vibration that results in de-fluidized zones and formation of large bubbles. Conversely, if too large, circulation of particles and back-mixing occur (Yang *et al.*, 2013b). Although proven to be dependent on bed geometry, coal and fluid properties as well as application, some guidelines are stipulated by He *et al.* (2015) and that can be useful. Frequencies ranging from 20 – 50Hz and amplitudes of 0 – 10mm are suggested.

A 0.18kW oscillatory vibration motor was selected as a suitable means of inducing vibration across the bed. A 2-pole BM 200/3 model OMB vibration motor was attached to the frame of the bed, accompanied by variable speed drive to adjust the input frequency of vibration. The motor has a maximum capability of 3000 revolutions per minute (RPM) with frequency and amplitude specifications of 50Hz and 10mm, respectively. Moreover, a motor efficiency of 69.4% is expected along with a 1.83KN force if weights are set to 100%. The frequency as stipulated on the motor refers to the electrical frequency received by the motor. The frequency of vibration for 2-pole motors is, by rule of thumb, generally the same as the electrical frequency, however this differs for 3 and 4 pole motors (Conrads, 2009). The amplitude output of the motor can be adjusted by means of adjusting the weights, which either increases or decreases the force delivered, thereby increasing or decreasing the amplitude, respectively.

The motor is attached to the base of the bed frame and induces a horizontal shaking motion of the bed structure. A protective steel brace is bolted onto the base of the bed to reinforce the bed structure during vibration. The minimum frequency requirement of 20Hz is considered for the experiments that follow to ensure a vibration that is not too vigorous. The frequency and amplitude are inter-related parameters, a change in one has an effect on the other. However, according to He *et al.*, (2015) the amplitude has the largest effect of the two. Consequently, the weights of the motor were set to a value 60% similarly to how it is portrayed in *Figure 3.3* (C), but only with 70%. This causes a reduction in the maximum force output of the motor by decreasing the amplitude of vibration for the same frequency. The associated decreased amplitude is obtained experimentally by holding a pen steady against the motor and recording the length of the lines drawn once switching it on. The amplitude values ranged from 0 – 7mm for the combined weight adjustments of 60% to 100%. The vibratory motor and adjustment of the weights are portrayed in *Figure 3.3*.

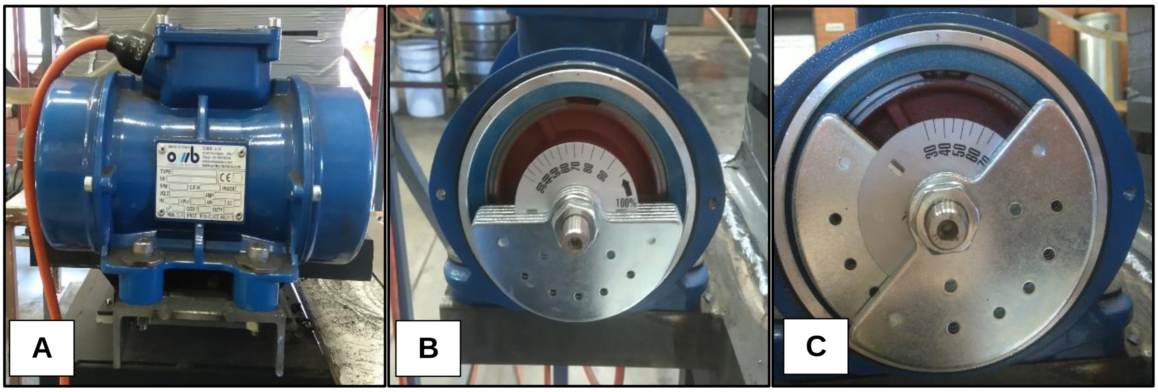

Figure 3.3: Oscillating vibration motor (A) adjustments of weights (B and C)

3.5 Air distribution

A constant and even air distribution was accomplished by means of an air distribution mechanism constructed from an air plenum, bed of marbles and 0.1mm wire mesh sandwiched between two 4mm perforated steel plates. This was designed so as to ensure only a slight air pressure drop across the distribution layer.

The centrifugal fan delivers air at desired volumetric flow rates ranging from 0 – 30m^3/min through a 2m long circular duct of 0.15m in diameter. A tapering air plenum is attached to the duct so as to increase the duct area to the desired square shape and 0.3m bed width. This plenum further aids in the air flow requirements and distribution as the gas collects within it and disperses from the centre (entering through the duct) to inhabit the entire volume of the chamber. The chamber further allows the air to be distributed to the corners and sides of the square bed.

A perforated steel plate is fixed to the top of the air dispersal chamber which forms the structure onto which a bed of ceramic marbles were placed. This aids in the even distribution of air to the bed as the gas is forced to percolate through the marbles. The third and final component of the air distribution mechanism forms the bottom portion of the first bed layer which is placed on top of the marbles. This section consists of 0.1mm wire mesh that is sandwiched between two 4mm perforated steel plates. This combination is designed to ensure further air distribution but also to prevent any fine particulates from falling into the duct which may have implications for the centrifugal fan. The air plenum (A), distribution marbles (B) and plate distributer (C) are shown in *Figure 3.4*.

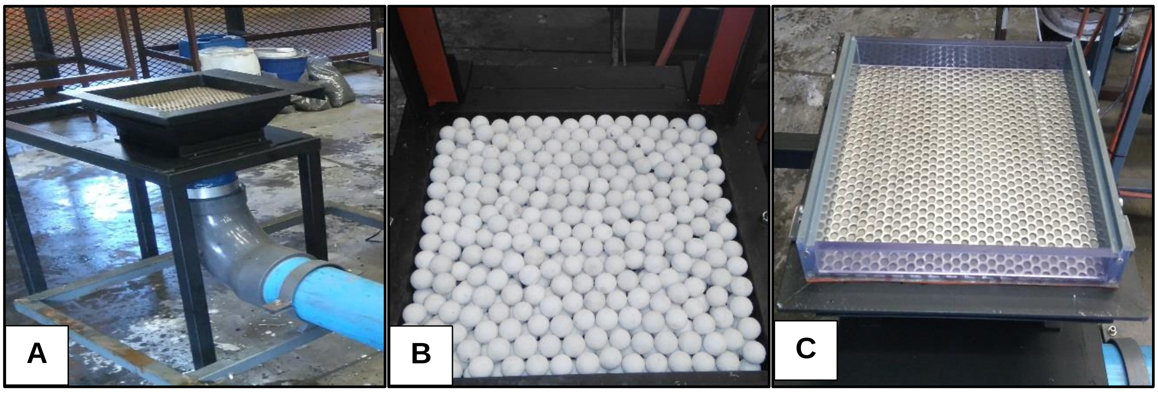

Figure 3.4: Air dispersion plenum (A), distribution marbles (B) and plate distributor (C)

The bed structure as described in *Section 3.4* is stacked above the distributor plate layer that is portrayed in *Figure 3.4*. This forms the final structure of the bed inclusive of the first four design objectives as stipulated in *Section 3.2.2*.

3.6 Control and measuring systems

The flow of the air, the MFV and bed pressure, are controlled by means of a variable speed drive through which the frequency input to the centrifugal fan can be adjusted. A decrease in input frequency causes the blower to deliver air at a lower velocity and vice versa. In order to protect the fan, a minimum frequency of 20Hz is ensured throughout all experimentation and the maximum is detailed by the frequency of the 3-phase input as 50Hz. The speed of the air was measured by a WIKA Model Air2G air velocity transmitter that is inserted into the air flow duct approximately 1m from the fan. The air velocity and temperature are recorded by the sensor as a 4 to 20mA signal and converted to values readable in m/s and °C, respectively. The Air2G model is best suited for gas systems in circular conduits and is capable of reading air velocities up to 22 m/s.

For the purpose of this study air velocity could not be directly altered, as the air velocity to the bed is controlled by the frequency inverter of the blower. Therefore, a correlation between air velocity (as measured by the flow transmitter) and input frequency of the blower was determined in order to calibrate the bed for the apparatus at hand. This correlation is explained by a representative experimental variable: PSD of +6.7 -8.0 mm, static and pure coal optimization run. *Figure 3.5* provides a depiction of the interaction between the input frequency of the blower and the velocity of the air in the conduit. It further portrays the reproducibility and extent to which this relationship is considered linear with the aid of linear regression models.

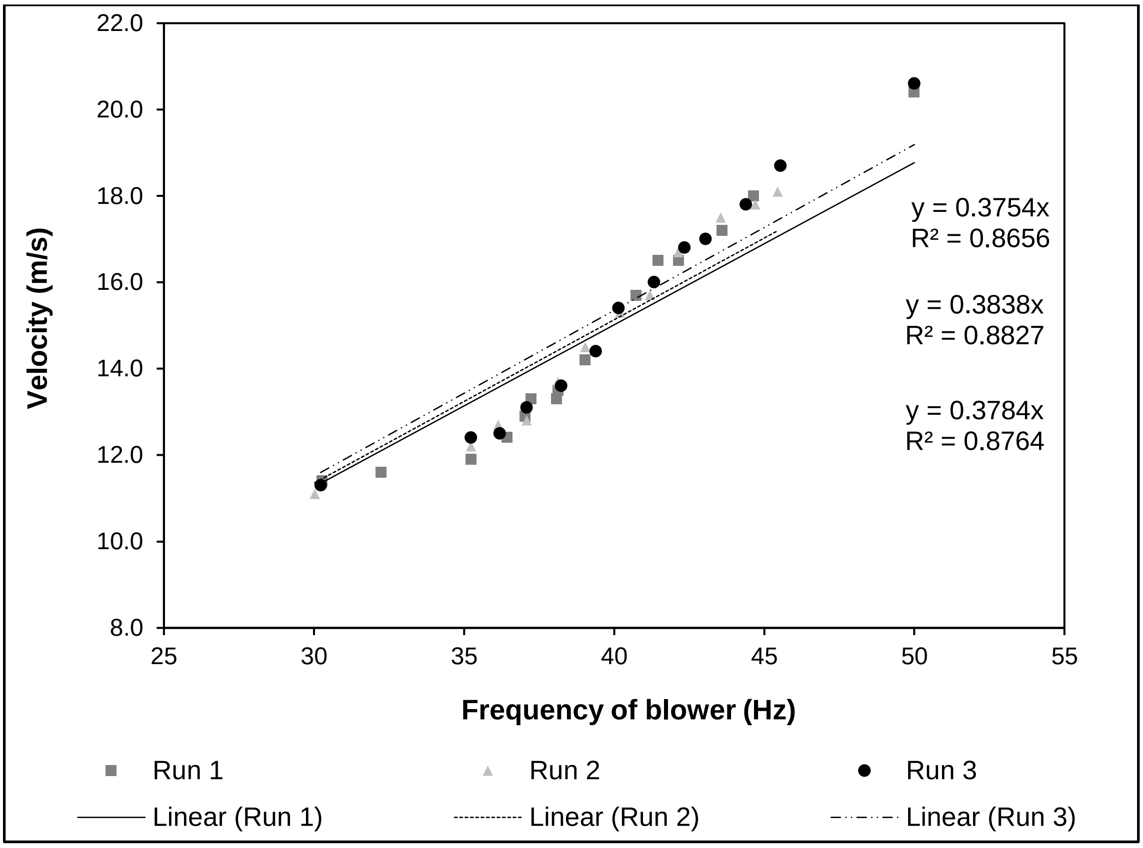

Figure 3.5: Relation between the blower frequency (Hz) and air velocity (m/s)

As in *Figure 3.5*, a moderately linear relation exists between the frequency of the blower and the velocity of the air. The gradient obtained is however slightly different when considering different variables. As such the velocity reading utilized for the runs are controlled by manually adjusting the frequency input to the centrifugal fan until the desired flow of air is achieved. Consistent observance of the velocity throughout operation is thus imperative so as to ensure that the necessary frequency adjustments can be made. Similar linear correlations for each of the investigation variables were constructed and yielded an average deviation from linearity of approximately 0.14. Since *Figure 3.5* is a representative, it can be said that the manually manipulated variable for the experimental procedure is the frequency of the blower (Hz) and is adjusted according to this relation to achieve the desired air velocity (m/s). This converse-calculation method therefore allows this study to comply with the Ergun pressure-velocity relation.

The bed pressure is measured in mm H_2O by means of a water based U-tube manometer connected to a probe that is inserted into the bed from the top. The probe can be adjusted to determine the pressure drop at any point along the bed height. Of importance to the accuracy of experimentation are the readings obtained for the pressure and velocity. Without these values, the MFV cannot be effectively determined and fluidization would be unpredictable and difficult to reproduce. *Figure 3.6* represents the air velocity sensor (A) and water based pressure manometer (B).

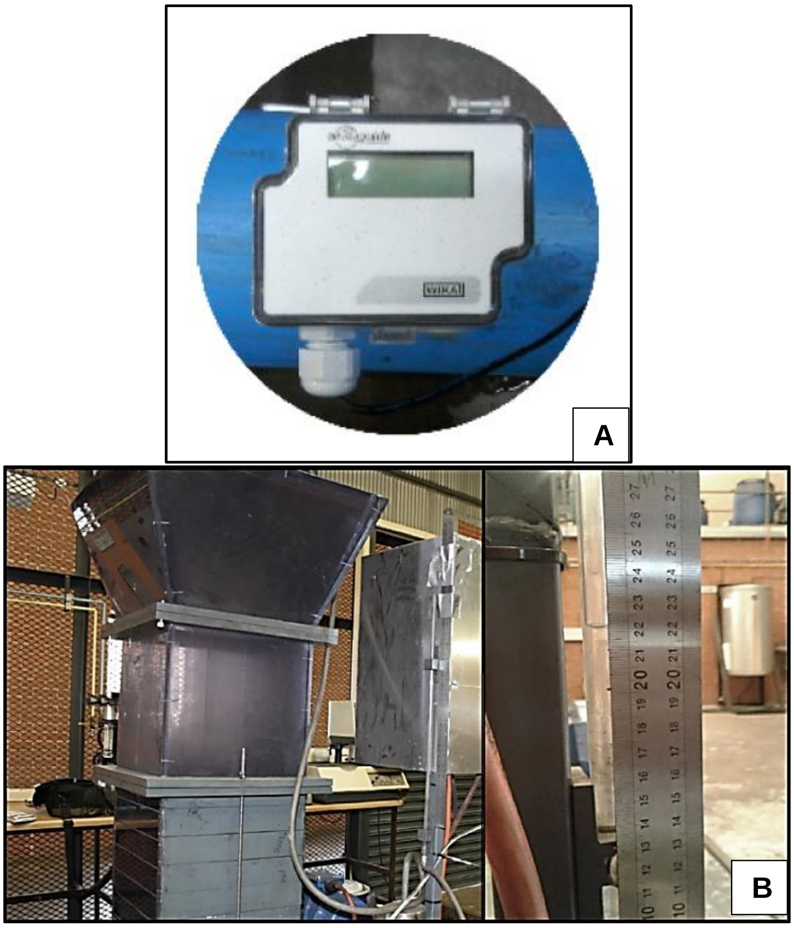

Figure 3.6: Depiction of the flow sensor (A) and water based manometer (B)

As noted in *Section 3.4.2*, the control system of the vibration motor is made up of a variable speed drive which controls the frequency input in a similar manner to that of the centrifugal fan. The adjustment of the amplitude was further discussed as being controlled before experimentation by a setting of the motor weights. An image of the control unit is given in

Figure 3.7 showing the starter boxes and frequency inverters for both the centrifugal fan and vibration motor.

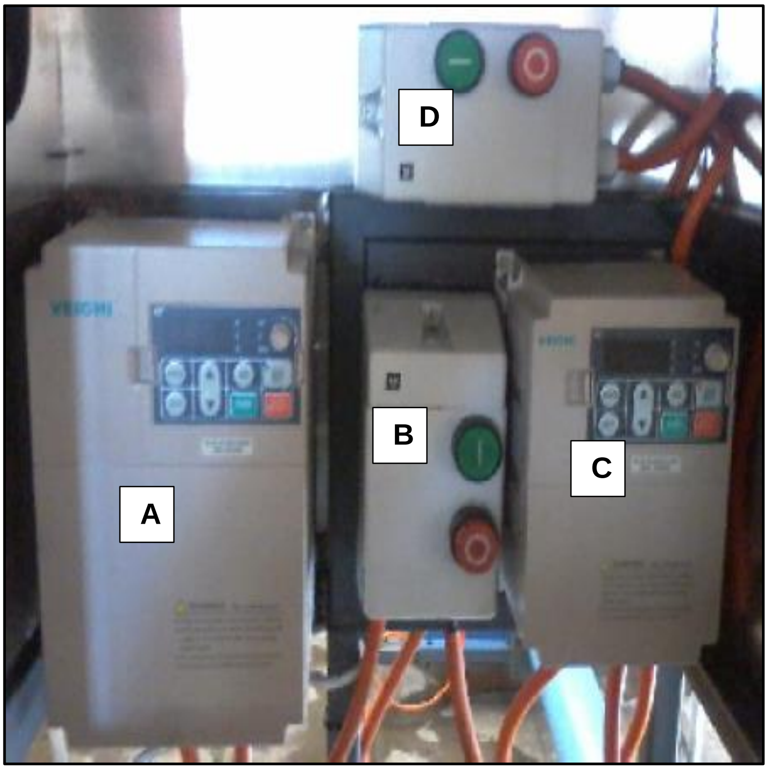

Figure 3.7: Control unit for the centrifugal fan and vibration motor

In *Figure 3.7,* (A) and (B), respectively, show the frequency inverter and starter box for the blower and (C) and (D) portrays the same for the vibration motor. These are enclosed in a containment unit fixed with a cooling fan to prevent any damage as a result of coal and magnetite dust and also overheating.

3.7 Final bed structure and dimensions

The main design objective was to implement an enlarged ADMFB that is capable of beneficiating large coal fractions and increased bed loads. From the fundamental process design, as in *Section 3.3*, theoretical parameters were determined and from these the scaled up dimensions were obtained. The overall bed structure complete with blower, distribution mechanism, fluidization layers, particle transport disengagement, dust control, flow sensor, vibration motor and control box is portrayed in *Figure 3.8*.

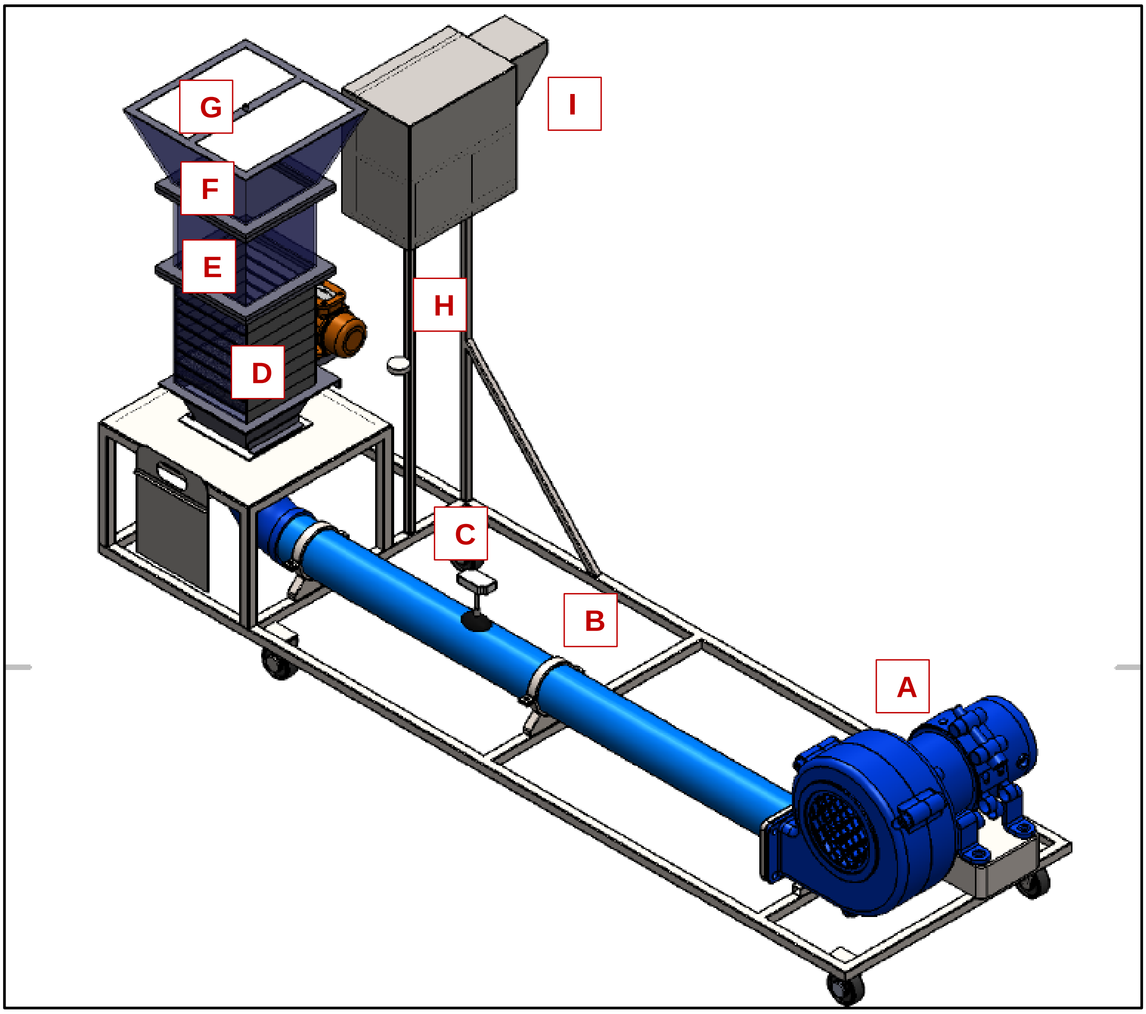

Figure 3.8: Overall bed structure

As shown in *Figure 3.8*, an electrical blower (A) supplies air for fluidization through the circular air duct (B). The air flow transmitter (C) is positioned approximately 1m from the blower outlet. Thereafter, the duct makes a 90° bend, which is connected to a flexible hose that clamps to the inlet of the distribution chamber. The hopper-like air distribution chamber (D) ensures even air distribution to the fluidized bed and reduces the effects of air channelling. The fluidized bed layers (E) are mounted onto the distribution chamber. In order to ensure particle transport disengagement, a ninth layer is added to the fluidized bed, as illustrated by *Figure 3.8* (F). The last section is bolted onto the ninth layer and comprises a tapered trapezoidal head (G) to prevent loss of particulates to the air as mentioned in *Section 3.4.1*. Previously discussed, an air flow transmitter and water based manometer are used to measure the air flow velocity and bed pressure drop, respectively. Lastly depicted in *Figure 3.8* by labels (H) and (I) are the oscillating vibration motor and control unit discussed in *Sections 3.4.2* and *3.6*, respectively.

Given the considerations for control and measurement of the crucial parameters as given above and also the fundamental process design and basic mechanical considerations, the ADMFB is completely specified in terms of the design objectives as stipulated in *Section 3.2.2* as well the desired application of the bed. Some additional engineering drawings stipulating the overall bed dimensions and various viewpoints of the assembly are provided in *Appendix A*.

3.8 Basic HAZOP study

A hazard and operability (HAZOP) study is defined as a structured and systematic examination of an operation in order to identify and evaluate problems that may represent risks to persons or equipment. This section is dedicated to a basic HAZOP study of the fluidized bed design which entails an evaluation of each of unit, line and instrument utilized in the operation. A study such as this is aimed at determining possible deviations from the intended purpose of the considered unit and highlight the causes thereof along with any consequences that may result.

For the purposes of this evaluation only those deviations relating to flow and pressure in the bed are detailed with the most appreciable variances in the other units briefly discussed afterwards. With an ADMFB, flow and pressure are interlinked, an increase in the one causes an increase in the other. As a result only the effects of flow are discussed with any necessary reference made to the related behaviour of pressure. The possible causes and consequences of probable operating deviations relating to the inlet (air duct, air distribution chamber), fluidizing layers and dust control head of the ADMFB are summarized in *Table 3.5*.

Table 3.5: HAZOP concerning the ADMFB

Guideword	Deviation, causes, consequences and actions
No flow	**Cause:** No flow in the bed inlet (air duct and air distribution mechanism) could be caused by a malfunction in the blower or a blockage downstream the air conduit. No flow in the fluidizing layers could be as a result of poor distribution of the air in the dispersion chamber. No flow in the dust control bed layer may be attributed to either poor air flow through the air distribution chamber and particulate bed or a blockage in the mesh cover atop the bed.
	Consequence: No flow signifies no pressure and in the inlet and fluidizing layers would seize the fluidization operation entirely, when as a result of a blower that malfunctioned. If a blockage in air line is the cause, a pressure increase in the line is possible and could lead to damage of the downstream process units, lines and instrumentation. Poor air flow through the dispersion chamber and bed may result in pressure accumulation in the air pipe and the air plenum, respectively. With regard to the outlet blockage cause (dust control head), it may result in a large pressure build-up in the bed and ultimately the suppression of fluidizing particles as well as bed leakages.
	Action: For mitigation, it is essential to ensure that the blower is operated correctly at all times and that the lines, air dispersion unit and dust control layer are free from blockages before operation of the bed.
More flow	**Cause:** More flow in the bed inlet may be as a result of incorrect readings from the sensors and therefore poor control of the frequency input to the blower.
	Consequence: An increase in the inlet air flow could yield an unstable fluidization of the particulates and if increased to a large extent could cause a

	pressure build-up in the bed resulting in leakages and possible suppression of fluidization. This is because the air cannot escape the top of the bed fast enough and accumulates in the head.
	Action: Action that can be taken to prevent this is to ensure that the flow sensors and control unit are in correct working condition and operated as accurately as possible and within the relevant design specifications.
Less flow	**Cause:** Less flow in the bed inlet can result once again from improper flow meter readings and poor control of the blower input frequency. A blockage in the air duct may also be a possibility. Poor air distribution in the dispersing mechanism may yield less flow to the fluidizing layers. Less flow from the outlet layer of the bed would most likely be caused by blockages in the mesh cover.
	Consequence: Less flow in the bed inlet and fluidizing layers may lead to ineffective fluidization of the particles within the bed. Additionally, a pressure build-up within the bed is possible if less flow is experienced in the bed outlet.
	Action: Once again, the importance of ensuring the optimal operation of all instrumentation is essential and observing and clearing of blockages before experimentation is vital.

From *Table 3.5* it is clear that adequate flow in the ADMFB is essential and that this relates closely to bed pressure. Note must be made of consequences of and mitigations required for these deviances throughout experimentation. With regards to the blower, vibration motor and sensors, it is essential that the correct input signals are ensured in order to prevent needing to replace any machinery and instrumentation due to overloading.

3.9 Commissioning

During the commissioning of the new ADMFB assembly some light was shed on certain shortcomings in the design of the previous bed. The enlarged bed was to be retrofitted to the same structure as the previous bed made up of the centrifugal fan, air duct, framing and flow and pressure sensors. As such, the existing equipment was evaluated to ensure its adequacy for the current application. Furthermore some additional adjustments in the new bed design were required as the behaviour and integration of certain components were unpredictable.

Modifications were made to the flow sensor, pressure manometer and means of vibration in order to improve the applicability to the current problem. The air velocities required for fluidization in the larger bed assembly are beyond the capability of the previous flow sensor, thus, a better suited air velocity transmitter was implemented (as discussed in *Section 3.6*). Some adjustments to the probe and piping of the water based manometer was required as the length was insufficient for the overall height of the new assembly. Therefore longer piping was attached to the water bath and an extended adjustable probe was implemented.

Previously, the ADMFB was vibrated by means of an industrial sieve shaker affixed to the bed frame. It was anticipated that this form of vibration would yield instability in the bed structure and as a result the alternative oscillatory vibration motor was selected. Additionally, adjustment of the frequency and amplitude of the sieve shaker was not possible. When implementing the OMB vibrating motor with weights to a maximum force of 1.83KN and operated at the minimum frequency of 15Hz, breakage of the bed frame to which the motor is attached was observed due to an amplitude of vibration that is too vigorous. The frame was then reinforced with steel bars and the motor weights adjusted to 60% of the maximum force. This prevented destruction of the bed frame when operated at approximately 20Hz but reduced the amplitude of vibration from 5-7mm to more or less 3-5mm.

As a result of poor dust control in the previous bed, some fine magnetite and coal particulates entered the control and starter box for the blower. This caused a short circuit and ultimately led to a fuse in the frequency inverter. New frequency inverters for the centrifugal fan and vibratory motor where consequently installed. In order to prevent similar destruction of the instrumentation, a sealed unit was constructed over the control instruments that prevents any particulates from entering. A cooling fan was further installed to make sure that the heat is controlled within the unit thereby further protecting the variable speed drives and starter boxes.

Some primary experiments were conducted using the enlarged assembly. This was done to ensure that the blower was capable of delivering the required air velocity for effective fluidization of the particles at the increased bed loads. In these investigations, coal of the smallest and largest size range considered for this study was loaded into the bed and the blower frequency incrementally adjusted so as to obtain a general idea of the minimum and maximum operating conditions. Similarly, this was investigated with the addition of magnetite which further gave an indication of any possible areas of leakage in the bed. Any spillage of air or fine dense medium powder from the bed during operation was inhibited by sealing the bed with adhesive tape.

During commissioning, another consideration regarding magnetite was made. It was found that when making use of a magnetite PSD of +0.12-0.3mm, a large amount of ultra-fine dense medium escaped the top of the bed through the dust control layer even with a 0.1mm wire mesh guard. This is due to large amount of ultra-fine magnetite particles agglomerating, and appearing as larger particles during screening. These agglomerates ultimately break up into the smaller counterparts once fluidized. The addition of an extra air filtration layer to the top of the bed, however, caused a build-up of pressure in the bed as the air could not escape entirely. For this reason, magnetite was sieved to +0.3mm, fluidized to break up any agglomerates and then utilized in the experiments conducted.

3.10 Chapter summary

At this point in the thesis entitled "*The dry beneficiation of South African small coal in a dense medium fluidized bed",* the fundamental process design and basic mechanical considerations of the bed are comprehensively detailed. With this the fluidized bed used for the investigation is well defined. A simple HAZOP study pertaining to the risk free operation of the equipment is also detailed along with a description of the necessary equipment commissioning phase. The chapters that follow endeavour to characterise the materials used, procedure followed for the experimentation portion of the study and detail the results obtained therefrom.

Chapter 4: MATERIALS, EQUIPMENT AND EXPERIMENTAL

This chapter presents a characterization of the materials utilized during the experimental entitled *"The dry beneficiation of South African small coal in a dense medium fluidized bed"*. It further provides a description of the procedure and method of experimentation. *Chapter 4* consists of the following sections:

- **Section 4.1:** Provides an overview of the study problem and details the necessary materials required for the experiments.
- **Section 4.2:** Discusses the coal used during the investigation and details the characterization thereof.
- **Section 4.3:** Considers the classification of the magnetite used as dense medium during the investigation experiments.
- **Section 4.4:** Consists of the experimental procedure followed during the investigations most specifically related to operating and sampling of the bed and also to the analyses required thereafter.
- **Section 4.5:** Presents the necessary safety measures implemented during the initial analyses and characterization.
- **Section 4.6:** Details some observations made with regard to the behaviour of the bed during optimization and operation
- **Section 4.7:** Provides a conclusion to the chapter and brief introduction to the chapter that follows.

4.1 Overview

The materials of importance to the experiments are magnetite as dense medium, coal and fluidizing air. The characteristics of these and their preparation are detailed in the sections that follow along with an extensive experimental plan and necessary procedures.

4.2 Coal

Two coal samples of different qualities were obtained from the Witbank coalfield (Seam 4) situated in Mpumalanga, South Africa. The coal deposits within this region are of the biggest in the country and are predicted to deplete entirely by 2050 (Cairncross, 2001; Jeffrey, 2005). The principal product originating from the Witbank coalfield is a bituminous steam coal primarily extracted for export, with some generated for the local market (Jeffrey, 2005). The SAWS (2017) reports an average annual rainfall of 533 mm in this region during the July 2016 and June 2017 season. Water and coal are therefore scarce commodities and proper utilization thereof is imperative.

Of importance to note, for this study, is that a set of initial experiments were conducted on the first coal quality which yielded less than desirable results. From this it was anticipated that the initial feed quality of the coal may have an effect on the degree to which the separation is possible. As a result, a second coal sample of superior quality to the first was obtained from the same coalfield and seam. The experiments were repeated with a blend of the first and second coal samples in the hopes of obtaining more desired results. From here, a fourth variable was introduced to the study as the effect of coal quality on the degree of separation in the ADMFB.

4.2.1 Preparation

The preparation of both coal specimens consisted of five procedures namely; drying, crushing, sieving, sampling and storage. For the purposes of this investigation, as pointed out in the introduction, it is necessary that the surface moisture of the coal is less than $5\%_{wt}$ by weight (Sahu *et al.,* 2009; Terblanche, 2011). Drying of the coal as received was thus required and was undertaken by spreading the sample and allowing it to air dry in ambient conditions, according to the South African National Standard (SANS) 18283:2007, for a period of time. Once dry, the coal was preserved in a number of large air tight barrels to prevent any contamination by undesirable materials or moisture.

In order to obtain the desired coal PSD, crushing and sieving was required. Both coal samples were crushed in a jaw crusher (Samuel Osborne (SA) LTD 66YROLL model) set to ensure a product size smaller than approximately 20mm. Sieving then commenced in order to separate the particles into the five desired particle size ranges. This was done using a sieve shaker and a stack of industrial sieves from which the relevant over and under size were stored in sealed containers and labelled accordingly. The coal of the first sample was used as is for the initial experiments and analyses (discussed in *Chapter 5*) and is hereafter referred to Q-01. The second coal quality was formed from a 50% by mass blend of Q-01 and the other sample obtained (hereafter termed Q-02). Coal quality Q-02 was utilized for the main experimental as is discussed in *Chapter 6*.

It is furthermore of utmost importance to obtain a sample that is representative for the analyses and experimentation to follow. A method known as coning and quartering (SANS 195:2006) was used to secure a representative specimen for the initial interpretation of the coal and all experimental runs. A verification study was conducted on the coning and quartering method to ensure its reproducibility as sampling technique. Three samples were individually generated from the feed batch of +6.7-8.0mm particles and analysed for ash content. The results obtained were 40.60, 40.53 and 37.38$\%_{wt}$ yielding a standard deviation of 1.5 and therefore being within the specifications for good repeatability.

4.2.2 Characterization

The characteristics of each of the prepared coal PSD's were determined by conducting a series of initial analyses. The classification of feed coal is crucial as it stipulates a bench mark from which it is possible to establish whether an upgrade occurred during fluidization or not. From the many characterizations, as discussed in *Chapter 2 Section 2.2.2*, of most importance to this study are density, proximate and CV analyses. A representative portion of the feed coal was obtained from the sample by means of coning and quartering and prepared to the desired -212µm PSD as required by the standard for coal characterization. This was done with the aid of a Fritsch pulverisette 6 that works on the same basis as a regular ball mill. The initial coal characterization analyses are discussed, along with the results obtained, in the sub-sections to follow.

4.2.2.1 Proximate study

A proximate study is conducted in order to ascertain the mass percentage of moisture, volatiles, ash forming minerals and fixed carbon present in a coal sample. It takes advantage of the differences in heat required for the vaporization of moisture and volatiles and also for the combustion of the fixed carbon element. More specifically, the mass loss of a coal specimen under rigid and controlled temperature conditions is used to determine both the moisture and volatile contents. The ash value is then determined by the mass of residue remaining after complete combustion and the fixed carbon content is obtained by difference. The proximate analysis was conducted on both qualities and for each PSD in four consequent stages by determining the following:

- Moisture content in a vacuum oven placed within a climate controlled room and operated at 105°C for 3 hours as stipulated by the SANS 5924:2009;
- Volatile matter in an oven placed within a climate controlled room and operated at 900°C for 7 minutes as stipulated by the SANS 50:2011;
- Ash value in an oven placed within a climate controlled room and operated at 900°C for 6 hours as stipulated by the SANS 50:2011
- Fixed carbon content by difference as stipulated by the SANS 50:2011
- Alternatively, all four stages can be completed in one machine by means of a thermogravimetric analysis (TGA) by the SANS 17246:2011

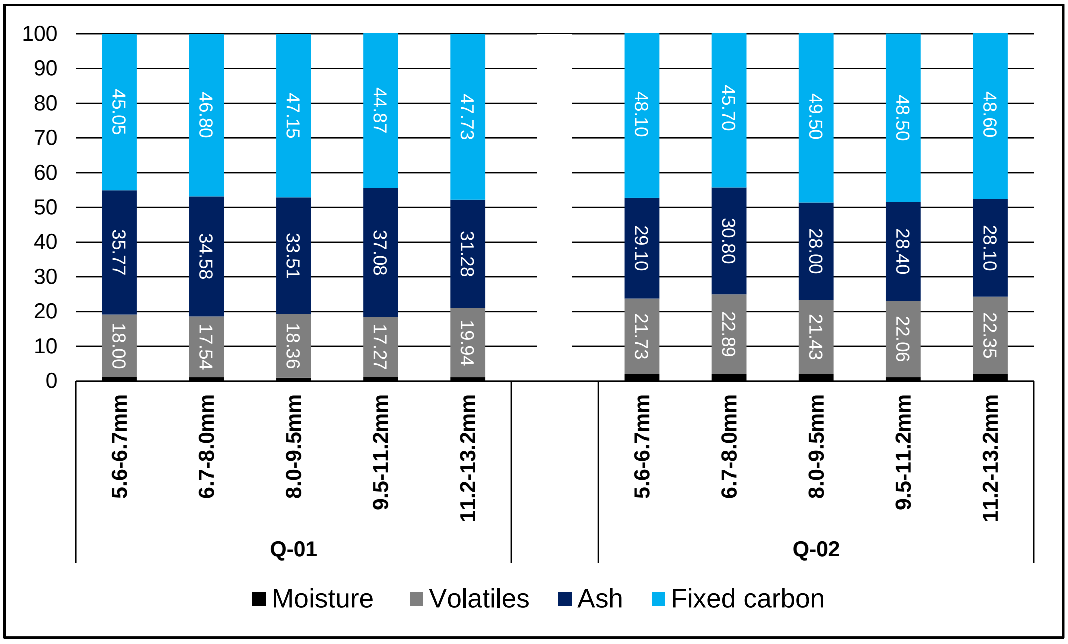

Figure 4.1: Average initial proximate analysis results for each size range of coal Q-01 and Q-02

The clustered stacked column chart portrayed in *Figure 4.1* provides the average initial proximate analysis results as obtained for each PSD of both coal qualities. As depicted, not much difference is noticed between the initial moisture, volatile, ash and fixed carbon values over the PSD's for Q-01. All five particle size ranges contain coal with average moisture-, volatile-, ash- and fixed carbon values ranging in 1.1%$_{wt}$, 18.2%$_{wt}$, 34.5%$_{wt}$ and 46.3%$_{wt}$, respectively. When considering Q-02, the same trend over each PSD is observed with the volatile content being slightly higher than that of Q-01 and conversely the ash value being lower. This provides an initial indication that Q-02 is of somewhat better quality than Q-01 and as a result, may behave differently during fluidization.

The repeatability of the proximate analysis was investigated by analysing the portions of the same sample three times. *Table 4.1* provides the results obtained for the proximate analysis of a sample collected from the top layer of an experimental run with +5.6-6.7mm PSD and no dense medium or vibration.

Table 4.1: Verification studies conducted on the procedure used for proximate analysis

Analysis repeat number	Moisture content (%wt$_{ad}$)	Volatile content (%wt$_{ad}$)	Ash content (%wt$_{ad}$)	Fixed carbon (%wt $_{by\ difference}$)
1	0.62	17.89	36.26	45.23
2	0.66	17.76	34.19	47.39
3	0.95	18.85	31.48	48.73
STD DEV.	0.15	0.48	1.96	1.44

From the low standard deviations listed in the above table, it is clear that the procedure followed for the proximate analysis of the coal samples yields repeatable and accurate results.

4.2.2.2 Calorific value

The calorific or heating value (HV) of a specimen is described as the specific energy required for complete combustion of a unit mass of solid fuel burned in oxygen under specific conditions in a calorimetric bomb. This value can provide an indication of the possible energy (MJ/kg) that a coal sample can release during combustion. An initial gross CV of the two coal qualities (Q-01 and Q-02) was determined in a bomb calorimeter according to SANS 1928:2009. The results obtained for each PSD are summarized in *Table*

4.2 which clearly shows that the calorific values of the different PSD's are comparable to one another ranging in 19 MJ/kg and 22 MJ/kg for Q-01 and Q-02, respectively. The moderately higher calorific values for Q-02 once again prove it consisting of a superior quality when compared to Q-01. Repeatability analyses conducted on the bomb calorimeter reported a standard deviation of 0.68 which proves the accuracy of the equipment

Table 4.2: Initial calorific values (MJ/kg)

PSD (mm)	Calorific value (MJ/kg)	
	Q-01	**Q-02**
+5.6-6.7	18.9	22.3
+6.7-8.0	19.5	21.7
+8.0-9.5	19.8	22.8
+9.5-11.2	18.5	22.5
+11.2-13.2	20.5	22.6

4.2.2.3 Optical analysis

As discussed in *Chapter 2*, particle shape plays a major role in fluidization and can affect the extent to which the particles may fluidize as well as fluidization stability. This in turn affects the efficiency of separation. According to Prusti *et al.* (2015), triangular prisms fluidize easiest followed by the cubical, rectangular and then spherical shapes. An initial visual analysis on the shape of the coal particles was done and *Figure 4.2* shows the general particle shapes present in the sample considered.

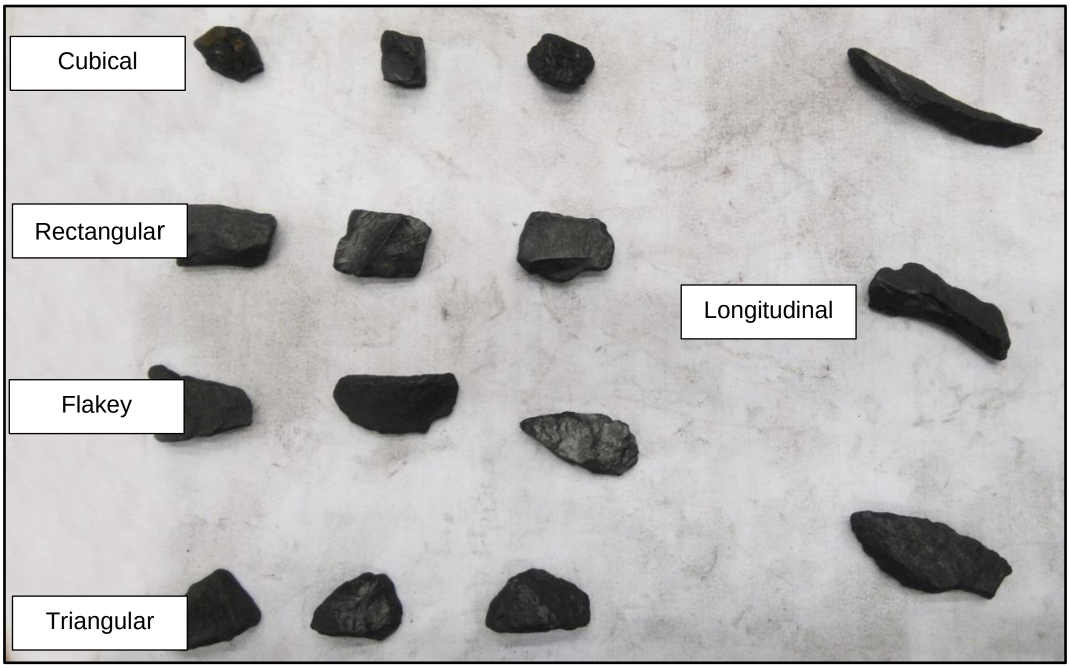

Figure 4.2: General particle shape contained within the sample

There was determined to be no regular pattern to the shape of the particles. Cubical, rectangular and triangular shapes are present along with longitudinal particles and coal flakes. The non-uniform particle shape may have some effect on efficient and stable fluidization and can also contribute to the particle misplacement phenomenon.

4.2.2.4 Density

As detailed in *Section 2.2.2.6* of the literature review, three different forms of density are classified and these are TRD, ARD and BD. The analytic methods used to determine these also differ and as a result, slightly different values can be observed for the same sample depending on density class. An initial TRD was determined for each coal quality and PSD by means of helium pycnometry (SANS 1014:1985). In this method, a sealed sample of known volume is pressurized with a displacement gas and the pressure is recorded. The gas is then allowed to expand into a reference chamber of known volume and once stabilized a second pressure is recorded. The ratio of the pressure drop is compared to a standard and from there a density value can be determined. The helium pycnometer proves to reproduce data well with a standard error of approximately 0.04. *Table 4.3* provides the

TRD results obtained for the +5.6-6.7mm and +6.7-8.0mm PSD's of Q-01 and all five PSD's of Q-02.

Table 4.3: Initial true relative density (g/cm^3)

PSD (mm)	True relative density (g/cm^3)	
	Q-01	**Q-02**
+5.6-6.7	1.88	1.63
+6.7-8.0	1.88	1.61
+8.0-9.5	-	1.63
+9.5-11.2	-	1.63
+11.2-13.2	-	1.60

Due to the heterogeneous nature of coal, the density may vary from particle to particle in a certain population. A more holistic representation of the density of a coal sample can be obtained by means of a washability or float and sink analysis. A mass of coal particles is immersed in a liquid of known density and the proportions floating or sinking are determined (Van der Walt, 1984). This provides a density profile of the entire sample from which an understanding of the coal quality and degree of theoretical separability can be obtained.

A washability study was conducted on the Q-01 and Q-02 samples for each of the specified PSD's. The test was conducted according to SANS 7936:2010 by using zinc chloride solutions for cut-point densities that are increasing by 0.1g/cm^3 from 1.4 to 1.8 g/cm^3. In order to comply with the minimum requirements as stipulated by SANS 7936:2010, a mass of 6kg of coal was used to conduct each study. Four curves are drawn from the data obtained during the study, densimetric, cumulative floats, cumulative sinks and difficulty. *Figure 4.3* contains the densimetric curves obtained from the float and sink analysis of qualities Q-01 and Q-02 for each PSD.

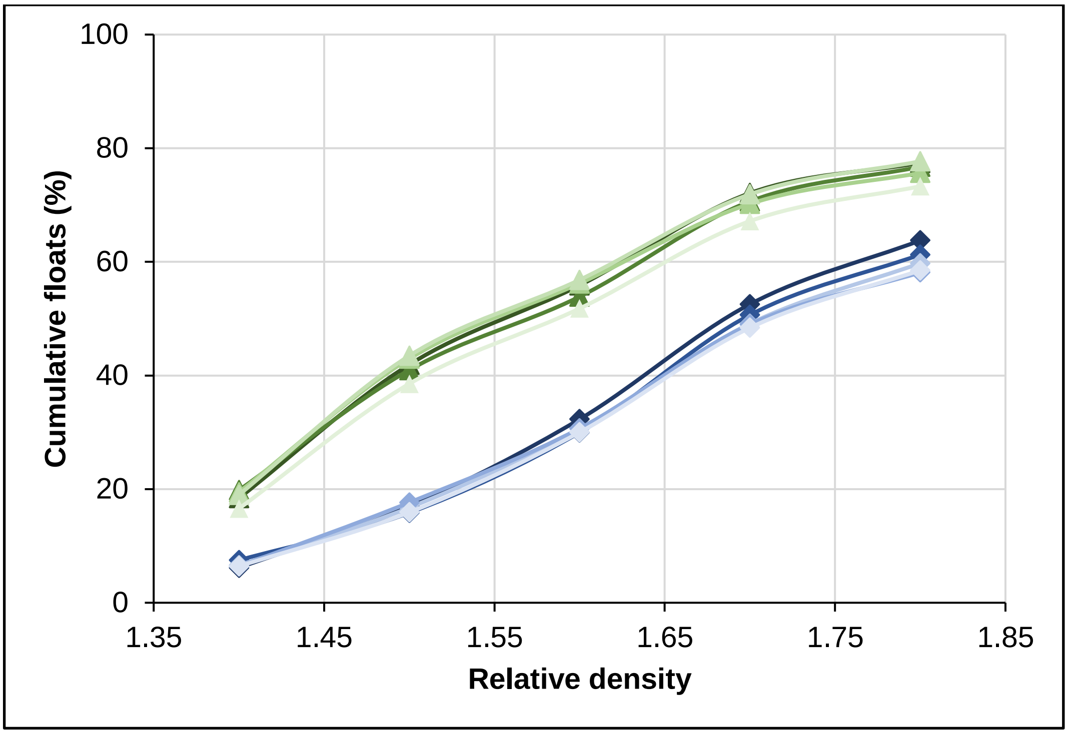

Figure 4.3: Densimetric curves for coal qualities Q-01 (Blue) and Q-02 (Green) across all PSD ranges considered

The curves in *Figure 4.3* provide an idea of the quality of the coal by portraying the percentage of a sample that floats at a specific relative density. The densimetric curves for coal Q-01 are portrayed by the data series depicted by blue diamond shaped markers. The different shades of blue depict the various PSD's. Similarly, the shades of green and triangular markers show the densimetric curves for all PSD's of Q-02. For the coals of quality Q-01 and Q-02, the densimetric curves of all five PSD's are nearly identical. This provides an indication that the mineral content of the coal (dense material) is intrinsic and therefore not extensively liberated through further crushing in the sizes that are considered. Furthermore, for Q-01, 40% of the material sinks at an SG of 1.8 which proves that the sample is largely made up of dense material. The second coal quality (Q-02) can be described as that of better quality because up to 80% of the mass of material floats at a relative density of 1.8.

The cumulative float and cumulative sink curves consist of a plot of cumulative floats yield to cumulative floats ash and cumulative sinks yield to cumulative sinks ash, respectively. From these diagrams the ash value of a product (cumulative floats) and discard (cumulative sinks) can be predicted for a desired yield. The cumulative floats curves for coal qualities Q-01 and Q-02 in sizes (+5.6-6.7mm) and (+11.2-13.2mm) are provided in *Figure 4.4*.

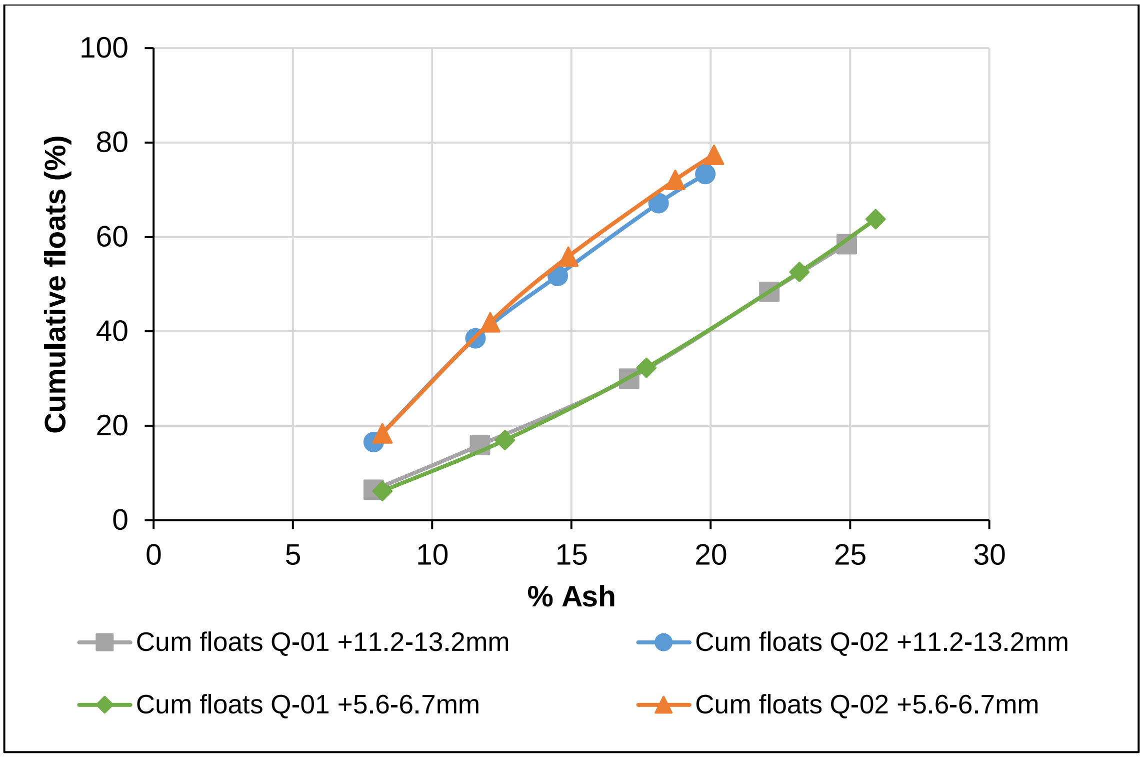

Figure 4.4: Cumulative floats curves for Q-01 and Q-02, PSD (+5.6-6.7mm) and (+11.2-13.2mm)

Apparent from *Figure 4.4* is that a higher yield is obtainable for Q-02 at lower ash content when compared to Q-01 and that the smallest and largest PSD's behave similarly. Not portrayed on the graph, for ease of reading, are cumulative floats for the three middle size ranges because they are similar to the ones shown. The cumulative sinks curves are also not displayed but are available in *Appendix B.*

An index of coal washing difficulty can be used to determine the degree of ease of separability and was proposed by Byron Bird as the amount of near dense material between arbitrary relative density limits (Van der Walt, 1984). The so called ± 0.1 distribution at a particular relative density (*X*) is merely the amount of material lying between the densities of (*X-0.1*) and (*X+0.1*). A low D_X value is indicative of a simple degree of difficulty and a sample with value above 25 proves formidable to separate (Van der Walt, 1984). Tabulated, in *Table 4.4*, are the degree of difficulty values calculated for an assumed range of relative densities from 1.5 – 1.8 as obtained from the densimetric data.

Table 4.4: Degree of difficulty of washing of the coal samples for a range of relative densities

PSD	Q-01				Q-02			
	$D_{1.5}$	$D_{1.6}$	$D_{1.7}$	$D_{1.8}$	$D_{1.5}$	$D_{1.6}$	$D_{1.7}$	$D_{1.8}$
+5.6-6.7	26	36	31	47	37	30	22	28
+6.7-8.0	22	35	31	49	34	30	23	29
+8.0-9.5	24	32	29	51	37	27	19	30
+9.5-11.2	24	31	27	51	38	28	21	28
+11.2-13.2	24	32	29	52	35	29	22	33

As visible from *Table 4.4*, most of the data points report to a difficulty value above 20 which Van der Walt (1984) stipulates as very difficult to wash. It is clear that a cut-point density of 1.5 for Q-01 and 1.7 for that of Q-02 provide the lowest degree of difficulty.

4.3 Magnetite

A standard coarse grade magnetite sample was obtained from the Witbank region situated in Mpumalanga, South Africa. Magnetite, as previously mentioned, is available in South Africa as a by-product from copper mining operations. Consequently, it has been extensively processed and generally reports to a very fine size fraction that contains a large amount of moisture (De Korte, 2016).

4.3.1 Preparation

Upon arrival of the magnetite sample, it was oven dried at 100°C to ensure a moisture level below 5% by weight. This is in conjunction with the requirement of low moisture in the coal as stipulated by Sahu *et al.* (2009) and Terblanche (2011). In a moist magnetite sample, particles could agglomerate and further stick to the coal and bed walls, thus inhibiting proper fluidization. Once dry, the magnetite sample was preserved in a number of large air tight containers to prevent any contamination by undesirable materials or moisture.

Due to the extreme powdery nature of the magnetite as received, it was necessary to sieve out the larger particles to be used during fluidization. He *et al.* (2016a) stipulated that magnetite particles ranging from +0.074-0.3mm produced a stable fluidized bed. Therefore, only the magnetite particles that reported to the +0.3mm particle size range, after sieving, were utilized.

4.3.2 Characterization

The characteristics of the magnetite sample was determined by conducting a series of initial analyses with regards to size, shape and density. These, along with the results obtained, are elaborated upon in the subsections below.

4.3.2.1 Size determination

A sizing analysis was conducted on a representative sample of the magnetite in order to determine the average size of the particles. This was done with a Malvern Mastersizer 2000 that makes use of laser diffraction and blue light technology to determine the size of each individual particle in the sample. From this, it was determined that the d(10), d(50) and d(90) size values of the magnetite are 0.31mm, 0.49mm and 0.93mm, respectively. Of the total sample, 10% therefore reports below 0.31mm, which confirms that most of the magnetite sample is above the range as stipulated by He *et al.* (2016a) and will most likely yield a stable fluidization.

4.3.2.2 Shape and density

If viewed under a microscope, the shape of the minute individual magnetite particles can be described as spherical. These particles do however agglomerate and form irregular shaped specimens that report to the (+0.3mm) size fraction. Upon fluidization, these composites break up into their finer counterparts and may have an effect on the fluidization stability and dust control measures applied to the bed. As with the coal sample, helium pycnometry was used to determine the initial TRD of the magnetite powder. The operation of the apparatus is discussed in *Section 3.2.2.*4. A TRD of 4.8 g/cm^3 was found for the magnetite sample yielding a percentage error of 0.12.

4.4 Experimental procedure

Section 4.4 elaborates on the procedure undertaken during the experiments. A clear and reproducible method is imperative during investigation to ensure that deviations in operating and sampling of the bed do not affect the results.

4.4.1 Experimental plan

An experimental plan was constructed as a guideline to aid in meeting the aim and objectives of this study as stipulated in *Section 1.2*. An array of experimental runs are required in order to test the influences of the different parameters, namely; variation in coal PSD, addition of dense medium in two different mass ratios and activation of vibration. The experiments were divided into two main groups. Initially the study was conducted using coal quality of Q-01 but seized after the first two size ranges (+5.6-6.7mm and +6.7-8.0mm) due to the poorer quality of Q-01 seeming to have an effect on fluidization. The coal was then blended as described in *Section 3.2.1* to form Q-02 and the experiments completed on Q-01 were repeated along with the conductance of the rest of the required studies. A schematic representation of the experimental plan is given in the flow chart in *Figure 4.5*. From this figure, it is clear that a number of 12 experiments are needed for the Q-01 sample and that 30 are required for Q-02 in order to meet the objective of study. Furthermore, a set of random verification experiments are planned for each variable in consideration. For each of the 42 runs, proximate, CV and TRD analyses are conducted on a sample of the feed and each of the bed layers.

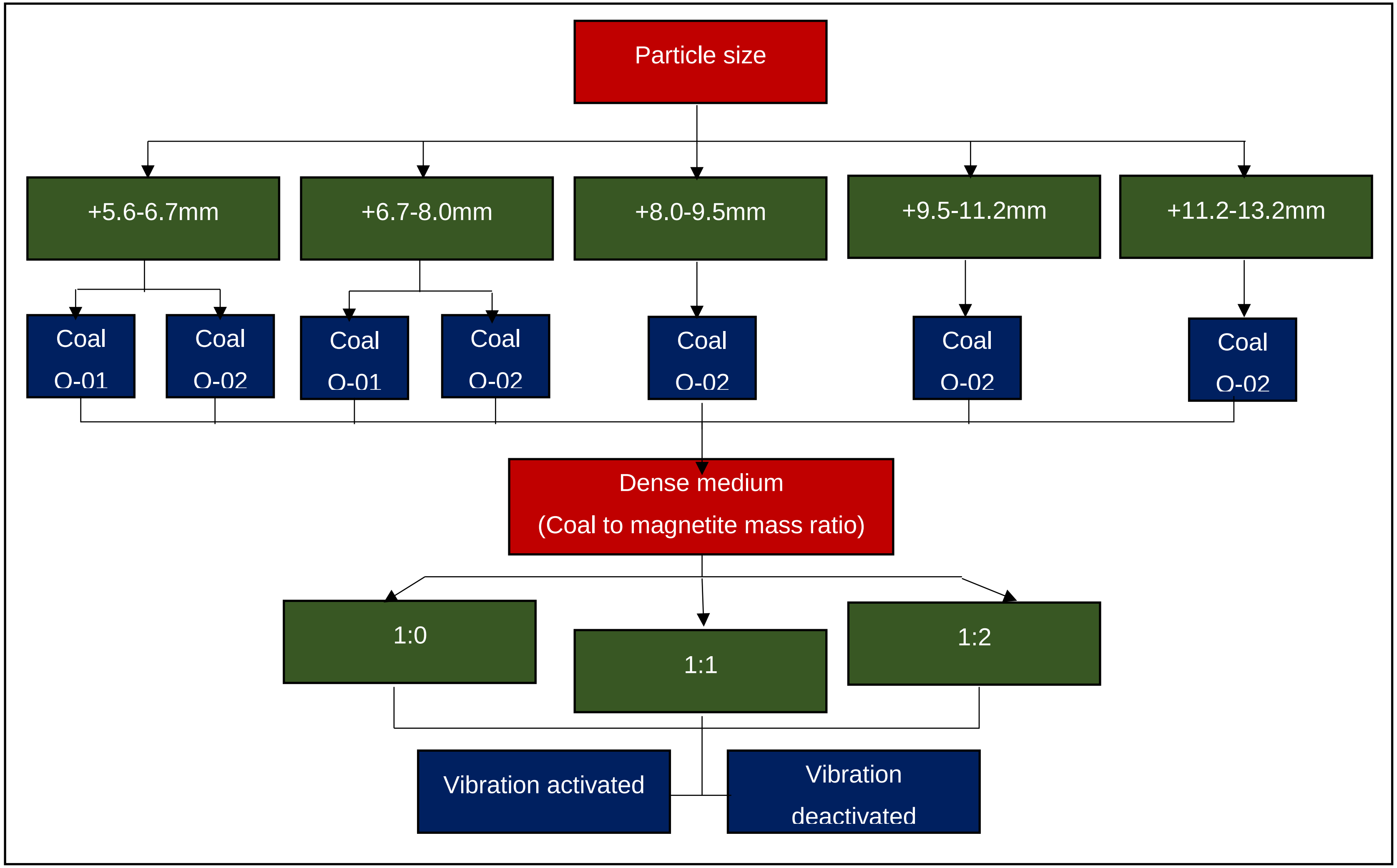

Figure 4.5: Experimental plan

4.4.2 Bed and sample preparation

The ADMFB is assembled as portrayed and discussed in *Section 3.4* and loaded with a specific mass of the desired sample. For beds of coal running without magnetite, the mass ranges from 15 – 18kg and fills approximately 4 bed layers (static bed height of 0.2m) and for those running with magnetite, a total mass load of 15kg is used attaining a bed height of approximately 0.15m in 3 layers.

Firstly, the correct mass of coal and magnetite were measured and a representative sample of the coal was collected by means of coning and quartering (for analyses). Coning and quartering further aids with mixing the sample beforehand to ensure a homogenous distribution of the varying density coal particles. For the experiments where magnetite is not considered, the bed was loaded with the coal alone. Where magnetite is considered in a 1:1 ratio, 7.5kg each of coal and magnetite were weighed, mixed and loaded into the bed and for the 2:1 ratio 5 and 10kg of coal and magnetite, respectively, were similarly prepared. The mixing of the sample prior to loading is necessary to ensure that the coal and magnetite are evenly distributed. An uneven distribution of material may lead to ineffective fluidization as a result of the uneven density distribution across the bed. Once the bed was loaded and assembled, the pressure probe was inserted so that it is positioned approximately 1 cm from the distributer plate.

4.4.3 Fluidization

The air was then initiated by setting the input frequency of the fan to approximately 20Hz, delivering an average air velocity ranging from 0.1 – 8.5m/s depending on the amount of dense medium used. The air flow was gradually increased by adjusting the frequency inverter and the associated velocity, temperature and pressure were recorded for each increment. As discussed in the literature study under *Section 2.4.3*, the dip in pressure drop across the bed indicates the incipient fluidization point. At this stage the bed expands slightly as a result of bubble formation. A number of factors dictate the MFV, as listed in *Section 2.4.2*, and consequently the construction of pressure drop vs. superficial velocity curves for each variable is crucial. It is however necessary to operate the bed at a velocity just above the minimum fluidization point. As detailed in *Section 2.4.2*, no concrete guidelines are available for the exact amount that the velocity should be higher than MFV. It is therefore imperative to closely observe the bed and thereby ensure that bubble formation is adequate and that slugging and turbulence are not experienced in the bed. This was manually approached by means of adjusting the air flow to increase if the bubbles are too small and conversely if the bubbles are too large, the air flow is reduced slightly. Additional to these curves a study to determine the bed pressure and density was undertaken. This was done by means of extracting the pressure probe in increments of 0.05m and reading the water height on the manometer. Once adequate fluidization was achieved the particles were allowed to settle and then once again fluidized at the predetermined velocity for a selected amount of time.

4.4.4 Activation of vibration

For the experiments where vibration is considered, the vibration to the bed was introduced at a point before complete fluidization was established. The parameters of vibration remained constant at 20Hz and 0.3-0.7mm for frequency and amplitude, respectively. Upon the initiation of vibration to the system, the pressure drop vs. superficial velocity curve was drawn to determine the MFV. A study conducted by Macpherson and Gavin (2010) proved that the addition of vibration to an ADMFB reduces the minimum fluidization velocity. Further elaborated upon by He *et al.* (2015), the addition of vibration also allows for a more stable pressure behaviour in the bed and thereby a steady fluidization occurs. Some emphasis is placed on both increased and decreased frequency and amplitude values in *Section 2.5.2* but there is also evidence that if activated too early, the vibration causes the finer particles to segregate to the bottom making the bed more compact and proving difficult for the air to move through the bed evenly. Upon completion of the experiment, the vibration was deactivated before gradually decreasing the air flow and allowing the particles to settle back into packed bed state.

4.4.5 Sampling

After the fluidization commenced and the airflow and vibration were switched off, the bed was allowed to stand for a short period of time to ensure that the particles have in fact settled and therefore no further movement was expected if the bed were to be disturbed. It further made certain that no ultra-fine particles escaped during disassembly of the bed. The bed was then disassembled layer by layer from the top. Once the point where the material resides (bottom four layers) was reached, each layer was individually sampled with the aid of a sample cutting plate. This is illustrated in *Figure 4.6*.

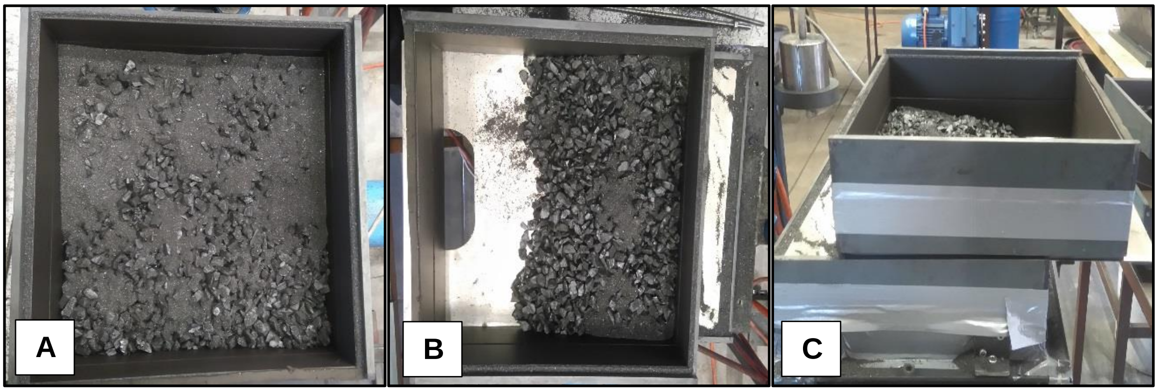

Figure 4.6: Illustration of sampling technique

In *Figure 4.6*, the image on the left (A) illustrates an aerial view of the packed bed after fluidization for a sample of coal and magnetite. The picture in the centre (B) shows the cutting tool inserted as from left to right and the figure on the right (C) provides a side view of this. The sampling tool was inserted at the bottom of the layer to be collected and slid across the area of the equipment effectively cutting the bed. The sample on top of the plate was collected into a bucket through the opening in the sampling plate (as seen in *Figure 4.6 B*) and then weighed. This was repeated for each layer of the bed until empty.

4.4.6 Medium recovery

After sampling of the bed, the magnetite and coal required separation. If this is not done effectively, some medium can remain in the coal sample, influencing the proximate, CV and density values. Magnetite consists mostly of mineral matter and therefore adds to the ash yield fraction of the coal if analysed along with the coal.

This separation was completed in two stages. Firstly, the coal and magnetite were separated by sieving and due to the large particle size difference; a sieve with an aperture of 0.85mm was used. This was approached manually until the magnetite was visibly removed from the coal sample after which advantage was taken of the magnetic properties of the dense medium. A hand magnet placed in a plastic bag was drawn across the coal sample to remove any magnetite residue that remained after sieving. Once separated, the coal and magnetite were weighed in order to conduct a mass balance over the system and so ensure that minimal losses occurred.

4.4.7 Analyses

On completion of weighing, the separated samples were pulverised in a ball mill until an adequate amount of -0.21mm was obtained. The pulverised samples of the feed and each layer of the bed were analysed to determine the separation efficiency of the ADMFB by conducting the following analyses:

- Ash value (weight %) according to SANS 131:2011,
- Calorific value (MJ/kg) according to SANS 1928:2009 and
- Density (g/cm^3) according to SANS 1014:1985

The results obtained from each run and the various repeats thereof as described by the experimental plan are presented and discussed in *Chapters 5* and *6*.

4.5 Safety measures

The safety of practices occurring in an around a laboratory are of the utmost importance. It is essential to consider the harmful and dangerous effects of the experimentation upon oneself, fellow colleagues and equipment. This is to ensure that measurements and mitigations can be set into place to prevent any permanent damage to oneself or laboratory equipment. Consequently, a hazard identification risk assessment (HIRA) was conducted in order to make sure that all participants in the experimentation are aware of any dangers that the operations possess and how to, from there, ensure their safety. The HIRA conducted for this study is given in *Appendix C*.

4.6 Observations during optimization and bed operation

Some observations regarding the behaviour of the bed during optimization and operation were noted. These relate to pressure stability, bed vibration, particle attenuation, material losses and medium behaviour. The procedure for optimizing the ADMFB in terms of MFV and time is extensively discussed in *Chapter 5 that follows*.

4.6.1 Minimum fluidization requirements

Some trends regarding the MFV were observed in that it was found that the incipient fluidising velocity decreases if vibration is activated and also for increasing DM ratio, but shows no significant difference as a result of PSD. This correlates with what is found in literature and remained unaffected by the change in quality of the coal.

4.6.2 Observations of bed behaviour

4.6.2.1 Pressure

One of the bed design objectives was to ensure that the flow of air out of the bed was not hindered as this causes a build-up of air within the bed which ultimately supresses the fluidized particles. This phenomenon was observed the previous small scale ADMFB employed at the NWU and negatively affected the separation efficiency. As detailed in *Chapter 3*, an additional 0.3m bed layer and a final tapered trapezoidal layer was considered necessary to ensure enough room for movement of the particles and no accumulation of air within the top section of the bed. The tapered trapezoid further contains a large surface area and 0.1mm wire mesh through which air can easily diffuse. In terms of the above design structures put in place, effective prevention of air accumulation in the bed was observed and fluidization was not affected thereby.

4.6.2.2 Vibration

Some observations were made concerning the influence of vibration on the operation and structure of the ADMFB. As stipulated, a clear decrease in MFV was noted along with a more stable pressure drop within the bed. However some additional occurrences should be highlighted. A larger backpressure was experienced when activating vibration, indicating that segregation has occurred resulting in the particles packing more densely in the bed. This may have a negative effect on fluidization and consequently the ability for particles to move in the bed. A further indication of this behaviour is that when sampling the bed after fluidization with vibration the static bed height was slightly lower than before experimentation had commenced. *Figure 4.7* illustrates the particle packing before and after the bed was switched on with vibration.

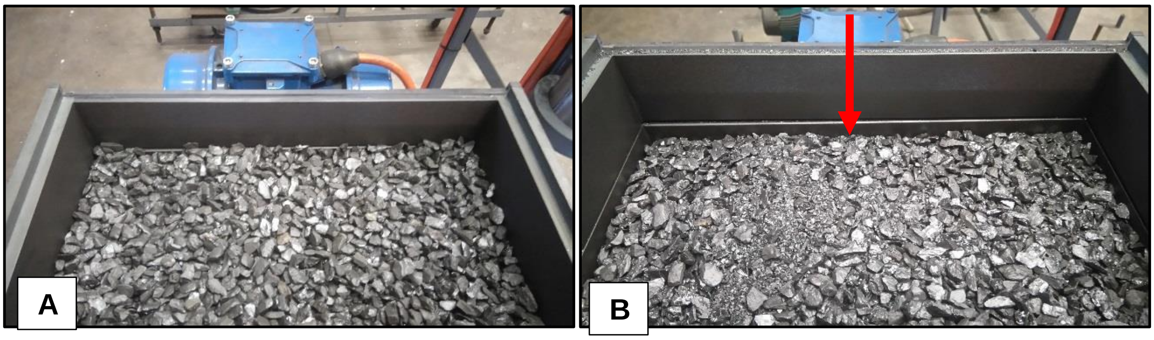

Figure 4.7: Dense packing from vibration on static bed height (A) initial (B) post experiment

Figure 4.7 shows a decrease in bed height after experimentation with the addition of vibration. This is shown by the red arrow in *Figure 4.7 (B)* illustrating the decreased bed height after experimentation as in comparison to that in *Figure 4.7 (A)* before onset. This may indicate that the vibration frequency, amplitude, onset, and offset timing were not ideal for the experiments conducted.

4.6.2.3 Particle attenuation

Also visible from *Figure 4.7 (B)* in comparison to *(A),* is the formation of fine coal particulates due to attrition in the bed. When fluidizing the bed, coal particles may fragment into smaller particles due to particle-particle interactions, particle-medium interactions, particle-wall interactions or breakage during sampling. These smaller particles were observed to fluidize in the higher portions of the bed and contribute generally to the top layer of the bed after the air flow is terminated. Even though the extent of particle fragmentation was not measured quantitatively, it may have affected the accuracy of the material balances executed on all experimental runs by adding to the medium portion of the bed. Furthermore the effect of the broken coal pieces on the stability of the fluidized dense medium bed is not known and may lead to insufficient fluidization.

A study conducted by Lagner *et al*. (2016) brought to light some points regarding the attenuation in an ADMFB. Lagner *et al*. (2016) established that coal attenuation is not as a result of vibration or coal-medium interactions and is most likely a cause of coal particle abrasion with each other, the bed walls and during sampling. Additionally found was that the coal particle breakage in fact reduced with the use of dense medium during fluidization. This is due to the fact that the medium is less abrasive than that of the coal particles. Since the addition of medium reduces the coal interactions with one another and increases those with the medium. The addition of a medium therefore reduces the effect of particle attenuation (Lagner *et al*., 2016).

4.6.2.4 Material losses

Experimental losses recorded for the coal across all variables ranged from 0.35 to 9.6% and may be attributed to loss of particles during sampling. Losses observed for magnetite were between 0 and 6.5% and are most likely as a result of magnetite blowing from the bed during operation and sampling losses. The magnetite powder has an extremely fine nature and a tendency to form the ultra-fine particulate agglomerates which break up during fluidization. This results in magnetite excreting from the bed crevices and also the top of the bed. In order to prevent this, only magnetite of +0.3mm was used and the tapered trapezoidal head layer (presented in *Chapter 3*) prevents most of the ultra-fine de-agglomerated particles to escape the bed. Furthermore, the use of adhesive tape over the crevices where the layers join prevented the fine material from escaping the bed. Even though these preventative measures were undertaken, it did not fully prevent the spillage of the medium entirely. It is unlikely that magnetite contamination in the coal is the cause of dense medium losses due to the large relative difference in size of the coal magnetite particles and the extensive magnetic separation procedure followed, after size separation. This further allows for the repeated use of the same magnetite but one must note that effective separation is required as a too large a contamination of the medium with fine coal particles could change the manner in which the medium fluidizes and also the stability thereof.

4.6.2.5 Medium behaviour

A major issue during operation was the behaviour of the magnetite during fluidisation. As established by Zhang *et al*. (2014) and He *et al*. (2016) medium size is directly proportional to the degree of fluidization stability in the bed. A +0.074-0.300mm medium size was recommended; however, the introduction of coarser magnetite was anticipated to improve medium performance during fluidization (Zhang *et al*., 2014). As previously determined, magnetite finer than 0.074mm will cause severe instability (He *et al.,* 2016), and therefore, medium preparation was essential in ensuring that magnetite with a mean particle size of 493.59µm was used for the execution of this study. Despite the employment of coarser magnetite, the mean coal size to mean medium size ratio is approximately 13.4; hence, classifying the magnetite particle type as a Gerhard type C. As previously predicted, a degree of fluidization difficulty was experienced during operation, due to the solid-like behaviour of the magnetite, which will be explained in the subsequent paragraph.

The congealed-state of the magnetite can be explained by the gas-solid forces being weaker than the inter-particle forces, causing the coagulation behaviour. More specifically, the resistance caused by the firmly packed medium inhibits air flow through the inter-particulate voids of the magnetite, and therefore causes a slight pressure build-up underneath the bed of magnetite. Once the air velocity reached a point where the upward force was extensive enough to overcome the inter-particulate forces, a normal particulate fluidization behaviour was experienced in the bed.

Similar behaviour was observed when coal was introduced in addition to the magnetite. The packing of the coal-magnetite beds was of importance as it may influence the initial superficial velocity experienced in the bed in a similar manner as previously explained. These beds were made up by adding a third of the feed coal onto the bed surface, then half of the required magnetite. This was repeated until all the material was homogeneously mixed in the bed.

4.6.2.6 Air channelling

Some channelling of air was observed in the bed but mostly in the corners, along the sides or in the middle were the pressure probe was inserted, as illustrated in *Figure 4.8.*

Figure 4.8: Air channelling visible in the bed

It is believed that the channelling was attributed to the properties of the medium and square shape of the bed instead of the distributor unit. These effects will influence the beneficiation of the coal with the use of magnetite as medium, as perfect fluidisation of these runs may not be established due to the formation of dead zones within the bed.

4.7 Chapter summary

At this point in the thesis, the characteristics of the materials, planning and experimental procedure are well understood. The fundamental process and basic mechanical design of the bed is also comprehensively detailed and the equipment used for the investigation is well defined. The chapters that follow endeavour to display and explain the results obtained from the array experiments as discussed in this chapter and conclude as to the effectivity of the ADMFB considering the objectives as stipulated in *Chapter 1*.

Chapter 5: RESULTS ON POORLY LIBERATED (HIGH ASH) COAL

This chapter presents the data obtained for the set of preliminary experiments conducted on the poorly liberated (high ash) coal, as described in *Section 4.4*. The experimental work began with investigating two of the considered PSD's (+5.6-6.7mm and +6.7-8.0mm) using coal quality Q-01. However, the poor quality of Q-01 seemed to have an effect on the extent of separation in the bed. As a result a coal of improved quality was blended with $50\%_{wt}$ of a new sample and Q-01, forming the Q-02 quality with which those listed, and more PSD's were tested. *Chapter 5* consists of the following sections:

- **Section 5.1:** Provides an overview of the study problem and details the associated objectives. It further focusses the reader to the initial data obtained and explains the variables considered.
- **Section 5.2:** Details the procedure undertaken to optimize the fluidization process for the +5.6-6.7mm and +6.7-8.0mm particle sizes in terms of minimum fluidization requirements and operating time.
- **Section 5.3:** Presents the experimental and analysis results obtained for the two Q-01 PSD's while considering amount of dense medium and activation of vibration along with the discussions thereof.
- **Section 5.4:** Consists of the results and associated discussion from a set of auxiliary experiments conducted to aid in describing the phenomena observed with regard to the extent of separation as a consequence of coal quality.
- **Section 5.5:** Concludes the chapter and highlights the most important points named therein. It further links the initial findings chapter to that of the chapter that follows with the results of an improved coal quality blend.

5.1 Overview

The main aim of the project is to determine the separation efficiency of ADMFB technology in beneficiating South African small coal and to test the effects of (1) PSD, (2) the addition of dense medium (DM) and (3) vibration. As mentioned, in Chapter 4, selected initial tests were conducted on a coal of quality Q-01 through which some observations of the effect of feed coal quality were noted. For the purposes of *Chapter 5*, these tests were then repeated on specific runs for the coal quality of Q-02. A modified experimental flowchart is provided in *Figure 5.1*, detailing the experiments that were considered as part of the runs conducted on the poor (high ash) coal and those repetitions conducted on the better (low ash) coal.

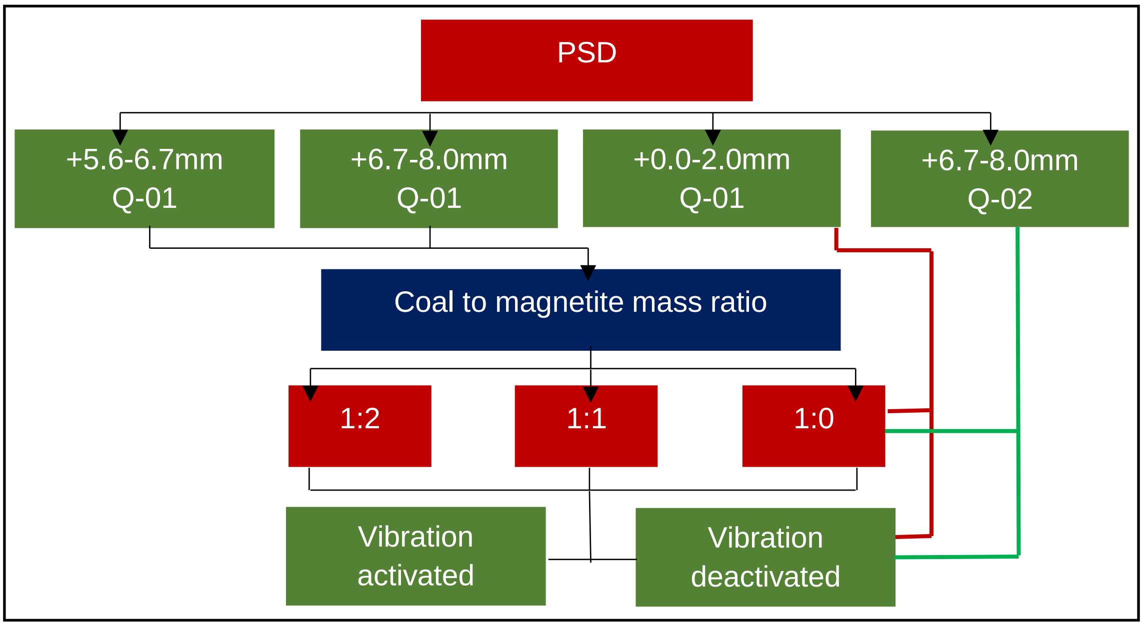

Figure 5.1: Schematic of the experimental flow for the initial findings chapter

It is apparent, by following the black arrows in *Figure 5.1*, that two particle size ranges were arbitrarily selected for investigation and subsequently tested alongside three medium to coal ratios and two states of vibration. A study on the effects of complete liberation of the particles was then done by crushing the sample to below 2mm and conducting a fluidization experiment therewith - the red line in *Figure 5.1* indicates this. Moreover, the green line indicates a test conducted on a sample of +6.7-8.0mm Q-02 coal to see the effect of utilizing and improved coal quality blend. During the initial study, an extensive set of data was generated with each ADMFB run consisting of approximately 4 layers and a feed sample. Determinations of CV, ash yield percentage and density were completed for the feed sample as well as each individual bed layer as discussed in *Section 4.4.7*. Furthermore each experimental run was first optimized for MFV and operating time.

5.2 Optimization

Operation of the ADMFB equipment at optimal conditions cannot be stressed more and therefore some additional experiments were required. Optimization of the bed consisted of MFV determination and tests conducted to determine the most effective operating time.

5.2.1 Minimum fluidization requirements

A theoretical approach for determining the minimum incipient point in a fluidized bed is obtained from an adjusted form of the Ergun equation, as discussed in *Section 2.4.2*. However, one must note that the results obtained are only related to a singular particle suspended in a fluid. In order to observe the minimum fluidizing point for a particulate bed, an experimental procedure was followed as explained throughout *Sections 2.4.3* and *4.4.3*. By this method, the MFV was experimentally determined by incrementally increasing the superficial velocity until such a point where the observed static pressure of the bed was visibly lower than that of the bed pressure.

5.2.1.1. Pure magnetite bed

The experimental determination of the MFV in an ADMFB packed with only magnetite is portrayed in *Figure 5.2.* It provides a typical bed pressure drop vs. superficial velocity curve for a run conducted with +0.3mm magnetite particles yielding a packed bed height 0.15m with vibration deactivated.

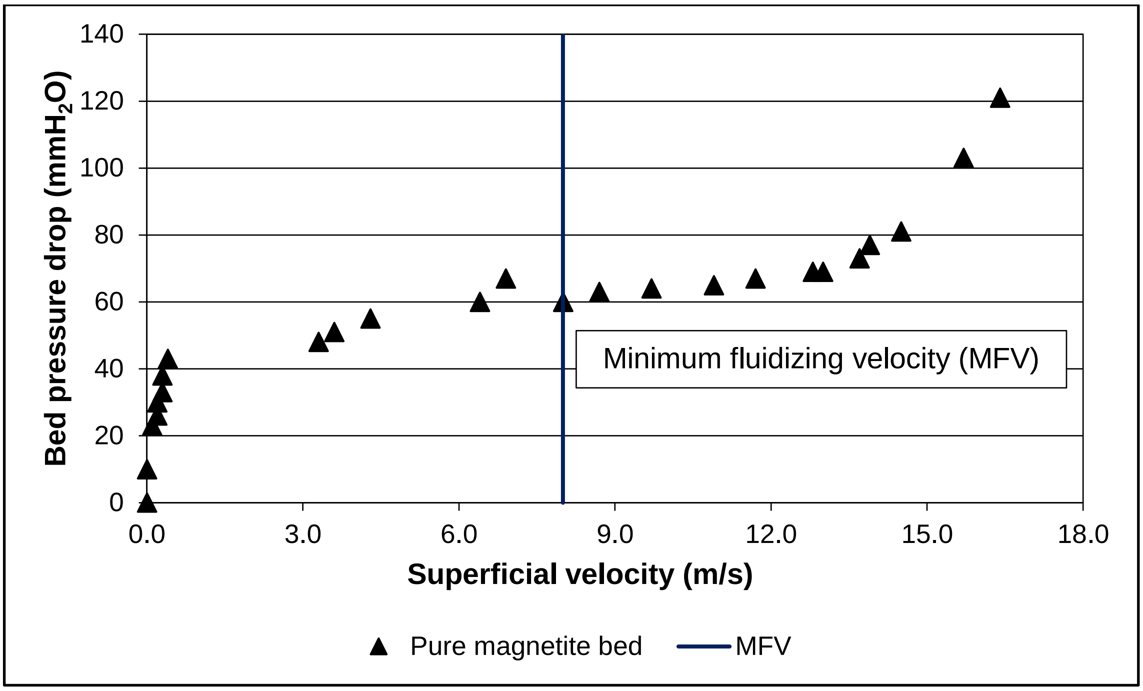

Figure 5.2: Bed pressure drop vs. superficial velocity for bed packed entirely with magnetite

The trend observed in *Figure 5.2*, is characteristic of a typical pressure vs. velocity curve with the exception of the initial points. As the superficial velocity is increased from 0m/s the pressure drop climbs until a pressure drop of 67mmH_2O is observed. At a velocity of 8.0m/s the pressure drop slightly decreases (60mmH_2O), corresponding to the minimum fluidizing velocity which is indicated by the line in the graph above. Henceforth, the pressure stabilizes slightly for velocities ranging from 8.7-12.6m/s and then rises as the bed reaches a more turbulent flow regime. From the bed height and pressure readings, the density of the magnetite particulate suspension was found as 1.31g/cm^3.

The anomaly observed with the velocity of the initial points (Figure 5.2) is attributed to the dense packing caused by the very fine magnetite particles and the means of controlling the blower output. A slight back pressure is experienced in the bed as a result of the closely packed magnetite particles. This affects the velocity reading as air flow is not directly controlled but measured as a consequence of adjusting the blower input frequency. The back pressure however dissipates at a point well below minimum fluidization.

5.2.2.2 Pure coal and coal-magnetite beds

As a comparison, a typical bed pressure drop vs. superficial velocity curve for an experiment conducted on a +5.6-6.7mm pure coal bed and no vibration is given in *Figure 5.3*. The bed mass and height report to 10.8kg and 0.15m, respectively.

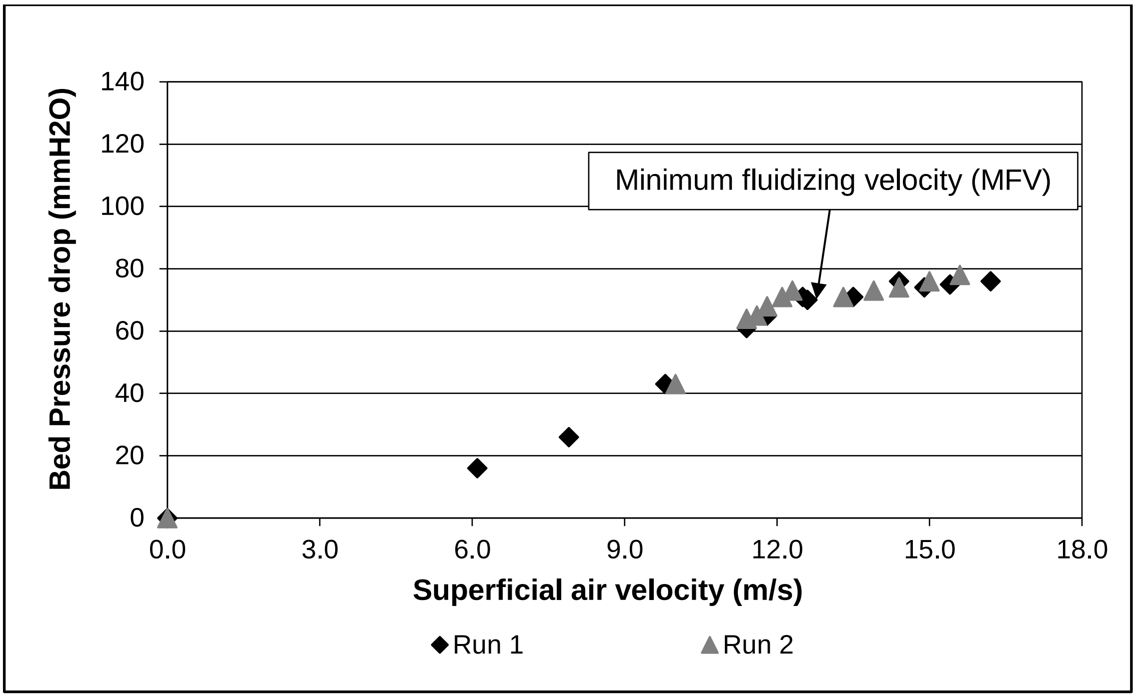

Figure 5.3: Bed pressure drop vs. superficial velocity (Q-01; PSD +5.6-6.7mm; DM 0:1; VD)

The expected trend is visible for the curves in *Figure 5.3*, with MFV, bed pressure drop and bed density of 13.3m/s, 71mmH_2O and 0.67g/cm^3, respectively. Literature provides some guidelines for operating an ADMFB bed, with regards to MFV. He *et al*. (2015) and Zhao *et al*. (2015) found that factors of 1.6 to 1.8 times MFV were optimal for operation; however, one should keep in mind that these guidelines might be bed and coal specific. As a result, the point above MFV at which the current commissioned ADMFB was operated was chosen for each experiment individually by a MFV determination as depicted in *Figure 5.3*. Close observation of the behaviour of the fluidized material in the bed was ensured and from there the point of fluidization was manually controlled. A relation for the fluidizing velocity mentioned above is provided in *Equation 5.1*.

$$U = U^* \times U_{mf} \tag{5.1}$$

U and U_{mf} represent the fluidized- and minimum fluidized velocity, respectively. U* denotes a scaling factor in order to achieve fluidization stability in the bed. A summary of the minimum fluidization and operating fluidization requirements for all 12 initial runs is provided in *Table 5.1*.

Table 5.1: Minimum and operating fluidization requirements for the initial study

PSD	Medium	Quality	Vibration	Bed mass (g)	Layer	u_{mf} (m/s)	u*	u (m/s)
(+5.6 -6.7) mm	DM (0:1)	Q-01	VD	11010	4	13.30	1.21	**16.10**
	DM (1:1)			15000	4	13.50	1.10	**14.80**
	DM (2:1)			15000	3	11.50	1.33	**15.30**
	DM (0:0)		VA	6700	3	10.40	1.21	**12.60**
	DM (1:1)			15000	3	13.00	1.08	**14.10**
	DM (2:1)			15000	3	10.90	1.05	**11.50**
(+6.7 -8.0) mm	DM (0:1)	Q-01	VD	15160	4	13.50	1.20	**16.20**
	DM (1:1)			15000	4	12.40	1.16	**14.80**
	DM (2:1)			15000	3	10.80	1.22	**13.20**
	DM (0:1)		VA	15760	4	12.20	1.09	**13.30**
	DM (1:1)			15000	3	10.00	1.23	**12.30**
	DM (2:1)			15000	3	10.50	1.00	**10.50**

From *Table 5.1*, it is clear that a slight decrease in U_{mf} is expected for increasing DM ratio in most cases with some deviations observed. As expected, a slight decrease in MFV is observed when vibration is activated and can be seen with almost all of the experimental runs in *Table 5.1*. The minimum incipient point did not seem to be significantly affected by the change in PSD. In some cases, the +6.7-8.0mm particles produced either lower or higher MFV's than the +5.6-6.7mm range. This could be as a result of the differing number of layers and bed masses. In *Table 5.1*, the scaling factors used to determine the point at which to operate the bed above MFV are listed, and range from 1.00 to 1.33.

A final note with regard to minimum fluidization - when fluidizing a particulate bed containing a dense medium and coal mixture, the magnetite is suspended and the coal merely separates according to the relative density difference. The MFV of a pure dense medium bed of 15kg was found to be 8.00m/s (*Figure 5.2)* with a bed density of 1.31g/cm^3. As a result, the minimum incipient point of the dense medium beds should not differ drastically if the static bed height remains relatively constant. The decrease in U_{mf} observed when increasing DM ratio is most likely as a result of the slight difference in the static bed height and not as a result of the amount of magnetite added.

In this study, the determination of the minimum incipient point for dense medium beds occurred in a similar manner to that of the pure coal beds. This is because of the slight variation in static bed height occurring due to the maximum load of the bed. A note is made of the scaling factor as compared to the MFV of a pure magnetite bed. The results obtained for the scaling factor of the magnetite-coal beds as compared to the magnetite only bed ranged from 1.25 to 1.69 which moderately correlates with the factors as stipulated by He *et al*. (2015) and Zhao *et al*. (2015).

5.2.2 Operating time

Fluidizing time plays a significant role in obtaining optimal separation as a prolonged operating time may lead to back-mixing in the bed (Luo, *et al.*, 2015). Therefore, time optimization experiments were conducted by operating the fluidized bed for five, ten and fifteen minutes at the operation velocity conditions as determined in *Table 5.1*. From the values for ash obtained in the top and bottoms layers of the time test runs, it was decided which time requirement is best. Proximate analyses for the static, pure coal bed, packed with +5.6-6.7mm particles revealed ash yield percentages given by *Figure 5.4* below.

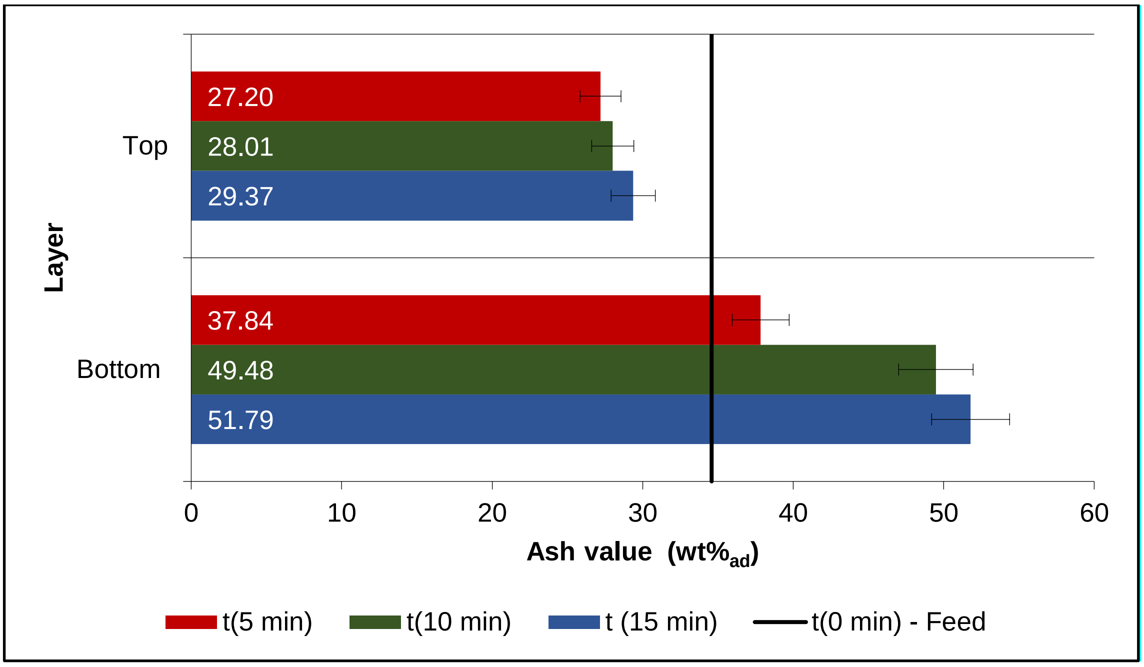

Figure 5.4: Ash yield %$_{wt}$ for time optimization (Q-01; PSD +6.7-8.0mm; DM 0:1; VD)

In *Figure 5.4*, the ash values for the bottom and top layers of the bed, operated at 5, 10 and 15 minutes is portrayed by means of a bar chart. The solid black line indicates the feed ash value at time t = 0 minutes and is 34.58%$_{wt}$. It is clear from *Figure 5.4* that a separation occurred after 5 min as the ash value obtained in the top bed layer reduced to 27.20%$_{wt}$ and that of the bottom layer increased to 37.84%$_{wt}$. Further evident is that the ash value in the top bed layer no longer reduced when operating longer than 5 minutes (considering the error bars portrayed), however de-stoning of the high ash coal discard to the bottom layer significantly improved from 5 to 10 minutes. Furthermore, the ash yield percentages in both top and bottom layers report similar values between 10 and 15 minutes of operation. As such, all experimental runs were operated between 10 and 15 minutes. From this data it may be concluded that the process separates the coal mostly by the sinking of heavy (high ash) coals to the bottom of the bed, rather than the floating of light (low ash) coal to the top of the bed. This is observed by the fact that effective destoning of the middling layers only occur after 10 minutes whereas no change is observed in the ash values of the top layer after 5 minutes. The optimization results, in terms of operating time, for each of the experimental variables are provided on the accompanying digital video disc (DVD).

5.3 Experimental results

Of the 12 experiments that make up the initial investigation matrix, a selected run will be portrayed and comprehensively discussed in *Section 5.3.1*. This experiment is deemed the control run and forms the baseline to which all other results are compared.

5.3.1 Control experimental run

The +6.7-8.0mm PSD with no addition of dense medium (DM 0:1) and vibration deactivated (VD) is selected as the control run. The extent of separation in the bed is observed by the relative comparisons of the ash value (wt%$_{ad}$), CV (MJ/kg) and TRD (g/cm^3) obtained for the feed coal and each bed layer of a specific experiment. *Figure 5.5* depicts a bar chart that is used to portray the stratification in the bed as according to the ash content determined for each layer and the feed.

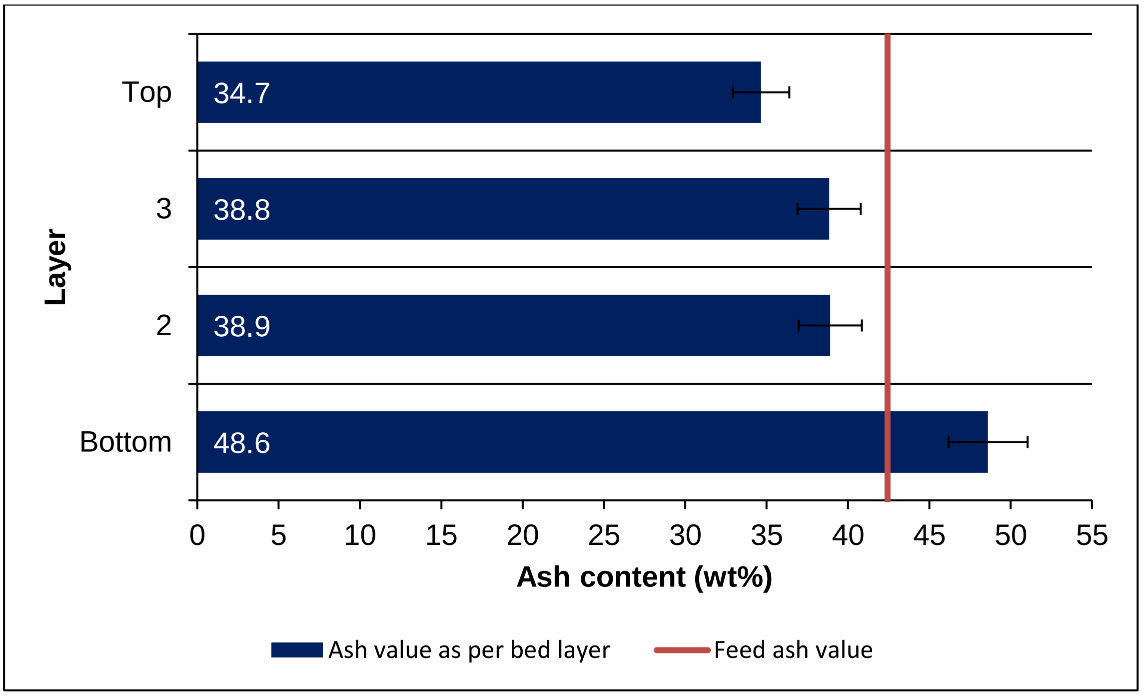

Figure 5.5: Particle stratification according to ash value (Q-01; PSD +6.7-8.0mm; DM 0:1; VD)

The bars in *Figure 5.5* depict the ash value relating to the various coal layers in the bed. The bottom layer is the lowest layer of the bed where most of the low quality coal, associated with a low CV and related high ash and density values, accumulate. The top layer consists of the beneficiated coal, generally of good quality and the red vertical line provides an indication of the ash value of the feed. For this experimental run, the feed coal consisted of an average ash value of 42.43$\%_{wt}$ and after fluidization the bed yielded four distinct layers with ash yields of 34.66, 39.84, 38.91 and 48.61$\%_{wt}$ as read from top to bottom, respectively. These results were obtained for a bed of 15.16kg at a static height of 0.2m that was fluidized at an air velocity of 17.5m/s, which corresponds to a factor of 1.3 times minimum fluidization and for a duration of 15 minutes.

The ash yield results, as portrayed in the bar chart, prove that a density separation was undertaken by the particles. The dense coal particles, associated with a high mineral content, reported to the bottom layer, yielding an ash value of 47.74$\%_{wt}$ and corresponding SG and CV of 1.98 and 14.6 MJ/Kg. The lighter and better quality particles moved to the top layer providing a final ash yield of 34.66$\%_{wt}$ and relating CV and TRD of 19.9MJ/Kg and 1.66 g/cm^3, respectively. Layers 2 and 3 represent a middling fraction with an ash yield that remained only slightly improved from the feed.

It is of importance to note that an improvement of the ash yield of the feed coal to the top layer by approximately 8 percentage points is observed. This provides an indication of the efficiency of the separation in terms of beneficiation in the ADMFB at these conditions. With regard to destoning a discard of a 6% differential increase in ash was produced and the middling fractions improved by 3.5% points. Provided below are *Figures 5.6* and *5.7,* showing the corresponding results for the CV and TRD of the run as discussed above.

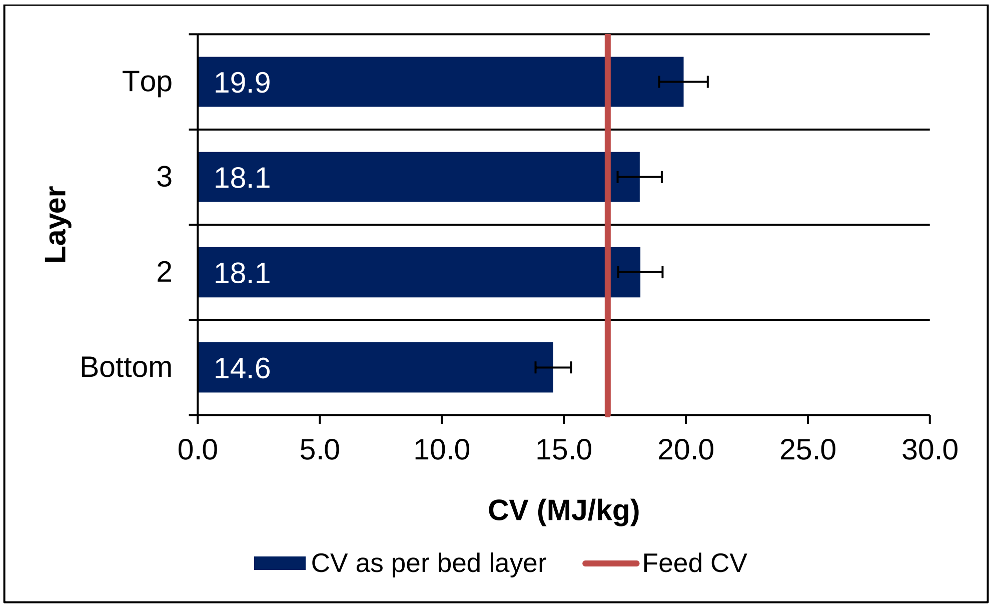

Figure 5.6: Particle stratification according to CV (Q-01; PSD +6.7-8.0mm; DM 0:1; VD)

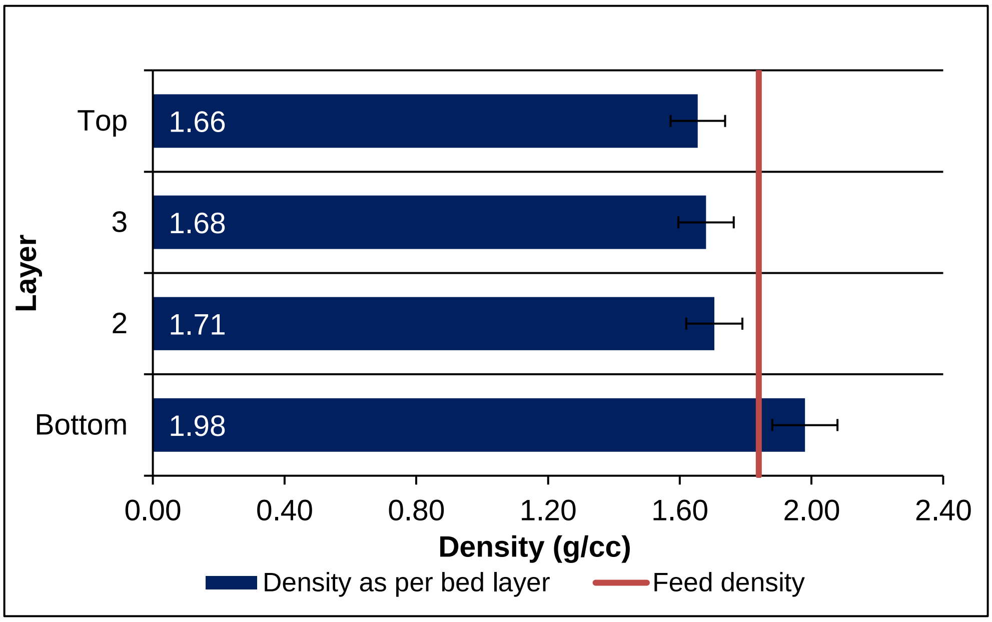

Figure 5.7: Particle stratification according to TRD (Q-01; PSD +6.7-8.0mm; DM 0:1; VD)

From *Figures 5.6* and *5.7* the same stratification of particles is observed, yielding four distinct layers of a general gangue, middling and product quality. A coal sample of low ash value is generally associated with a higher CV and lower TRD as evident from the corresponding results in *Figures 5.5, 5.6* and *5.7*. For the control experimental run, heating value results of 14.6, 18.1 and 19.9MJ/kg were obtained for the bottom, middle and top layers showing a 3.1MJ/kg improvement in CV from the feed. The corresponding TRD values of 1.98, 1.71, 1.68 and 1.66g/cm^3, further indicate a 0.18g/cm^3 decrease in density. In this chapter only the ash value results will be considered for determining the separation efficiency of the process. The associated CV and TRD data is provided on the accompanying DVD.

Total mass balances as well as ash content balances were conducted for each of the experimental runs. This was done to further validate the proximate results obtained for each layer and to quantify mass loss during operation. *Table 5.2* provides the total mass and amount of ash contained in the feed and each sampling layer.

Table 5.2: Mass balances conducted for the control run of the initial study

Mass (g)	Feed	Top	3	2	Bottom	Bed total
Coal (g)	15160	4310	4260	4330	2780	15680
Ash (g)	6432	1494	1655	1685	1351	6185
Coal balance error (%)		**3.43**		**Ash balance error (%)**		**3.85**

From *Table 5.2*, it is clear that relatively small percentage errors (<5%) are expected for the mass balance over the bed. The 3.85% deviation is ash balance over the layers validates the proximate results obtained for the feed and bed layers. Similar balances were conducted over all experiments and are available on the accompanying DVD.

5.3.2 Effects of differing variables

5.3.2.1 Particle size distribution

When compared to the control run, the +5.6-6.7mm PSD yielded similar results across all the layers for DM (0:1) and no vibration. The ash contents in the lower bed layers observed for the larger particle size are however slightly higher. In terms of beneficiation, the +6.7-8.0mm particles produced more desired results in that it upgraded the feed coal by an ash differential of 7.52% whereas the smaller PSD only managed 2.44%. Generally, the ash values obtained in the top layer of the bed do not differ for the two particle sizes across all

DM ratios for vibration deactivated and activated. More specifically, a decrease in PSD has no effect on the ash value of the beneficiated coal reporting to the top layer. Slight variations are however encountered in the intermediate and bottom layers of the bed for the different PSD's.

Those values in the intermediate and bottom bed layers that differ slightly from the smaller to larger PSD could be as a result of the higher ash content in the feed of +6.7-8.0mm particles. More dense material is present in the feed and therefore yields bottom and middling's layers with slightly higher ash values. *Figure 5.8* provides a depiction of this trend for the PSD's with the DM (0:1) ratio where vibration is not considered.

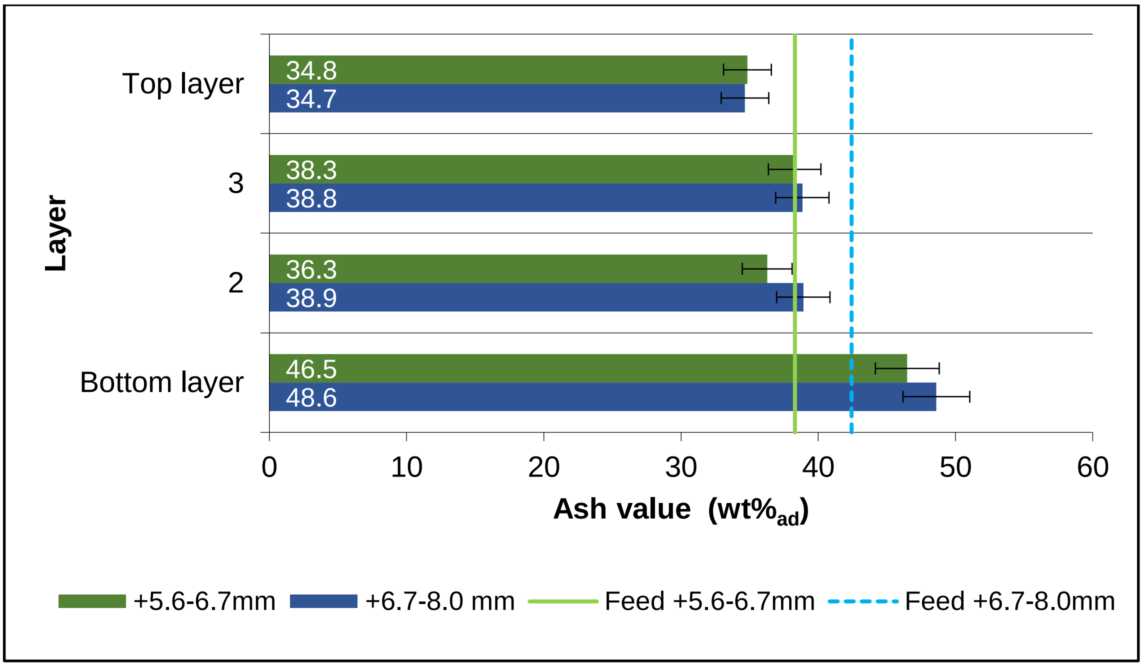

Figure 5.8: Comparison of the ash values for different PSD's (Q-01; DM 0:1; VD)

In *Figure 5.8*, a comparison chart for PSD is displayed, that shows the ash content in each layer of the bed for a dense medium ratio of 0:1 and vibration deactivated. It is apparent that the layers report relatively similar ash contents for both +5.6-6.7mm and +6.7-8.0mm particles with slight variation in the intermediate and bottom layers. The trends as described above and displayed in *Figure 5.8* hold true for all dense medium ratios considered as well as for both deactivated and activated vibration with some anomalies observed. These anomalies occur mostly when comparing the two PSD's of DM 1:1 and 2:1 for vibration active. With these variables, the larger PSD seems to perform better in terms of the ash content obtained in the top layer. This observation may be attributed to the operating conditions of the bed and sampling procedure. Although extensively and accurately determined, it is possible that these runs were conducted at inadequate fluidization conditions most especially relating to optimized vibration of a DM bed.

5.3.2.2 Dense medium consideration

When taking into account the DM ratio, it was evident that no substantial difference was identified in the ash values obtainable in the top layer for vibration both deactivated and activated (*Figure 5.9* below). When comparing the vibration deactivated 1:1 and 2:1 DM ratios with the control run, it is clear that the ash contents in the top layers are similar. This implies that the addition of increasing amounts of dense medium will yield no better results than a bed operated without dense medium entirely. This may be as a result of the batch type experiments conducted for this study and a continuous process where the magnetite is fluidized before addition of the coal may yield different results.

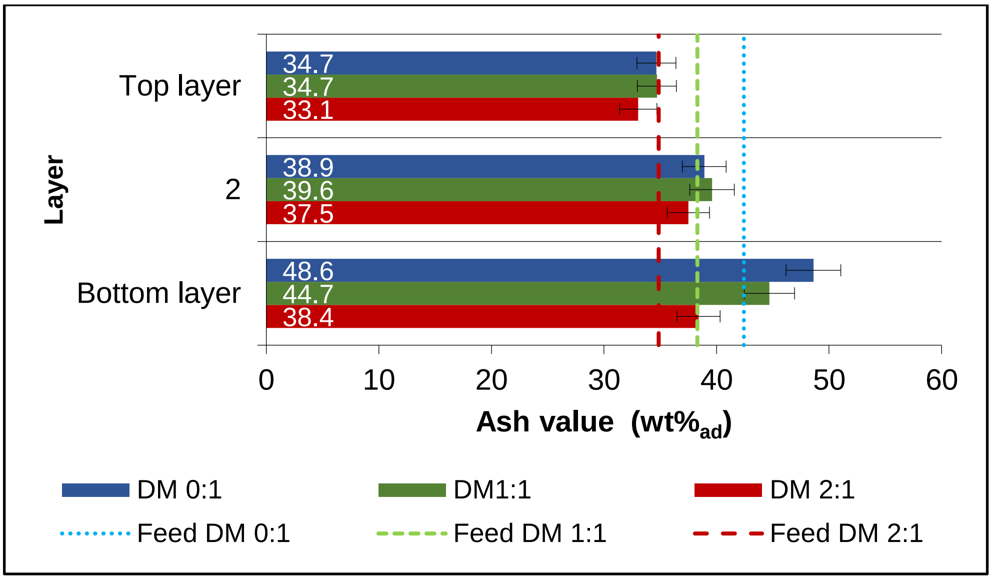

Figure 5.9: Comparison of ash values for different DM ratios (Q-01; PSD +6.7-8.0mm; VD)

A noticeable difference in the ash values between the bottom layers is however observed in *Figure 5.9*. The ash value in the bottom layer decreases with increasing DM ratio from 0:1, 1:1 and 2:1 and for both PSD's and states of vibration. The highest ash values in the bottom layer of the bed (as desired) are obtained from beds containing no dense medium. This may be as a result of the larger inter-particulate voids present in a bed made up of purely coal. No fine magnetite powder occupies these openings and the movement of particles in these voids are therefore not hindered. A similar trend is noted in the intermediate bed layers of all variables considered. Similar graphs for the other PSD and vibration variables, which ultimately show the same behaviour, are available on the accompanying DVD.

5.3.2.3 Influence of vibration

The addition of vibration to the ADMFB lowers the MFV and increases the stability of fluidization (He *et al.,* 2015). This is due to the formation of smaller bubbles that rise to the top of the bed and a resulting loosening effect is experienced on the particulates. This may be the cause of the more desired separation observed when the vibration of the bed is activated. *Figure 5.10* provides the comparison chart for vibration deactivated (VD) and activated (VA) for the +6.7-8.0mm PSD with a corresponding DM ratio of 0:1.

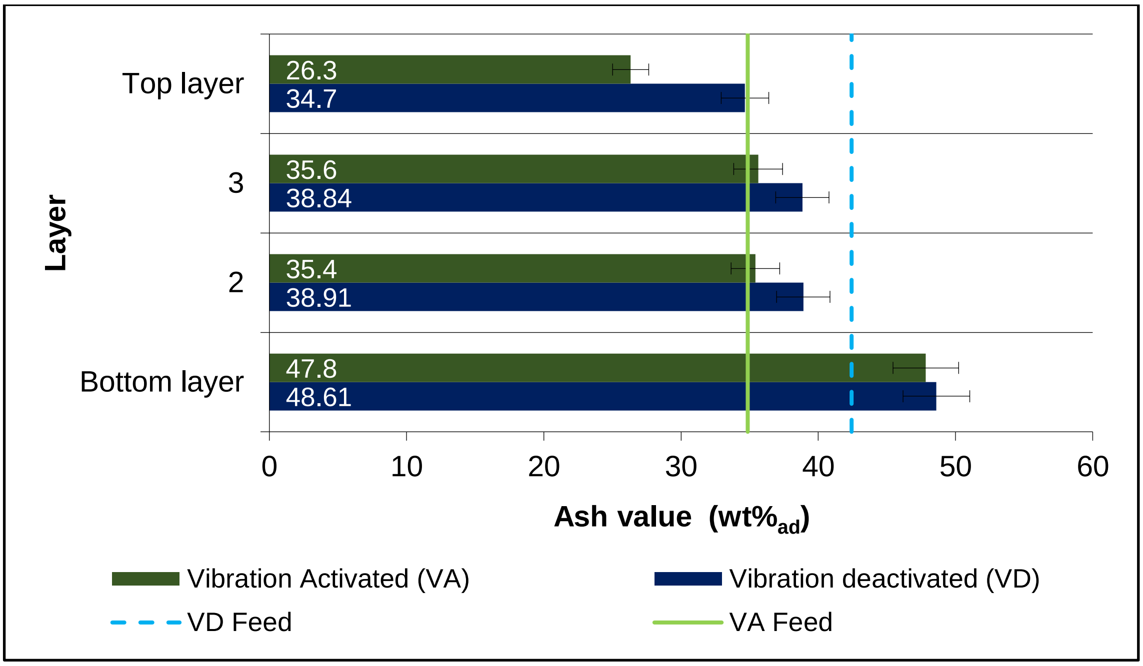

Figure 5.10: Comparison of ash values for vibration (Q-01; PSD +6.7-8.0mm; DM 0:1)

Figure 5.10 illustrates that only marginal differences were experienced across the bed layers except when considering the top layer, as previously mentioned. The proximate results for the intermediate and bottom layers are for the most part similar, with some anomalies noted especially with respect to the middling layers. These variances could be attributed to the effect of frequency and amplitude of vibration on the bubble formation of the specific run. It may also result from closer packing in the bed due to the vibration which leaves little space for movement. The slightly increased proximate ash value of the feed for the run where vibration is deactivated (+6.7-8.0mm) may also provide a reason for the differences in the intermediate layers.

5.3.2.4 Verification and repeatability

Verification of data obtained by the ADMFB experimental runs, sampling as well as various analyses is particularly important. This is done by means of repeatability studies conducted on selected runs. The bar chart in *Figure 5.11* provides an indication of the repeatability of +6.7-8.0mm coal particles, in the absence of dense medium or and vibration. Run 1, 2 and 3 were conducted at an air flow between 15.5 and 17.5m/s with masses ranging close to 15 kg and a static bed height of 0.2m. The feeds for the verification runs contained ash values of 40.60, 42.43 and 39.60%$_{wt}$ for runs 1, 2 and 3 respectively.

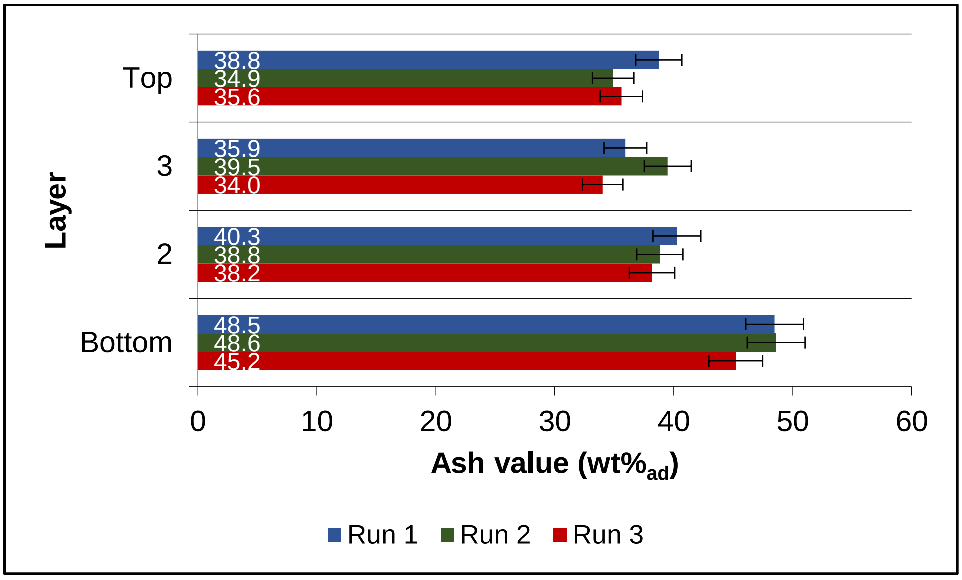

Figure 5.11: Bed repeatability (Q-01; PSD +6.7-8.mm; DM 0:1; VD)

Good repeatability of the experimental runs are visible from Figure *5.11*. Three runs conducted on the same material at relatively similar conditions yielded ash values for each layer that are closely comparable and within standard deviations below 2.3 and a confidence interval of 95%. This, along with the low standard deviations for the sampling and analytical methods as portrayed in *Section 4.2.2* of *Chapter 4*, proves that the procedure is repeatable and will therefore yield accurate results. Similar verification results are found when comparing all of the repeated runs and are available in *Appendix D.*

5.3.2.5 Summative description of variable effects

In accordance with the study objectives, the effect of PSD, DM ratio and added vibration on the extent of separation of the ADMFB was investigated. *Table 5.3* contains the ash values pertaining to the feed as well as top and bottom sampled layers of the bed for both PSD's considered as well as all dense medium ratios with vibration activated or deactivated.

Table 5.3: Ash value results for all variables considered during initial study

Ash value (%wt$_{ad}$)	Vibration Deactivated (VD)			Vibration Activated (VA)		
	DM (0:1)	DM (1:1)	DM (2:1)	DM (0:1)	DM (1:1)	DM (2:1)
PSD: +6.7-8.0mm						
Feed	42.43	38.30	37.72	34.86	35.54	32.25
Top layer	34.66	34.70	33.05	26.33	25.85	27.30
Bottom layer	48.61	44.70	38.40	47.84	40.19	39.40
Ash differential (% points)	7.52	3.6	4.67	8.53	9.69	4.95
PSD: +5.6-6.7 mm						
Feed	37.28	37.49	37.70	38.68	33.43	33.95
Top layer	34.84	33.27	32.19	26.81	31.81	32.50
Bottom layer	46.49	40.02	40.00	47.74	39.52	37.70
Ash differential (% points)	2.44	4.22	5.11	11.87	1.62	1.45

Even though some trends are clear from the results discussed, a less than desired outcome was obtained in the top layers of the experimental runs. Stratification occurs to some degree but is not considered sufficient for effective coal beneficiation as it is not comparable to that found in literature. It was therefore necessary to conduct an investigation into the possible reasons for the results obtained. The method used during the experimental runs was verified through a series of repeatability tests, as given in Section 4.3.2.4 above, and could therefore not be the major cause of the undesired and varying results. Consequently, a deeper inspection into the quality of the feed coal was undertaken in order to attempt an explanation for the above.

5.4 Auxiliary investigations

As stated above, supplementary investigations into the quality of the feed coal were conducted. This was done in order to determine the cause of the less than desired results obtained, even after the addition of dense medium and vibration which have proven useful in many studies (He *et al.,* 2015; Zhao *et al*., 2015). From the washability studies conducted on the coal qualities (as discussed in Section 4.2.2.4) some conclusions regarding Q-01 coal quality are drawn:

- The coal feed sample (Q-01) contains a large portion of near dense material which is due to the fact that approximately 40%$_{wt}$ of the material sinks at an SG of 1.8.
- Reduction in the PSD had no influence on the float sink results because the densimetric curves for the two PSD's considered are nearly identical.

The above findings were indicative of a coal sample that is largely composed of dense material and may contain a great portion of intrinsic ash forming minerals. As detailed in *Section 2.2.2.4*, intrinsic mineral matter is comprised of the inorganic matter that was present during the original formation of the coal specimen and is intimately bound to the carbon in such a way that only extensive crushing could liberate it.

5.4.1 Investigation into liberation

A liberation study was undertaken, in which the coal sample was crushed to +0-2mm particles and beneficiated in an ADMFB. This study was conducted on a smaller scale with the previous ADMFB setup as designed for fine coal fractions. Details regarding the bed used for this study are available in *Appendix E*. The results obtained for the ash values as per layer of the bed are shown in *Figure 5.12* and those are obtained for a bed mass and height of 1.5kg and 0.15m, respectively, that was fluidized at an air flow of 175L/min for a period of 10 minutes. Sampling and preparation for analyses were conducted as described in *Section 4.4*.

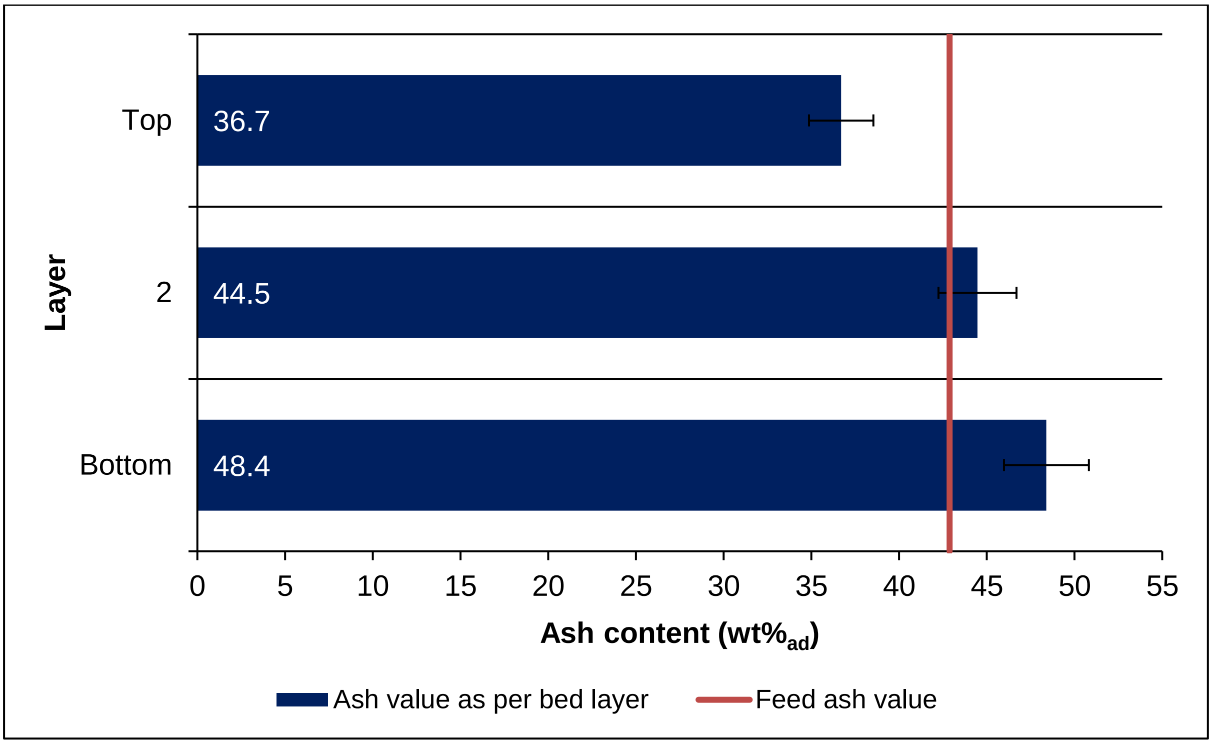

Figure 5.12: Stratification of extensively liberated coal (Q-01, +0-2mm; 0:1 DM; VD)

From *Figure 5.12*, it is clear that three layers are produced with ash values closely comparable to the results obtained for the +5.6-6.7mm and +6.7-8.0mm particles. Therefore, it was established that even after extensive crushing of the particle, no improvement is observed in the separation efficiency of the coal. From this the conclusion drawn from the washability study, in that the coal of quality Q-01 may be intrinsic in ash forming minerals, and is consequently mostly comprised of near dense material, is corroborated.

5.4.2 Coal quality

To further validate the finding as stated above, Energy Dispersive X-ray Spectroscopy (EDS) analyses were conducted on a representative sample of the Q-01 coal. *Figure 5.13* provides the some of the images obtained therefrom.

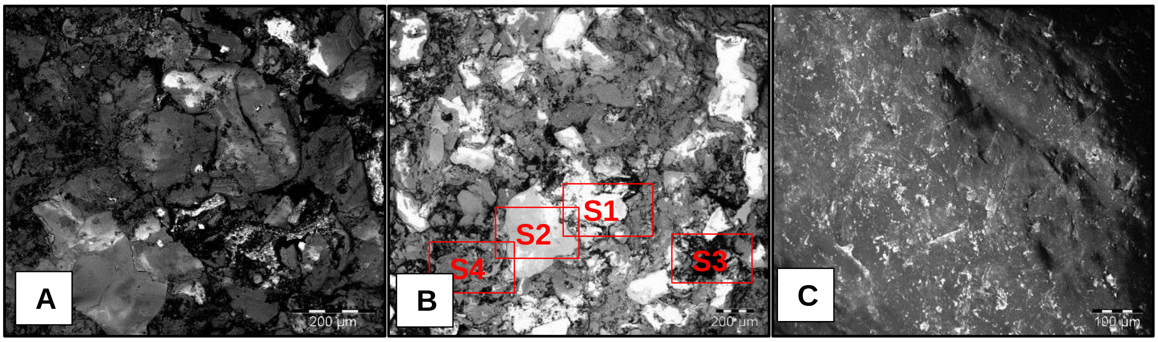

Figure 5.13: Magnified photographs of the coal Q-01

In *Figure 5.13*, some magnified images of the coal Q-01 sample are portrayed. Figure 5.13 shows the varying portions of black, grey and white colours which are expected to depict either coal (black) or mineral matter (grey and white). Clearly seen from *Figure 5.13 (A)* and *Figure 5.13 (B),* is that the specimen contains a large amount of grey and white areas and consequently a large amount of mineral content. These mineral and carbon constituents that form part of the coal are further intimately bound into a heterogeneous mixture. A Scanning Electron Microscopy (SEM) analysis was then conducted on the areas of differing colour to obtain a general idea of the composition thereof. The results for the elemental composition of spots labelled S1 to S4 in *Figure 5.13 (B)* are portrayed in *Table 5.4*.

Table 5.4: Elemental composition of specific portions of the coal Q-01 specimen

wt%	C	O	Na	Mg	Al	Si	S	K	Ca	Ti	Fe
S1	0.01	66.22	0.29	0.5	12.64	16.29	-	3.63	-	-	0.42
S2	6.17	53.81	0.4	0.41	14.05	17.56	-	5.9	-	-	1.41
S3	79.24	18.54	-	-	0.95	0.97	0.3	-	-	0.29	-
S4	15.35	50.31	-	-	12.77	14.38	0.34	-	0.27	6.58	-

From the above data (given in *Table 5.4*), it is apparent that the white, light grey and darker grey areas corresponding to S1, S2 and S4, respectively, are made up of very little carbon and larger amounts of aluminium, silica and oxygen. These are the main components of a quarts mineral and it can therefore be concluded that these areas are mostly mineral matter. The portion labelled S3 contains 79.24%$_{wt}$ carbon which is indicative that this (black) area is made up of coal. It can also be concluded that *Figure 5.13 (C)* is a coal of large carbon content and therefore, good quality.

It is clear that the sample contains a wide range of particle qualities with a large portion being near dense and intrinsic in ash forming minerals that are intimately mixed with the regions high in carbon. This makes the complete liberation of the coal at the overall PSD of +5.6-8.0mm nearly impossible when considering the magnification of 0.2mm during the EDS analysis. Effectively, a new coal sample of arguably better quality needed to be investigated in order to determine if it would yield a more desired result.

5.4.3 A note on coal quality

A new coal sample (Q-02) was obtained by making use of a 50% by mass blend of a new coal sample, also obtained from the Witbank coalfield (Seam 4), with the coal used for the experiments thus far. From the washability studies conducted in *Section 4.2.2.4*, it was concluded that Q-02 is of better quality when compared to Q-01 in that the sample contains less near dense material. This is concluded from the fact that approximately 80% of the sample floats at an SG of 1.8.

A representative sample of Q-02 was prepared in a similar manner to that of Q-01 (as discussed in *Chapter 4*) and a selected experimental run was conducted thereon. A mass of +6.7-8.0mm particles made up of the coal blend (Q-02) was beneficiated under similar conditions in the ADMFB, as described in *Section 5.3.1*, and the results obtained are displayed in the bar chart in *Figure 5.14* in terms of the ash value obtained in the bed layers compared to that of the feed.

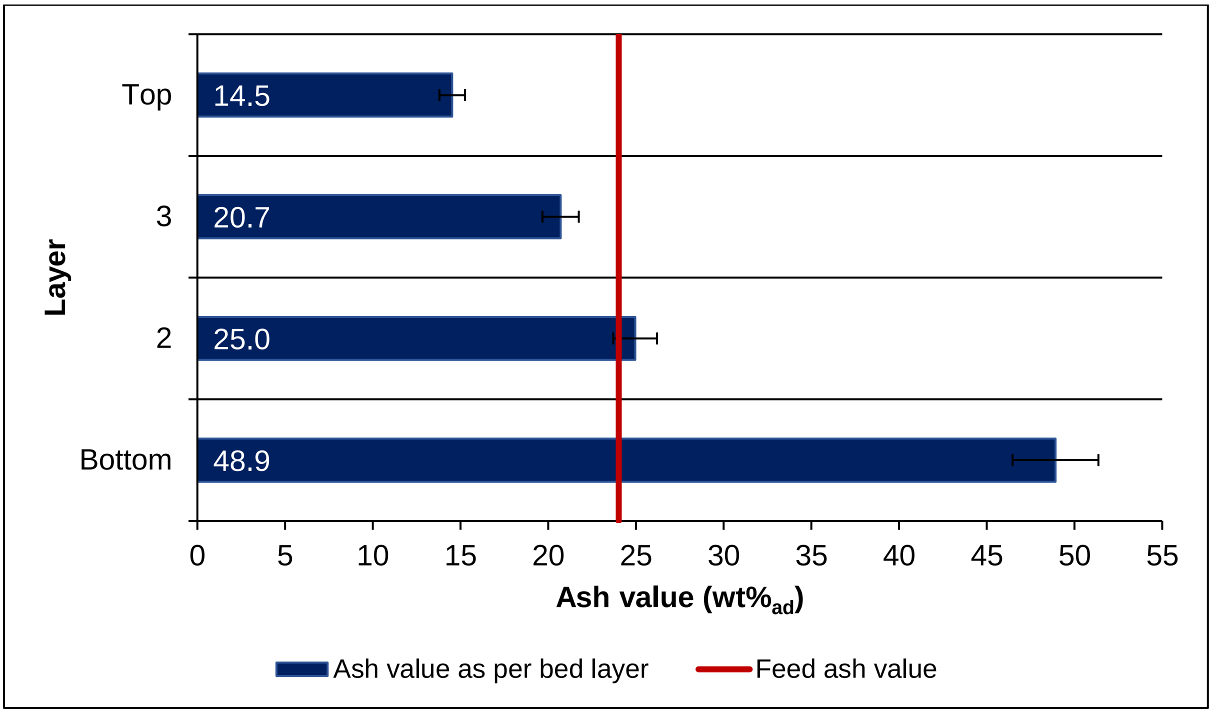

Figure 5.14: Particles Stratification according to ash value (Q-02; PSD +6.7-8.0mm; DM 0:1; VD)

From *Figure 5.14*, it is apparent that a more desired coal beneficiation outcome was obtained. The separation yielded a top layer with an ash value of 14.53%$_{wt}$ and destoned the feed to produce a 48.92%$_{wt}$ ash value in the bottom layer. It can be seen that an upgrade in 10 percentage points from the feed ash value was obtained in the top layer and two distinct intermediate layers of 24.96 and 20.71%$_{wt}$ were produced. The behaviour of the bed layers yielded more desired results with a clear and significant decrease in ash content per layer. With regard to the South African specifications for coal products given in *Section 2.2.3.1* a clear gangue, middling and product coal can be achieved with the Q-02 coal quality.

5.5 Chapter summary

With the data as portrayed in this chapter it is clear that some trends are observed for a change in particle size, amount of dense medium and state of vibration. The beneficiation result is however less than desired for the experimental runs with most regard to the ash values in the top layer of the bed. Slightly lower ash values were expected in accordance with literature. As a result a closer look into the experimental method and quality of the feed coal was endeavoured to explain the behaviour observed. From this, coal quality was proved to have a definite effect on the extent to which the ADMFB can beneficiate the coal. This could in turn affect the performance of the dense medium ratios as well as activation of vibration.

Chapter 6: RESULTS ON BETTER LIBERATED (LOW ASH) COAL

This chapter presents the data obtained for the experiments conducted on the better liberated (low ash) coal in the investigation of *"The dry beneficiation of South African small coal in a dense medium fluidized bed"*. As previously described, the experimental work began with investigating two of the considered PSD's (+5.6-6.7mm and +6.7-8.0mm) using coal quality Q-01. However, the poor quality of Q-01 seemed to have an effect on the extent of separation in the bed. As a result a coal of improved quality was blended with 50% by mass of a new sample and Q-01, forming the Q-02 quality with which all five particle sizes are additionally tested. *Chapter 6* consists of the following sections:

- **Section 6.1:** Provides an overview of the study problem and details the associated investigation objectives.
- **Section 6.2:** Presents the results obtained for the Q-02 sample with regard to the investigation into the effect of PSD, amount of dense medium and activation of vibration on the extent of separation.
- **Section 6.3:** Concludes the chapter and highlights the most important points named therein. It further links the initial findings chapter to that of the chapter that follows with the results of an improved coal quality.

6.1 Overview

As stated, this study undertakes to determine whether ADMFB technology is adequate for beneficiating South African small coal. This is done by determining the effects of the following variables (using Q-02):

- Particle size distribution (PSD)
  +11.2-13.2; +9.5-11.2; +8.0-9.5, +6.7-8.0 and +5.6-6.7mm
- Dense medium to coal mass ratio (DM ratio)
  0:1; 1:1 and 2:1
- Vibration
  Activated (VA) and deactivated (VD)

In a similar manner as approached in *Chapter 5*, the extent of separation in the bed will be portrayed by means of the ash value obtained per bed layer as compared to the feed. Notation of the corresponding CV and density data will be made along with that of the associated minimum fluidization requirements, mass balances, bed stability and performance of separation.

6.2 Discussion of experimental results

Of the 30 experiments that make up the main investigation matrix, as illustrated in *Figure 4.5*, a selected run will be shown and comprehensively discussed in *Section 6.2.1*. This experiment is deemed the control run and forms the baseline to which all other results are compared. As detailed, the extent of separation for this study is determined from the ash value in each bed layer as compared to the feed. Consequently only notation will be made of the associated CV and density results. Detailed graphs and relevant discussions of these are available on the accompanying DVD. The discussion comprising the data of the control run further extends to minimum fluidization requirements; bed pressure and density; performance curves and lastly, mass and ash balances.

6.2.1 Control run

The +11.2-13.2mm PSD with no addition of dense medium (DM 0:1) and vibration deactivated (VD) is selected as the control (normal) run. *Figure 6.1* depicts a bar chart that is used to portray the stratification in the bed as according to the ash content determined for each layer and the feed.

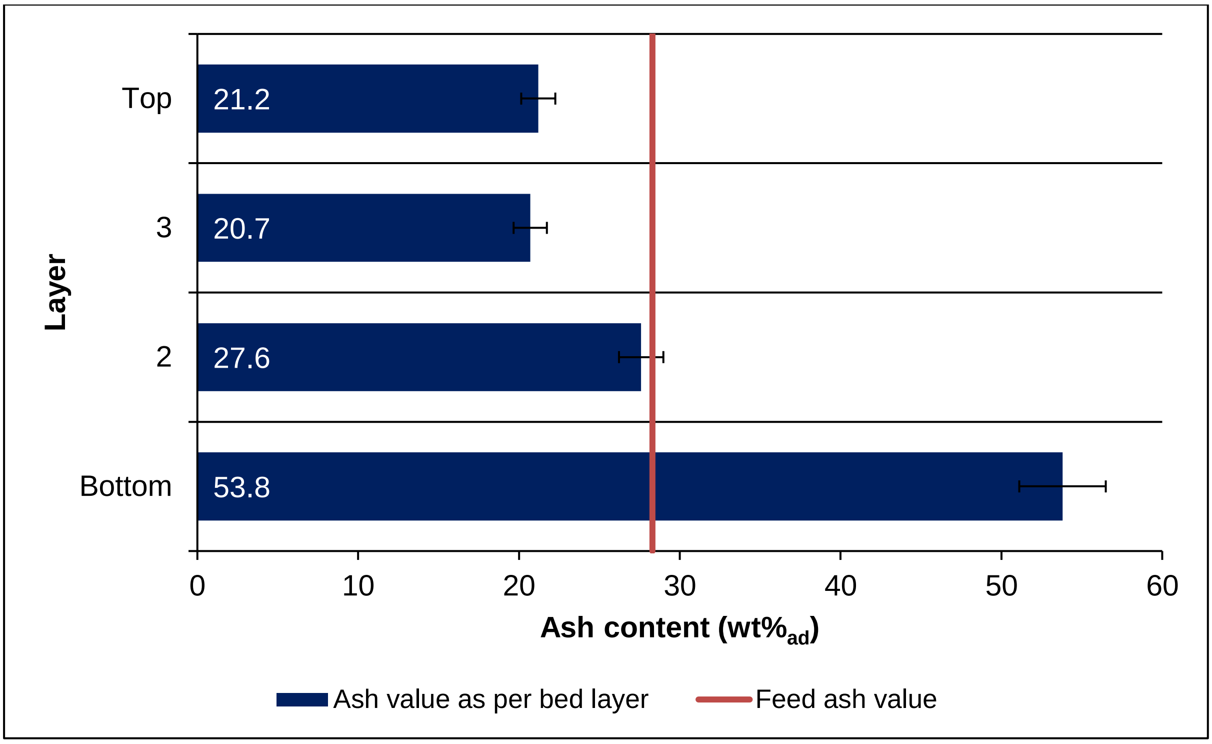

Figure 6.1: Particle stratification as per ash content (Q-02; PSD +11.2-13.2mm; DM 0:1; VD)

Figure 6.1 shows that a bed fed with +11.2-13.2mm coal particles and an average feed ash value of 28.3%$_{wt}$, yields an effective separation that relates to a 7.1% ash differential to the top bed layer. A clear stratification is observed across the bed layers, with an immense increase in ash content to the bottom bed layer as compared to the feed (25.5% points). Further visible from *Figure 6.1* is that no significant difference is observed between the ash values in the third and top layer of the bed but a clear middling fraction with ash content of 27.6%$_{wt}$ (close to that of the feed) was produced.

This experimental run behaved considerably well in de-stoning due to the immense increase in ash yield to the bottom layer. This may be as a result of the size of the particles and associated larger inter-particulate voids. These increased void spaces leave more room for the more dense particles to sink to the bottom. This observation is supported by the findings of Yang *et al.* (2013), which states that bed performance decreases for decreasing particle size. Some minor back-mixing is observed in the third and top bed layers and may be as a result of inadequate fluidizing conditions for this run. The associated CV and density results as per feed and bed layer are given in *Table 6.1*.

Table 6.1: CV and TRD for the control run (Q-02; PSD +11.2-13.2mm; DM 0:1; VD)

Layer	CV (MJ/kg)	Density (g/cm^3)
Feed	21.8	1.61
Top	24.9	1.54
2	25.1	1.54
3	22.3	1.62
Bottom	11.4	1.96
Differential (Feed to Top)	**-3.1**	**0.07**

The results portrayed above were obtained for a coal sample of 15kg and static bed height of 0.2m. The minimum and operating velocities reported as 15.6 and 16.1m/s, respectively, corresponding to a scaling factor of 1.07. Fluidization commenced at a bed pressure drop of 110mmH_2O and approximate bed density of 0.67g/cm^3 for a duration of 10 minutes.

Total mass and ash mass balances were conducted for the experimental run as discussed above. The results are used to validate the results obtained from the proximate analysis and to determine the extent of material losses. *Table 6.2* provides the total and ash masses attributed to the feed and each bed layer of the control run (PSD +11.2-13.2mm; DM 0:1; VD).

Table 6.2: Mass balances conducted for the control run (Q-02; PSD +11.2-13.2mm; DM 0:1; VD)

Mass (g)	Feed	Top	3	2	Bottom	Bed total
Coal (g)	15 060	4 690	3 630	3 790	2 950	14 700
Ash (g)	4 262	994	751	1 046	1 393	4 185
Coal balance error (%)		**2.39**		**Ash balance error (%)**		**1.80**

From *Table 6.2*, it is clear that relatively small percentage errors (<5%) are expected for the mass balance which are further deemed well within a 95% confidence interval (CI). The 1.80% deviation is ash balance over the layers validates the proximate results obtained for the feed and bed layers. Furthermore, observed from *Table 6.2*, was the mass distribution over the bed layers. Although the stratification of ash contents produced are as desired, the mass of each layer may affect the overall yield obtainable. More specifically, the mass of coal removed from each of the four bed layers may differ from the expected 25% of the bed mass due to the effects of density and particle size. *Figure 6.2* provides a depiction of this distribution with regard to product and discard yield as compared to bed height.

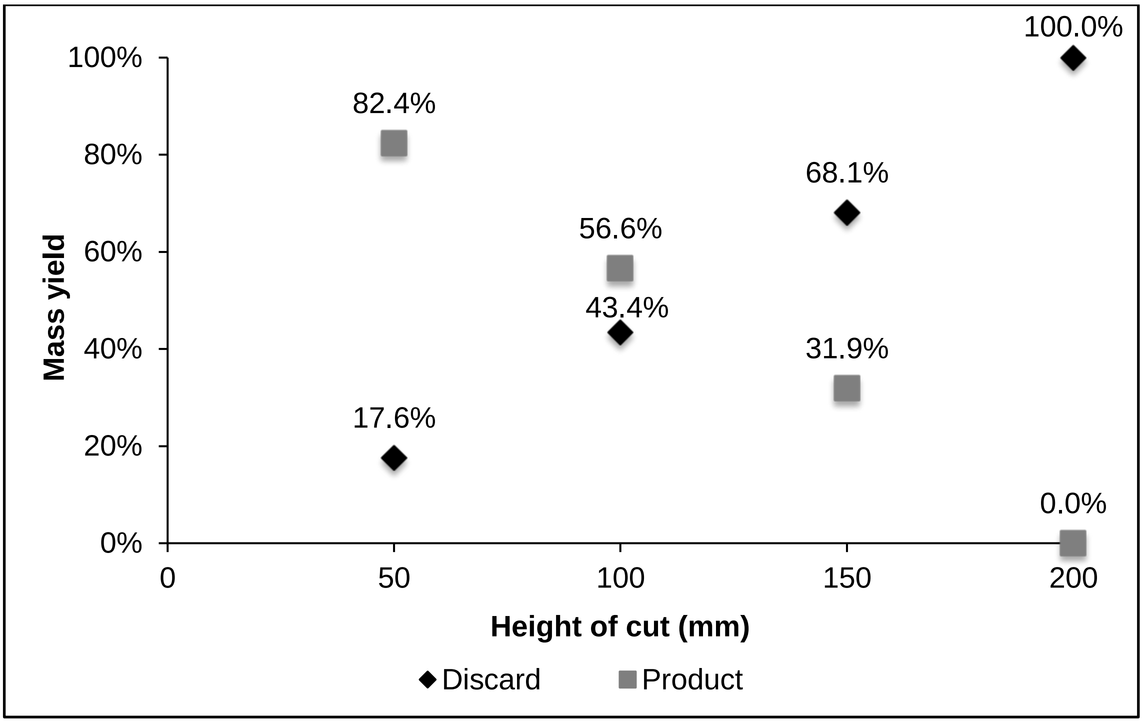

Figure 6.2: Mass yield vs. bed height for the control run (Q-02; PSD +11.2-13.2mm; DM 0:1; VD)

From *Figure 6.2*, a theoretical percentage yield can be viewed in terms of a product and discard as per cut-point along the bed height. More specifically, if selecting a theoretical split at a height of 50mm (choosing the bottom layer as discard and top 3 layers as product), an 82.4% mass yield is expected with a corresponding 22.3% ash yield which is not significantly improved from the feed ash value of 28.3%$_{wt}$. Alternatively, if only the top layer is selected as product (a cut-point of 150mm), a mass yield of 31.9% is obtainable with a corresponding ash yield of 14.2%$_{wt}$. A much improved ash value when considering desired product qualities but is however coupled with a reduced output or mass yield. This implies that from cutting the bed above layer 2 or 3, a suitable ash yield is obtainable but the reduced mass outputs are not necessarily desirable. Figure 6.3 provides a depiction of the ash yields for product and discard that correspond to the varying cut points along the bed.

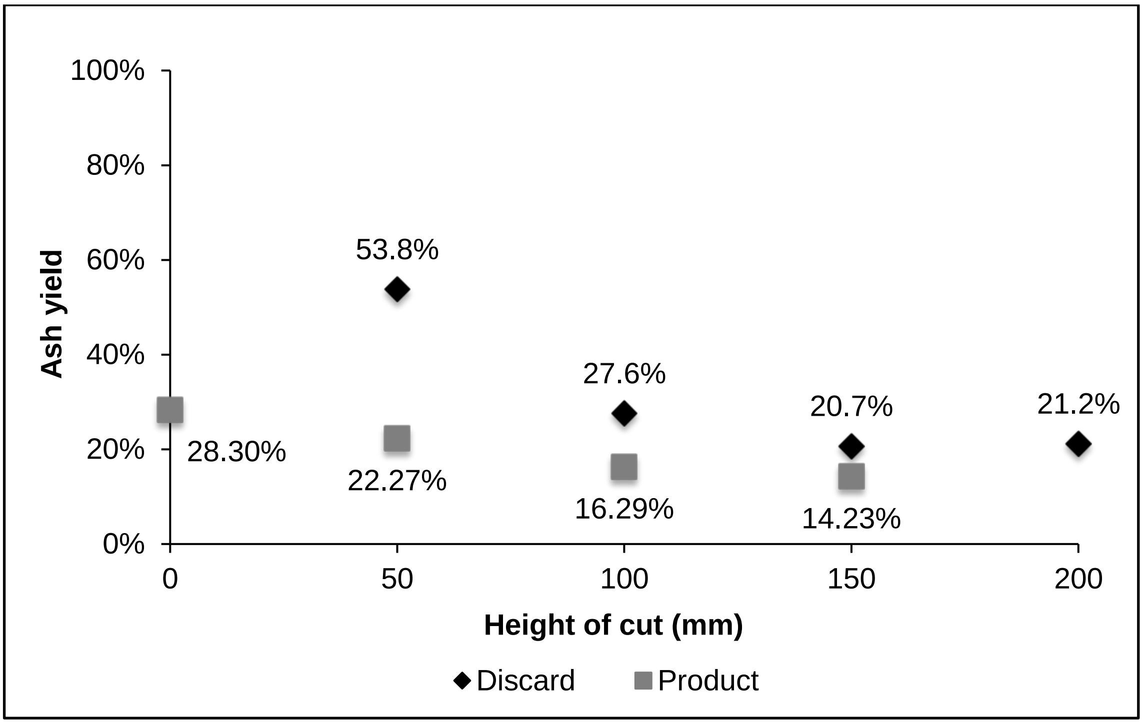

Figure 6.3: Ash yield vs. bed height for the control run (Q-02; PSD +11.2-13.2mm; DM 0:1; VD)

When considering the ash yield with regard to the discard in *Figure 6.3,* it is clear that the discard ash value decreases as theoretical cut point increases along the bed height. This is as expected since the most high ash coal particles report to the bottom layer of the bed and with an increase in cut point height, a dilution of the gangue with good quality coal is experienced and the ash values decrease. The sharpest separation efficiency is observed at the 50mm height given that the largest difference in ash values of the product and discard are observed. This may indicate that a cut point of 50mm along the bed height yields the best result when considering ash value and also mass output of the process.

To further provide an idea of the extent to which the ADMFB stratified, given the data from the control run, a performance curve is provided. This represents the yield obtainable for the cumulative ash percentage in the product. *Figure 6.4* below displays this performance curve.

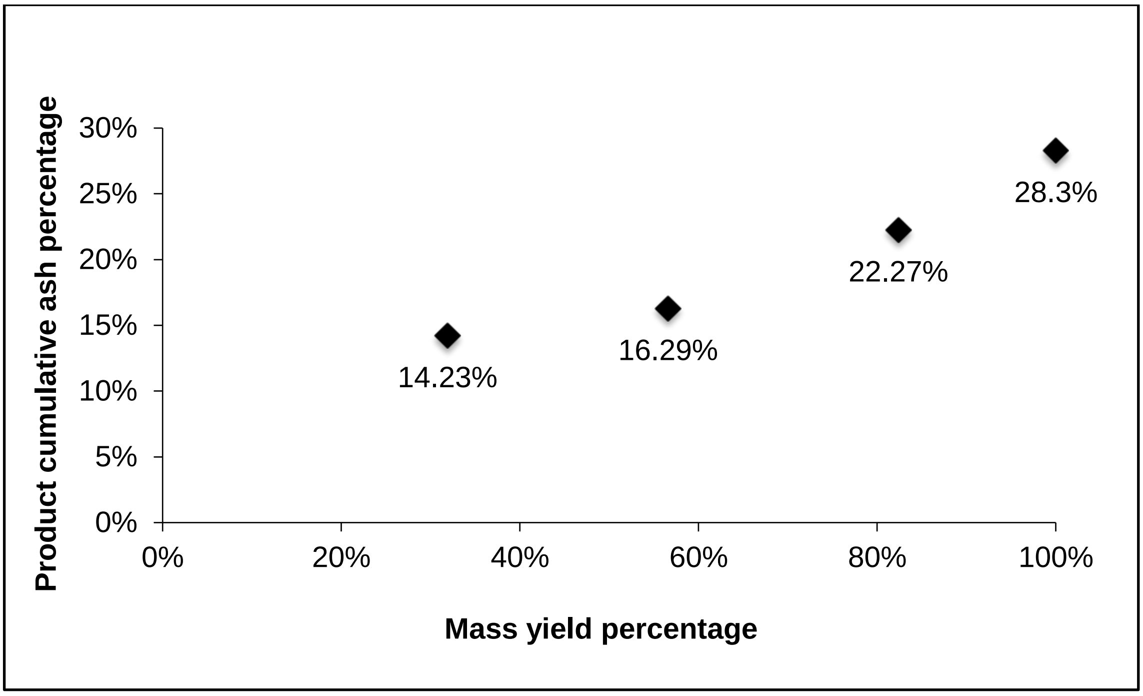

Figure 6.4: Performance curve for the control run (Q-02; PSD +11.2-13.2mm; DM 0:1; VD)

The performance curve may be used to determine the percentage yield that is obtainable in the ADMFB at the conditions stipulated for the control run. From *Figure 6.4* it is clear that 100% yield (using the entire feed mass as theoretical product) will result in a coal that remained unimproved from the feed ash value and is therefore not desired. The lowest cumulative ash percentage (as desired product) is obtained at a yield of 31.9%. An increase in theoretical yield clearly leads to an increased cumulative ash content and it is therefore essential to select a point where a sufficient coal quality is produced - but in an adequate quantity as well.

A comparison of the performance of the control run with the cumulative floats curve from the initial washability study is provided in *Figure 6.5*. The cumulative floats curve (washability curve) provides the limiting yield vs. ash value which is an indication of the best performance that the coal can achieve. As visible in *Figure 6.5*, the performance of the ADMFB is on par as the ash value vs. yield trends portrayed are quite similar. A slight difference is however observed in the lower bed yields. Since these generally occur when the top and second bed layer of the bed are selected as product, it could indicate some measure of particle back mixing which ultimately affects the separation outcome achievable in the bed at the conditions specified.

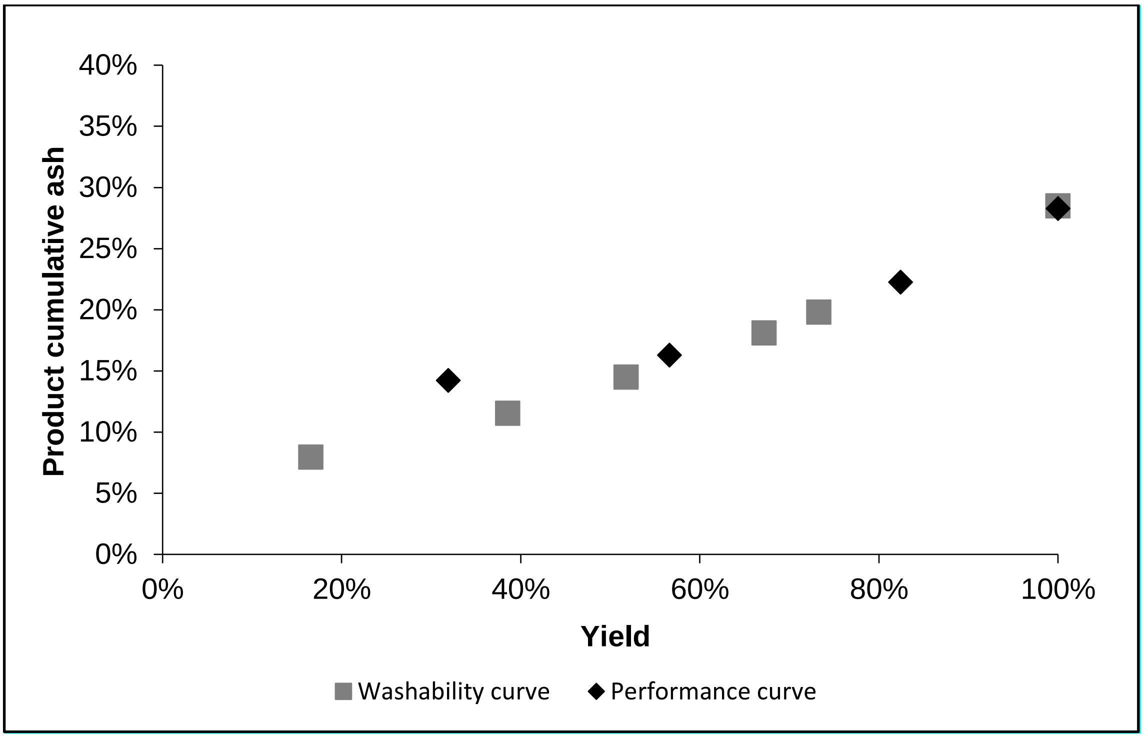

Figure 6.5: Comparison of bed performance to limiting performance curve (PSD +11.2-13.2mm; DM 0:1; VD)

6.3.2 Influence of differing variables

This section, in accordance with the study objectives, determines the influence of PSD, DM ratio and vibration on the fluidization operation and also the extent of separation. The results obtained from these variables are provided in comparison to the control run discussed in Section 6.3.1.

6.3.2.1 Particle size distribution

Firstly, a look into the influence of PSD on the minimum and operating velocities of the bed is presented. *Table 6.3* provides comparisons relating to PSD for the conditions where magnetite was not utilized.

Table 6.3: Comparison of minimum and operating fluidizing conditions for PSD (Q-02; DM 0:1; VD)

PSD (mm)	Bed mass (g)	Layers	U_{mf} (m/s)	U*	U (m/s)
Vibration deactivated (VD)					
+11.2-13.2	15060	4	**15.1**	1.07	**16.1**
+9.5-11.2	14210	4	**14.4**	1.09	**15.1**
+8.0-9.5	15350	4	**14.7**	1.01	**14.8**
+6.7-8.0	14490	4	**11.2**	1.13	**12.6**
+5.6-6.7	15200	4	**9.2**	1.13	**10.4**

Foot note: U_{mf} – Minimum fluidizing velocity (m/s), U* - Velocity scaling factor, U – Superficial velocity (m/s)

From *Table 6.3* it is evident that PSD influences the minimum fluidization velocity to some extent. A general decrease in U_{mf} is marked in conjunction with a decrease in particle size. This is due to the increased surface area of the larger particles, which require a larger buoyant force to suspend and therefore an increased MFV is essential. For particulate beds comprised entirely of coal, it was observed that operating at a velocity closer to U_{mf} produced a more stable fluidized bed that consequently yielded a reduced amount of turbulence and back mixing. As such, scaling factors ranging between 1.01 and 1.13 were maintained. The same general trend is observed when also considering the addition of vibration and dense medium. It is useful to note that this trend differs from that observed in *Chapter 5* in that PSD shows no significant effect on the results. This difference may be attributed to the larger PSD range considered during the main experimental runs.

When considering the control run (*Figure 6.1*) it is observed that a reduction in PSD had no significant effect on the extent of separation in the bed. *Figure 6.6* provides this comparison in the form of a bar chart for selected PSD's, in the absence of dense medium and vibration.

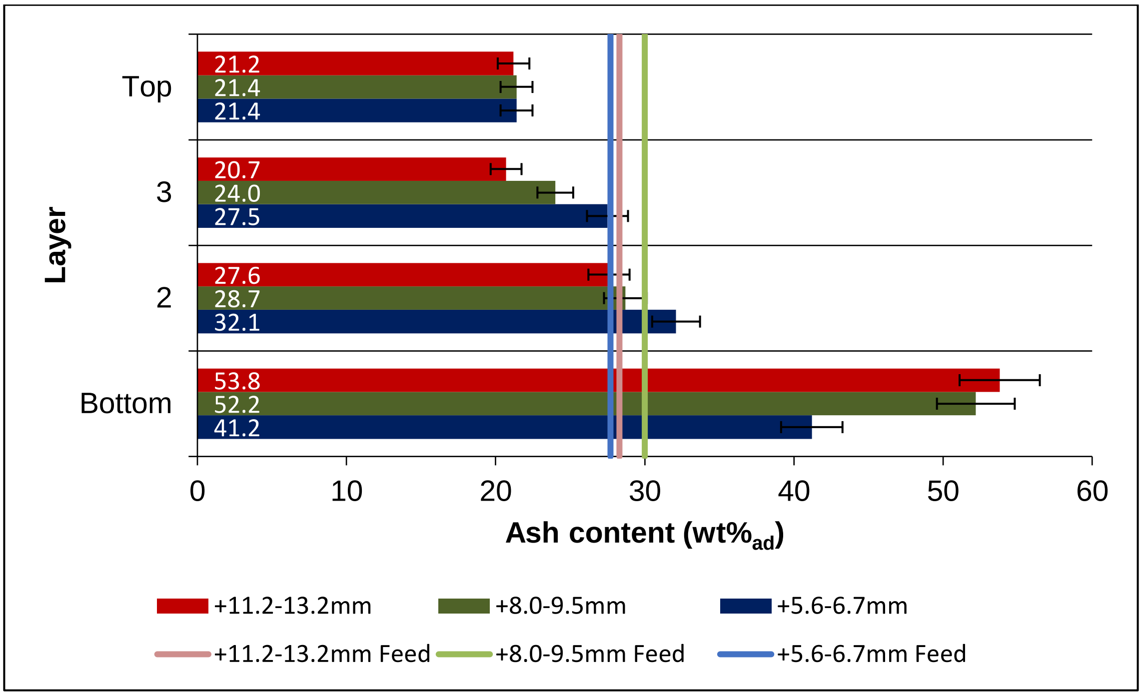

Figure 6.6: Comparison of PSD with regard to ash value (Q-02; DM 0:1; VD)

From *Figure 6.6*, comparable ash values were obtained in each of the bed layers when considering the three particle sizes displayed. The two sizes not depicted follow the same trend and charts with these are available on the accompanying DVD. Some appreciable variances from the above mentioned trend are however observed in the intermediate and bottom sections of the bed. When compared to the +11.2-13.2mm PSD (indicated by the red bar in *Figure 6.6*), the +5.6-6.7mm particles produced much lower ash values in the bottom layer. This is observed with the +6.7-8.0mm and +9.5-11.2mm ranges as well. These deviances may be as a result of the lower ash content of the feed for these ranges, meaning that less dense material is available to sink to the bottom and contribute to the poorer quality of coal therein. Similar results are seen for the +9.5-11.2mm PSD in the intermediate bed layers. The +5.6-6.7mm and +8.0-9.5mm size ranges however produced the highest ash values of all of the PSD's when considering the middle bed layers. These findings however correlate with the research conducted by Yang *et al.*, 2013, which concluded that the separation efficiency in the bed decreases with decreasing particle size.

The performance curves for the three PSD's discussed above are portrayed in Figure 6.7 along with the limiting performance curve obtained from the initial washability study of the

+11.2-13.2mm PSD (*Figure 6.6*). The limiting performance curves are generally similar for all particle sizes considered (as portrayed by the similar cumulative floats curves in *Chapter 4*).

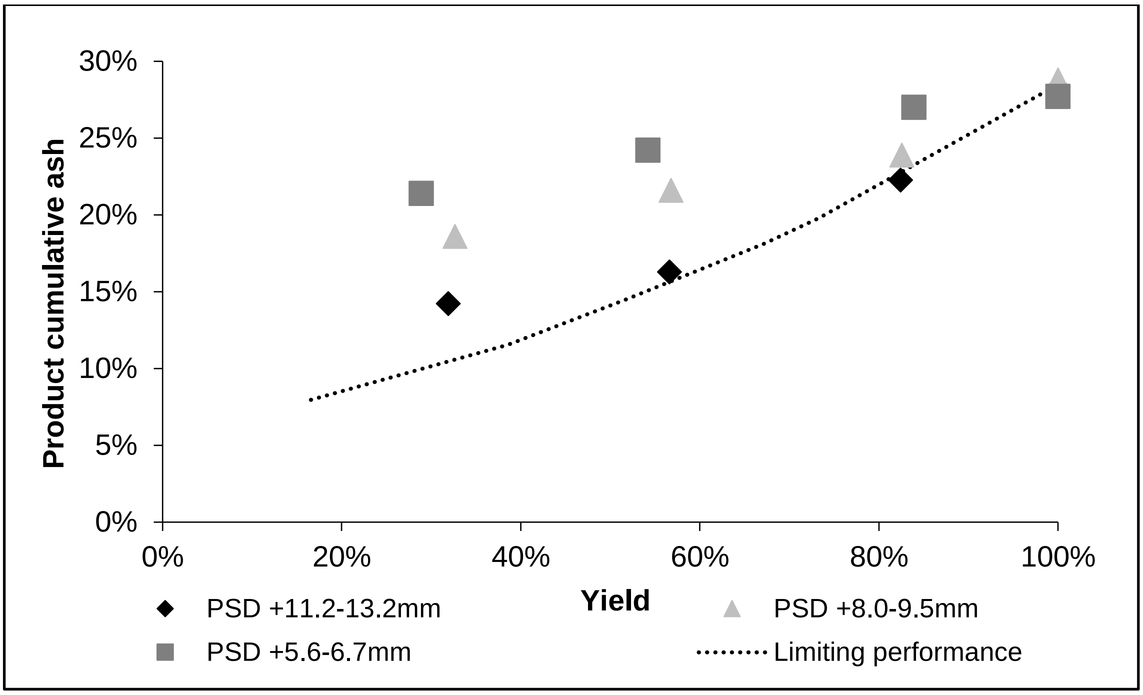

Figure 6.7: Comparison of bed performance curves when considering differing PSD (DM 0:1; VD)

From the data displayed in *Figure 6.7*, one can see that the conclusion drawn above, that the performance of the bed increases with increasing particle size, is validated. The +11.2-13.2mm particles behaved, for the most part, similarly to the limiting performance curve, indicating that a relatively good separation had occurred. The +8.0-9.5mm and +5.6-8.0mm particles vary significantly from the limiting performance curve in so indicating that these did not yield the optimal separation in the ADMFB. Furthermore, the smallest PSD (+5.6-8.0mm) yielded the largest deviation from the curve showing that this size fraction performed the worst as anticipated from the results found by Yang *et al.*, 2015.

When considering the particle size range comparison when DM and vibration are considered, the ash values produced in the top bed layer of the bed generally do not appreciably differ for the five particle size ranges across all magnetite ratios for vibration deactivated and activated. Slight variations from this trend are however encountered when considering the DM 1:1 and 2:1 ratios with activated vibration and the 2:1 DM ratio with vibration deactivated. In the former, the ash value in the top layers of the two smaller PSD's are considerably higher than that of the rest. When noting that dense medium and vibration are considered for these experiments and that a similar trend is observed for the intermediate and bottom layers, it is safe to assume that operating conditions of the bed may have been the cause. Even if extensively optimized, the batch-type procedure may affect the fluidization process where dense medium is considered and inadequate vibration parameters could contribute as well. With regard to the top layers in the 2:1 DM, VD experiments, a clear trend is observed (*Figure 6.X*). The ash values slightly decrease as PSD increases. This may be as a result of sampling however, a similar trend is observed in the bottom layer for all of the DM and vibration variables. Although not repeated in the top or intermediate bed layers for all variables, this trend appears in the bottom layers across all PSD's considered for DM 0:1 VA, DM 1:1 VA and DM 2:1 VA. *Figure 6.8* provides these results in bar chart form and this trend is clearly visible in the top layer.

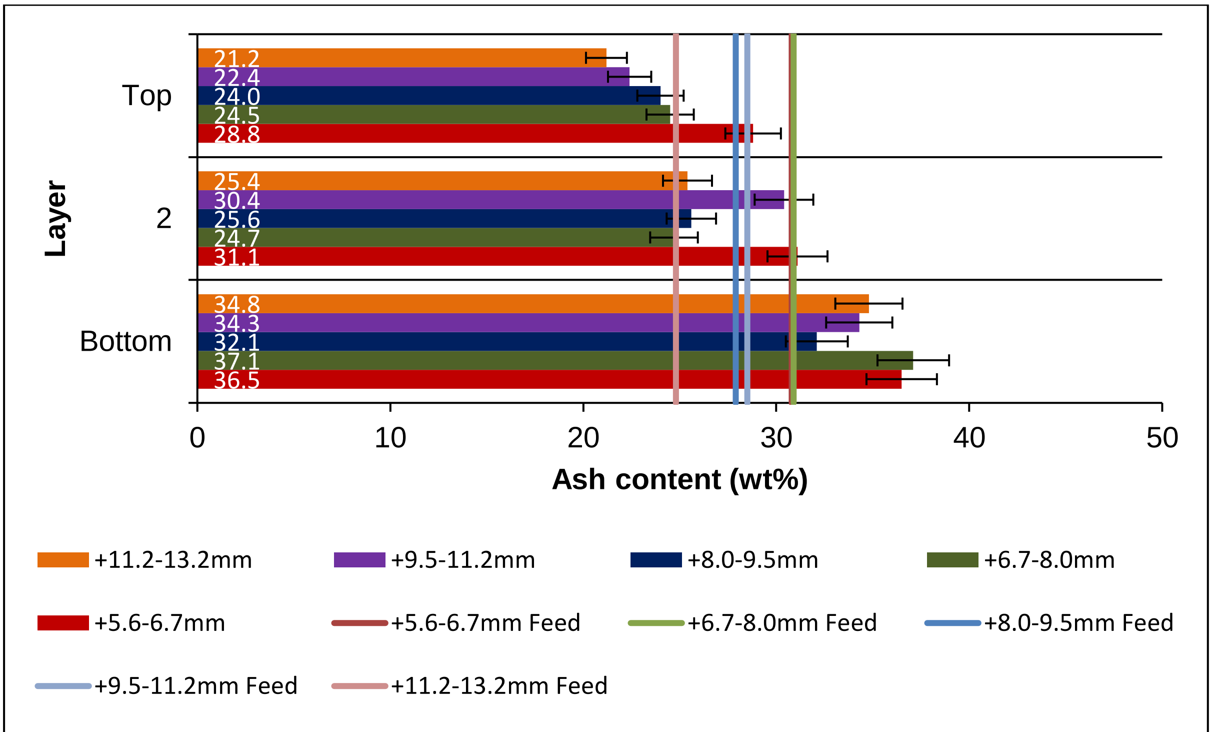

Figure 6.8: Comparison of PSD with regard to ash value (Q-02; DM 2:1; VD)

In summary, a change in PSD may seem to have insignificant effect on the ash value obtainable in the top bed layer. However, when considering the performance curves and some of the trends described above, it is clear that a larger PSD (+11.2-13.2mm) undergoes a more efficient separation as when compared to the smaller size ranges considered for this study. This is in accordance with the findings regarding PSD reported in literature and as described in Chapter 2.

6.3.2.2 Dense medium consideration

When taking into account the runs that made use of the +11.2-13.2mm PSD (vibration deactivated), the DM ratio proves no significant difference in the ash values obtained in the top layer. *Figure 6.9* displays the dense medium ratios (DM 1:1 & 2:1) compared to the control run discussed in Section 6.3.1.

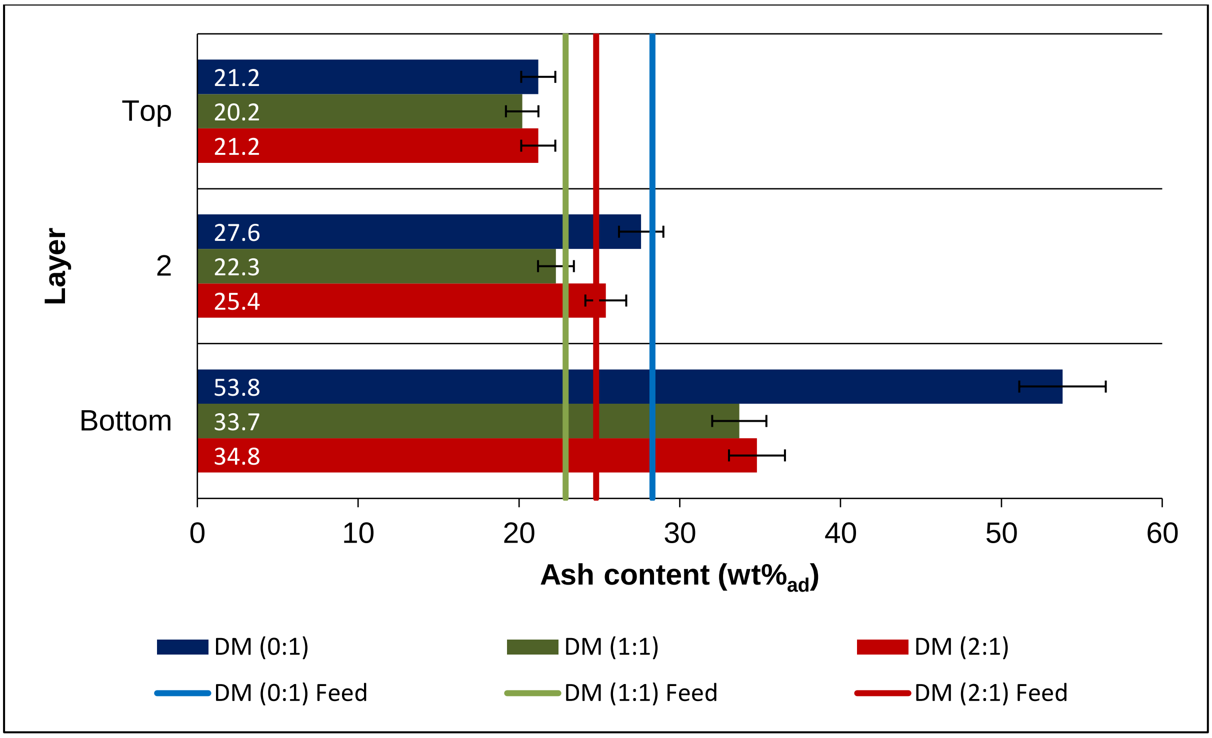

Figure 6.9: Comparison of DM ratio with regard to ash value (Q-02; PSD +11.2-13.2mm; VD)

From *Figure 6.9*, only slight variation is observed in the top layers when comparing DM to coal mass ratio. This implies that the addition of increasing amounts of dense medium will yield no better results than a bed operated without dense medium entirely. A noticeable difference between the bottom layers is however observed in that the ash value in the bottom layer decreases with increasing ratio from 0:1, 1:1 and 2:1 (most appreciably from DM 0:1 to 1:1 and only slightly from DM 1:1 to 2:1). The highest ash values in the bottom layer (as desired) are obtained from beds containing no dense medium. This observation holds true for all five particle sizes even upon initiation of vibration and may be as a result of the increased size of the inter-particulate voids present in a bed made up of purely coal. These openings were clear of any fine magnetite powder and the movement of particles in these voids is easier.

The performance curves comparing the dense medium ratios for the +11.2-13.2mm PSD with vibration deactivated are depicted in *Figure 6.10*. From this data it is once again clear that the 0:1 DM ratio yielded the best performance in terms of separation efficiency.

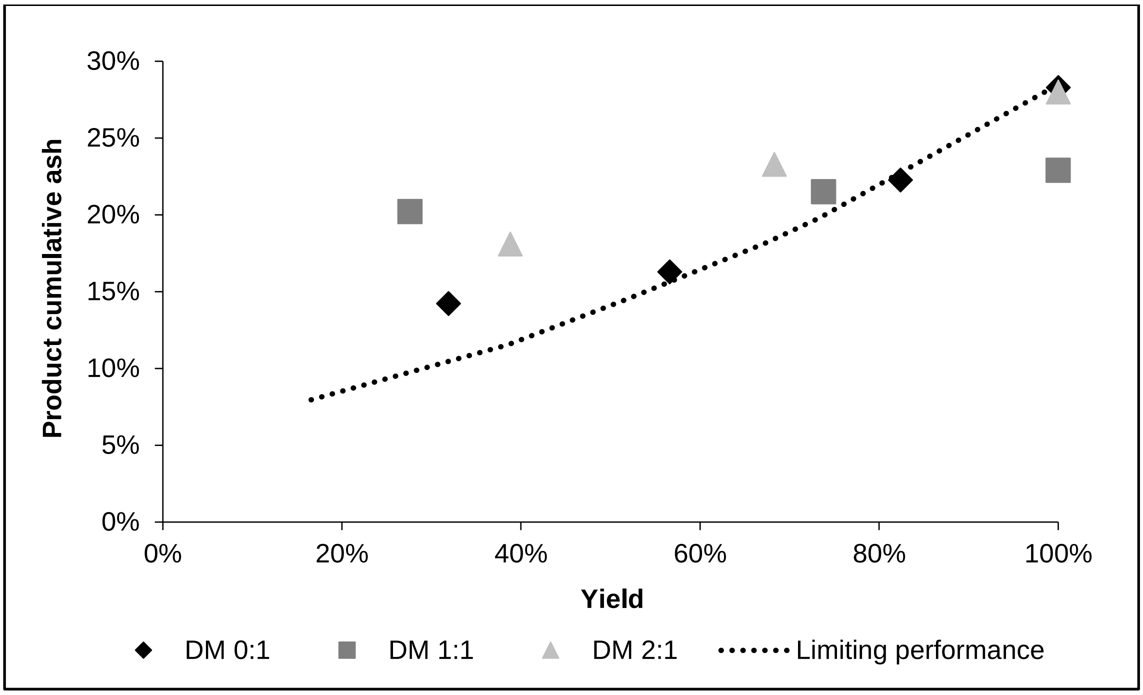

Figure 6.10: Comparison of bed performance curves when considering differing DM (PSD +11.2-13.2mm; VD)

When considering the other PSD ranges (+5.6-11.2mm), some variances from the above-discussed trend for the top layer of the bed were observed. A lower ash content is obtained in the top layer of the 0:1 DM beds when compared to the 1:1 and 2:1 ratios. This trend proves true for a number of the runs in varying ash differentials. When considering the overall stratification of dense medium runs, it is apparent that the separation undertaken in the bed was poor. *Figure 6.11* provides a bar chart portraying this poor separation trend.

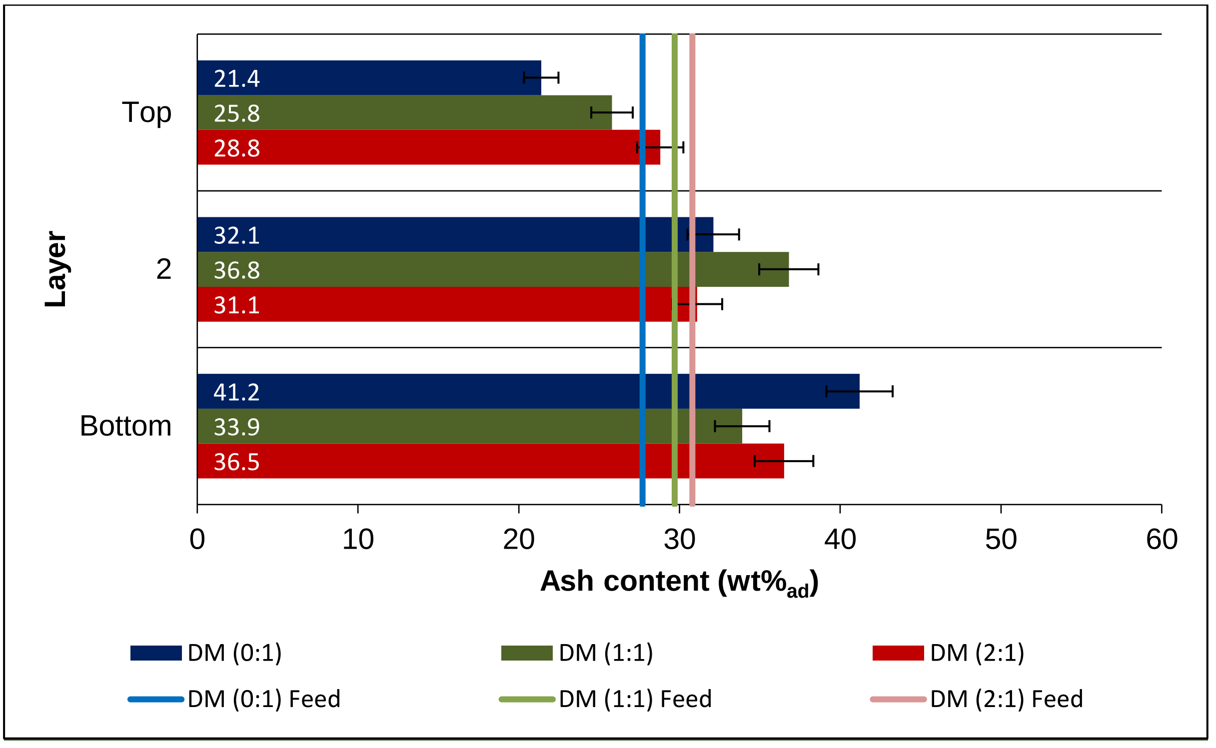

Figure 6.11: Comparison of DM ratio with regard to ash value (Q-02; PSD +5.6-6.7mm; VD)

Figure 6.11 shows that the 0:1 DM bed produced the most acceptable results of the three dense medium ratios compared. A distinct difference is observed in both the top and bottom layers. The green and red bars depicting the bed layer ash values for DM 1:1 and DM 2:1, respectively, show very little improvement from the feed ash value. This may be as a result of the batch type experiments conducted for this study and a continuous process where the magnetite is fluidized before addition of the coal may yield different results.

Furthermore, it is useful to note that the dense medium to coal mass ratio influences the minimum fluidizing velocity of a specific bed. As previously stated, a fluidized bed containing medium induces a suspension of the magnetite and the coal merely separates according to the relative density difference. Determined in *Chapter 5*, the MFV of a pure dense medium bed of 15kg was found to be 8.0m/s with a bed density of 1.31g/cm^3. As a result, the minimum incipient point of the dense medium beds should not differ drastically if the static bed height remains relatively constant. *Table 6.4* presents the U_{mf} values observed for coal PSD's of +11.2-13.2mm and +5.6-6.7mm with vibration deactivated.

Table 6.4: Comparison of minimum and operating fluidizing conditions for DM and PSD (Q-02; VD)

PSD (mm)	Bed mass (g)	Layers	U_{mf} (m/s)	U*	U (m/s)
		+11.2-13.2mm			
0:1	15060	4	**15.1**	1.07	**16.1**
1:1	15000	3	**8.6**	1.14	**9.8**
2:1	15000	3	**9.2**	1.14	**10.5**
		+5.6-6.7mm			
0:1	15200	4	**9.2**	1.13	**10.4**
1:1	15000	3	**7.2**	1.15	**8.3**
2:1	15000	3	**5.2**	1.33	**6.9**

As seen in *Table 6.4*, a decrease in MFV is expected when adding medium to system. The extent of the decrease as observed for the +11.2-13.2mm PSD is probably attributed to the amount of layers that decrease from 4 to 3. This is in order to conform to the bed load specifications and capability of the blower. Further visible is that the MFV for the dense medium experiments range close to that of the 8.0m/s obtained for a pure magnetite bed, with pure magnetite bed to coal-magnetite bed scaling factors in the range of 0.89 and 1.33. The latter is in accordance with the values as stipulated by He *et al.* (2015) but the former is slightly low. The control of this scaling factor in the batch tests may provide some further reasoning for the poor separation observed with the beds utilising dense medium.

6.3.2.3 Vibration

As discussed in *Chapter 2*, the addition of vibration to the ADMFB lowers the MFV and improves the stability of fluidization as a result of adequate bubble formation and movement (He *et al*., 2015). *Table 6.5* provides an indication of the influence of vibration on each coal

PSD studied. The bed masses were 15kg with 4 layers for all experiments considered in this comparison.

Table 6.5: Comparison of minimum and operating fluidizing conditions for vibration (Q-02; DM 0:1)

Vibration	U_{mf} (m/s)	U*	U (m/s)
	+11.2-13.2mm		
VD	**15.1**	1.07	**16.1**
VA	**14.7**	1.04	**15.3**
	+9.5-11.2mm		
VD	**14.4**	1.09	**15.1**
VA	**14.1**	1.00	**14.1**
	+8.0-9.5mm		
VD	**14.7**	1.01	**14.8**
VA	**11.1**	1.15	**12.8**
	+6.7-8.0mm		
VD	**11.2**	1.13	**12.6**
VA	**10.3**	1.05	**10.8**
	+5.6-6.7mm		
VD	**9.2**	1.13	**10.4**
VA	**8.0**	1.15	**9.2**

A clear decrease in MFV is observed for every PSD when activating vibration. This is as expected from literature. *Figure 6.12* provides the comparison chart of vibration deactivated (VD) and activated (VA) for the control run of +11.2-13.2mm PSD and corresponding DM ratio of 0:1.

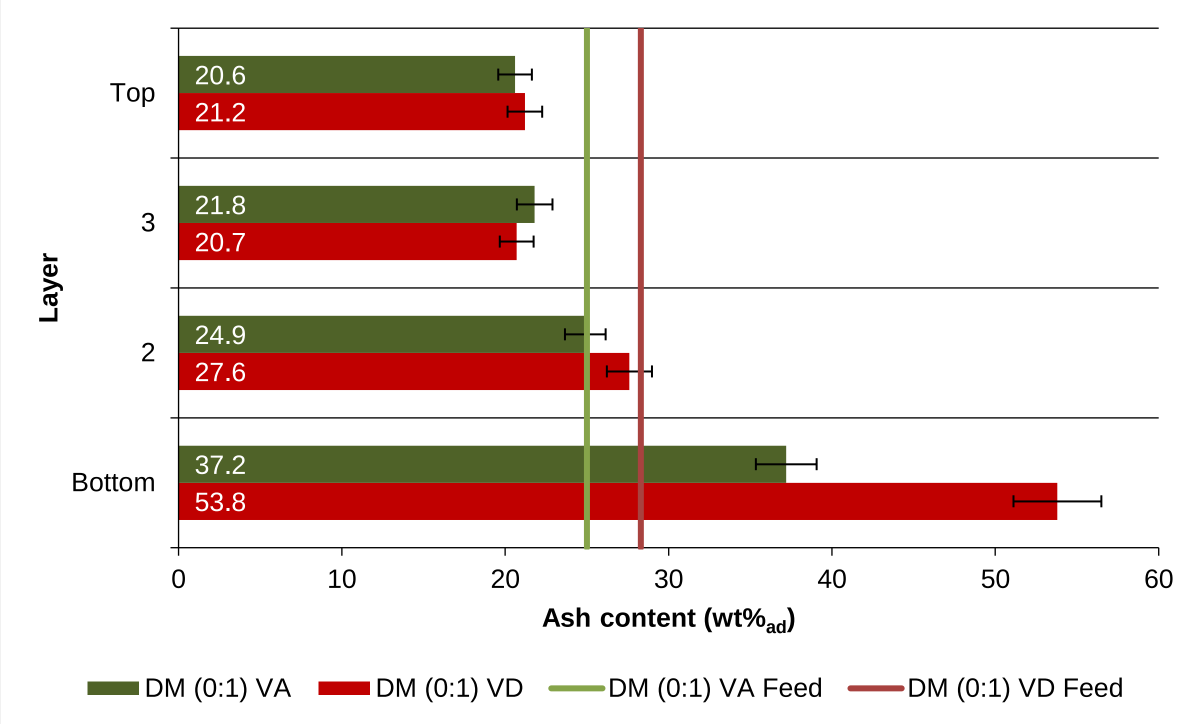

Figure 6.12: Comparison of vibration with regard to ash value (Q-02; PSD +11.2-13.2mm; DM 0:1)

Figure 6.12 illustrates that a marginal difference is experienced across the bed layers except when considering the ash values of the bottom layer. The bed operated without vibration produced a bottom layer with much larger ash content than the bed with vibration activated. A similar observance is made for all PSD's conducted on pure coal beds. This may be as a result of the particles in the intermediate layers moving into the bed voids and packing tightly thereby inhibiting the further downwards movement of more dense particulates. A vibration frequency and amplitude that is too vigorous and also the initiation of vibration too early may be plausible explanations for the dense packing and hence the occurrence in the bottom layer of the bed.

These results differ from that which is published in literature which report the addition of vibration to improve the stability of fluidization and thereby the separation efficiency of the bed (Yang et al., 2013a; He et al., 2015 and Dwari & Rao, 2007). The difference in findings may be as a result of vibration parameters (frequency and amplitude) that induced a vibration that was not optimal proper separation. The performance curves for the runs operated with vibration activated (VA) and vibration deactivated (VD) for the +11.2-13.2mm

PSD at a DM ratio of 0:1 are provided in *Figure 6.13*. It is clear from this figure that the run conducted with vibration deactivated performed much more efficiently than when vibration was activated.

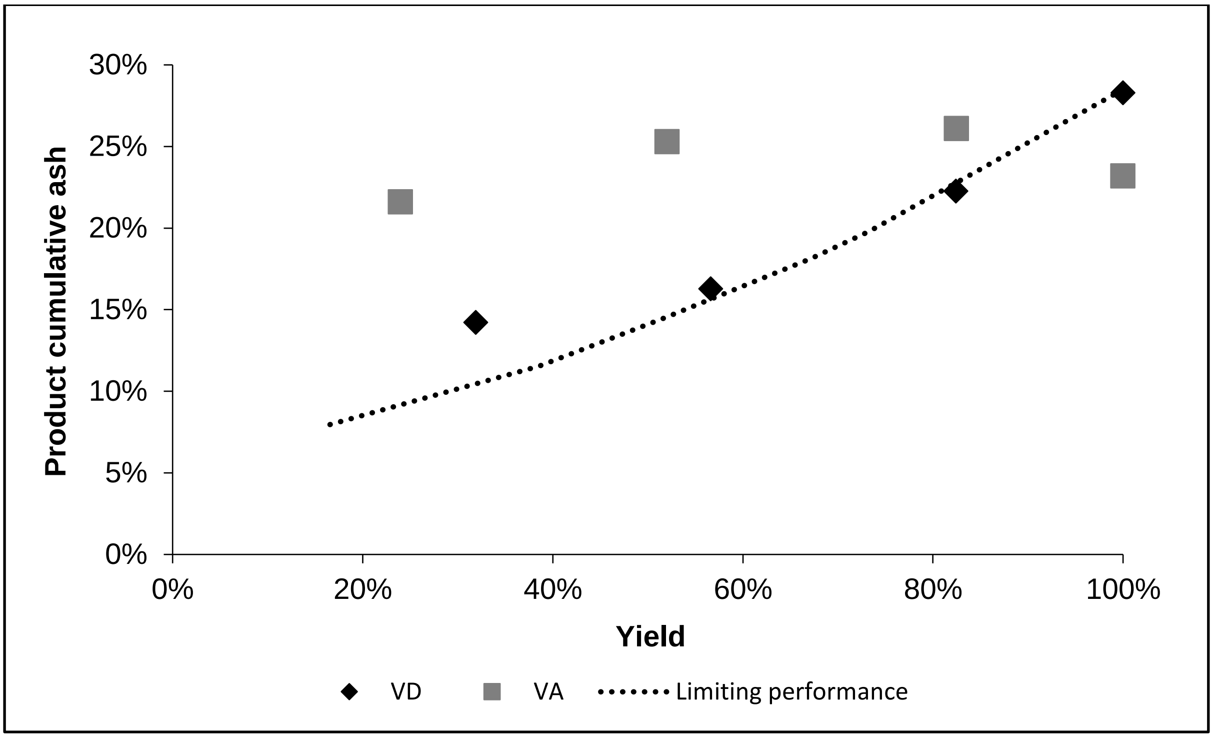

Figure 6.13: Comparison of bed performance curves when considering differing vibration (PSD +11.2-13.2mm; DM 0:1)

When considering the other DM ratios, relatively poor separation is found in the beds that consider dense medium in 1:1 and 2:1 ratios and furthermore the addition of vibration proves no improvement of ash values throughout the bed layers. When comparing the results of +11.2-13.2mm PSD, DM 2:1 for vibration deactivated and activated, minimal variances between ash values are observed across all of the bed layers. Differences are observed where the VD bed produces a better result but are so insignificant that it cannot be deemed concrete. This is however noticed for most of the runs conducted with DM. The slight improvement may be attributed to the particles being able to move freely when vibration is deactivated even in the presence of magnetite. The addition of vibration with increased amounts of DM most likely caused and even denser packing in the bed which hindered particle movement and thereby rendered no extensive separation. Once again, it must be noted that this is probably as a cause of the batch experimentation method followed. The effect of a vibration that may have been inadequate can also be considered in that an unstable fluidization commenced and thereby hindered the separation efficiency of the bed. *Figure 6.14* provides the bar chart depicting the trend that was discussed in the above deliberations.

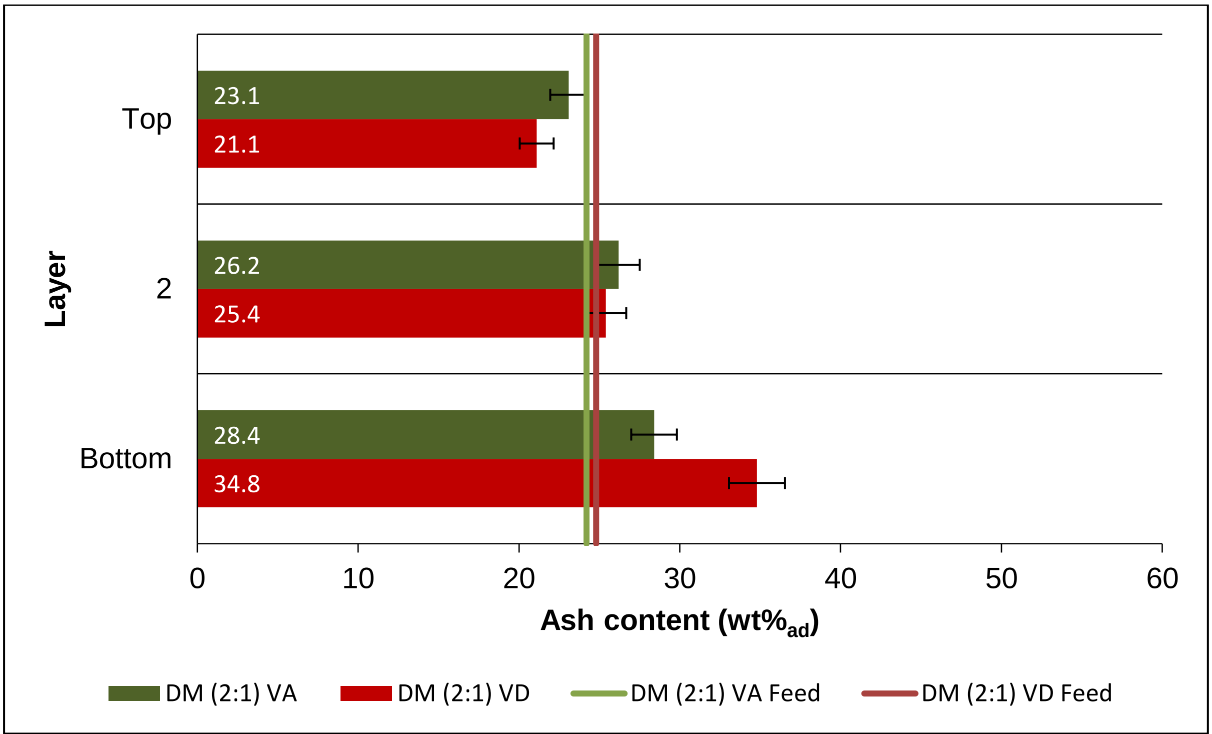

Figure 6.14: Comparison of vibration with regard to ash value (Q-02; PSD +11.2-13.2mm; DM 2:1)

From *Figure 6.14,* it is clear that an insignificant extent of improvement is expected when adding vibration to a system containing dense medium.

6.3.2.4 Observation of anomalies

Two major anomalies were observed throughout the experiments considering the various dense medium and vibration parameters. These are (1) severe back mixing in the bottom layer and (2) ash mass balances that do not correlate. *Figure 6.15* provides a case in point of both anomalies.

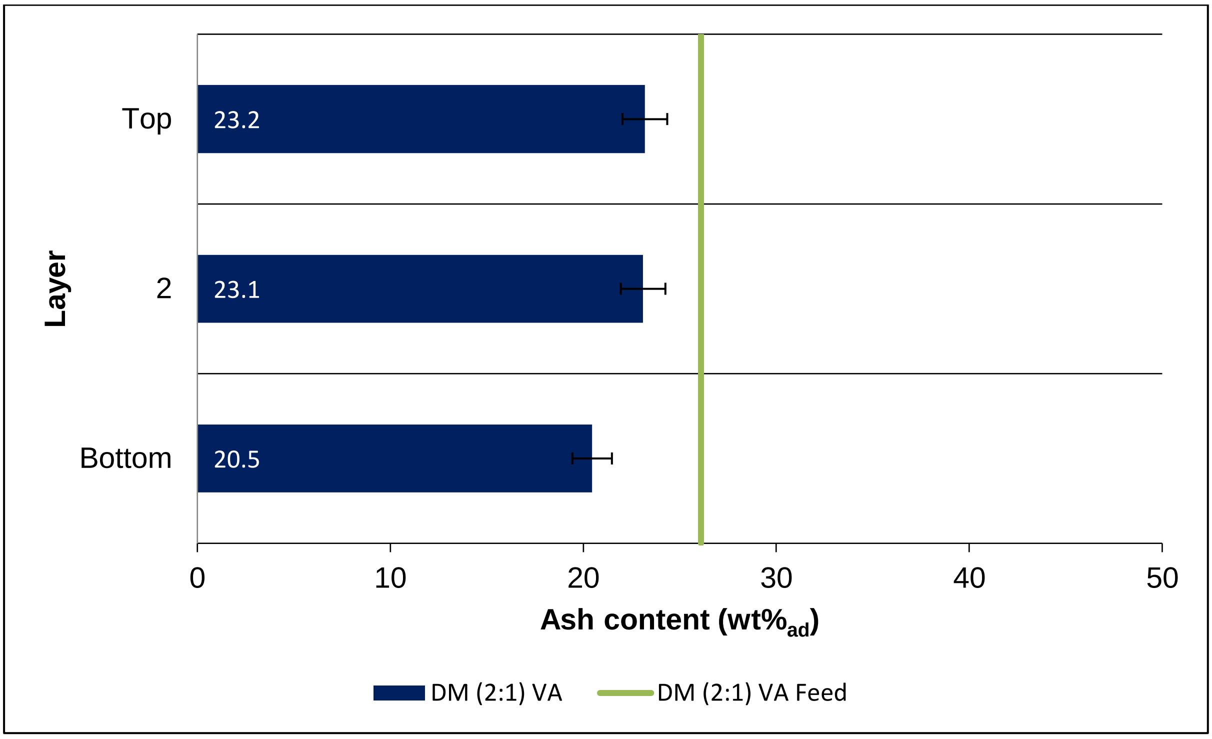

Figure 6.15: Back mixing and incorrect ash balance (Q-02; PSD +5.6-6.7mm; DM 2:1; VA)

Evident from *Figure 6.15*, is that the bottom layer contains a lower ash content than the second and top layer and that feed ash is higher than all three layers. This is indicative of a bed that was poorly operated and experienced severe back mixing in the bottom layers. This is once again attributed to the inadequate fluidizing environment as a result of dense medium and vibration that behaved unexpectedly. A more vigilant approach to the optimizing of dense medium vibratory beds during batch testing is inevitable. The ash balance that is inaccurate could be as a result of experimental errors during analysis of the feed coal as very little sample loss and magnetite contamination is experienced.

6.3.3 Verification and repeatability

The reproducibility of the fluidization process and all analyses have been established in *Chapters 4* and *5* with the characterization and initial runs. Selected runs were repeated during the main investigation. *Table 6.6* contains the statistical error percentage values achieved for the +8.0-9.5mm PSD, 0:1 DM with VD and those of +11.2-13.2mm, 2:1 VD. All representations of the conducted verification studies are available in *Appendix F* or the associated DVD.

Table 6.6: Verification and repeatability data

Run description	Layer	Ash (% error)	CV (% error)	TRD (% error)
PSD +8.0-9.5mm DM 0:1 VD	Feed	0.23	0.14	0.14
	Top	0.35	0.50	0.24
	3	0.51	0.12	0.12
	2	0.02	0.03	0.03
	Bottom	0.69	0.23	0.07
PSD +11.2-13.2mm DM 2:1 VD	Feed	0.76	0.14	0.07
	Top	0.74	0.14	0.06
	2	0.11	0.23	0.12
	Bottom	1.03	0.12	0.05

From *Table 6.6*, it is apparent that good repeatability of the experimental runs was achieved. Three runs conducted on the same material at relatively similar conditions yielded ash values for each layer that are closely comparable and within standard percentage errors well below 1.03. Similarly low standard deviations are visible for the CV and TRD data of the same run. This, along with the low standard deviations for the sampling and analytical methods as portrayed in *Section 4.2.2* of *Chapter 4*, proves that the procedure is repeatable and is able to reproduce accurate results.

6.3.4 Statistical significance

The probability that a randomly chosen sample is not representative of the population is broadly termed as the statistical significance. A reduction in the significance of a sample leads to more certainty that the results are reproducible. Two statistical significance tests are considered applicable to the data, (1) ANOVA and (2) t-test. The former is a one-way analysis of variance and is used in the cases where three and more parameters are tested

(PSD and DM). The t-test is generally referred to as significance testing and was made use of in cases where less than three parameters are present (Vibration).

For both tests a p-value is calculated for the population and forms a criterion from which the statistical significance of a sample can be deduced. Ellis and Steyn (2003) provided the following guideline in that a p-value below 0.05 indicates statistical significance and a result above 0.05 proves statistical insignificance.

Relevant ANOVA or t-tests were conducted on the final ash, calorific and true relative density values obtained for changes in (1) PSD, (2) DM to coal mass ratio and (3) state of vibration. The ANOVA results regarding the ash values obtained in the bottom and top bed layers with respect to particle size and dense medium ratio are provided in *Table 6.7*.

Table 6.7: ANOVA statistical significance results

Manipulated variable	Measured variable	Sum of squares	d_f	Mean square	F-value	p-value
Top bed layer						
Particle size	Ash value	54.19	4	13.55	1.97	0.13
DM ratio	Ash value	68.08	2	34.04	5.80	0.008
Bottom bed layer						
Particle size	Ash value	10.51	4	2.62	0.048	4.88E-20
DM ratio	Ash value	805.30	2	402.65	19.01	7.02E-06

From the p-values summarized in Table 6.7, it is clear when focussing on the ash values obtained in the bottom layer, that both the particle size and amount of magnetite are governing parameters during the fluidization process. Further obtained from Table 6.7 is the F-value which provides an indication of the variability between groups to that within groups. Clearly the DM ratio shows more variance when considering ash content in the bottom (discard) layer. For the top (product) bed layer, the p-value obtained for PSD is higher than 0.05 and thereby proves that PSD has no major influence on the ash value obtainable in the top bed layer. However, the DM ratios p-value is below 0.05 and does bear influence on the separability of the ADMFB. The response of the t-test when regarding the ash value in the top and bottoms layers of the bed is provided in *Table 6.8*.

Table 6.8: T-test statistical significance results

Manipulated variable	Measured variable	Mean	Standard deviation	t	d_f	p-value
Top bed layer						
Vibration	Ash value	23.41	7.69	-1.51	14	0.15
Bottom bed layer						
Vibration	Ash value	39.23	7.33	2.303	28	0.029

From the p-values displayed in *Table 6.8*, it is clear that the ash value obtained in the bottom layer is affected by the activation of vibration whereas the top bed layers are once again not influenced thereby.

6.3.5 Conclusion on variable influences

In conclusion, with regard to the influence of PSD, a slight decrease in minimum fluidizing velocity is observed as particle size decreases, most likely due to the smaller surface area associated with these sizes. No significant difference is observed in the ash values obtained in all layers when comparing PSD at a DM ratio of 0:1 vibration deactivated. The performance curves do indicate that the beds operated with larger PSD yield a better separation efficiency, in terms of mass yield, when compared to the smaller size fractions. Some trends do appear in the top and bottom layers of the experiments conducted with medium. From these it appears that the larger PSD yields better results in the top bed layer when compared to the smaller sizes. The slight differences observed between the layers of each PSD are possibly attributed to the bed operating conditions and differing ash contents observed in the feed of that specific PSD. Some of these findings are highlighted in *Table 6.9*, which provides a summary of the ash content data pertaining to the experiments discussed above.

Table 6.9: Comparison of data obtained using the better liberated (low ash) coal (ash values per selected bed layer in $\%_{wt}$)

Vibration	Layer	+11.2-13.2 mm	+9.5-11.2 mm	+8.0-9.5 mm	+6.7-8.0 mm	+5.6-6.7 mm
0:1 DM						
VD	Feed	28.3	22.3	30.0	26.3	27.7
	Top	**21.2**	**18.6**	**21.4**	**20.1**	**21.4**
	Bottom	**53.8**	44.5	52.2	46.5	**41.2**
	Differential	7.1	3.7	8.6	6.2	6.3
VA	Feed	23.2	25.0	28.1	25.8	28.0
	Top	**21.6**	20.6	24.0	23.1	**23.1**
	Bottom	**36.2**	37.2	41.6	40.0	**43.2**
	Differential	1.6	4.4	4.1	2.7	4.9
1:1 DM						
VD	Feed	22.9	26.4	25.9	40.0	29.7
	Top	**20.2**	23.9	24.0	21.8	**25.8**
	Bottom	**33.7**	34.6	34.0	34.6	**33.9**
	Differential	2.7	2.5	1.9	18.2	3.9
VA	Feed	23.7	27.3	26.2	28.7	33.4
	Top	**21.4**	22.3	23.4	30.0	**27.4**
	Bottom	**23.0**	30.0	29.8	30.3	**34.8**
	Differential	2.3	5.0	2.8	-1.3	6.0
2:1 DM						
VD	Feed	24.8	28.5	27.9	30.9	30.8
	Top	**21.2**	22.4	24.0	24.5	**28.8**
	Bottom	**34.8**	34.3	32.1	37.1	**36.5**
	Differential	3.6	6.1	3.9	6.4	2.0
VA	Feed	23.1	24.2	24.2	26.1	33.0
	Top	**23.1**	26.5	23.7	28.0	**25.8**
	Bottom	**28.4**	30.0	29.7	32.8	**31.5**
	Differential	0.0	-2.3	0.5	-1.9	7.2

Highlighted in red, are the cells illustrating that no difference is observed within ash contents obtained in the top bed layers for varying PSD at a DM of 0:1 and VD. This trend is similar for all data displayed and is further corroborated by the 0.13 p-value obtained from the ANOVA test.

The effect of DM is highlighted in green for the +11.2-13.2mm PSD within *Table 6.9*. Once again no appreciable improvement is observed in the ash yield obtained in the top layer upon increasing amounts of medium for vibration activated and deactivated. A noteworthy difference is however observed, with the bottom layers of the DM beds compared to the pure coal runs. The ash value obtained in the bottom layer decreases as DM is increased from 0:1 to 1:1 and 2:1. This observation was proven true for all variable considered when comparing the effect of added dense medium and may be attributed to the hindering of particle movement as a result of fine magnetite occupying the bed voids. The ANOVA results portrayed in *Section 6.3.4* further validate this conclusion.

The MFV is also affected by the increase in amount of medium in that it decreases slightly but remains relatively close to 8.0m/s. This is due to the fact that the magnetite fluidizes and causes a separation of coal by density. A general observance upon the addition of medium to the bed is that a poorer degree of stratification was experienced and that fluidization did not yield desired results as when compared to beds operated without DM.

Indicated in blue for all DM ratios of +5.6-6.7mm particles is that the difference in the ash contents, when comparing a run with vibration deactivated to that when vibration is activated, was trivial. However, a large variation was observed in the ash content reporting to the bottom layer. The VD runs produce a bottom layer with significantly larger ash value than the opposing VA experiments. This indicates that destoning is more effective in a bed without vibration and may result from more freedom of particle movement. This observation is validated with the very low p-value obtained for the bottom layer from the t-test. In a bed that is vibrated the intermediate and bottom layers may pack densely, hence inhibiting the downwards movement of the more dense particles. Once again, much poorer separation efficiency was observed when vibration was activated, which could be attributed to inadequate vibration conditions and the operation of the bed as a batch process. In regard to bed operation, vibration (as expected) reduces the MFV considerably and yields a more stable fluidized bed. Further validation of the trends as discussed above is seen when focussing on the ash differential (percentage points). This provides an indication of the extent to which the coal in the top layer was upgraded from the feed. Visible from *Table 6.9* is that the largest differential values mostly correlate to the pure coal beds with vibration deactivated.

6.4 Chapter summary

From the data as described above it is clear that beneficiation of the coal is possible, to some extent, by the ADMFB method. This is however, greatly affected by the feed and bed operating conditions as well as the utilization of inadequate vibration parameters. The data as observed in Chapter 5 correlates with that which is discussed above and together this provides a comprehensive idea about the ADMFB process for the beneficiation of South African small coal. Even more specifically to the effects of (1) particle size, (2) addition of dense medium and (3) activation of vibration.

Chapter 7: CONCLUSION AND RECOMMENDATIONS

Chapter 7 presents the conclusions that were drawn from the data obtained as well as any further recommendations for the project entitled "*The dry beneficiation of South African small coal in a dense medium fluidised bed*".

- **Section 7.1:** Provides an overview of the study problem and details the associated objectives as stipulated in the introduction.
- **Section 7.2:** Presents the main operating observations and conclusions drawn from the study as a whole.
- **Section 7.3:** Provides recommendations for future work on a similar project and the ADMFB as designed for this study.

7.1 Overview

South Africa, an arid country, is exploring ways to utilise water responsibly, especially pertaining to the coal processing industry. In recent years, focus has shifted to processing of coal by dry means instead of wet and as a result, air dense medium beneficiation technique has received much attention. The purpose of this project was therefore to investigate the extent to which a dense medium fluidized bed can beneficiate South African small coal with these specific objectives in mind:

An established design, commissioning and operation of an enlarged ADMFB with the capabilities of effectively fluidizing (1) 5.6-13.2mm coal particles and (2) increased bed loads while considering:

- Investigation into the final ash, density and calorific values obtainable from the ADMFB and noting if a significant improvement was made to the separation efficiency while considering the following variables:
- Coal quality

  (High intrinsic ash content Q-01; low intrinsic ash content Q-02)
- Coal feed PSD

  (+5.6-6.7mm; +6.7-8.0mm; +8.0-9.5mm; +9.5-11.2mm & +11.2-13.2mm)

- Mass ratio of dense medium to coal
  (0:1, 1:1 & 2:1)
- Vibration state of the ADMFB
  (Activated & deactivated)

7.2 Conclusions

Observed from the results obtained for the study is that the newly designed ADMFB proved to successfully de-stone the Witbank ROM coal (+5.6-13.2mm). The coal was mostly stratified according to density which can generally be associated with increased ash values and reduced CV. The dense material mostly reported to the bottom layer of the bed and the better quality coal remained in the top sections. Additional to the effective beneficiation of the ADMFB, the bed design proved to be most applicable for the following:

- Capable of effectively fluidizing the 5.6-13.2mm coal particles and increased bed loads considered for this study.
- Provided enough properly dispersed air into the bed through the improved air distribution chamber and distributor plate mechanism.
- Severely reduced the dust pollution to the air with a modified tapered trapezoidal head layer providing an increased outlet area covered by 0.1mm wire mesh.
- Ensured accurate measuring and control of the air flow and bed pressure drop with the improved sensors and control unit.

The main conclusions as related to the influence of varying coal feed particle size distribution, the mass ratio of dense medium to coal, the coal feed quality and the addition of vibration are detailed in the following sections.

7.2.1 Yield and stratification

When assuming a cut-point of 50mm along the bed height (discarding the bottom layer), the best cumulative yields obtained for each PSD are as follows:

- The best cumulative product for +11.2-13.2mm was obtained with no dense medium or vibration. The lowest ash yield, CV and density values of 14.2%$_{wt}$, 24.1MJ/kg and 1.56g/cm^3 were produced, respectively at a theoretical cut point of 150mm (using only the top layer as product). This corresponds to a mass yield of 31.9% whereas the best mass yield obtainable is 82.4% with a theoretical cut point of 50mm (using the top 3 layers as product) but corresponds to an ash value of 22.27%$_{wt}$. This was for a feed ash value of 28.3%$_{wt}$.

- The best cumulative product for +9.5-11.2mm was obtained with no dense medium or vibration. The lowest ash yield, CV and density values of 13.0%$_{wt}$, 25.0MJ/kg and 1.54g/cm^3 were produced, respectively at a theoretical cut point of 150mm (using only the top layer as product). This corresponds to a mass yield of 27.6% whereas the best mass yield obtainable is 82.2% with a theoretical cut point of 50mm (using the top 3 layers as product) but corresponds to an ash value of 18.3%$_{wt}$. This was for a feed ash value of 22.3%$_{wt}$.
- The best cumulative product for +8.0-9.5mm was obtained with no dense medium or vibration. The lowest ash yield, CV and density values of 18.6%$_{wt}$, 23.7MJ/kg and 1.56g/cm^3 were produced, respectively at a theoretical cut point of 150mm (using only the top layer as product). This corresponds to a mass yield of 32.7% whereas the best mass yield obtainable is 82.6% with a theoretical cut point of 50mm (using the top 3 layers as product) but corresponds to an ash value of 23.9%$_{wt}$. This was for a feed ash value of 28.8%$_{wt}$.
- The best cumulative product for +6.7-8.0mm Q-02 was obtained with no dense medium or vibration. The lowest ash yield, CV and density values of 13.7%, 24.0MJ/kg and 1.57g/cm^3 were produced, respectively at a theoretical cut point of 150mm (using only the top layer as product). This corresponds to a mass yield of 27.9% whereas the best mass yield obtainable is 80.6% with a theoretical cut point of 50mm (using the top 3 layers as product) but corresponds to an ash value of 12.8%$_{wt}$. This was for a feed ash value of 26.3%$_{wt}$
- The best cumulative product for +5.6-6.7mm Q-02 was obtained with no dense medium or vibration. The lowest ash yield, CV and density values of 17.6%, 22.7MJ/kg and 1.64g/cm^3 were produced, respectively at a theoretical cut point of 150mm (using only the top layer as product). This corresponds to a mass yield of 28.9% whereas the best mass yield obtainable is 83.9% with a theoretical cut point of 50mm (using the top 3 layers as product) but corresponds to an ash value of 17.6%$_{wt}$. This was for a feed ash value of 27.7%$_{wt}$.

Given the ash and mass yield data as listed above, it is clear that an extremely low ash yield is obtainable but at a moderately low mass production. It must be noted that mass yields comparable to that in literature (as stated in the hypothesis as 78.3%) were attained but at slightly higher ash yields than the 8.2%$_{wt}$ expected. Also evident from above is that the beds utilizing no dense medium and vibration achieved the best overall performance. Some further elaboration is made with respect to this in *Section 7.2.2*.

7.2.2 Particle size distribution

The particle size ranges considered for this investigation proved to have no significant effect on the ash values obtained from the top layers if the bed. Comparable ash values are obtained in in each layer across all PSD's with the consideration of each study variable. When additionally considering the ash and mass yield data summarized in Section 7.2.1 above, it is clear that the larger PSD however performed best and this decreases as particle size decreases. The PSD does affect the operating conditions of the bed in that an appreciable difference is noted in the minimum fluidizing requirements of the varying PSD's. A clear decrease in MFV is observed for a reduction in particle size which is attributed to the associated decrease in particle surface area and the lower buoyant force therefore required for suspension.

7.2.3 Addition of dense medium

By adding magnetite dense medium, the density separation of the coal-magnetite beds suffered whereas the pure coal beds delivered results that were more promising. When considering bed stratification, the top layers for each dense medium ratio considered produced similar ash contents with some deviances where the beds of no medium produced slightly lower values. However, substantial differences were observed in the ash yields pertaining to the bottom bed layer. Much higher ash values were observed in the bottom most layers because better de-stoning achieved for the "no medium beds" – this held true for the majority of variables considered for this study. This is attributed to the occupation of the inter-particulate bed voids with fine magnetite powder. Increased difficulty of the particles to move within the bed is thus experienced as a result of the batch-type experimentation.

The poor separation observed with dense medium beds as compared to those of pure coal, may additionally be attributed to the more sensitive nature of a fluidized dense medium bed.

Furthermore, the occurrence of back mixing, channelling and the formation of dead zones inside the bed was found to be more severe when a dense medium was introduced. Poor separation in the bed is expected when considering the above mentioned occurrences. An increase in mass ratio from 1:1 to 2:1 additionally showed no consistent positive or negative impact on the separation capability of the bed. The above conclusions are corroborated by the comparison of the performance curves for each DM ratio in which that of the pure coal beds exhibited a better separation efficiency.

A definitive effect of the addition to, and increase of dense medium during experimentation is observed for the minimum fluidizing requirements. The addition of magnetite reduced the MFV drastically when compared to a bed operated without magnetite. This is as a result of the reduced particle size of the magnetite even when considering particle and wall interactions. In a dense medium bed, effectively, the magnetite fluidizes and the coal merely floats or sinks according to density. As such the reduction in MFV is expected as the amount of dense medium increases. To note is that the incipient velocity of the dense medium beds range closely to that obtained when determining the MFV of a “magnetite only” bed.

7.2.4 Activation of vibration

The addition of vibration yielded no significantly improved results in the bed layers but worsened the ash value obtainable in the bottom layer. This may be because of the particles in the intermediate layers moving into the bed voids and packing tightly, thereby inhibiting the further downwards movement of more dense particulates. A vibration frequency and amplitude that is too vigorous and also the initiation of vibration at too early an instance may be plausible explanations for the dense packing. It was found that the beneficiating of the coal within the ADMFB is heavily reliant on the separation capabilities of the two bottom bed layers. In cases where ineffective separation was found between the bottom and second layer, the coal was not improved and the top layer was also discarded in order to improve the coal quality. The fluidised bed is less sensitive to the sharpness of separation in mid-to-top section of the bed.

Relatively poor separation was found in the beds that consider 1:1 and 2:1 dense medium ratios and furthermore the addition of vibration proves no improvement there upon. The addition of vibration with increased amounts of DM most likely caused an even denser packing in the bed, which hindered particle movement and thereby resulted in no extensive separation. Once again, it must be noted that this is probably due to the batch experimentation method followed and some inadequacies regarding the procedure and equipment optimization.

7.2.5 Influence of quality

An observable improvement in the sharpness of separation noted when considering the coal quality Q-02 as compared to Q-01. Clearer stratification of the layers, in terms of ash value, is obtained and a much more desired product and middling fraction is formed. Comparably large ash values in the bottom layer is observed for both qualities which further proves that Q-02 behaved better. The latter quality consists of a sample that constitutes less intimately mixed dense material when compared to Q-01. This is the cause of the sharper separation observed for this sample.

7.2.6 Statistical significance

The response obtained from the ANOVA and t-test statistical significance analyses validate the conclusions drawn with regard to the influence of particle size, dense medium to coal mass ratio and activation of vibration. Very low p-values are reported for the bottom bed layers alongside all variables considered which indicates that the influence on ash value from variation of these have a significant impact on the separation. A change in PSD and activation of vibration proves to have no effect on the ash value obtained in the top layer due to the p-values reporting above 0.05. Dense medium does however seem to have an appreciable effect on the ash value obtainable in the top layer (p-value = 0.008).

7.3 Recommendations

The following recommendations are made in order to support future test work on the dense medium fluidised bed and ensure that the technology can be introduced to the South African coal processing industry.

7.3.1 Operation and optimization

It may be useful to operate the bed in a semi-continuous cycle as compared to batch testing. This may yield significantly different results most especially when considering dense medium beds. Ensuring a stable fluidized magnetite bed and simply adding the coal to the already fluidized bed may result in sharper separation efficiencies than when mixing the two materials initially as done in the batch test. The extent to which the coal particles affect the movement and fluidization of the magnetite in the initial stages is not known. It is possible that the dense medium does not reach a fully developed and stable fluidized bed state because of these coal-magnetite interactions.

It is further recommended that extensive optimization studies be conducted on the enlarged ADMFB. These should include, minimum fluidization requirement, vibration frequency and amplitude tests. It will comprehensively benefit the study to ensure that the most optimal MFV is obtained for each change in variable and that the oscillating vibratory motor is vibrated optimally for the application at hand.

7.3.2 Medium

An autogenous dense medium may be beneficial to a project such as this. If mixed with fine coal discard, the issue of contamination of the magnetite by coal fragments as formed from attrition is eliminated. It is however essential to ensure that the amount of fine coal added does not significantly affect the density and stability of the fluidized bed obtainable.

Some benefit may be found from a more comprehensive understanding of the medium behaviour in the bed. This can be achieved with the use of density tracers and may provide an idea of the sensitivity of fluidization to varying certain parameters without needing to consider the particle effects as related to coal. Density tracers provide a means to determine the effect of particle size more accurately, density and shape on stable fluidization and effective separation. As coal mining operations generally use copious amounts of water, ROM coal is relatively high in moisture content. The study of dry dense medium separation may further benefit from a deeper understanding of the effects of moisture on the fluidization of the medium and the limitations thereof.

The addition of a secondary visual control system can be implemented in order to visually study the behaviour, formation and effects of bubble formation at various air flow rates. This will especially be beneficial with the use of a dense medium, as bubble formation during test runs that were conducted with the addition of a medium is more severe. The installation of a video camera will therefore aid in explaining the behaviour, formation and effects of bubbles.

The economic aspects of adding medium to the bed should also be considered. By adding a dense medium, a reduction in coal throughput over a time will be experienced, which will increase the processing time required. It will therefore be necessary to ensure that the performance of the bed, with the addition of a medium, is far better than that of a normal fluidisation of the coal particles to ensure the feasibility of the technology.

7.3.3 Particle size and quality

It is highly recommended that various coal blends be investigated in future studies to validate the finding relating the effects of coal quality. Many investigations, as referred to in *Chapter 2*, utilized a coal with an array of qualities from which the destoning effects seemed much better. This may give a more comprehensive idea of the sensitivity of fluidized bed separation to the feed characteristics of the coal. Moreover, the investigation may benefit from a knowledge of the type and positioning of mineral matter in a coal sample and therefore, Quantitative evaluation of minerals by scanning electron microscopy (QUEMSCAN) studies of the feed coal may be useful. A QUEMSCAN may provide a good idea of the relating particle size to use for a specific sample to ensure proper liberation.

Furthermore, it is recommended that the particle size of the feed coal should be broader. It has been proved in this paper that a narrow particle size distribution can be effectively upgraded in the ADMFB. However, various authors made use of a much wider particle size range. It is therefore recommended that tests should be performed on +5.6-9.5mm and +9.5-13.2mm particle sizes as well as on coarser size fractions +13.2mm. Of use to understanding the capability of scaling the process, it may be useful to conduct investigation into the finer fraction of -5.6mm as previously investigated by the NWU in the smaller set-up.

7.4 Conclusive remark

From the study detailed in this dissertation it is clear that ADMFB technology can be implemented to successfully beneficiate South African small coal. An enlargement of the process is also possible which is beneficial for industrial applicability. Some additional research, regarding the ADMFB utilized, is however required to ensure optimal operation especially with the addition of dense medium and activation of vibration.

REFERENCES

Cairncross, B. 2001. An overview of the Permian (Karoo) coal deposits of Southern Africa. *J. Afr. Earth Sci., 33*:529–562.

Chen, Q. & Wei, L. 2003. Coal dry beneficiation technology in China: The state-of-the art. *China Particuology*, 1(2):52–56.

Chen, Q. & Wei, L. 2005. Development of coal dry beneficiation with air-dense medium fluidized bed in China. *China Particuology*, 3:42.

Chen, Q. & Yang, Y. 2003. Development of Dry Beneficiation of Coal in China. *Coal Preparation*, 23:3–12.

Chikerema, P. & Moys, M. 2012. Effects of Particle Size, Shape, and Density on the Performance of an Air Fluidized Bed in Dry Coal Beneficiation. *International Journal of Coal Preparation and Utilization*: 80–94.

Choung, J., Mak, C. & Xu, Z. 2006. Fine Coal Beneficiation using an Air Dense Medium Fluidized Bed. *Coal Preparation*, 26(1):1–15.

Conrads, G. 2009. Simple measurement of the frequency and amplitude of vibration. Concrete technology, Concrete Plant International. Retrieved from www.cpi-worldwide.com Date accessed: 15 June 2017.

De Korte, G.J. 2016. Dry Dense Medium processing of raw coal – progress report [correspondence]. 14 Jun., Potchefstroom.

Department of Energy, 2017. Coal resource. Retrieved from http://www.energy.gov.za/files/coal_frame.html. Date of access: 11 May 2017.

Department of Mineral Resources, 2014. South African Yearbook. In: Johannesburg, South Africa: s.n., pp. 301-311.

Dwari, R.K. & Rao, K.H. 2007. Dry beneficiation of coal - A review. *Mineral Processing & Extractive Metall*, 28:177–234.

Eberhard, A. 2011. The future of South African coal: Market, investment, and policy challenges. Retrieved from http://iis-db.stanford.edu/pubs/23082/WP_100_Eberhard_Future_of_South_African_Coal.pdf Date of access: 24 Feb. 2016.

Escudero, D. & Heindel, T.J. 2011. Bed height and material density effects on fluidized bed hydrodynamics. *Chemical Engineering Science*, 66: 3648–3655.

Falcon, R. & Ham, A.J.1988.The characteristics of Southern African coals. *Journal of the South African institute of mining and metallurgy*, 88(5):145-161.

Fan, M., Chen, Q., Zhao, Y., Guan, Z.L.Y. & Li, B. 2001. Magnetically stabilized fluidized beds for fine coal separation. *Powder Technology*, 123: 208–211.

Firdaus, M., O'Shea, J.P., Oshitani, J. & Franks, G.V. 2012. Beneficiation of coarse coal ore in an air-fluidized bed dry dense-medium separator. *International Journal of Coal Preparation and Utilization*, 32(6): 276–289.

Ghosh T. 2013. Modelling of an air-based density separator. Theses and Dissertations-Mining Engineering. Paper 7. Obtained from http://uknowledge.uky.edu/mng_etds/7.
Date accessed: 18 August 2017

Honaker, R.Q., Saracoglu, M., Thompson, E., Bratton, R., Luttrell, G.H. & Richardson, V. 2008. Upgrading coal using a pneumatic density-based separator. *International Journal of Coal preparation and Utilization*, 28 (1): 51-67.

He, J., Tan, M., Zhao, Y., Zhu, R. & Duan, C. 2016a. Density-based segregation/separation performances of dense medium gas–solid fluidized bed separator (DMFBS) for coal cleaning and upgrading. *Journal of the Taiwan Institute of Chemical Engineers,* 59: 252–261.

He, J., Tan, M., Zhu, R., Zhao, Y., Luo, Z. & Duan, C. 2016b. Process optimization for coal cleaning by enhancing the air-distribution stability of dry separator. *Powder Technology*, 288: 45–54.

He, J., Tan, M., Zhu, R., Zhao, Y., Hong, P. & Jiang, Y. 2016c. Density-based separation performance of a secondary air-distribution fluidized bed separator (SADFBS) for producing ultra-low-ash clean coal. *Fuel*, 172: 178–186.

He, J., Zhao, Y., He, Y., Luo, Z. & Duan, C. 2013. Separation performance of raw coal from South Africa using the dense gas-solid fluidized bed beneficiation technique. *The Journal of the Southern African Institute of Mining and Metallurgy*, 113: 575–582.

He, J., Zhao, Y., Zhao, J., Luo, Z., Duan, C. & He, Y. 2015. Separation performance of fine low-rank coal by vibrated gas–solid fluidized bed for dry coal beneficiation. *Particuology*, 23: 100–108.

Houwelingen, J.A. & De Jong, T.P.R. 2004. Dry cleaning of coal: Review, fundamentals and opportunities. *Geologica belgica*, 7: 335–343.

International Energy Agency (IEA). 2014. Medium-term coal market report 2014 factsheet. https://www.iea.org/media/news/2014/press/141215_MTCMR2014_Factsheet.pdf
Date of access: 24 Feb. 2016.

International Energy Agency (IEA). 2011. Power generation from coal. Retrieved from https://www.iea.org/publications/freepublications/publication/Power_Generation_from_Coal2011.pdf Date of access: 24 Feb. 2016.

IPC Coal. 2016. IPC Africa. Retrieved from http://www.ipcafrica/products_coal.htm Date of access: 11 September 2017.

Jeffrey, L. S. 2005. Characterization of coal resources of South Africa. *The Journal of the Southern African Institute of Mining and Metallurgy, 105*: 95–102.

Jun Oshitani, Kazuhiro Teramoto, Mikio Yoshida, Yasuo Kubo, Shing Nakatsukasa, George V. Franks. 2016. Dry beneficiation of fine coal using density-segregation in a gas–solid fluidized bed. *Advanced Powder Technology*, *27*:1689-1693.

Jun Oshitani , Tetsuya Kawahito, Mikio Yoshida, Kuniaki Gotoh, George V. Franks. 2012. The influence of the density of a gas-solid fluidized bed on the dry dense medium separation of lump iron ore. *Minerals Engineering 24*:70–76.

Kumar, P., Sah, R., Ari, V., & Das, A. 2010. Dry beneficiation of coal fines using air table. *Mineral Processing Technology*, 1: 446-451.

Kunii, D. & Levenspiel, O. 2001. Fluidization Engineering. Newton: Butterworth-Heinemann.

Langer, D. J., 2016. *The dry beneficiation of duff coal in a dense medium fluidised bed,* Potchefstroom: Dissertation submitted in fulfilment of the requirements for the degree Masters in Chemical engineering at the Potchefstroom Campus of the North-West University.

Luo, Z. & Chen, Q. 2001. Dry beneficiation technology of coal with an air dense-medium Fluidized bed. *International journal of mineral processing*, 63: 167–175.

Luo, Z., Fan, M., Zhao, Y., Tao, X., Chen, Q. & Chen, Z. 2008. Density-dependent separation of dry fine coal in a vibrated fluidized bed. *Powder Technology*, 187:119–123.

Luo, Z.F., Tang, L.G., Dai, N.N. & Zhao, Y.M. 2012. The effect of a secondary gas distribution layer on the fluidization characteristics of a fluidized bed used for dry coal beneficiation. *International Journal of Mineral Processing*, 118: 28–33.

Luo, Z., Zhao, Y., Chen, Q., Fan, M. & Tao, X. 2002. Separation characteristics for fine coal of the magnetically fluidized bed. Fuel Processing Technology, 79: 63–69.

Luo, Z., Zhao, Y., Tao, X., Fan, M., Chen, Q. & Wei, L. 2003. Progress in dry coal cleaning using air-dense medium fluidized beds. *Coal Preparation*, 23: 13-20.

Luo, Z., Zhu, J., Fan, M., Zhao, Y. & Tao, X. 2007. Low density dry coal beneficiation using an air dense medium fluidized bed. *Journal of China University of Mining & Technology*, 17: 306–309.

Macpherson, S.A. & Galvin, K.P. 2010. The effect of vibration on dry coal beneficiation in the reflux classifier*. International Journal of Coal Preparation and Utilization*, 30(6): 283–294.

Maoming, F., Qingru, C., Yuemin, Z., Zhenfu, L., Xinxi, Z., Xiuxiang, T. & Guohua, Y. 2003. Fine coal dry classification and separation. *The European Journal of Mineral Processing and Environmental Protection*, 3(2): 196–201.

Mohanta, S., Rao, C.S., Daram, A.B., Chakraborty, S. & Meikap, B.C. 2013. Air dense medium fluidized bed for dry beneficiation of coal: Technological challenges for future. *Particulate Science and Technology*: 31(1): 16–27.

Mohanta, S., Chakraborty, S. & Meikap, B.C. 2011. Influence of coal feed size on the performance of air dense medium fluidized bed separator used for coal beneficiation. *Industrial and Engineering Chemistry Research*: (50): 10865–10871.

Encyclopaedia Britannica. 2010. 'Gondwana' in Encyclopaedia Britannica. Retrieved from https://www.britannica.com/place/Gondwana-supercontinent Date of access: 12 April 2018.

Prusti, P., Sahu, A.K. & Biswal, S.K. 2015. Prediction of the position of coal particles in an air dense medium fluidized bed system. *International Journal of Mining Science and Technology*, 25: 421–427.

Rao, A., Curtis, J.S., Hancock, B.C., & Wassgren, C. 2010. The effect of column diameter and bed height on minimum fluidization velocity. *AIChE Journal:* 56(9): 2304-2311.

Rand water. 2017. Water Wise. Retrieved from http://www.waterwise.co.za/site/water/environment/situation.html
Date of access: 11 May 2017.

Rhodes, M. 2008. Introduction to Particle Technology. Australia: Monash University. Wiley & Sons, Ltd. Second edition.

SACPS (South African Coal Processing Society). 2011. *Coal preparation in South Africa.* Pietermaritzburg: Natal witness commercial printers.

SACPS (South African Coal Processing Society). 2015. *Coal Preparation in South Africa.* Pietermaritzburg: Natal witness comercial printers.

Sahu, A.K., Tripathy, A. & Parida, A. 2013. Study on particle dynamics in different cross sectional shapes of air dense medium fluidized bed separator. *Fuel*, 111: 472–477.

Sahu, A.K., Bismal, S.K. & Parida, A. 2009. Development of air dense medium fluidized bed technology for dry beneficiation of coal – A review. *International Journal of Coal Preparation and Utilization*, 29: 216–241.

SANEDI.2011. SACRM. Retrieved from http://www.fossilfuel.co.za/initiatives2013/SACRM-roadmap.pdf Date of access: 25 Jun 2014.

SAWS (South African Weather Service). 2017. Weather SA. Retrieved from http://www.weathersa.co.za/climate/historical-rain-maps Date accessed: 11 May 2017

SAWS (South African Weather Service). 2017. Drought monitoring March 2017. Retrieved from http://www.weathersa.co.za/images/climate/pdf/CLS-CI-Drought%20Monitoring-2017-04.pdf Date accessed: 11 May 2017

SAWS (South African Weather Service). 2017. Seasonal climate watch February to June 2017. Retrieved from http://www.weathersa.co.za/media/data/longrange/gfcsa/scw.pdf Date accessed: 11 May 2017

Sobrino, C., Acosta-iborra, A., Santana, D. & De Vega, M. 2009. Bubble characteristics in a bubbling fluidized bed with a rotating distributor. *International Journal of Multiphase Flow*, 1: 1–23.

Stats SA, 2013. The importance of coal. *Mining Industry (Report No.20-01-02).*

Schweinfurth, S.P. 2009. An introduction to coal quality, Chapter C, in Pierce, B.S. and Dennen, K.O., ed., The National Coal Resource Assessment Overview: US Geology Survey Professional Paper 1625-F, 20 p.

Terblanche, A.N. 2011. Dry beneficiation of fine coal using a fluidized bed. Final year project Report. Potchefstroom: NWU. (Unpublished).

Van der Walt. 1984. Lecture notes on coal washability.

WCA (World Coal Association). 2017. Coal. https://www.worldcoal.org/coal/where-coal-found. Date of access: 22 May 2017

WCI (World Coal Institute). 2009. The Coal Resource: A Comprehensive Overview of Coal. Retrieved from https://www.worldcoal.org/sites/default/files/coal_resource_overview_of_coal_report (03_06_2009).pdf Date of access: 25 Feb. 2016.

Wei, L., Chen, Q. & Zhao, Y. 2003. Formation of Double-Density Fluidized Bed and Application in Dry Coal Beneficiation. *Coal preparation*, 23: 21–32.

Wen C, Yu Y. 1966. Mechanics of fluidization. *Chem Eng Prog Symp.,* 62:100–111.

Wills, B.A. & Napier-Munn, T.J. 2006. Wills' mineral processing technology. Burlington: Elsevier Ltd.

World Energy Council. 2017. World Energy Council. Retrieved from https://www.worldenergy.org/data/resources Date of access: 11 May 2017.

Xie, K.C. 2015. Coal gasification. In: Structure and reactivity of coal. Springer, Berlin, Heidelberg

Yang, X., Zhao, Y., Zhou, E., Luo, Z., Fu, Z., Dong, L. & Jiang, H. 2015. Kinematic properties and beneficiation performance of fine coal in a continuous vibrated gas-fluidized bed separator. *Fuel*, 162: 281–287

Yang, X., Zhao, Y., Luo, Z., Song, S., Duan, C. & Dong, L. 2013a. Fine coal dry cleaning using a vibrated gas-fluidized bed. *Fuel Processing Technology*, 106: 338–343.

Yang, X., Zhao, Y., Luo, Z., Song, S. & Chen, Z. 2013b. Fine coal dry beneficiation using autogenous medium in a vibrated fluidized bed. *International Journal of Mineral Processing*, 125: 86–91.

Yang, X., Zhao, Y., Li, G., Luo, Z., Chen, Z. & Liang, C. 2012. Establishment and evaluation of a united dry coal beneficiation system. *International Journal of Coal Preparation and Utilization*: 32(2): 95–102.

Zhao, Y.M., Zhang, B., Luo, Z.F., He, J.F., Dong, L., Peng, L. & Cai, L. 2015. Effect of lump coal shape on separation efficiency of gas-solid fluidized bed for dry coal beneficiation. *Procedia Engineering*, 102: 1123–1132.

Zhao, Y., Li, G., Luo, Z., Liang, C., Tang, L., Chen, Z. & Xing, H. 2011. Modularized dry coal beneficiation technique based on gas-solid fluidized bed. *National Natural Science Foundation of China*, 18: 374–380.

Zhao, Y.M., Luo, Z.F., Chen, Z.Q., Tang, L.G., Wang, H.F. & Xing, H.B. 2010a. The effect of feed-coal particle size on the separating characteristics of a gas-solid fluidized bed. *The Journal of the Southern African Institute of Mining and Metallurgy*, 110: 219–224.

Zhang, B. et al., 2014. Effect of high density coarse-particle layer on the stability of a gas-solid fluidized bed for coal beneficiation. *International Journal of Mineral processing,* pp. 8-16.

Appendix A: ENGINEERING DRAWINGS

- Engineering drawings stipulating the dimensions of the ADMFB and its various additions

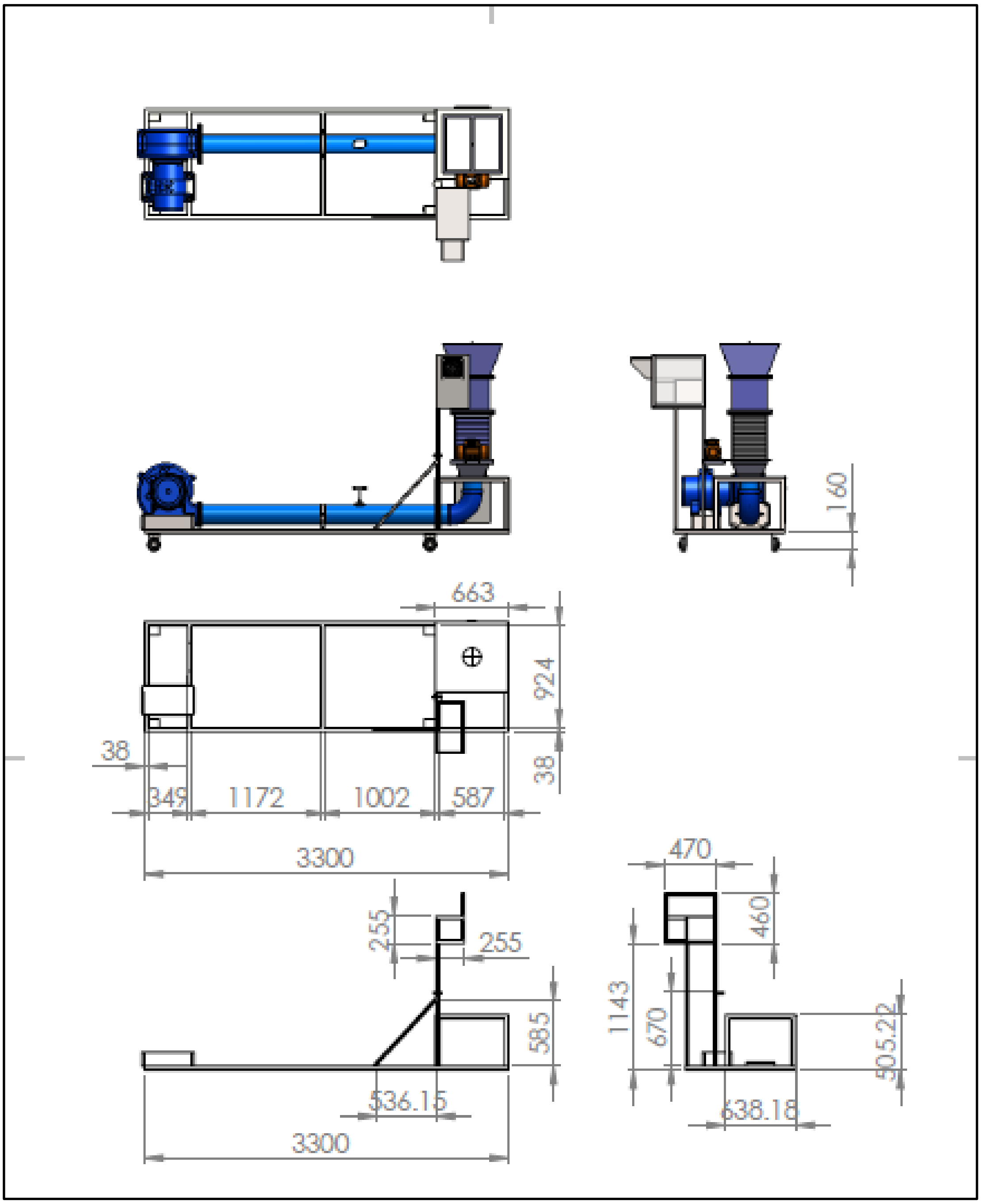

Figure A 1: Bed dimensions

- Three dimensional rendered sketches of the ADMFB from differing viewpoints

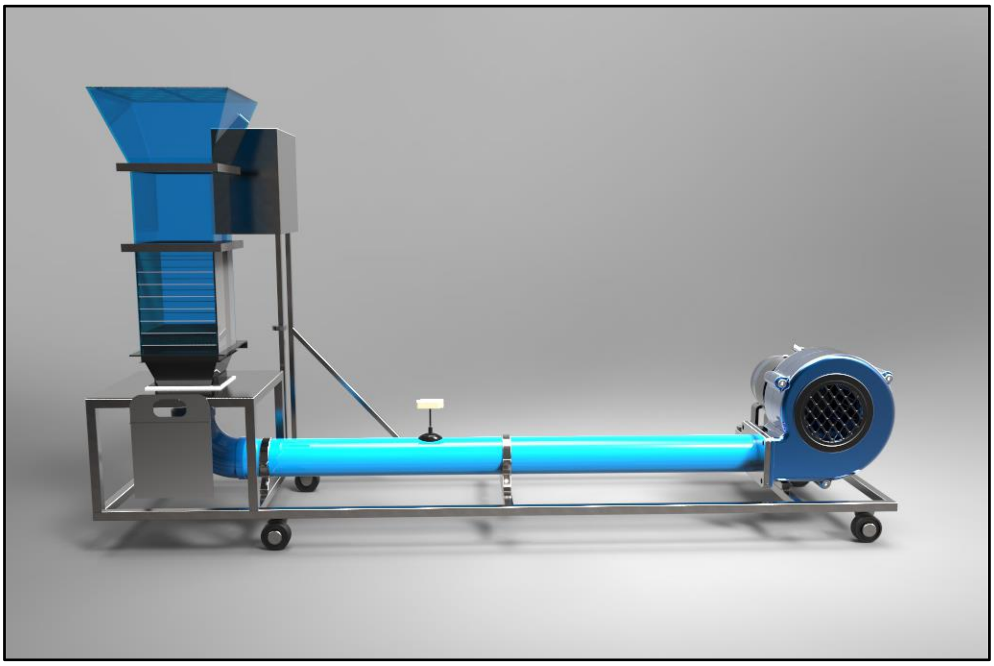

Figure A 2: Front view

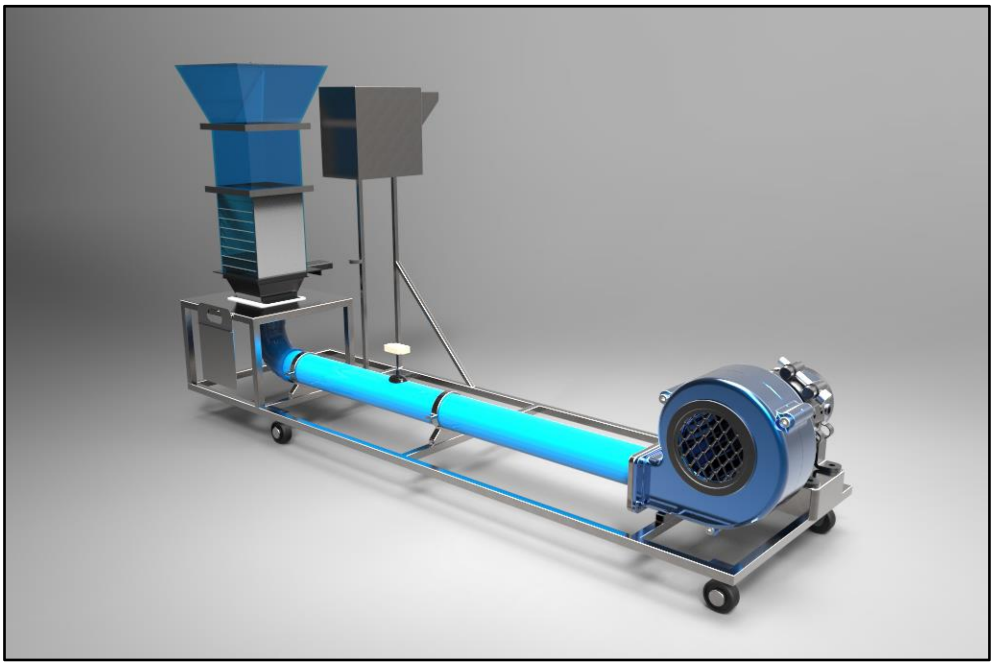

Figure A 3: Front diagonal view from blower

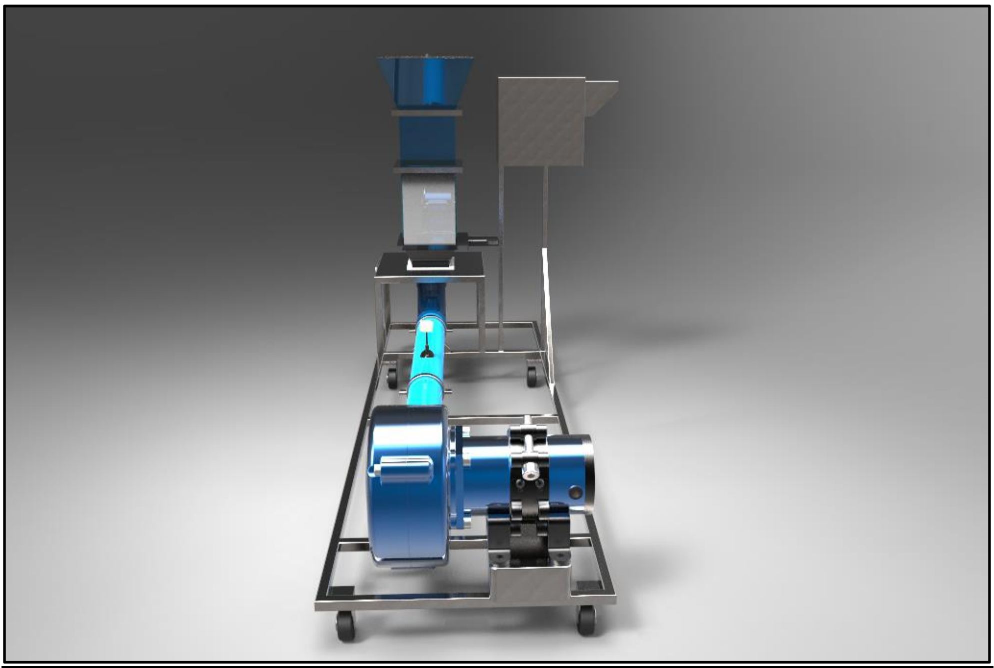

Figure A 4: Side view from blower

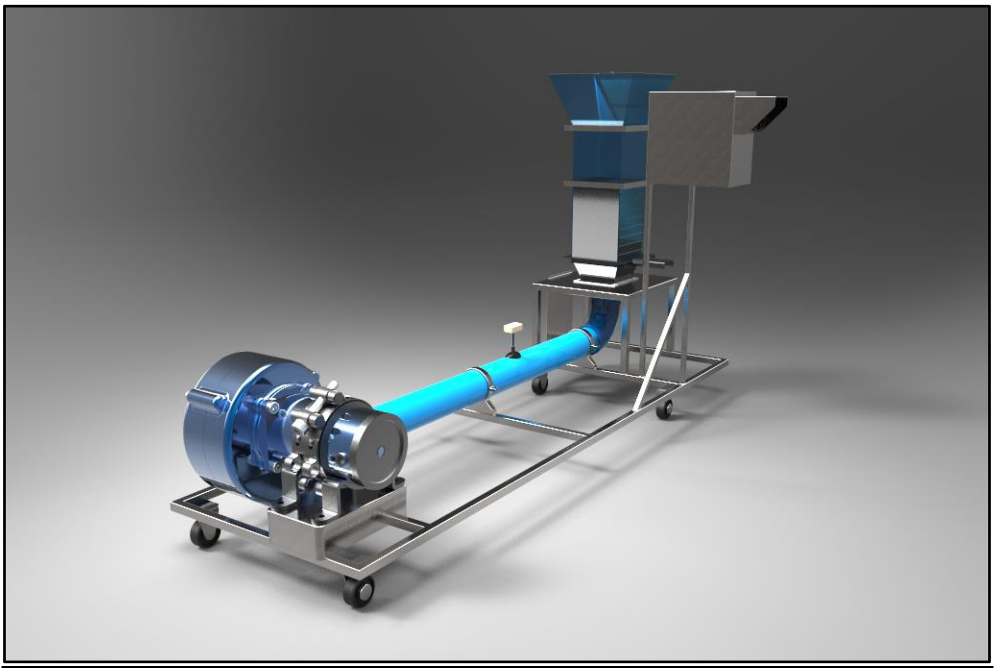

Figure A 5: Rear diagonal view from blower

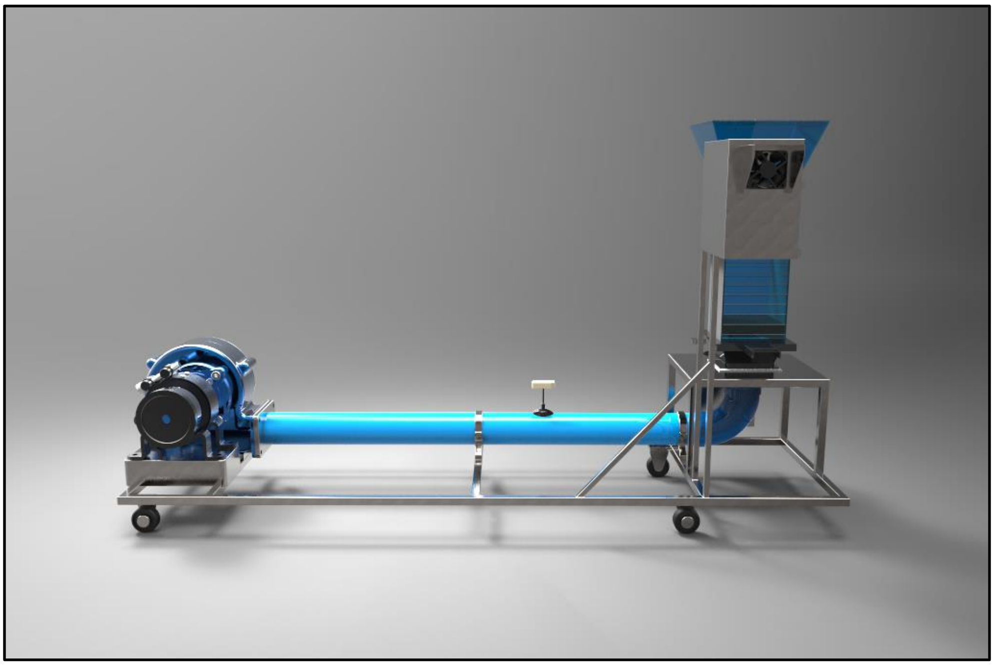

Figure A 6: Rear view

Figure A 7: Diagonal rear view from control unit

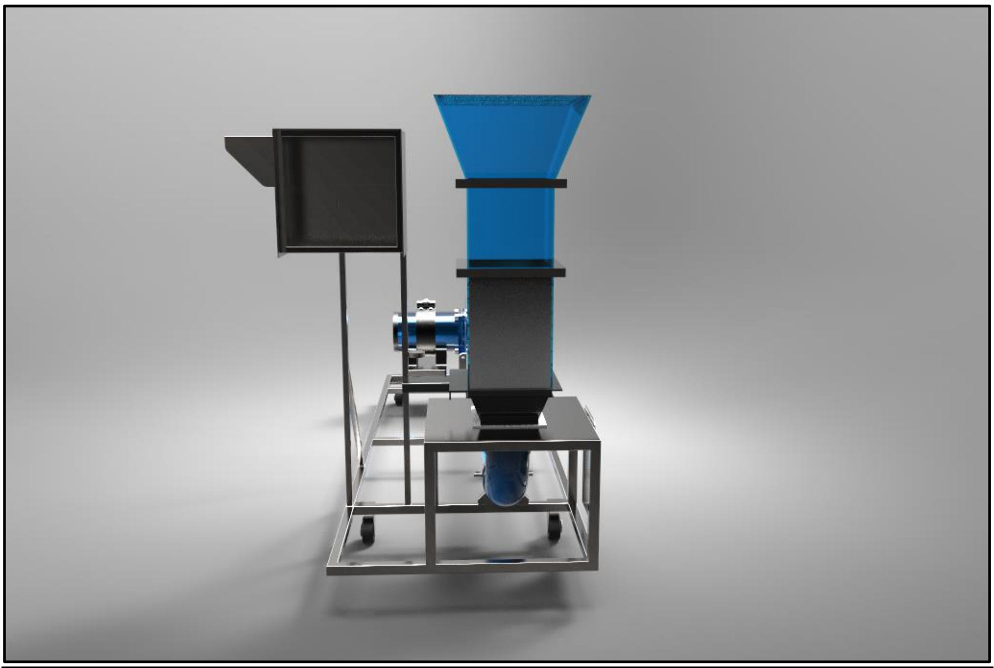

Figure A 8: Side view from control unit

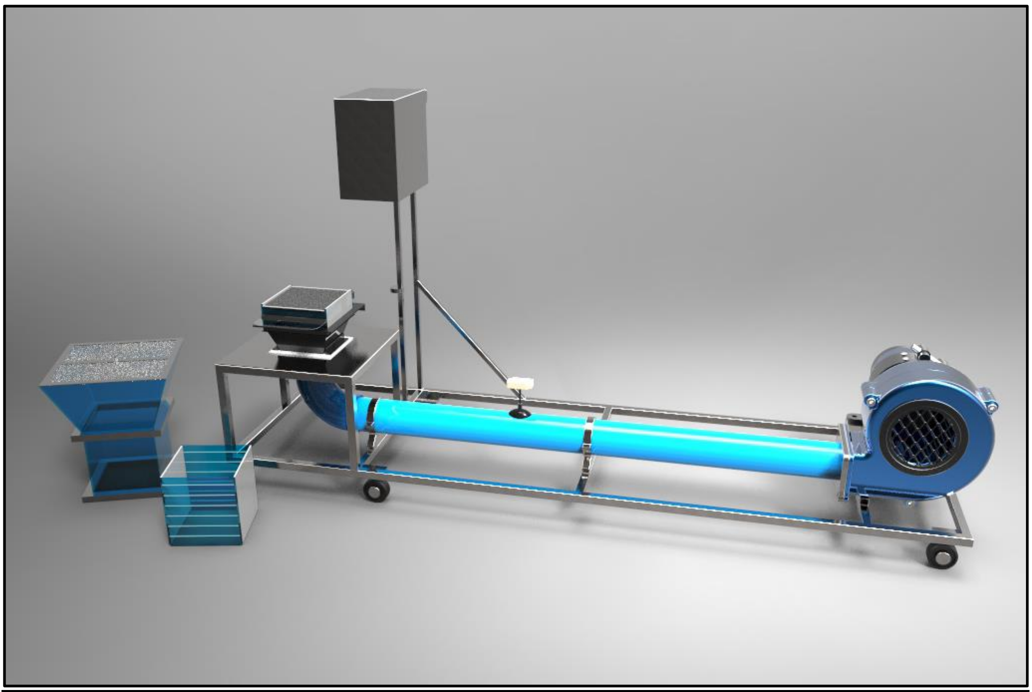

Figure A 9: Front view of disassembled bed

Appendix B: COAL WASHABILITY STUDIES

Presented in this appendix are the following results from the washability studies for each PSD of both Q-01 and Q-02 coal qualities

- Densimetric curves,
- Cumulative floats curves,
- Cumulative sinks curves and
- Difficulty curves

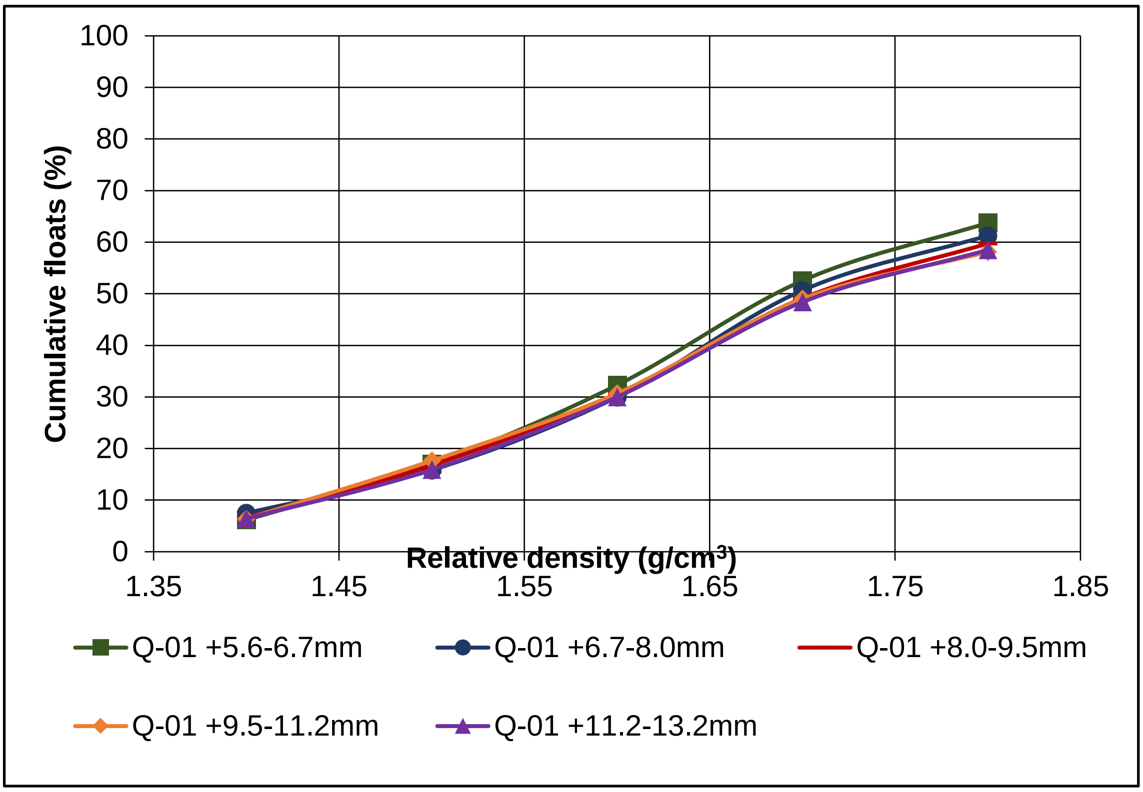

Figure A 10: Densimetric curves for Q-01

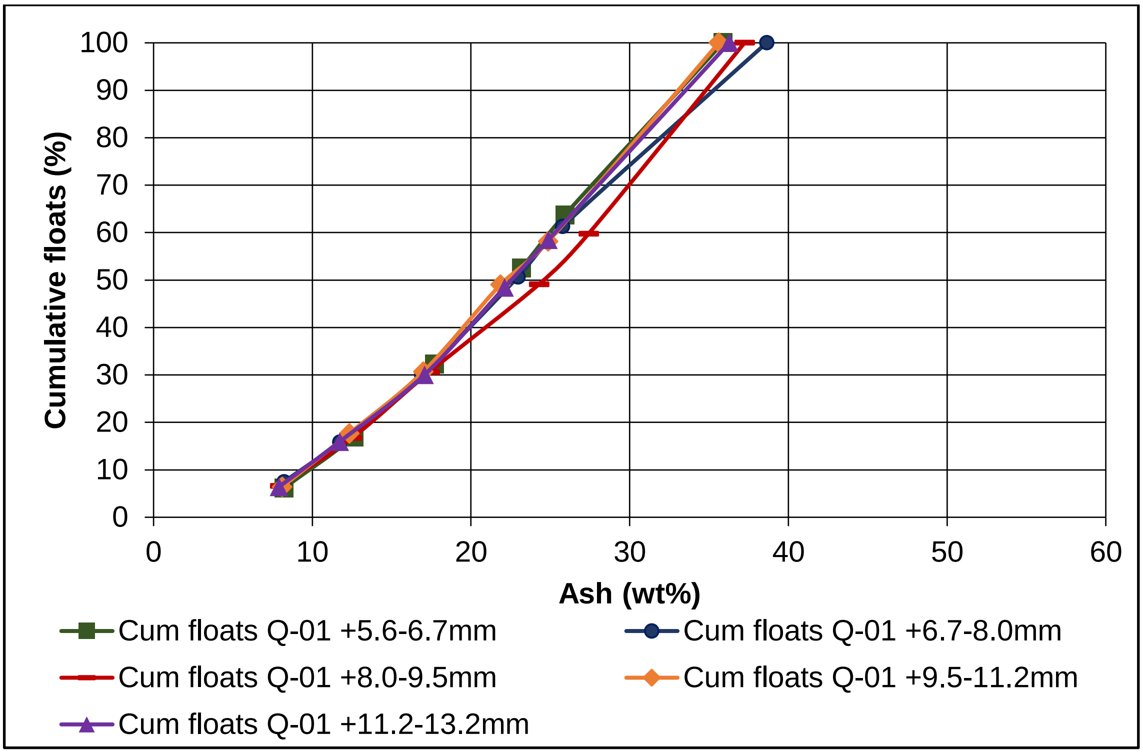

Figure A 11: Cumulative floats curves for Q-01

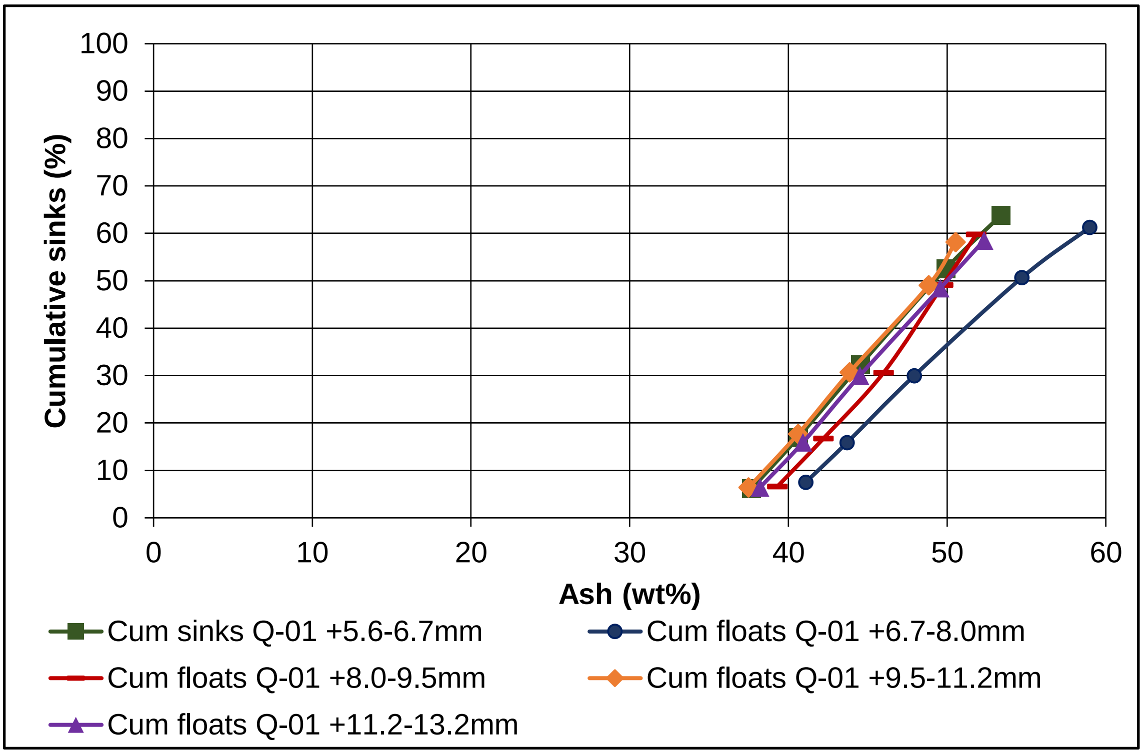

Figure A 12: Cumulative sinks curves for Q-01

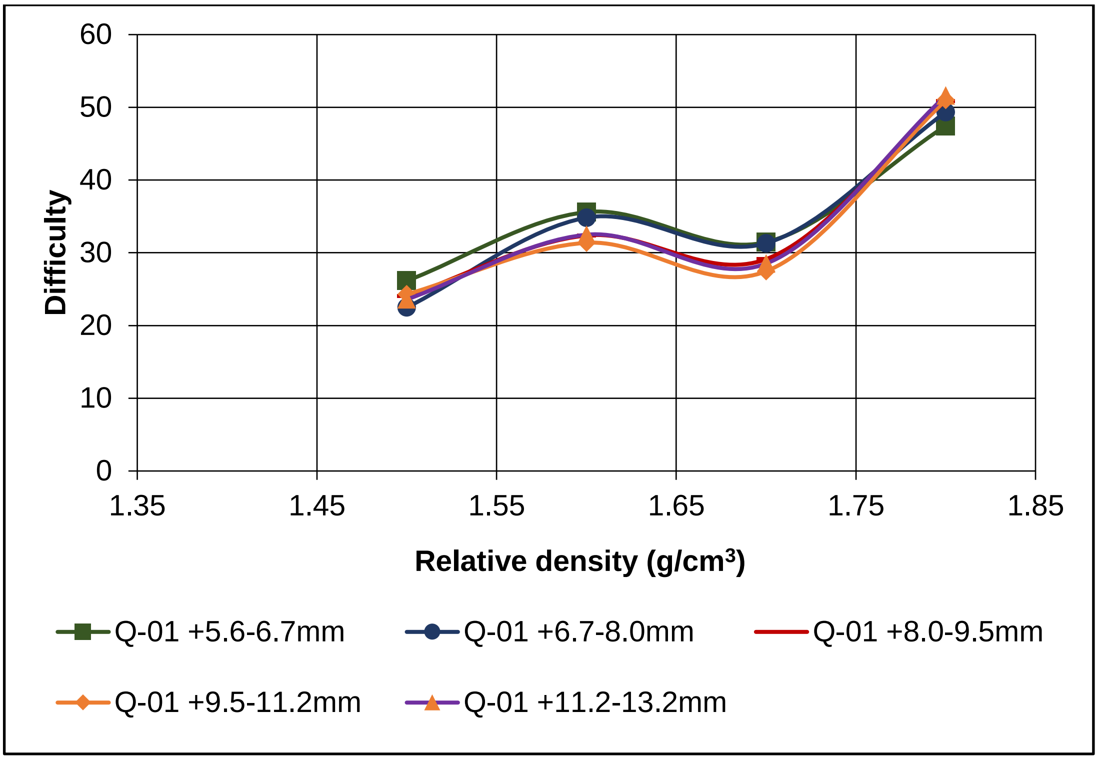

Figure A 13: Difficulty curves Q-01

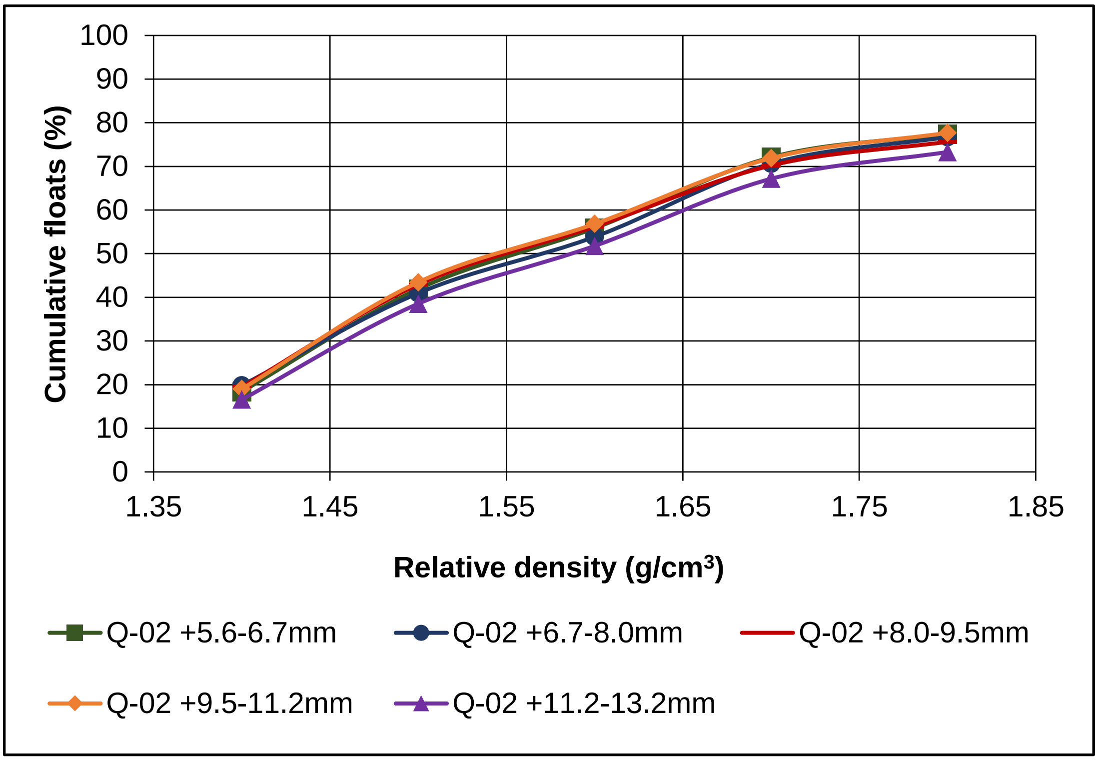

Figure A 14: Densimetric curves Q-02

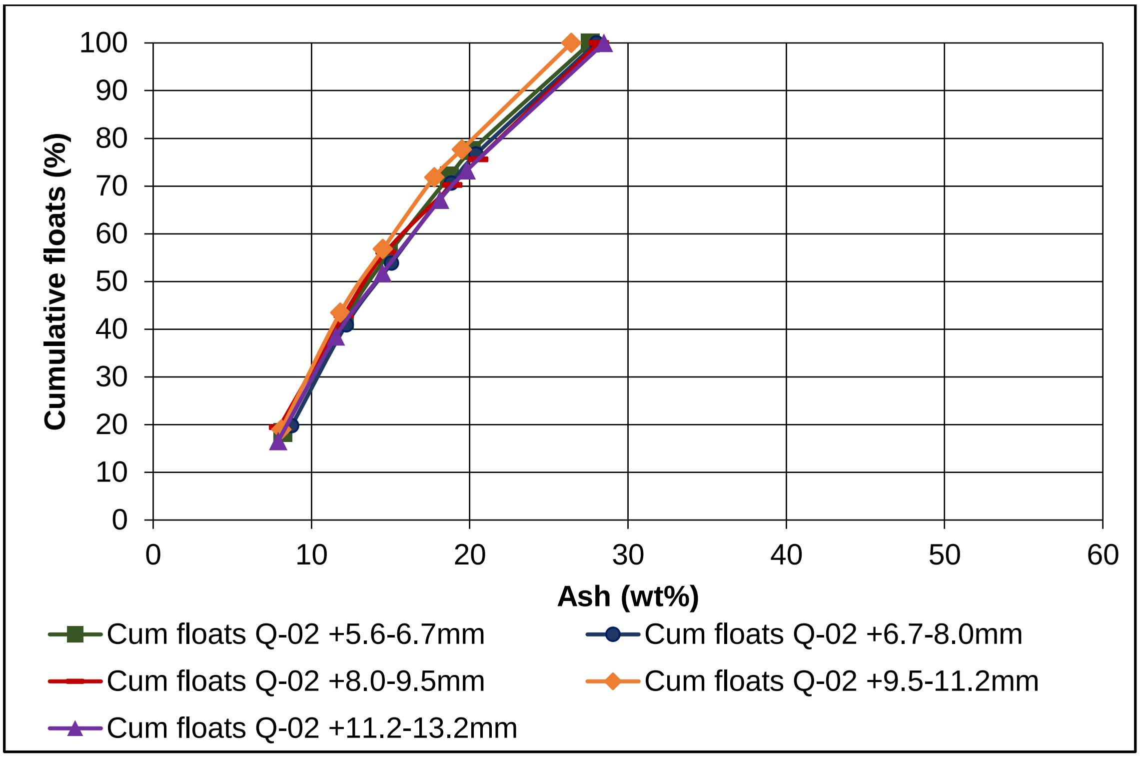

Figure A 15: Cumulative floats curves Q-02

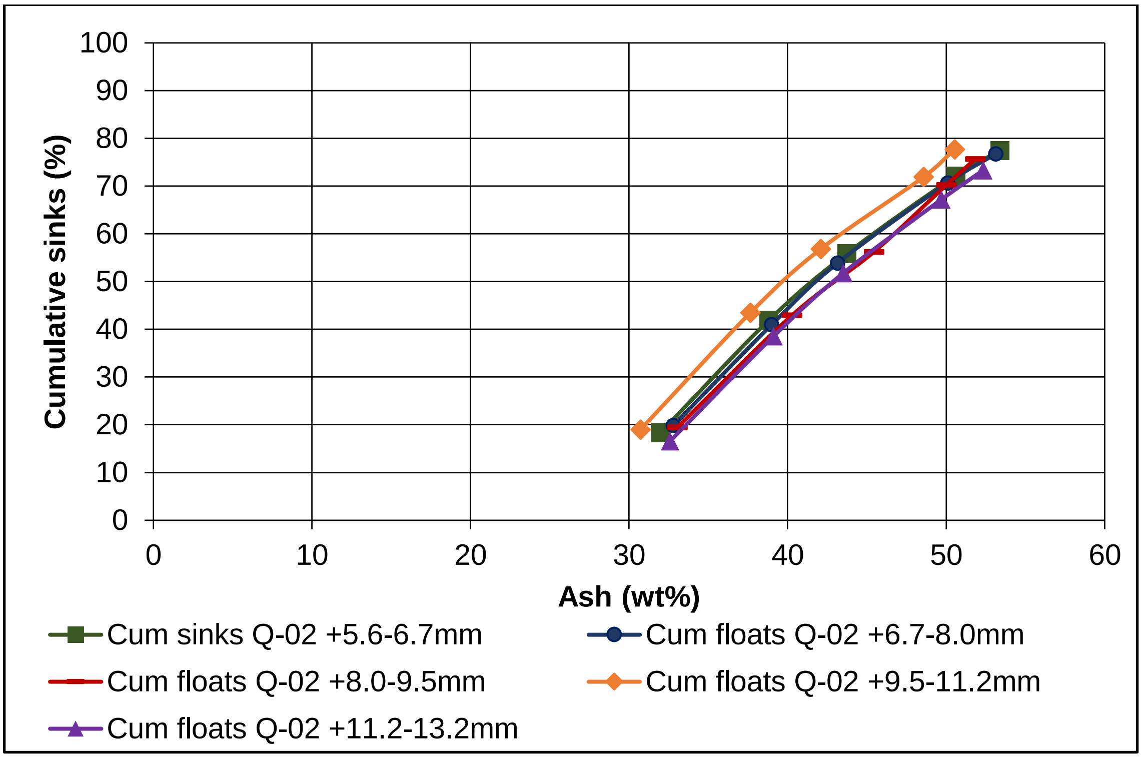

Figure A 16: Cumulative floats curves Q-02

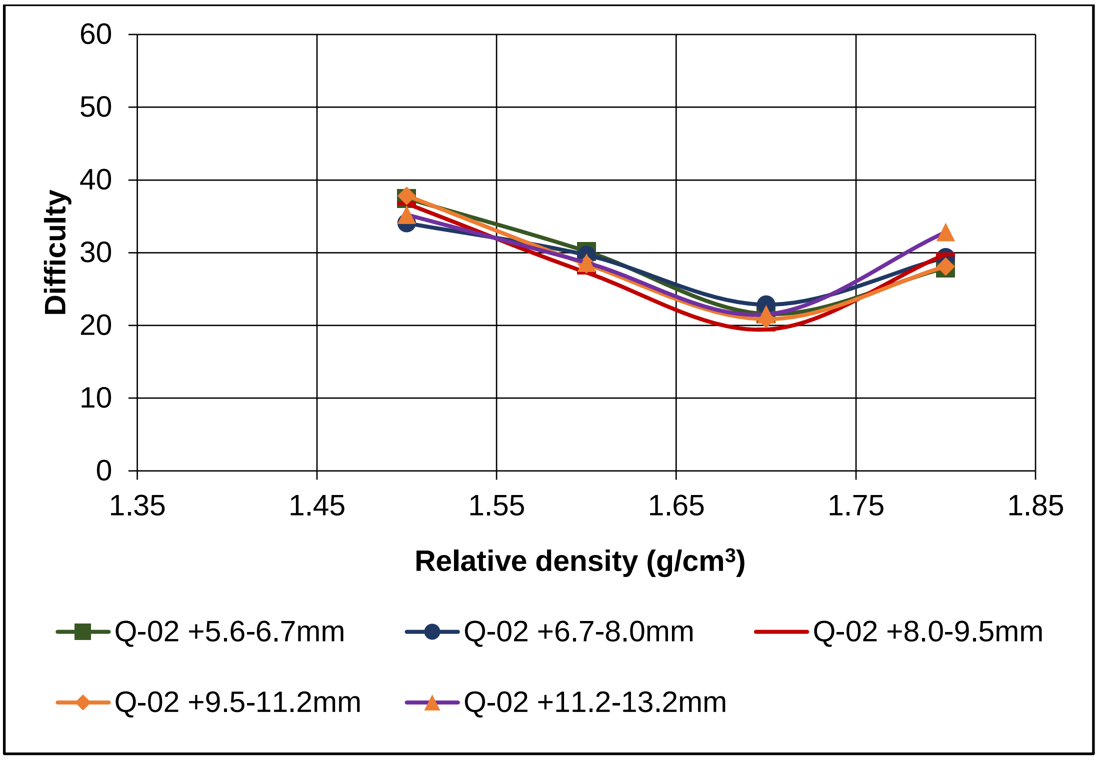

Figure A 17: Difficulty curves Q-02

Appendix C: HAZARD IDENTIFICATION RISK ASSESSMENT

PART 1: HAZARD IDENTIFICATION

Table C.1 lists those major hazards regarding the persons, materials, equipment and laboratory environment during the investigation. This is inclusive of hazards associated with sample preparation, experimental runs and the analyses performed, along with a short description of each.

Table A 1: List of hazards and descriptions

Fine coal powder
Experimental procedures, such as crushing, sieving, fluidizing and sampling of coal particles, may cause dust formation. Inhalation of coal dust poses a threat to the respiratory function and reduces the pulmonary capability. Coal dust can cause irritation when in contact with the skin or eyes and if ingested. The proper use of personal protective equipment (PPE) such as dust masks, protective goggles and protective clothing will aid in the necessary prevention. In occurrence of an incident rinse the affected area and clothing thoroughly with water and if any symptoms persist, seek medical attention.
Fine magnetite powder
Handling, fluidization, screening and sampling of fine magnetite powder with air may cause the particles to suspend in the air, increasing the risk inhalation, ingestion and contact with the skin and eyes. Various respiratory and pulmonary deficiencies such as metal fume fever can occur from inhalation of large amounts of magnetite powder and ingestion leads to problems with the liver and digestive tract. Fine magnetite powder may cause irritation when in contact with the eyes and skin. PPE such as dust masks, protective goggles and protective clothing is essential when working with fine magnetite powder. In occurrence of an incident rinse the affected area and clothing thoroughly with water or and if any symptoms persist, seek medical attention.
Zinc chloride powder and solution
Zinc chloride is a corrosive chemical solution that reacts exothermically with water and has potentially harmful health concerns. Zinc chloride can cause corneal damage and blindness

when in contact with the eyes and blistering and inflammation when in contact with skin. Ingestion can result in irritation of the gastro-intestinal and respiratory tracts. Airborne contaminates, produced from heating the zinc chloride solution, are extremely harmful to the pulmonary edema function. Prevention can be aided by the correct utilization of PPE including dust masks, respirators, eye protection and full protective clothing. In occurrence of an incident rinse the affected area and clothing thoroughly with water or move to an area of fresh air and if any symptoms persist, seek medical attention.
Explosions
Dust explosions could occur when suspended material (such as coal and magnetite powder) responds to frictional forces, impact or an ignition spark and rapidly combusts, subsequently releasing profuse amounts of energy. Zinc Chloride becomes highly explosive when in contact with potassium. Gas leaks of damaged or misused equipment are a cardinal cause of explosions resulting in severe physical injuries and death. Proper housekeeping and routine maintenance on all equipment is of utmost importance in prevention of explosions. In case of physical injury during an explosion, seek medical attention.
Ejecting particles
Crushers or vibrating sieves occasionally eject particles, which could cause injury to a person especially regarding the eyes. High-pressure systems (e.g. bomb calorimeter) can result in material eruptions, as equipment could be forced open, if not sealed appropriately. An induced pressure drop introduced across fluidized bed implies that the bed is not operated at an ambient pressure, thus posing a possible physical hazard to people close by, if the fluidized bed is not secured properly. Prevention of injury from ejecting particles remains in good housekeeping.
Physical injuries
Machinery with moving parts or that are portable can cause physical harm to those in the immediate surroundings if not secured properly. Repeatedly moving heavy equipment or containers may impose physical strain resulting in musculoskeletal injuries. If nozzles and pipes connected to a high-pressure system, such as the air dense medium fluidized bed, are not reinstated correctly, the sudden displacement may cause injury to those nearby.
Burn wounds

High temperatures analyses (e.g. Proximate analyses) pose a threat of acute burn wounds, as operating temperatures are as high as approximately 900°C. The correct use of heat resistant gloves is essential in prevention of burn wounds during such procedures.
Electrocution
Damaged electrical wiring positioned in areas where they are frequently subjected to spills on surfaces, wet floors and humid conditions pose an electrocution hazard. It is important to ensure that all electrical machinery and wiring is insulated and to clean up water spills as quickly as possible.
Noise
Noise produced from the jaw crusher, sieve shaker, pulverizer and fluidized bed may result in discomfort or hearing damage for the people working in the area. Proper use of ear plugs aids in prevention of hearing damage.

Location (building/room)

Experimental and analysis procedures will be completed in the mineral laboratory and the coal beneficiation laboratory, rooms N3B-G04 and N1-G08, respectively. All exploratory assessments will be conducted at the North West University's Engineering Campus situated in Potchefstroom. *Table C.2* provides a list of the activities which will be taking place during the investigation along with the required equipment and associated hazards.

Table A 2: List of activities, equipment/ substances and applicable hazards

	Activity	Equipment/substances	Hazard
1	Washability analysis	Coal, magnetite and a zinc chloride solution will be used to complete this preparatory procedure along with stainless steel baskets, buckets and sieves.	Zinc Chloride Physical injuries
2	Coal preparation	In order to ensure the desired particle sizes (+5.6-13.2mm), jaw	Dust Ejecting particles

		crushers and sieves will be used.	Electrocution Noise
3	Sampling	The raw coal and coal from experiments will be divided into functional samples by means of the coning and quartering sampling technique.	Dust Physical injuries Ejecting particles
4	Fluidizing	Coal and magnetite will be fluidized with the use of air during the experimental procedure.	Dust Ejecting particles Explosions
5	Moisture analysis	A proximate analyser machine or a laboratory oven and scale will be used for the purpose of this analysis.	Burn wounds Electrocution
6	Volatile analysis	A proximate analyser machine or a laboratory oven and scale will be used for the purpose of this analysis.	Burn wounds Electrocution
7	Carbon and ash analysis	A proximate analyser machine or a laboratory oven and scale will be used for the purpose of this analysis.	Burn wounds Electrocution
8	Calorific value analysis	A bomb calorimeter will be employed to determine the heat value of the sample.	Explosions Burn wounds Electrocution
9	Density analysis	A gas pycnometer device can be used to determine an accurate displacement volume of solids, which in return will be used to determine the density of the coal	Electrocution Explosion (gas)

		sample.	
10	PSD analysis	The appropriate size sieves and a sieve shaker as well as PSD analysis equipment will be used for this procedure.	Dust Electrocution Ejecting particles Noise
11	Housekeeping	Wash water and appropriate tools to ensure a clean and practical work environment is necessary.	Dust Physical injury

Coarse coal particles (+5.6-13.2mm) will be beneficiated using air dense medium fluidisation. The effectiveness of this dry beneficiation technique will be evaluated by analysing the performance of coarse coal particles in the ADMFB. This will be assessed in order to optimize separation efficiency of the bed for a desired density cut point. Whether coarse coal particles can be effectively beneficiated, will be determined by studying the influence the variables listed in **Error! Reference source not found.** have on the dependent ariable, which is the separation efficiency.

Table A 3: Independent variables and descriptions

Independent variable	Description
Initial/feed PSD of the coal	Investigate the effect of the initial PSD (5.6-6.7; 6.7-8.0; 8.0-9.5; 9.5-11.2 and 11.2-13.2mm) on the separation efficiency.
Coal to medium concentration	Investigate the effect of coal to medium concentration ratio's (1:0, 1:1 and 1:2) on the separation efficiency,

Vibration	Investigate the effect of a vibrated fluidised bed opposed to no vibration on the separation efficiency.
Media	Investigate the influence of two different media, magnetite and sad, on the separation efficiency.

A brief description of the activities performed for the beneficiation of coarse coal particles using an air dense medium fluidised bed will follow in **Error! Reference source not found.**.

Table A 4: A brief description of activities

	Activity	Description
1	Washability analysis	A preparatory analysis essential to determine the ability of the coal used in subsequent experimental procedures to separate effectively.
2	Coal preparation	A preparatory procedure ensuring suitable coal particle sizes for further investigations. This includes jaw crushing and sieving in order to acquire the desired particle sizes from the PSD and also air drying to ensure the correct initial moisture content of the coal.
3	Sampling	A Standard Operating Procedure (SOP) that entails retrieving a representative of the coal by using splitting apparatuses (Department of Natural Resources Management and Environment, 1998).
4	Moisture analysis	An analysis executed by making use of the proximate analyser machine or a laboratory oven to establish the moisture content at a temperature of $108 \pm 2℃$ (Majumder, *et al.*, 2008).

5	Volatile analysis	An analysis performed by the proximate analyser to establish the volatile content of the examined sample at a temperature of $900 \pm 15°C$ (Majumder, et al., 2008).
5	Carbon and ash analysis	An analysis performed as part of the proximate analyses to determine the remaining incombustible ash and the difference representing fixed carbon content (Majumder, et al., 2008).
6	Calorific value analysis	An analysis executed by an apparatus known as the bomb calorimeter that determines the heat value of a sample.
7	Density analysis	A conclusive analysis executed by a pycnometer that determines the density of the sample.
8	PSD analysis	An analysis to determine the particle size distribution of the desired particle size range which varies between +5.6-6.7mm.
9	Housekeeping	An essential activity assuring that the workstation is always clean and tidy.

PART 2: RISK ASSESSMENT

Risk = Likelihood (of event occurring) **x Severity** (seriousness of harm caused)

Table A 5: Risk assessment scale

Guideline for ranking: Rating	Likelihood	Severity
1	Very unlikely	Minor injury - No treatment or only first aid required
2	Might happen eventually	Injury requiring doctor's treatment; brief hospitalization

3	Likely to happen eventually	Severe injury causing permanent damage; disability
4	Will happen	Very severe injury; fatality

Table A 6: Hazard identification survey

Hazard Identified		**Likelihood of Incident occurring**	**Severity**	**Risk** (likelihood x Severity) (A x B)
Dust	Impaired respiratory function	3	2	6
	Eye sight restrictions	3	1	3
	Skin irritation	3	1	3
	Explosion	1	4	4
Chemicals	Tissue damage	2	2	4
Explosions	High pressures	2	3	6
	Dust	1	4	4
Ejecting particles	Impaired eye sight	1	3	3
	Physical injuries	2	2	4
Physical injuries	Carrying and handling	2	3	6
	High pressures eruptions	2	3	6
Burn wounds	High temperatures	2	3	6
Electrocution	Electrical shock	1	2	2
Noise	Impaired hearing	2	1	2

PART 3. CONTROL MEASURES

For Control Measures consider and implement the *Hierarchy of Controls* in order of preference:

1. Elimination
2. Substitution
3. Mechanical controls
4. Administrative controls
5. Personal protective equipment (PPE)

It is imperative that the hazards with the highest risk receive priority for control and that they have the highest practical order of control measure.

Table A 7: Hazards and control measures

Hazard	Controls
	Sample managing
Physical injuries	• Move samples loads of physically manageable quantities. • Request assistance if a task is too physically challenging. • Wear safety gloves to avoid coming into contact with the sharp edges of samples and ultimately avoid hand injuries.
Storage casualties	• In order to avoid sample arrangements collapsing, stack sample containers beside each other on flat surfaces, rather than on top of each other. • Ensure the workstation is dry and tidy before storing sample containers.

Contamination initiating fire	• To ensure an area does not result in a fire hazard, clean the contaminated area or surface. • Always operate at conditions that comply with standard operating regulations.
Milling and sieving procedures	
Dust	• During the milling process, wear dust mask to avoid inhaling dust fines. • Wear safety glasses to avoid eyesight irritation caused by suspended dust particles. • Wear the appropriate PPE in the laboratory to minimize contact with dust. • Rinse eyes or any irritated area thoroughly with large quantities of water to relieve irritability.
Noise	• Frequent exposure to sound pressure more than 85 decibels can cause permanent damage to a person's hearing. Use earplugs as required for continuous milling processes (Creighton University, 2016).
Ejecting particles	• Wear safety glasses and long-sleeve PPE to protect skin and eyes from sudden impact. • Seek medical attention if bleeding or blindness occurs.
Electrocution	• Restore faulty wiring and dry areas near electrical appliances. • Switch off electrical equipment if they are not used.
Experimental procedure	
Physical injury	• Secure and shut off gas valves properly with suitable claps to prevent pipes to lash out violently, which may cause physical injury to the operator.

	• Open pressure valves carefully to avoid a forceful release of a high-pressure system. • Tighten and secure any lose clamps on high-pressure equipment. • Wear long sleeve PPE, safety glasses and closed shoes as prevention in case of possible harmful incidents.
Analysis	
Chemicals	• Use chemical resistant rubber gloves and long sleeve PPE when performing the washability analysis. • Keep chemicals dry and locked up. • If zinc chloride makes contact with eyes and skin, rinse with plenty of water and soap. • Work in a well-ventilated room since zinc chloride airborne particles or smoke lead to pulmonary edema and metal fume fever (U.S. Services, 2014).
Burn wounds	• Wear safety oven gloves when operating the proximate analyser machine or ovens, since the crucibles are hot and will cause severe burns.
Explosions	• Verify that the equipment whilst operating the bomb calorimeter is secure and fastened properly. • Clean the bomb is properly to avoid contamination. • Make sure not to drop or damage bomb of the calorimeter. • Keep a safe distance from the bomb calorimeter when firing.

Appendix D: COMPARISON AND VERIFICATION DATA FOR INITIAL FINDINGS

This appendix provides all of the comparison tables and bar charts for the initial findings and discussion (*Chapter 5*).

Table A 8: Summary of initial findings data

Ash value (%wt_{db})	Vibration Deactivated (VD)			Vibration Activated (VA)		
	DM (0:1)	DM (1:1)	DM (2:1)	DM (0:1)	DM (1:1)	DM (2:1)
PSD: +6.7-8.0mm						
Feed	42.43	38.30	37.72	34.86	35.54	32.25
Top layer	34.66	34.70	33.05	26.33	25.85	27.30
3	38.84	36.30	-	35.62	-	-
2	38.91	39.60	37.50	35.42	32.11	32.30
Bottom layer	48.61	44.70	38.40	47.84	40.19	39.40
Upgrade Ash (% points)	7.52	3.6	4.67	8.53	9.69	4.95
PSD: +5.6-6.7 mm						
Feed	37.28	37.49	37.70	38.68	33.43	33.95
Top layer	34.84	33.27	32.19	26.81	31.81	32.50
3	38.28	38.42	-	-	-	-
2	36.28	37.73	32.98	38.39	32.11	34.00
Bottom layer	46.49	40.02	40.00	47.74	39.52	37.70
Upgrade Ash (% points)	2.44	4.22	5.11	11.87	1.62	1.45

The following table provides s standard error percentage for a selected run (Q-01; PSD +5.6-6.7mm; DM 0:1; VA) in order to establish statistical repeatability.

Table A 9: Verification of intitial findings data

Proximate analyses					Statistical calculations		
MV	**Sample**	**Run 1**	**Run 2**	**Run 3**	**Average ($\bar{x}$)**	**Confidence interval ($\bar{z}$)**	**Statistical error (%)**
Ash value (%)	Feed	36,30	37,55	38,68	37,51	1,64	4,4%
	Bottom	45,04	41,44	47,74	44,74	4,35	9,7%
	2	34,91	30,52	38,39	34,61	5,43	15,7%
	Top	27,49	27,08	26,81	27,13	0,47	1,7%
					Average statistical error:		**7.9%**

Appendix E: PREVIOUS ADMFB USED FOR LIBERATION STUDY

This appendix provides the details of the small scale ADMFB used for the liberation study conducted during the initial findings and discussion (*Chapter 5*).

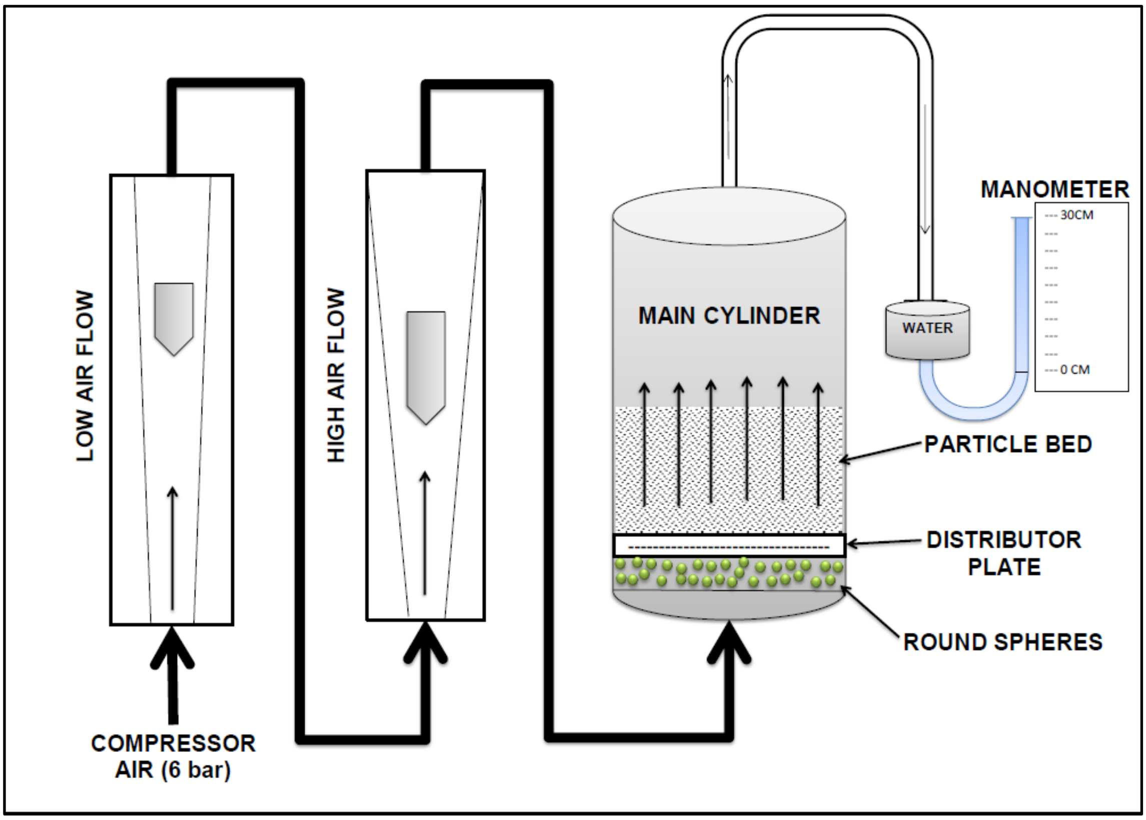

Figure A 18: Schematic of small scale ADMFB

The means of air flow and bed dimensions and geometry are the major differences noted when comparing the small scale ADMFB to that of the larger one used for experiments in this dissertation. For the prior bed, air was supplied by a laboratory compressor line controlled by a low and then high-flow meter. A similar distribution plate with perforated steel plating and marbles was utilized to aid in dispersion of the air. A U-tube water based manometer was used to record the pressure in the bed and a 212µm sieve was affixed to the top of the bed to prevent the coal from becoming airborne. The main cylinder of the bed consisted of 8 circular removable Perspex sections that fit onto one another. The diameter, layer height and bed height are 150mm, 40mm and 200mm, respectively. This specific configuration was designed according to recommendations made by Terblanche (2011) and Roux (2012) in order to ease sample cutting.

Figure A 19: Small scale ADMFB

Appendix D: COMPARISON AND VERIFICATION DATA FOR MAIN RUNS

This appendix provides a comparison table for the main experiments as discussed in *Chapter 6*. The associated bar charts are available on the accompanying DVD.

Table A 10: Summarized data for main experiments

Vibration	Layer	+11.2-13.2 mm	+9.5-11.2 mm	+8.0-9.5 mm	+6.7-8.0 mm	+5.6-6.7 mm
0:1 DM						
VD	Feed	28.3	22.3	30.0	26.3	27.7
	Top	21.2	18.6	21.4	20.1	21.4
	2	20.7	18.7	24.0	22.9	27.5
	3	27.6	24.9	28.7	26.0	32.1
	Bottom	53.8	44.5	52.2	46.5	41.2
VA	Feed	23.2	25.0	28.1	25.8	28.0
	Top	21.6	20.6	24.0	23.1	23.1
	2	28.5	21.8	24.0	24.7	26.0
	3	27.5	24.9	26.3	25.8	25.4
	Bottom	36.2	37.2	41.6	40.0	43.2
1:1 DM						
VD	Feed	22.9	26.4	25.9	40.0	29.7
	Top	20.2	23.9	24.0	21.8	25.8
	3	-	-	27.0	-	-
	2	22.3	25.7	28.8	26.2	36.8
	Bottom	33.7	34.6	34.0	34.6	33.9
VA	Feed	23.7	27.3	26.2	28.7	33.4
	Top	21.4	22.3	23.4	30.0	27.4
	3	-	-	-	-	-
	2	29.2	26.0	25.7	28.4	28.8
	Bottom	23.0	30.0	29.8	30.3	34.8
2:1 DM						
VD	Feed	24.8	28.5	27.9	30.9	30.8
	Top	21.2	22.4	24.0	24.5	28.8
	3	-	-	-		-
	2	25.4	30.4	25.6	24.7	31.1
	Bottom	34.8	34.3	32.1	37.1	36.5
VA	Feed	23.1	24.2	24.2	26.1	33.0
	Top	23.1	26.5	23.7	28.0	25.8
	3	-	-	-	-	-

	2	26.2	25.6	23.5	25.8	26.2
	Bottom	28.4	30.0	29.7	32.8	31.5

The ash results obtained for the verification studies conducted on selected main experimental runs are provided in the Tables below. Similar tables are available for CV and TRD in the accompanying DVD.

Table A 11: Verification data for main experiments

Q-02; PSD +11.2-13.2mm; DM 2:1; VD (Ash content)							
Proximate analyses					**Statistical calculations**		
MV	Sample	Run 1	Run 2	Run 3	Average ($\overline{x}$)	Confidence interval ($\overline{z}$)	Statistical error (%)
Ash value (%)	Feed	22.8	28	23.6	24.8	0.19	0.76
	Bottom	30.8	38.5	35.1	34.8	0.26	0.74
	2	25	25.4	25.8	25.4	0.03	0.11
	Top	18.1	24.6	20.8	21.2	0.22	1.03
					Average error (%)		**0.66**
Q-02; PSD +11.2-13.2mm; DM 2:1; VD (Ash content)							
Proximate analyses					**Statistical calculations**		
MV	Sample	Run 1	Run 2	Run 3	Average ($\overline{x}$)	Confidence interval ($\overline{z}$)	Statistical error (%)
Ash value (%)	Feed	22.20	24.40	22.80	23.13	0.08	0.33
	Bottom	27.70	28.49	29.00	28.40	0.04	0.15
	2	28.50	25.70	24.40	26.20	0.14	0.54
	Top	23.00	24.50	21.90	23.13	0.09	0.38
					Average error (%)		**0.35**
Q-02; PSD +9.5-11.2mm; DM 0:1; VA (Ash content)							
Proximate analyses					**Statistical calculations**		
MV	Sample	Run 1	Run 2	Run 3	Average ($\overline{x}$)	Confidence interval ($\overline{z}$)	Statistical error (%)
Ash value	Feed	21.90	23.50	25.00	23.47	0.10	0.44
	Bottom	35.90	40.50	37.20	37.87	0.16	0.42

(%)	2	23.50	25.80	24.90	24.73	0.08	0.31
	Top	18.90	22.60	21.80	21.10	0.13	0.62
					Average error (%)		**0.45**

Q-02; PSD +9.5-11.2mm; DM 1:1; VD (Ash content)							
Proximate analyses					**Statistical calculations**		
MV	Sample	Run 1	Run 2	Run 3	Average (x̄)	Confidence interval (z̄)	Statistical error (%)
Ash value (%)	Feed	27.30	24.00	27.80	26.37	0.14	0.52
	Bottom	33.50	34.10	36.30	34.63	0.10	0.29
	2	25.70	26.00	25.50	25.73	0.02	0.07
	Top	24.40	24.90	22.30	23.87	0.09	0.39
					Average error (%)		**0.32**

Q-02; PSD +8.0-9.5mm; DM 0:1; VD (Ash content)							
Proximate analyses					**Statistical calculations**		
MV	Sample	Run 1	Run 2	Run 3	Average (x̄)	Confidence interval (z̄)	Statistical error (%)
Ash value (%)	Feed	30.6	30.6	28.8	30.00	0.07	0.23
	Bottom	54.3	53.3	49.1	52.23	0.18	0.35
	2	31.1	28	26.9	28.67	0.15	0.51
	3	24	24	23.9	23.97	0.00	0.02
	Top	20.3	19.9	23.9	21.37	0.15	0.69
					Average error (%)		**0.36**

Q-02; PSD +8.0-9.5mm; DM 1:1; VA (Ash content)							
Proximate analyses					**Statistical calculations**		
MV	Sample	Run 1.00	Run 2.00	Run 3.00	Average (x̄)	Confidence interval (z̄)	Statistical error (%)
Ash value (%)	Feed	27.20	24.90	26.60	26.23	0.08	0.30
	Bottom	30.50	31.80	27.20	29.83	0.16	0.53
	2	26.60	26.00	24.50	25.70	0.07	0.28
	Top	26.10	21.00	23.20	23.43	0.17	0.73
					Average error (%)		**0.46**